NASA SP-229

PROCEEDINGS OF THE SEVENTH ANNUAL WORKING GROUP ON EXTRATERRESTRIAL RESOURCES

A meeting held at
DENVER, COLORADO
June 17–18, 1969

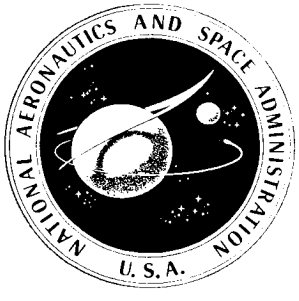

NATIONAL AERONAUTICS AND SPACE ADMINISTRATION

NASA SP-229

PROCEEDINGS OF THE SEVENTH ANNUAL WORKING GROUP ON EXTRATERRESTRIAL RESOURCES

A meeting held at

Denver, Colorado

June 17-18, 1969

Scientific and Technical Information Division
OFFICE OF TECHNOLOGY UTILIZATION 1970
NATIONAL AERONAUTICS AND SPACE ADMINISTRATION
Washington, D.C.

For Sale by the Superintendent of Documents,
U.S. Government Printing Office, Washington, D.C. 20402
Price $1.50
Library of Congress Catalog Card Number 68–62479

FOREWORD

This volume contains the proceedings of the Seventh Annual Meeting of the Working Group on Extraterrestrial Resources, which was held in conjunction with the Joint National Meeting of the American Astronautical Society (AAS) and the Operations Research Society (ORSA) on June 17–20, 1969, in Denver, Colorado.

The Working Group on Extraterrestrial Resources (WGER) is composed of scientists and engineers from the National Aeronautics and Space Administration, U.S. Air Force, U.S. Army, and the U.S. Bureau of Mines who have active interest in the utilization of extraterrestrial resources. Also contributing to the WGER studies are many invited participants from industry and universities.

The WGER was organized in 1962 with the following objectives:

> To evaluate the feasibility and usefulness of the employment of extraterrestrial resources with the objective of reducing dependence of lunar and planetary exploration on terrestrial supplies, to advise cognizant agencies on requirements pertinent to these objectives, and to point out the implications affecting these goals.

The WGER was one of six participating societies that aided AAS and ORSA in the planning of their national meeting, the theme of which was the "Planning Challenges of the 70's in Space and the Public Domain." Of the 137 technical sessions, the WGER planned and conducted one theme session, the "Use of Extraterrestrial Resources," and six specialist sessions which comprised its Seventh Annual Meeting. Theme session papers will be published by the AAS in the Advances in the Aeronautical Science series and the Science and Technology series. The six WGER sessions consisted of 11 invited and contributed papers and two panel discussions. Eight brief papers encompassing the panel discussions were prepared by the panel participants and are also included in this volume. All of the papers were technically edited by the staff of EXTERRA, Office of the Chief of Engineers, U.S. Army. Technical discrepancies were called to the attention of the authors for correction, but no attempt was made to interfere with an author's individual style. Primary responsibility for the technical accuracy of statements made reside with the author of each paper.

I believe that these proceedings will serve as a valuable reference in the field of extraterrestrial resource exploration and exploitation.

JAMES J. GANGLER,
Chairman, Working Group on Extraterrestrial Resources

CONTENTS

JAMES ADAMS
Stanford University

JOHN BILLINGHAM
Ames Research Center, NASA

MOONLAB: A Design for a Semipermanent Lunar Base

Under the direction of the authors, the 1968 Joint NASA–ASEE Summer Faculty Course on Systems Engineering prepared a design for a semipermanent lunar base. The base would be for the purpose of scientific exploration, with particular emphasis on astronomy; the site would be Grimaldi. The base would evolve over a 15-year period, requiring 37 launches of Saturn 5 delivery systems. The completed base would consist of 11 interconnected modules. Eight of these are for the shelter of the crew (24 men at base completion) and equipment.

The other three, which are inflated structures partially transparent to sunlight, contain a lunar farm of higher plants. This farm, a significant feature of the design, provides humidity control, oxygen generation, CO_2 removal, and a major part of the calorie requirements in food.

Power is supplied to the base by solar cell arrays during the day and fuel cells at night. Provisions are made for lunar surface exploration, use of lunar rocks and soil for many purposes, and emergency backup procedures.

BACKGROUND

A 10-week preliminary design study was undertaken in the summer of 1968 by a group of 20 visiting professors at Stanford University and Ames Research Center as a part of the NASA–ASEE Engineering Systems Design Summer Faculty Fellowship Program.

The primary purpose of this study was to acquaint the participants with the educational methods in space systems engineering used at Stanford in the hope that they would introduce similar techniques at their home universities. A second purpose was to acquaint the participants with NASA activities in space technology and research in order to identify areas of importance to engineering students both in course work and in graduate research. A third purpose was to perform a preliminary design of a lunar scientific laboratory. The study was purely for educational purposes and in no way was intended to be a part of NASA planning.

The problem originally assigned to the participants in this study was the design of a "semipermanent lunar surface observatory." The detailed definition of the mission and its objectives was an extremely difficult problem. Because of concern with overall national expenditures, a sizeable amount of effort was devoted to cost-benefit analysis. Unfortunately, because the benefits were primarily scientific knowledge, a rigorous cost-benefit analysis was not achieved. However, enough thought was given the relative benefits of various lunar missions and experiments and the relative benefits of manned and unmanned lunar, planetary, and Earth orbit missions to enable the study group to converge upon a mission.

Once a specific operational mission and its objectives were defined, the design of MOONLAB proceeded quite smoothly. The decision to include man in the lunar observatory was made fairly early in the program. Human intelligence and skills were considered essential to accomplish the desired scientific investigations. As an exercise in multi-disciplinary communication, the study was successful. As the design evolved, the areas of parametric conflict became apparent

and resolution by tradeoff was accomplished where possible. MOONLAB, as finally proposed, is designed to evolve over a 15-year period to a size capable of maintaining 24 men and of supporting scientific investigations in astronomy, selenodesy, selenology, selenochemistry, selenophysics, biology, biomedicine, behavioral science and agricultural science as well as particle and field experiments, lunar atmosphere studies, and remote observation of the Earth.

This chapter presents a few of the design conclusions which resulted from this study.

SITE SELECTION

The landing site selected for the proposed lunar base (MOONLAB) is in the crater Grimaldi at lunar coordinates 68°00′W, 3°30′S. The selected site is accessible to lunar landing vehicles using lunar orbit rendezvous and also accessible by line-of-sight to Earth bases for the purpose of direct radio and TV communication. Grimaldi was chosen primarily for its suitability as an astronomical site, although the site has many selenological features of interest as well. The site is just south of the lunar equator, a location characterized by extremes in thermal conditions. The polar regions are much more favorable from thermal considerations but were rejected because of poor astronomical promise, unfavorable abort capability, and plane change requirements in those phases of the program where lunar orbit rendezvous will be used.

MOONLAB BUILDUP

The early stages of the evolutionary phase of MOONLAB employ the Lunar Orbit Rendezvous (LOR) technique for personnel delivery and return. The study assumed the launch and landing vehicle configurations proposed by the Lockheed Missile and Space Company (ref. 1). Two assumptions concerning these delivery vehicles were made which were of paramount importance in establishing the abort capability for the base. These assumptions were (1) The LOR personnel carriers are capable of 180-day duration operation, and (2) The direct-mode personnel carrier is capable of 270-day dormancy on the lunar surface.

An alternate program was investigated which did not use LOR techniques. The results of that study indicated that the total cost of a direct-mode-only evolutionary program would be the same as the program described in the following pages; however, as the manned operations would occur over 5 years in the direct mode (instead of 9 years in the LOR mode), the peak annual funding of such a program would be larger. The direct mode would also not return scientific data until a later date. Accordingly the evolutionary program using LOR was selected.

A profile of the MOONLAB buildup is given in table I. A total of 37 launches is required, of which 23 are manned launches and 14 are cargo launches. The buildup of astronaut staytime from 6 months to a year is accomplished in three steps, with a period of 1 year of Earth post-mission observation of the astronauts before the lunar staytime is increased.

Abort during the first 3 years of the program is continuous since the astronauts will be able

TABLE I.—*Major Milestones in the Evolutionary Program*

Year	Development
0.....	Start development programs
3.....	Site certification mission
6.....	Deliver first cargo
	Establish three-man, 3-month staytime base
7.....	Staytime extended to 6 months
	Science program starts
8.....	Base grows to 6 men
	Hygiene shelter delivered
9.....	Staytime extended to 9 months
11.....	Staytime extended to 12 months
	Base grows to 12 men
	Sleeping and command shelters delivered
	Direct-mode personnel and advanced LLV used
12.....	Physical science and offsite activities shelters delivered
	Start phase C science program
13.....	Agriculture shelter delivered
	Base grows to 18 men
	Deliver lunar surface transportation
14.....	Astronomy shelter delivered
	Farms delivered
	Fourteen metric tons of science equipment delivered
15.....	Base grows to 24 men

to return to Earth via the same vehicle that delivered them. As personnel lunar staytime grows beyond the vehicle staytime in the ninth year, return from the Moon is accomplished by launching a personnel carrier from Earth. In the case of abort, the launch time reaction capability of this method (minimum of 3 days) may be unacceptable. By developing vehicles with staytimes equal to personnel staytimes, or vice versa, this problem may be avoided.

The total mass delivered in the evolution of MOONLAB is shown in table II. Table III gives the delivery requirements during evolution.

TABLE II.—*Mass Budget for MOONLAB Evolution*

System	Weight (kg)	Percent of total
Shelters, life support, farm, and radiator..	99 000	36
Water: use, reserves, and packaging.....	45 000	16
Power equipment and replacement.....	31 300	11
Lunar transportation and off-loading equipment.....	26 600	10
Gas: use, leakage, reserves, and packaging.....	30 400	11
Food: use, reserves, and packaging.....	19 400	7
Science equipment.....	19 200	7
Tunnels.....	2 700	1
Communications replacement.....	2 400	1
Total.....	276 000	.....

Since the requirements do not fall exactly into units deliverable by the cargo vehicles (16 000 and 23 000 kg), early delivery, particularly of expendables, allows the cargo to be partitioned into the specified units.

During the MOONLAB evolution eight shelter modules and three "farm" structures are to be delivered. The deployment of these shelters and farms is illustrated in figure 1; also indicated is the post-evolutionary function of each shelter. The total cost for the MOONLAB project was calculated to be 17.4 billion dollars. Figure 2 shows the annual cost as a function of the year from project initiation (assuming the project was initiated in the early 1970's).

MOONLAB LAYOUT

During design of MOONLAB, it was considered important to minimize the effects of isolation and maximize the effectiveness of the crew at their assigned tasks. Equipment layout and facility arrangement were carefully considered and habitability factors (odor, noise, illumination, temperature, humidity, recreation, etc.) were considered when it was demonstrated that they were potentially significant to the lunar crewman's total performance.

Some of the important design features that resulted from consideration of human factors were

(1) Separation of noise (offsite activities module) from quiet zones (sleeping)

TABLE III.—*MOONLAB Evolution Annual Delivery Requirements (Mass Is Given in Units of 10^3 kg)*

Item / Year	Shelters, farm and life support	Water	Power	Atmosphere	Off-loading and lunar transportation	Food	Science equipment	Miscellaneous	Total*
6.....	16	**	**	**	10	**	2.4		28.4
7.....		4	.6	2.8		0.8		.3	8.5
8.....	8	5	3.6	2.8		1.0		.6	21.0
9.....		8	1.2	4.4	5	1.6		.3	20.5
10.....		8	1.2	4.4		1.6		.3	15.5
11.....	18	8	7.2	4.4		2.8		1.2	41.6
12.....	16	8	2.4	3.6		3.2	2.8	1.2	37.2
13.....	10	2	7.8	3.6	11.6	3.6		.9	39.5
14.....	31	2	7.3	4.4		4.8	14	.3	63.8

*Included in first shelter.
**Payload constraints enforce early delivery of cargo.

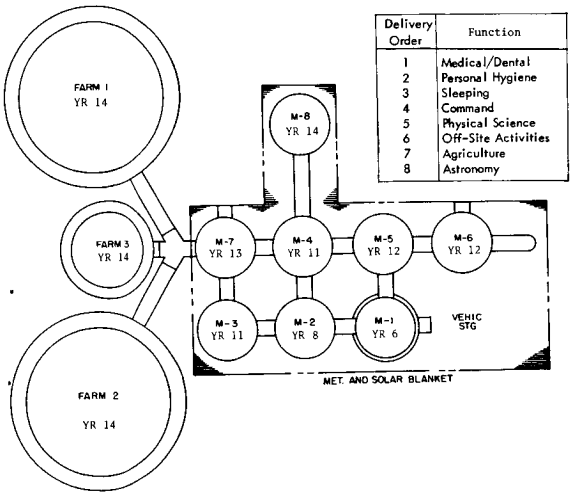

FIGURE 1.—Base evolution.

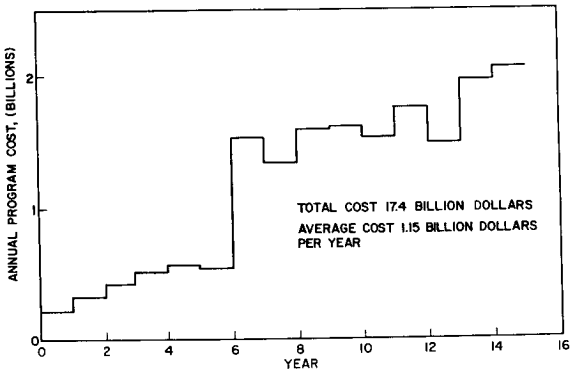

FIGURE 2.—MOONLAB funding schedule.

(2) Normal activity "flow" routines designed into adjacent canisters (e.g., sleeping, personal hygiene, eating)

(3) Provision for a continuum of social activity (individual quarters in M–3 to 24-man group meetings in dining/conference area M–4) and for individual and group recreation

(4) Work stations radiating out from the central command station

(5) Location of primary water storage (M–2) adjacent to the maximum security habitat (M–1)

(6) Emergency air locks to and from every shelter. Emergency monitoring of all shelters for air pressure fluctuations. Techniques of locating personnel and diagnosing their physical condition. Protection against sudden decompression, fire, explosion, and radiation, and provisions for search and rescue outside of the base.

The habitat, or base module, for all base operations is the space canister used to carry cargo and men to the Moon. This decision was made after a tradeoff between various methods of building shelters from lunar material, designing erectible shelters, utilizing lunar geological features, and operating without shelter. The first canister delivered (M–1) is to contain life-support and science equipment and facilities to accommodate three to six men. This structure is to be covered with lunar soil to a minimum depth of 1 meter in order to minimize micrometeorite and radiation damage. As other canisters are added, changes in module function will occur. For instance, by the fifteenth year, module M–1 is to be the bioscience laboratory, hospital, and maximum security habitat. However, functional changes have been selected so that minimal effort will be required for modification.

The principal parameters and/or constraints encountered in the design of the lunar shelter modules included internal pressure, temperature extremes, protection against ionizing radiation and meteoroid impacts, the dynamic structural loading of launch and landing, and the man-hour construction load on the lunar surface. These factors interacted directly with weight, size, and cost.

The base as designed consists of eight habitat/work-area modules connected by short tunnels of inflatable rigidized material. The modules are to be completely prefabricated on Earth and configured to fit atop a standard, direct landing lunar descent stage. Raceways in the tunnel floors will house plumbing, power, and gas ducting. Deployed over the eight-module cluster will be a flat shield, acting both as a meteoroid bumper and a heat moderator. Figure 3 shows the base configuration.

POWER AND COMMUNICATION

The power subsystem selected for the MOONLAB supplies electrical energy directly from solar cells during the lunar day. During the lunar night, electrical energy is produced from fuel cells. Hydrogen and oxygen for fuel cells are

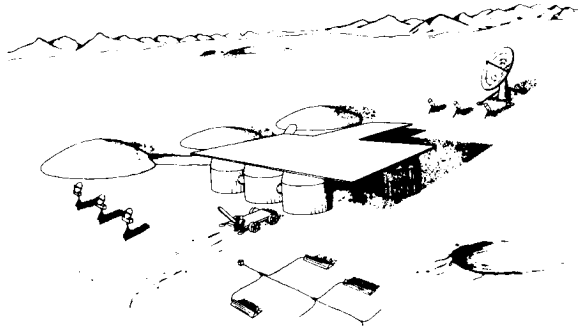

FIGURE 3.—MOONLAB.

obtained from electrolysis of water during the lunar day with cryogenic storage. Electrical power for electrolysis is supplied from the solar cells.

The power subsystem choice was influenced by the assumptions that (1) large quantities of fuel for Radioisotope Thermoelectric Generators (RTG) will not be available and (2) the useful life of a SNAP–8 reactor system at full power is approximately 1 year. If either of the above conditions were changed significantly, the power subsystem choice might be altered.

This is the least expensive of the five systems considered and has other inherent advantages:

(1) It is highly modular and can be supplied in units of virtually any size desired.

(2) Redundancy is readily achieved by adding units or by accepting a lower availability of power in event of failure of part of the system.

(3) Expansion of the system for additional power or for electrolyzing water to provide fuel for mobile vehicles of Earth return is readily achieved.

(4) Buildup of the system on the Moon is simple since components can be packaged in nearly any size desired and can be carried on any launch.

(5) There is no problem of radiation, thus allowing convenient location of the system relative to shelters.

(6) A peak power of 225 kW is possible if all electrolysis is shut off.

Fuel cells for the power system will be available from the navigational packages on the landing vehicles. Each vehicle has two cells, each of 2-kW capacity. With 40 or more landing vehicles, there will be more than enough fuel cell capacity, including replacement as necessary. There will also be ample cryogenic tankage that can be salvaged from landing vehicles. Fuel cells, tanks, and vehicles should be designed with this future use in mind.

The base proper will require 50 kW (electrical) during the lunar day and 40 kW during the lunar night. This does not include power for electrolysis of water to supply fuel for mobile vehicles or for return to Earth. Specific requirements are shown in table IV. Subsystem characteristics are shown in table V.

TABLE IV.—*MOONLAB Power Requirements*

System	Power (kW)
Lunar day	
Atmosphere circulation	5
Lighting	10
Heat rejection (living-working space and farm)	6
Water pumping (farm)	1
Harvesting and food processing	1
Waste processing	1
Communications	3
Experiments	15
Miscellaneous and contingency	8
Total	50
*Lunar night**	
Emergency life support	25
Lighting	4
Heating	10
Communications	1
Total	40

*Requirements determined by emergency conditions in the event of loss of the farm.

TABLE V.—*MOONLAB Power System**

Development cost	$110 million
Hardware cost	$115 million
System mass	21 500 kg
Deployment time	200 man-hr
Annual replacement rate	20 percent

*The cost of electrolyzing 2000 kg of water per year will be 3.16 M$.

Figure 4 shows modes of communication provided on the lunar surface. Because of the diverse nature of the MOONLAB mission, the communication subsystem design necessarily included a large amount of flexibility. Lunar equipment must be adaptable to changing needs of investigators. A new Earth-based network is required consisting of three ground stations spaced approximately equally around the Earth.

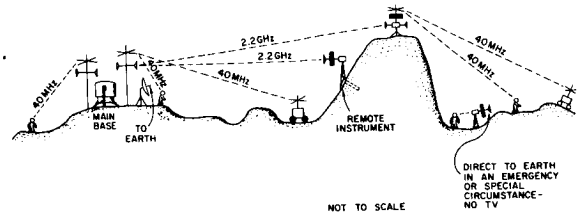

FIGURE 4.—Modes of communications on the lunar surface.

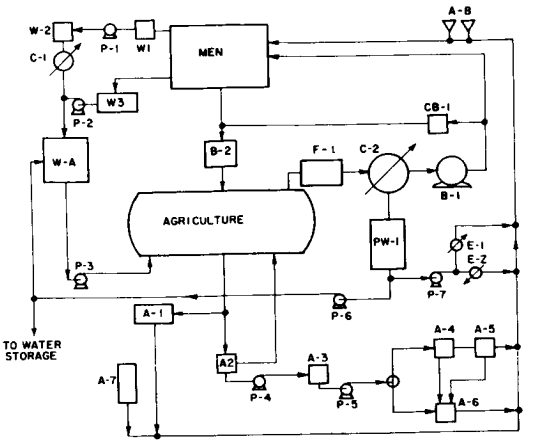

A-1 Freezer
A-2 Crusher
A-3 Cooker
A-4 Coagulum Washer
A-5 Dryer
A-6 Serum Freezer
A-7 Stored Food
A-8 Flavors
B-1 Circulation Fans
B-2 Adsorption System
C-1 Condenser
C-2 Dehumidifier
CB-1 Contaminant Removal
E-1 Water Cooler
E-2 Water Heater
F-1 Filter Sterilizer
P-1 Feces Pump
P-2 Urine Pump
P-3 Dilute Urine Pump
P-4 Juice Pump
P-5 Cooked Juice Pump
P-6 Water Recycle Pump
P-7 Potable Water Pump
PW-1 Potable Water Storage
W-1 Feces Storage
W-2 Feces Dryer
W-3 Urine Storage & Sterilization
W-4 Dilute Urine Storage

FIGURE 5.—MOONLAB life-support system.

LIFE SUPPORT

The life support subsystem for MOONLAB is unique for several reasons:

(1) It uses higher agriculture to both close the O_2–CO_2 cycle and to provide food.

(2) Because higher plants are used, man's waste products are almost completely used efficiently.

(3) By careful choice of crops, it is possible to operate with a minimum of mechanical equipment. Fundamentally only a fan and a dehumidifier are needed.

(4) A large fraction (75 percent) of the total food available is in a relatively fresh and aesthetic form.

(5) Resupply from Earth is greatly reduced.

(6) Water purification is greatly simplified, and as a consequence more water for washing and laundry is available because of the multiple use.

Some idea of the interrelationships in the life-support system can be seen in figure 5. A material balance is shown in figure 6. During the lunar night the agriculture is dormant and shelter air is bypassed through an absorber bed to keep the CO_2 from exceeding 1.5 percent during the lunar night. The CO_2 is then desorbed into the agriculture during the lunar day. A backup system requiring standby electrical power is available if the agricultural system should fail.

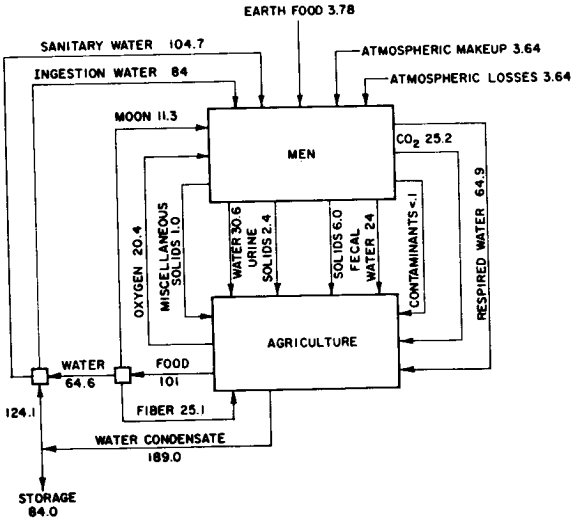

FIGURE 6.—Material balance relationships (kg/day).

Atmospheric leakage from the shelter will be principally due to air lock operation. Assuming that air locks will bound the tunnels and that there may be as many as three openings per day, losses have been calculated as 10 percent of a tunnel volume per day per opening. Farm leakage is based on probability of three punctures per year of meteorites 1.5 mm in diameter, and the

loss of one shelter volume (18 m shelters) at each hit before repair can be made.

During the base evolution all food will be from Earth-supplied stores. The diet will be 2800 k-cal with roughly 12-percent protein. As the agriculture develops, harvest of crops will begin to contribute to the diet. On the basis of 0.63 kg/day/man of dried food, the 24-man base will require 15.1 kg/day or k, 520 kg/yr. This relatively small weight makes it feasible to keep a year's supply of food on hand as backup for possible agricultural failure.

The MOONLAB water requirements are quite extensive, because of initial requirements for charging the farm and the necessity for an inventory for fire protection. Once the base reaches steady-state operation, a surplus of some 5000 kg will be produced each year due to metabolism by the farms and by the crew. This surplus will be electrolyzed to H_2 and O_2 for fuel and breathing air. However, during the evolutionary phase some 45 000 kg of water must be brought to MOONLAB.

Waste is to be disposed of by feeding it to the farm, in various forms. During construction, and if the farm is temporarily out of operation, waste will be disposed of by more conventional means. An electrodyalysis system will be used for urine reclamation and solid wastes will be heat-dried, sterilized, and stored.

THE LUNAR FARM

The reasons for developing MOONLAB agriculture are as follows:

(1) The MOONLAB farm provides the basis for a pleasant, expandable permanent colony on the Moon, and is also economically justifiable. For 75-percent food recycle, about 2 years at a base level of 24 men justifies the weight of the farm over the weight of required imported food and a CO_2 removal system.

(2) A system may be developed for maximum photosynthesis with minimum space and labor requirements.

(3) New plant forms, new genetic makeup, and new soils by exposure to unusual light, hard radiation, gravity, magnetism, and atmospheric composition may be developed. Useful plants produced in such an environment may produce seeds which are advantageous elsewhere.

(4) Crop adaptation and exploitation methods on the Moon may provide means for unlimited colonization without dependence on Earth.

(5) Moon farming may yield knowledge and techniques which can be applied on Mars without the need for shelters. Mars farming could lead to eventual conversion of the entire planet to useful purposes.

Several farm units are provided for safety and for variation in growing conditions. Figure 7 shows a plan view of a typical farm unit.

One 18 m diameter farm unit will be programmed for perennials, one 18 m diameter unit for annuals and diannuals, one 10 m diameter unit for vegetable crops, and one 6 m diameter agrilab for new work in hydroponics and tissue culture. The total farm area for a 24-man MOONLAB was calculated to be 500 m^2 ($\frac{1}{8}$ acre).

Figure 8 shows the layout of the farm and the

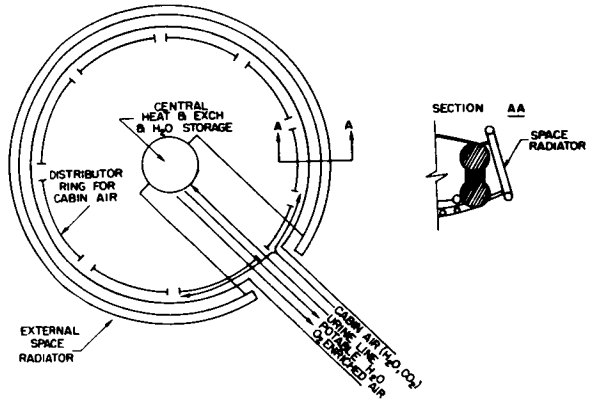

FIGURE 7.—Plan view of typical farm unit.

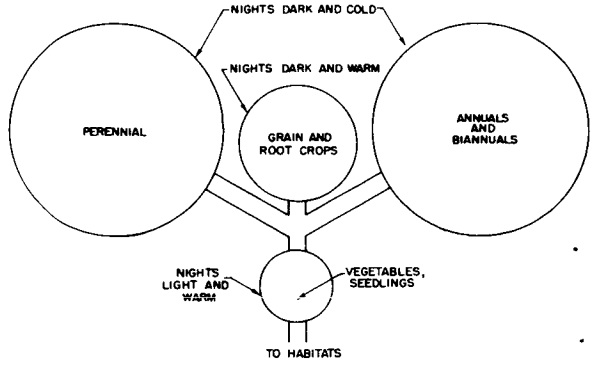

FIGURE 8.—Farm layout.

nighttime environment. Leaf crops will be removed from the 18 m farms at dusk. Highly reflective shades will be deployed over all windows to minimize heat loss at night.

Soil conditioning must be considered as a primary factor in designing the farm. Moon soil must be made from Moon dust since 160 tons are needed for the total farm assuming a 10-inch soil depth. Soil will be loaded before putting the window in place. Aggregate will be loaded first, followed by finer material. The soil will be watered by coarse sprays and drained into a sump. Water holdup of the entire farm in the soil will be 8000 kg.

The floor of each farm unit will consist of a sloping, gastight pan of high-density plastic placed on properly contoured Moon dust. Tables VI and VII summarize various characteristics of the agriculture complex. Figure 9 shows a cross section of one of the farm units.

Possible annual and biannual leafy crops included in the farm are rye, swiss chard, endive, lettuce, and Chinese cabbage. Other plants of interest are tomatoes, peas, beans, sweet potatoes, peanuts, and alfalfa. The various foods to be processed are leaves, cereals, root crops, vegetables, and hydroponic crops.

Leaf processing will include harvesting, packaging, and freezing at dusk. Leaves not directly edible will be cooked with hot water, while fibrous leaves will be crushed and fiber pressed out for return to the soil. The serum will be frozen for direct consumption if palatable, and unpalatable serum will be boiled to coagulate protein, which will be pressed out and dried. A safe scheme for removing leaf serum taste should be found as soon as possible.

TABLE VII.—*Life Support System—Agriculture Peak Power Requirements*

Item	kW	Mass
Feces dryer	0.22	10.0
Water heater	0.08	1.0
Agriculture machinery	4.0	100.0
Wash water system	0.50	12.0
Air circulation	3.8	320.0
Pumps at 0.093 kW each*	1.6	20.0
Lighting, UV sterilizers, adsorber	10.0	800.0
Total	20.2	1263.0

*Includes agriculture processing pumps.

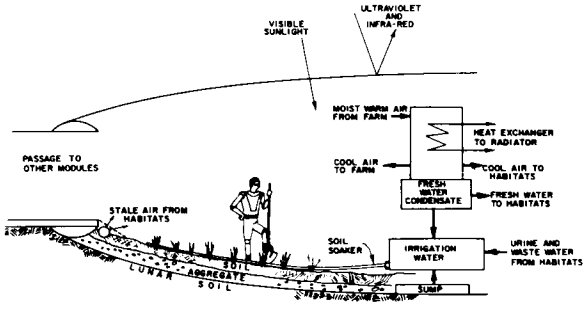

FIGURE 9.—Cross section of a farm unit.

TABLE VI.—*Characteristics of the Agricultural Complex*

Item	18m	18m	10m	6m	Total
Window area	250 m^2	250 m^2	75 m^2	25 m^2	600 m^2
Enclosed volume	800 m^3	800 m^3	450 m^3	50 m^3	2100 m^3
Window mass	370 kg	370 kg	110 kg	37 kg	900 kg
Floor mass	1000 kg	1000 kg	300 kg	.....	2300 kg
Beam mass number	1400 kg	1400 kg	800 kg	.....	3600 kg
Total structure	2800 kg	2800 kg	1200 kg	40 kg	6800 kg
Night power	0	0	2 kW	2 kW	4 kW
Soil mass	65 tons	65 tons	25 tons	5 tons	160 tons
Soil moisture	2000 kg	3000 kg	1200 kg	300 kg	7500 kg
Maximum biomass					10 000 kg
Total plant dry matter					1000 kg
Nitrogen in biomass					200 kg

Root crops and vegetables will be eaten after the usual preparation, and cereals will be boiled or dried and malted to improve taste. Hydroponic crops will be eaten as is or dried during the day, since dusk harvesting is not needed in this case. Tomatoes will be consumed immediately, and sweet potatoes will not need preservation.

CONCLUDING COMMENTS

The MOONLAB study, insofar as possible, was a complete system study. It included detailed considerations of scientific mission activities, experiments and equipment, personnel selection, training and organization, structural and thermal design, emergency procedures and backup subsystems, mobility, lunar resources exploitation, and post-evolution logistics. It is not possible to go into all of these considerations in this paper; interested readers may refer to reference 2 for the complete study results.

REFERENCES

1. ANON.: Improved Lunar Cargo and Personnel Delivery System. LMSC Report 7-28-64-4, June 28, 1968.
2. ANON.: MOONLAB. Final Report of Stanford University-Ames Research Center Summer Faculty Program in Engineering Systems Design, NASA Contract NSR 05-020-151, 1968.

PAUL R. MILLER
Office of Advanced Research and Technology, NASA
Washington, D.C.

High-Power, Long-Life Electrical Generating Systems for Lunar Base Missions

Large lunar bases will require high-power, long-life electrical power systems to provide power for sustaining mission personnel and accomplishing mission objectives. Nuclear and solar cell systems are potential power system candidates. This chapter presents an updated comparison of the primary performance characteristics of these two system types. The effects of possible lunar base mission constraints and requirements identified from previous studies on these characteristics are then reviewed.

INTRODUCTION

A large lunar base is a potential future NASA mission. Such a base will require electrical power in the tens of kilowatts for years. This chapter presents projected performance characteristics for several candidate base power systems that could be made available for this mission in the time frame of the mid- to late 1970's.

A variety of power systems could conceivably meet base power needs. This chapter, however, will be limited to those systems that develop most readily from power technology programs now in progress. This approach gives the greatest credence to system projections.

Studies of lunar base power systems have shown that mission factors can have a major impact on their design and configuration and hence on their eventual capabilities. A review is made of the more significant factors identified to date and their potential effects are discussed.

DESCRIPTION OF POWER SYSTEMS

The on-going NASA and AEC technology programs can potentially lead to five high-power, long-life power system candidates for a lunar base mission available in the time frame of the second half of the 1970's. These are a solar cell/fuel cell/reactant regeneration system, a system using multiple isotope/Brayton units, a SNAP-8 reactor/thermoelectric system, a SNAP-8 reator/Rankine system (SNAP-8), or a SNAP-8 reactor/Brayton system. The next section projects the primary characteristics of weight and size for each of these systems adapted to the lunar base mission. These projections are based on conceptual mission designs, the major features of which are described below. In addition, a brief indication of current development status is given.

It is believed that with adequate future funding and timely specification of mission requirements these systems can be readied for mission use in the second half of the 1970's, with the solar cell/fuel cell/reactant regeneration system and the isotope/Brayton system available earlier in this time period than the SNAP-8 reactor systems.

Solar Cell/Fuel Cell/Reactant Regeneration System

This system uses solar cells to provide base power during the lunar day and to provide power needed to regenerate fuel cell reactants. The regenerated reactants are then used in fuel cells to provide base power during the lunar night. This makes the system self-regenerating and there is no net consumption of expendables. Boretz and Miller (ref. 1) give a more detailed de-

382-451 OL-70-2

scription. Figure 1 illustrates the deployment of a 22.5-kW system on the lunar surface. Although general technology programs in the area of solar arrays and fuel cells are continuing, there is no specific program at this time aimed at developing the total technology for this system.

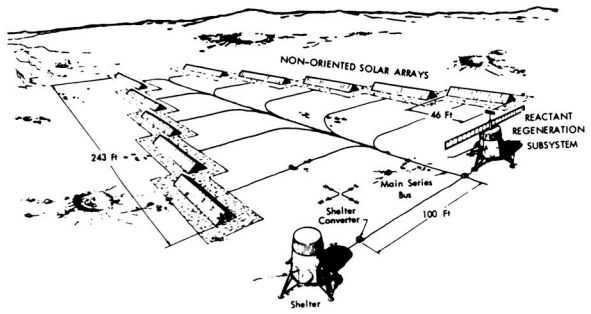

FIGURE 1.—22.5 kWe solar cell/fuel cell/reactant regeneration system.

System projections are based on non-oriented solar array capabilities (ref. 2), fuel cell capabilities (ref. 3), and reactant regeneration subsystem capabilities (ref. 4). It is assumed that equal power is to be supplied through the lunar day/night cycle and that the regenerated reactants will be liquefied. Redundancy is provided for in the key components of the regeneration subsystem, and a 20-percent overgenerating capacity is included in the solar arrays and in the fuel cell subsystem.

Isotope/Brayton System

NASA is developing the ^{238}Pu fueled isotope/Brayton system for use in a 2- to 10-kWe range. Basic fuel capsule work is being performed by AEC and the Brayton conversion system is being developed by NASA. The combined Brayton rotating unit has now been tested hot for about 600 hours. An electrically heated system test at 6-kWe output is expected to begin very shortly at the Lewis Research Center.

System projections are based on results from a study of this system in a space station mission (ref. 5). The system uses a single heat source coupled to two power conversion systems, each of which is capable of delivering rated power. Weight estimates include provisions for an intact reentry vehicle to provide for safe atmosphere reentry of the fuel in case of an abort and shielding to permit location of the power system immediately adjacent to the base.

Figure 2 illustrates an 8-kWe isotope/Brayton system off-loaded onto the lunar surface. Multiple isotope/Brayton units can be ganged together for higher power applications as illustrated in figure 3.

SNAP-8/Rankine System

The SNAP-8/Rankine system uses the NaK cooled, 600-kW_t/1300° F SNAP-8 reactor now in development by AEC, and the mercury/Rankine (SNAP-8) power conversion system now

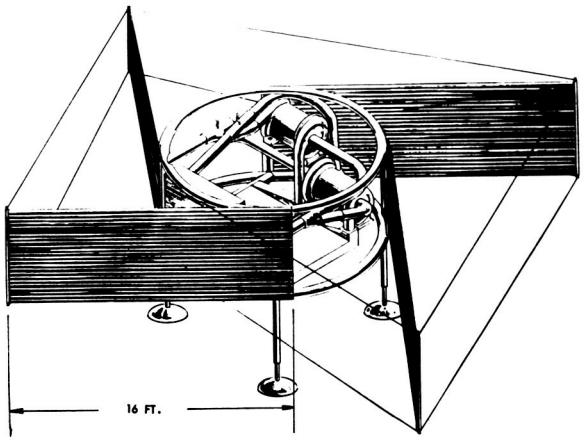

FIGURE 2.—8 kWe off-loaded isotope/Brayton system.

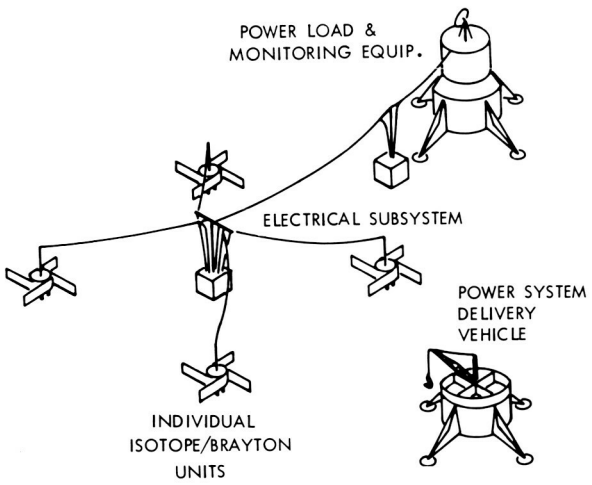

FIGURE 3.—Multiple isotope/Brayton system.

under development by NASA. Power conversion system endurance testing has reached 4500 hours and component run times from 6000 to 17 000 hours have been demonstrated to date. NASA is now working toward a test of the power conversion system coupled to the reactor. Nuclear test operations are expected to begin in 1973.

System projections are based on updating results from a study of SNAP–8 systems in the lunar mission (ref. 6). A single reactor is coupled to two power conversion systems, each capable of delivering rated power. The approach to system redundancy is illustrated in figure 4. This same basic approach to redundancy is also used in the previously discussed isotope/Brayton and in the SNAP–8/Brayton system to be described.

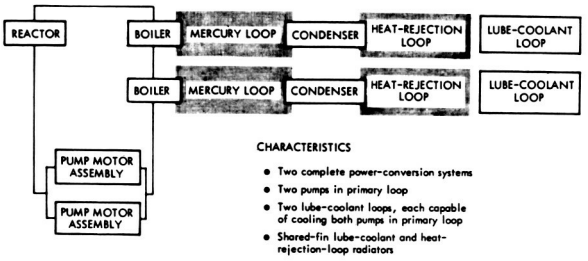

FIGURE 4. – Rankine system redundancy.

System weights are projected for two reactor shielding configurations. In one, all required shielding is earth-fabricated and transported with the system to the lunar surface. To save shield weight for this case, the power system is separated from the base by 0.5 to 1 mile. This gives a shield weight of about 14 000 pounds. Figure 5 illustrates this configuration; here the power system remains mounted on its landing vehicle for power operation.

In the second configuration, use is made of lunar "dirt" to supplement shielding, thus reducing the transported shield weight by about 10 000 pounds. Studies have shown this to be feasible if the lunar "dirt" can be compacted and large voids avoided. One method for using lunar dirt for shielding is to off-load the power system from its landing vehicle and bury the reactor beneath the lunar surface (fig. 6).

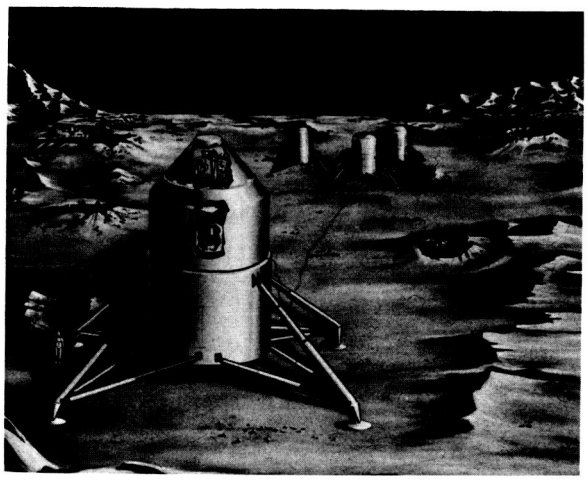

FIGURE 5. – 35 kWe Rankine system, landing vehicle mounted arrangement.

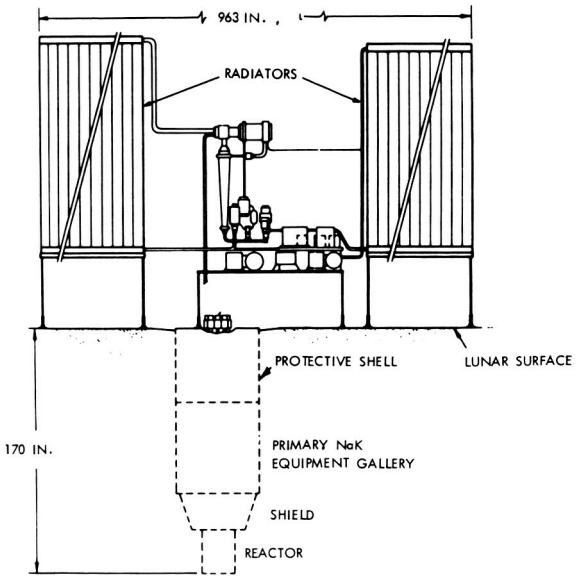

FIGURE 6. – 35 kWe Rankine system, off-loaded arrangement.

SNAP–8/Thermoelectric System

The SNAP–8/thermoelectric system also uses the SNAP–8 reactor as the heat source. Direct current power is generated by multiple compact thermoelectric converters that receive their thermal energy from the reactor loop, and unused thermal energy is rejected by a NaK radiator loop, one for each converter. Thermoelectric converter technology for this system

is being developed by AEC based on the lead telluride tubular module approach.

As with the Rankine system, system projections are based on updating results from reference 6. Performance is based on a reactor outlet temperature of 1250° F. A 20-percent overgenerating capacity is included to allow for outage of a single converter loop without a sacrifice in rated power capability. System weights are given for the same two shielding configurations described for the SNAP–8/Rankine system.

Development testing of individual thermoelectric modules has been underway for several years. Testing of multiple module converters using flowing NaK for heat transport is expected to begin late this year to be followed by test of a 6-kWe power conversion loop in 1971.

SNAP–8/Brayton System

NASA has conducted conceptual studies of the use, with the SNAP–8 reactor, of a Brayton power conversion system based on technology to be gained from the isotope/Brayton system. Because low heat-rejection temperatures can be easily accommodated with a gas conversion loop, efficiencies of up to 20 percent are possible. This extends the potential electrical power available from a single 600-kW_t reactor to over 100 kWe. There is no direct development underway on a conversion system, and no system designs have been engineered. Since this system can build on the conversion technology from the isotope/Brayton program, implementation of development program can wait several years if a flight availability date at the end of the 1970's is acceptable.

System projections are based on conceptual system analyses performed by Lewis Research Center and assume, as with SNAP–8/Rankine, a single reactor coupled with two independent power conversion systems, each capable of providing rated power. Weights are given for the same two shielding configurations discussed previously for the SNAP–8/Rankine and SNAP–8/thermoelectric systems.

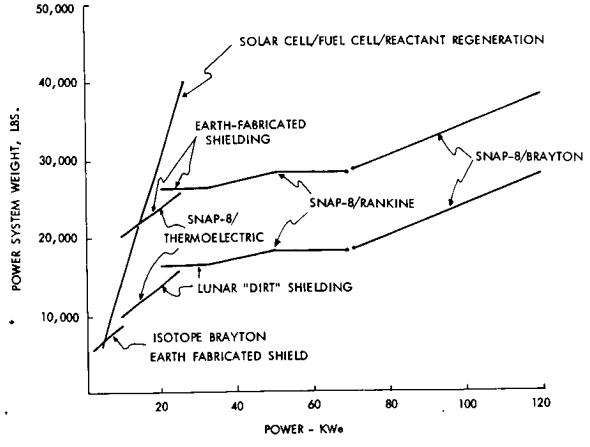

FIGURE 7. – Projected power system weight versus power.

POWER SYSTEM PRIMARY CHARACTERISTICS

Projected weights for the appropriate range of power level are given in figure 7 for each of the five power systems described above. These projections are subject to revision, however, as future development results indicate are necessary, or as lunar mission requirements become more definitive.

All the SNAP–8 system projections are based on the use of a 600-kW_t reactor regardless of electrical power level. The isotope/Brayton system projections are also based on the use of a heat source sized as necessary for the electrical output power indicated. The 10-kW power limit results from limitations in current conversion system hardware. Future improved hardware may raise the system power limit to about 15 kWe.

The significant results from figure 7 are that, for the conceptual systems projected, reactor systems are superior in weight to the solar cell/fuel cell/reactant regeneration systems at power levels above 10 to 20 kWe, and that multiple isotope/Brayton units ganged together as a single system are competitive in weight with the reactor systems for power levels up to 30 to 60 kW, depending on the approach taken to shield the reactor system.

Analyses of the SNAP–8/Brayton system have covered the power range down to 25 kWe. Weights for this system below 70 kW are not shown on figure 7 because they are approximated by Rankine system weights.

Table I summarizes the estimated logistics

TABLE I.—*Projected Lunar Logistic Payload Capabilities*

Launch vehicle/logistic landing vehicle	Landed payload
Current Saturn V using lunar module derivatives	Up to 10 000 lbs
Improved Saturn V using advanced, cryogenic landing vehicle	Up to 35 000 lbs
Major upgraded Saturn V using advanced, cryogenic landing vehicle	Up to 50 000 lbs

payload that could be delivered to the lunar surface, using three combinations of launch and logistic landing vehicles; except for the current Saturn V, all are unapproved future vehicles. Estimates are based on data from references 7 and 8.

Comparing the projected power system weights from figure 7 with the estimated landed payload capabilities of table I shows that only relative low power solar cell/fuel cell/reactant regeneration systems or the isotope/Brayton systems can be delivered with lunar module derivatives. An advanced logistics landing vehicle is required if a power system with an output of more than 10 kWe is to be landed by a single Saturn V launch.

The projection of SNAP–8/Rankine weights in figure 7 show nearly constant weight over the range of 25 to 70 kW. The Rankine (SNAP–8) power conversion system is currently aimed at a 35-kWe power level. Potentially available improvements in performance of key components (ref. 9) indicate that this power level can be doubled with only a modest weight increase and without requiring a larger reactor. For less than 35 kWe, the 35-kW power conversion system would be derated with essentially no weight saving credited.

The use of multiple isotope/Brayton systems to achieve high power appears to be an attractive alternative to the use of a reactor power system. However, there is a limit, not clearly definable at this time, as to how much ^{238}Pu fuel and, consequently, power will be available for the lunar mission because of its limited supply and because of potential needs for other missions. The use of other isotopes, which would require heavier shielding, cannot be ruled out, but presently no consideration is being given to this.

As apparent from the proceeding discussion on development status, only a nominal amount of test data are presently available for predicting the lifetime of any of the five projected lunar power systems. It is also apparent that projections of eventual system life at this time for any system are largely conjectural. However, both NASA and AEC recognize the importance of developing long life, and this aspect is receiving major development emphasis. It is believed that useful operating lifetimes of 2 to 3 years can be made available for any of these five systems by mission use time.

Power system dimensional requirements are another primary characteristic of importance, which strongly influence mission adaptation and can influence configuration design for transportation and lunar surface deployment. This aspect has been examined in a preliminary manner for the isotope/Brayton (ref. 10) and for the SNAP–8 system (ref. 6). It is apparent from these studies that, for power levels in the tens of kilowatts, the size of the heat rejection radiators is the controlling dimensional factor. Figure 8 gives the required radiator areas for each of the nuclear systems and for the reactant regeneration subsystem of the solar cell/fuel cell/reactant regeneration system. Special note should be

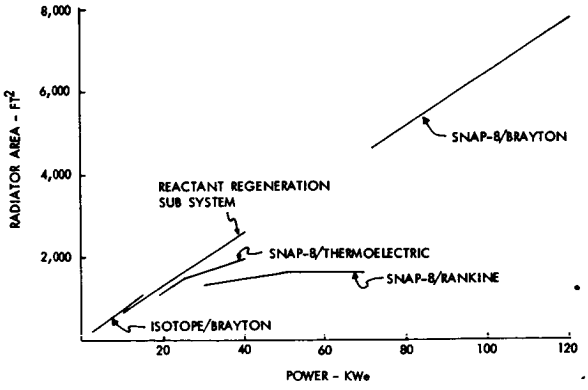

FIGURE 8.—Projected power system radiator area versus power.

made of the solar array area for this latter system which is estimated to be 1000 ft^2 for each day/night kW delivered to the base. The significance of these areas will be discussed in a subsequent section of this chapter.

The projections given in figure 7 imply that a potential lunar power capability from 5 to 120 kWe can be made available by the late 1970's. NASA and AEC are also developing the technology for even higher power systems with single heat source capabilities up to 500 kWe or more. It is estimated that these more advanced systems could be ready for mission applications by the mid-1980's if needed.

POTENTIAL IMPACT OF MISSION FACTORS

Mission factors, i.e., restraints and requirements imposed by mission-dictated considerations, have been shown in studies to have a major bearing on power system design features and configurational details and, consequently, on power system characteristics of weight and size. Undoubtedly the actual mission, when defined, will alter or add to the factors discussed below.

For some cases, a specific mission consideration can be accommodated with little or no penalty to either the power system or to the mission. In other cases, penalties may or will be involved. Where possible, those situations that could lead to an increase in system weight over that projected in figure 7 are noted.

Launch Vehicle Restraints

It may be desirable to use the surface of the payload volume above the logistic landing stage for power system heat rejection radiators. However, there will be restraints imposed on the overall launch/landing vehicle height and, consequently, on payload surface area. A principal restraint on overall height is imposed by consideration of winds aloft. This arises from consideration of structural bending moments in the overall vehicle as it achieves the point of maximum dynamic pressure and angle of attack in the launch trajectory. Wind conditions vary in intensity with months of the year and impose a probability that winds are suitable for launch. This probability also depends on overall vehicle and payload cylindrical height, assuming a conventional double cone nose shape as illustrated in figure 9.

Reference 6 indicates that the current Apollo launch criteria (95-percent probability for launch in March) applied to a Saturn V logistic launch limits total payload surface area to 1500 ft^2. By accepting a lower launch probability in March 1970, payload surface area could be increased, perhaps to 2500 ft^2. By comparing these areas with the required power system heat rejection areas given in figure 8, it can be seen that radiator deployment will be necessary for the high-power SNAP–8/Brayton systems and for the reactant regeneration subsystem of solar cell/fuel cell/reactant regeneration systems at power levels above 25 to 35 kWe.

Payload Sharing

Comparison of projected system weights in figure 7 with potential lunar logistic vehicle payload capabilities indicates that unused weight may be available for transporting other equipment or base expendables with the power system launch. The extent to which this unused weight can be effectively utilized reduces the cost of transporting the power system which is a major factor in overall cost to the mission for providing power.

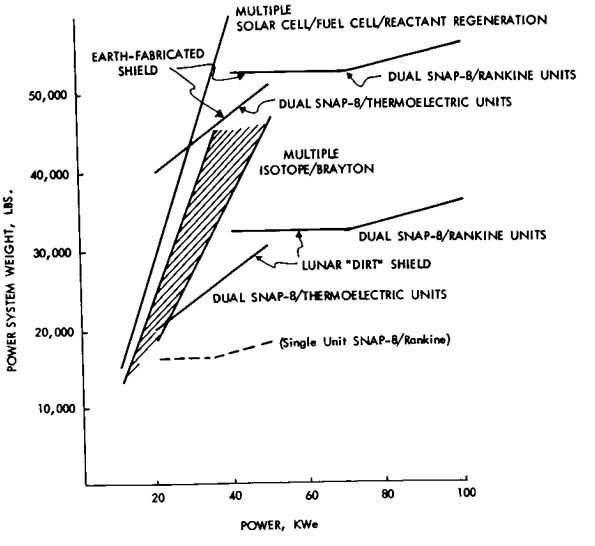

FIGURE 9.—Wind effects on Saturn V launch probability.

The degree to which payload sharing is possible depends on such factors as dimensional characteristics of the non-power cargo, the logistic logic supporting base build up, etc. Payload sharing cannot be studied until a mission model that adequately defines the influencing variables is available. It is axiomatic that this aspect can have a major bearing on whether one power system has a major advantage over another from a weight and, therefore, cost point of view.

Multiple Power Systems

Figure 7 gives the characteristics of nuclear power systems using single heat sources. At least two considerations direct attention to the use of more than one nuclear power system to meet base power needs.

The mission planner will undoubtedly want a backup power system available to supply base needs if there should be a failure in the primary power system. A review of potential power needs indicates that the backup level could be as high as 30 to 50 percent of full operational base load. One means for providing backup power is to use two or more independent power systems of the same type, which, when delivering bus bar power, meets full load needs. A failure in one system still leaves adequate power for continuance of the base until the failed system is repaired or a replacement system is delivered.

Figure 10 compares the weights of the five projected systems if multiple power systems are desired. The weight of the solar cell/fuel cell/reactant regeneration system is unchanged from figure 7 because this system can probably be modularized without a significant weight penalty. The isotope/Brayton system projection is based on the use of multiple 5- to 10-kW units. The reactor power system projections are based on the use of two independent systems, each supplying one-half of the total base power load. Weights for the individual power systems have been taken from figure 7. Two independent systems are the minimum system redundancy to meet a backup power criteria. Figure 10 shows that the weight advantage of the reactor systems is diminished if multiple systems are desired.

The second reason for considering multiple power units relates to mission approach in achieving the planned full base capability. Probably an evolutionary approach will be implemented, starting with a base camp followed by a build up to full operational capability. Power needs will then grow as base activation progresses, and the mission planner would probably prefer, from a logistics point of view, to match this growth by adding more power systems as the need arises. The choice of individual power system rating, then, depends on the desired initial and end point power levels and the rate of growth of required power. Of course, those systems that can be more easily modularized into small independent units offer greater flexibility to meet this kind of requirement.

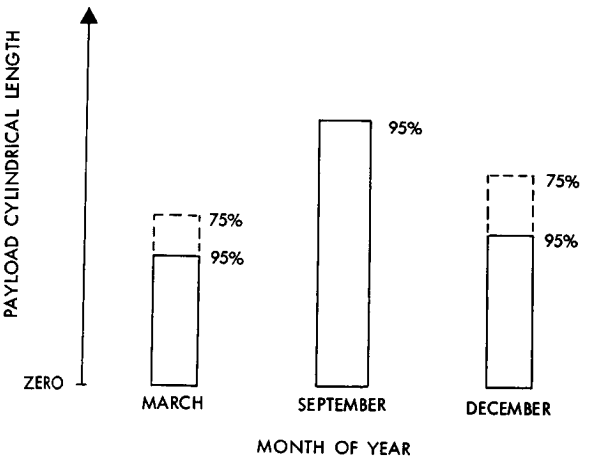

FIGURE 10.—Projected multiple power system weight versus power.

Pre-Operational Storage

References 4 and 6 suggest that a lunar base mission may require extended pre-operational, perhaps unattended, storage of the base power system. For the SNAP-8 reactor systems, reference 6 recommends that the stored power system be thermally protected from the low temperatures of the lunar night to avoid freezing of system fluids. Two possible schemes to accomplish this are suggested. One is to contain the fluids in fill and drain tanks that use isotope thermal heaters to prevent freezing. An allowance for these tanks is included in the reactor system weights of figure 7. An alternate heating scheme

is to start up the reactor following landing and bring it to low power, using reactor thermal energy to keep the plant warm. This latter approach should save weight; but, of course, it cannot be adopted if the reactor is to be buried to save shielding weight.

For the isotope/Brayton system, thermal energy is continuously available and, if not used for thermal control, it would have to be dissipated. Specific means for properly distributing this thermal energy within the individual power units have not been considered.

For the solar cell/fuel cell/reactant regeneration system, temperature limits will have to be maintained for at least the reactant regeneration subsystem during the storage period (ref. 11). Means for accomplishing this have not yet been specified.

Pre-Operational Preparations

Each of the five power systems projected will involve some degree of post-landing preparations before bus bar power is available. These preparations may impose a substantial work load on the base crew or special equipment requirements.

Figure 5 illustrated a reactor power system configuration that remains mounted on its landing vehicle for power operation. The payload surface area is used for the heat rejection radiators, and required shielding is shipped from the Earth. Greater detail is given in figure 11. Pre-operational preparations are the minimum possible, primarily involving running power lines to the station. Also, this arrangement allows system pre-launch checkout, thus giving the greatest possible confidence in successful operation following the lunar landing. The chief disadvantages of this approach are that all the necessary shielding must be shipped from Earth, and that power from the system is limited by the area available on the payload stage for heat rejection radiators. As noted in the discussion of launch vehicle restraints, the payload area for an advanced logistics landing vehicle on top of the current Saturn V is probably limited to between 1500 and 2500 ft^2. By comparing this limitation to the required heat rejection areas given in figure 8, it is seen that this mode of deployment is not available to the high power SNAP–8/Brayton systems. A major up-rating of the Saturn V, if undertaken, may influence payload area, but additional information is not available at this time.

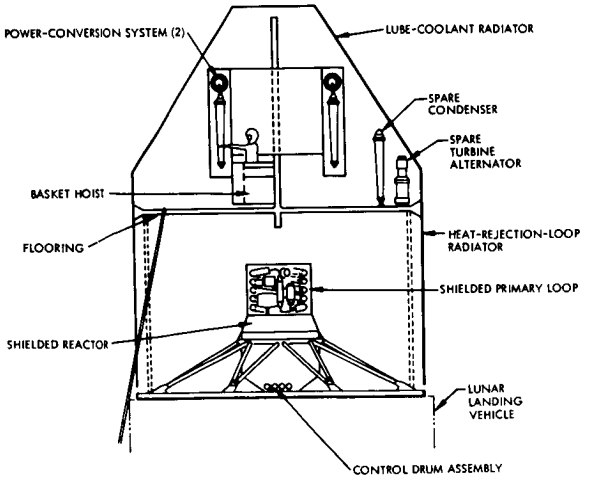

FIGURE 11.—Rankine system landing vehicle mounted configuration details.

SNAP–8 system weight projections in figure 7 indicate that a substantial weight saving can be realized if lunar "dirt" can be used to shield the reactor. A means for accomplishing this has not been reduced to an engineering design, but several conceptual approaches have been considered (ref. 6). In one approach, the power system is transported in a number of modules, all modules are off-loaded following landing, and the reactor/primary loop module is buried beneath the lunar surface. This approach was illustrated in figure 6. More detail on the buried reactor/primary loop module is shown in figure 12. The remaining modules are then placed on the surface above the reactor and interconnections, including welding of piping, are made. It was estimated that it would require three men 17 days to bring the system to operational readiness. It is apparent that savings in system weight are bought at the price of increased crew labor and perhaps the need for special skills. Other approaches, such as providing bins for lunar "dirt" around the reactor on launch, might produce a better balance of weight saving versus deployment envolvement.

Solar arrays for the solar cell/fuel cell/reactant regeneration system because of their large areas, will have to be deployed on the lunar surface to

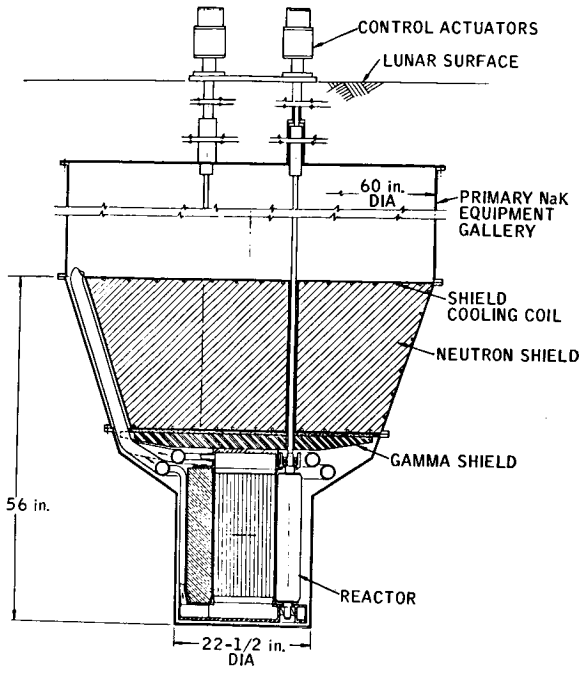

FIGURE 12. – Buried reactor details.

achieve operational readiness. This will involve, at least, off-loading of the arrays, their set up, and completion of the necessary electrical interconnections. It has been estimated that it would require three men 2.5 days to bring a 9-kWe system to operational readiness. At high power levels, it may also be necessary, as seen from the area requirements given in figure 8, to deploy radiators for the reactant regeneration subsystem. If total deployment man-hours is proportional to installed power level, it appears that the man-hours required to deploy either a high-power solar cell/fuel cell/reactant regeneration system or an off-loaded SNAP–8 system would be about the same, although setting up the solar system probably involves less complex operations.

Deployment does not appear to be a significant operations problem for a multiple isotope/Brayton system, providing means are available for moving individual off-loaded units to their final position (ref. 10), elected to off-load primarily because of radiator area considerations. After final placement on the lunar surface, it will be necessary to install isotope fuel capsules into the heat source heat blocks, to electrically interconnect the individual units, and possibly to place light-weight spectral covers on the nearby lunar surface to reduce the effective heat sink temperature during the lunar day. This later step may be necessary because of the low heat-rejection temperature of the Brayton conversion system. There appears to be no fundamental reason why off-loading could not be avoided by using the landing vehicle pay-load surface area for radiators, as suggested for the reactor power systems, if the power level limitation is acceptable.

Some of the deployment options involve movement of heavy loads from the landing vehicle to the final placement position. For example, individual isotope/Brayton units may weigh up to 9000 pounds. Data from reference 7 indicate that a self-propelled, short-distance cargo carrier will weigh approximately 1.4 times the cargo to be carried (ref. 7). Thus, if some power system deployment schemes require a larger cargo carrier than would otherwise be necessary for the mission, a substantial weight penalty could be charged to the power system.

The weight of individual units for the multiple isotope/Brayton system, at the time the off-loaded deployment mode was suggested (ref. 10), was under 3000 pounds. The higher unit weights shown in figure 7, caused primarily by nuclear safety considerations, suggest that a reexamination of preferred deployment mode is necessary because of the potential impact on mobile equipment.

Repair

As mentioned previously, power systems with a life of 2 to 3 years are expected to be available for the lunar base mission. Varying degrees of redundancy will be incorporated to increase reliability. The specific approaches to redundancy for each projected system have been described. Still the capability of effecting even minor repairs could avoid long-term power outages and extend the power system's useful life. A study on how repair of the SNAP–8/Rankine system might be effected (ref. 6) concluded that minor repairs, such as replacement of electrical and electronic components or modules, are entirely practical and that it is desirable to include means for accomplishing this in the design. However, to accomplish even minor repairs requires increased

shielding with a consequent increase in system weight. An allowance for this is included in the weights in figure 7. Major repair activities, such as replacement of fluid containing components or repair of piping leaks, were deemed feasible; however, reservations are in order about the practicality of this. Of course, repair of reactor loop malfunctions is not at all feasible because of radiation from the reactor and the activated NaK coolant. These same general conclusions would appear to apply to the SNAP–8/Brayton and thermoelectric systems as well.

Unlike the reactor systems, all major subsystems of the solar cell/fuel cell/reactant regeneration system may be modularized, including the reactant regeneration subsystem. Performance data (ref. 4) indicate that there are no significant power or weights penalties for this subsystem at regeneration rates down to an equivalent nighttime power of about 5 kWe. With total system modularization into small units, repair of major failures could be effected by module replacement.

The type of minor maintenance mentioned for the SNAP–8 could also be performed for the isotope/Brayton system, probably without incurring a significant shield weight penalty. Because heat transfer from the isotope heat source to the Brayton conversion unit is by radiation, it is feasible to replace the entire Brayton loop package. Cutting and rewelding the relatively low temperature liquid lines connecting it to the radiator would be necessary, but this does not appear to be a formidable problem. However, a specific design to accomplish this has not been engineered. Replacement of the Brayton loop package, if weight lifting and transportation means are available, appears more practical than accomplishing major maintenance on the SNAP–8 reactor systems.

Safety

Lunar mission use of nuclear systems imposes considerations of nuclear hazards to the Earth's populace and to the crew at the base. This has not been studied in depth for this mission, but some general views can be stated.

Reactor systems hazards to the general populace could result only during those phases of Earth-to-Moon transit where the reactor could return to Earth. Since the reactor will not have been operated at power prior to launch, it will not contain fission products, so the hazards to the populace do not appear to be of major concern. Analysis has indicated that should the reactor impact in water following an abort in transit, it might go critical. The consequences of this and a means for avoiding it are under study by AEC. There are no provisions included in system weight estimates for whatever protective means may be required.

Once the reactor is operated on the lunar surface, the possible consequences of radioactive fission product release need to be considered. In terrestrial applications where atmospheric, hydrological, and ecological factors can lead to wide distribution of fission products if a power accident causes loss of reactor integrity, a secondary containment vessel is used. The hazard to the lunar crew as a result of a similar accident is not clear because of absence of these factors. No allowance has been included in the projection of SNAP–8 systems weights for secondary reactor containment. Potential explosive energy released by the SNAP–8 reactor in special transient tests has been demonstrated to be small, on the order of a few tens of mW seconds. Separation of the power system from the base by a short distance should obviate this hazard.

As mentioned previously, the weights given here for isotope/Brayton system include an allowance for a reentry vehicle to provide against ^{238}Pu fuel dispersal during reentry should an abort occur during the transit phase. To further reduce potential hazards, the use of fuel with improved high temperature and impact characteristics is being investigated.

SUMMARY AND CONCLUSIONS

Weight remains the most easily discernible means for comparing the relative merits of lunar power systems. Assuming nearly equal lifetimes can be made available regardless of power system type, weight will be one of the foremost criteria for power system selection because of the high cost of Earth-to-Moon transportation. Figure 7 gives weights of lunar systems as they can be projected today. However, the discussion on

mission factors has shown that these could have a major effect on weight differences between candidate systems when real mission requirements and constraints are applied. Results from future power system development and evaluation tests could also change power system weight projections.

At higher power levels, it is apparent from figure 7 that the weight advantage of reactor power systems becomes overwhelming. However, it is concluded that, for power in the low tens of kilowatts, projected system weights are not a reliable measure of the relative merits of possible future lunar power systems. Not only might system weights that reflect the real constraints and requirements of a lunar mission differ significantly from those given in figure 7, but other criteria such as power system compatibility with overall logistic planning and desired base build-up sequence may become important in power system selection for the lunar base mission.

REFERENCES

1. BORETZ, J.; AND MILLER, J.: Large Solar Arrays for Multi-Mission Lunar Surface Exploration. Paper presented at Intersociety Energy Conversion and Engineering Conf., 1968.
2. BORING, R.: Large Surface Solar Array Characteristics. Paper presented at Intersociety Energy Conversion and Engineering Conf., 1968.
3. SCHULMAN, F.; AND SMITH, A.: Lunar Power Systems. Paper presented at the 4th Annual AIAA Meeting.
4. ANON.: Study and Design Optimization of a Water Electrolysis System. H6S–R47–68, NAS 8–21190, Space Division of Chrysler Corporation, June 1968.
5. ANON.: Study of Separately Launched Multi-Use Space Electrical Power System. GESP–7007, General Electric Missile and Space Division, Nov. 1968.
6. ANON.: Design Requirements for Reactor Power Systems for Lunar Exploration. LMSC–677879, Lockheed Missiles and Space Company, Sept. 1967.
7. ANON.: MIMOSA/Exploration Equipment Data Book. LMSC–A847943, Lockheed Missiles and Space Company, April 1967.
8. MORGAN, L.: AND JOHNSON, R.: Improved Lunar Cargo and Personnel Delivery Systems. NASA SP–177, pp. 173–191.
9. ANON.: SNAP–8 Performance Potential Study. Aerojet 3386, NASA CR–72254, April 1967.
10. ANON.: Study of an Electrical Power System for Support of a 12 Man Lunar Base. Doc. No. 67SD2006, Missile and Space Division, General Electric.
11. ANON.: Mid-Term Progress Report on Study of a Water Electrolysis System for a Lunar Base Power System. HGS–R125–68, Space Division, Chrysler Corporation, Dec. 1968.

J. H. BELL, JR.

The Boeing Company
Huntsville, Alabama

No-Loss Cryogenic Storage on the Lunar Surface

Lunar exploration and extended lunar stay requires the capability of storing oxygen and hydrogen for extended periods of time. A technique for storing these cryogens for a period of 6 months to a year is described. This theory is based on the best cryogenic information available at this time.

Under the Molab Study, Contract NAS8-20073, a study was made to determine the best method of storing propellants on the lunar surface; the results of this study are also presented. Curves were plotted for optimizing the design, and equipment layouts are presented showing designs and materials selected for best results.

INTRODUCTION

If hydrogen and oxygen could be stored on the Moon for a 6-month period without loss, the Moon geological expeditions in the 70's would prove more feasible. This study will show the possibility of such no-loss storage.

The studies conducted on the heat leak being discussed showed that it was possible to store frozen methane and hydrogen for 12-month periods in a superinsulated vessel under controlled temperature and pressure conditions (ref. 1). Calculations from a previous study under the Molab Study (Contract NAS8-20073) were used as a basis for determining optimum long-term storage of cryogens on the lunar surface. A system is described for loading and freezing the cryogens on Earth. Storage vessels filled with solid cryogens are than transported to the lunar surface for future use. The storage vessels each contain heater elements for use in expelling the cryogens on demand.

SOLID CRYOGENIC STORAGE SYSTEM CONCEPT

Description

The system would consist of a solid (solidified liquefied gas) in a superinsulated container and a low-pressure relief system for solidification of the liquid with the minimum amount of heat leak to the outside. The outer surface properties determine the surface temperature of a spherical tank on the lunar surface. Figure 1 shows the surface temperature of a sphere with various coatings located on the equatorial zone of the lunar surface (ref. 2). White paint on the lunar sphere gives the lowest absorptivity-to-emissivity ratio (α/ϵ) and hence the lowest temperature of the sphere; $\alpha = 0.2$ and $\epsilon = 0.86$; therefore, $\alpha/\epsilon = 0.232$ for the values shown in figure 1.

All cases in this study were based on the use of SI-62 superinsulation in a vacuum between the two shells of the sphere. Multilayers of aluminum foil separated by glass paper serve as the insulation. The K value for this insulation is 2.5×10^{-5} Btu/hr$-^\circ$R in the range of cryogenic temperatures when subjected to 10^{-6} Torr vacuum. This value cannot always be reached, and a degradation factor of 2 was assumed for this study. Based on the increased Δh due to freezing, freezing of the liquid oxygen can increase storability by a factor of 1.5. For hydrogen this factor is 1.38.

In a cryogenic solid, the quantity of heat that a given weight of solid cryogen can absorb is dependent on the heat of fusion and the amount of heat required to bring the mass up to super-

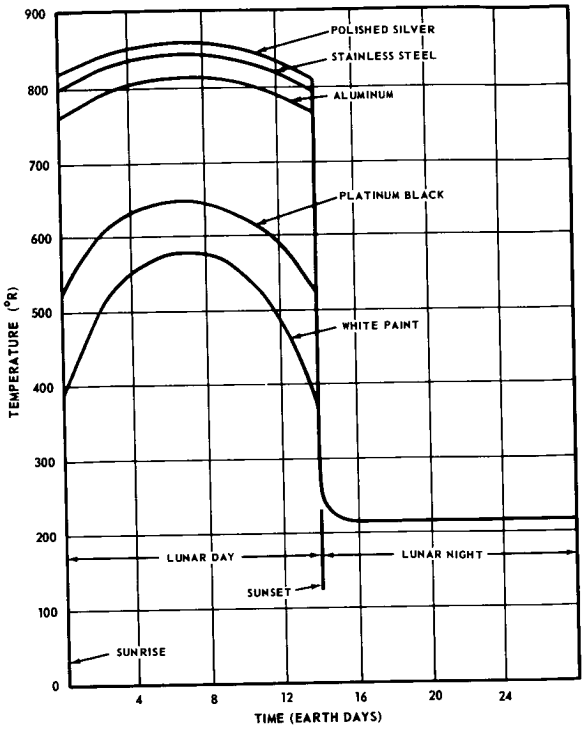

FIGURE 1.—Surface temperature of spherical object on Moon equator.

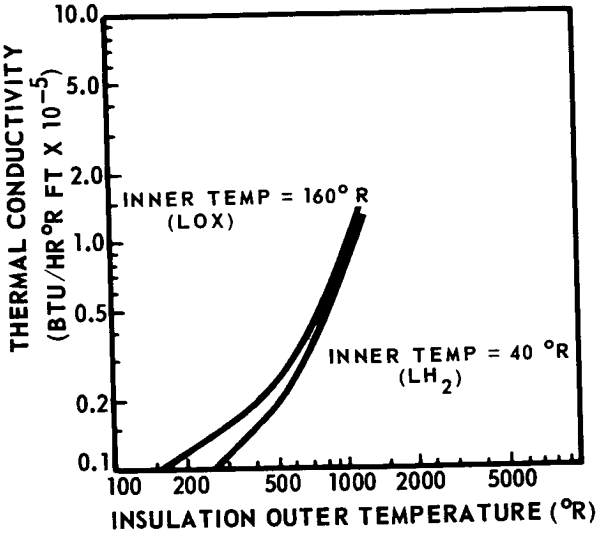

FIGURE 2.—Apparent thermal conductivity of Linde SI–62 superinsulation.

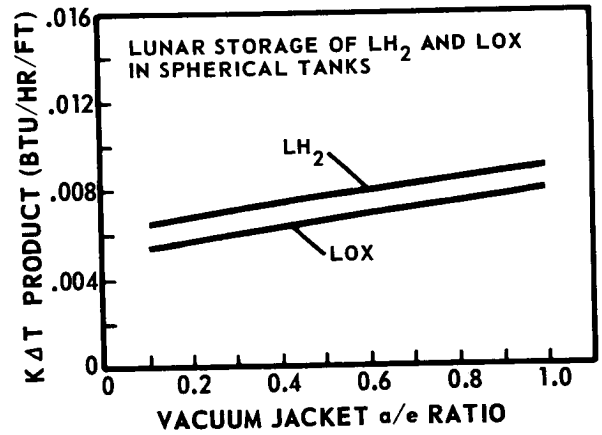

FIGURE 3.—Thermal-conductivity temperature difference product, Linde SI–62 superinsulation (ref. 3).

critical conditions, assuming heating is uniform and phase changes occur in sequence throughout the mass. When solid hydrogen at 0 Btu/lb is melted and brought to 350 psia, supercritical conditions will have 264 Btu/lb, which is the allowable heat input for the storage period on the lunar surface.

The success of the lunar storage project is based on the Linde SI–62 Insulation. The density of the insulation is 4.7 lb/cu ft, and the characteristics of this insulation are shown in figures 2 and 3. Figure 2 shows the effect of the outer and inner vessel temperatures on the thermal conductivity of the insulation; figure 3 shows the effect of the outer surface α/ϵ ratio on the thermal conductance of the insulated walls. In both cases the charts are for both lox and hydrogen, the most common cryogens needed in space and on the lunar surface. This will also require a special design to reduce the heat leakage to a minimum. The storage time depends on the quantity of the solid and the heat leak rate. Once the liquid was solidified, the vent system could be closed and sealed. Figure 4 shows the system used to fill the storage system.

Operation of the No-Loss Storage System

The cryogenic storage sphere is filled to capacity with the liquid cryogenic material, and a vacuum is then pulled on the vent system to reduce the pressure over the liquid. As the liquid vaporizes, the vapor is drawn off and the remaining liquid freezes. Table I shows the temperature and pressure range at which various cryogens solidify (ref. 1). More liquid is fed in as

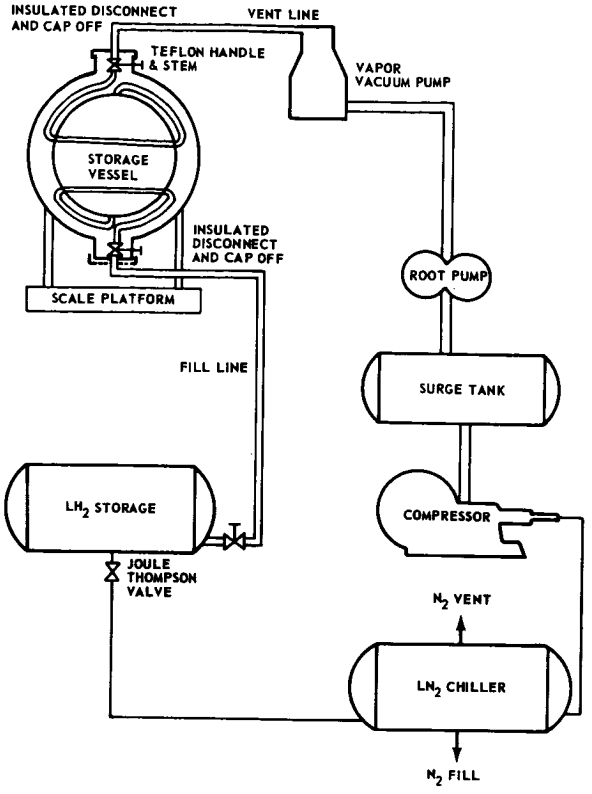

FIGURE 4.—Storage vessel filling schematic diagram.

TABLE I.—*Temperature and Pressure Ranges of Solid Coolants*

Material	Temperature range		Pressure range torr*
	°K	°R	
Methane	90 to 67	162 to 120	80 to 1
Argon	83 to 55	149 to 99	400 to 1
Carbon dioxide	68 to 51	122 to 92	10 to 1
Nitrogen	62 to 47	112 to 84	73.6 to 1
Neon	24 to 16	43 to 39	260 to 1
Hydrogen	14 to 10	25 to 18	56 to 2

*Below these pressures only a 1°-to-3° K temperature drop takes place.

the vapor is drawn off until the proper weight of required gases is in the sphere and frozen. The fill line is then closed, removed from the source, insulated, and capped off. The vent line will be the outlet line when the supercritical fluid is drawn off for use 6 to 12 months later.

In a cryogenic solid the quantity of heat that a given weight of solid can absorb is dependent on the heat of fusion and the amount of heat required to bring the mass up to supercritical conditions based on the assumptions above. For example, solid oxygen with enthalpy of 10 Btu/lb, when melted and brought to 1050 psia and to the supercritical condition, will have 120 Btu/lb for 6 months of storage. The design criteria for a 200-pound oxygen storage system then becomes 200×110, or 22 000-Btu heat leak for a 6- to 12-month period.

Tank plumbing and structural support of the inner tank play an important part in the overall operation of the system. Since support systems were kept to a minimum in each case, the support rods could be used as fill and vent lines for the inner sphere. A factor of 0.2 loss for structures was used for the computer study, but actual calculation showed this to be very low.

The thermodynamic variables are (1) the surface temperature of the outside sphere, (2) the temperature of the cryogen over the storage period from the solid (frozen) state to the liquid state and to the supercritical state, and (3) the increased temperature of the cryogen caused by the addition of heaters in spheres to drive out the residual propellants so they can be used in the lunar systems. Some of the dependent variables are the size of the sphere to hold the amount of cryogen for a definite period, the thickness of the shell to withstand the pressure, and the thickness of insulation to contain the cryogen for the required storage period.

The goal of the cryogenic study is to design a supercritical storage vessel to keep cryogenic fluids for 6 to 12 months on the equatorial zone of the Moon.

A preliminary computer study was made to determine the feasibility of such a design using state-of-the-art materials and superinsulation. The temperature and radiant energy on the lunar surface were thoroughly analyzed to determine the feasibility of the project under adverse conditions. The results of the computer study determined the appropriate thickness of insulation and the weights of the systems required and provided information for optimizing the system design based on the propellant to be stored.

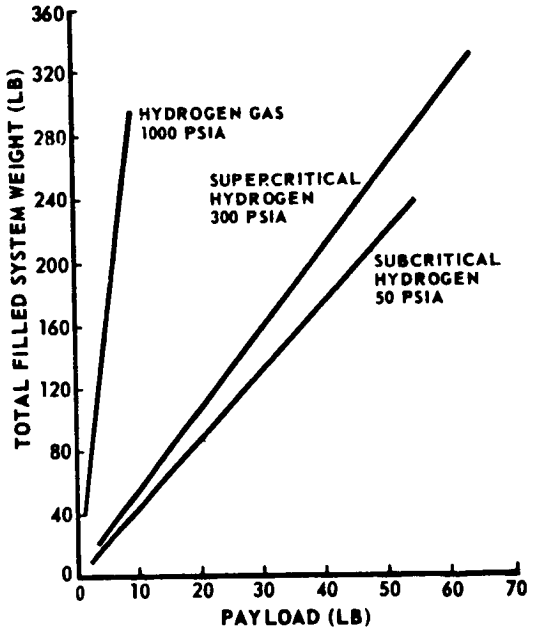

FIGURE 10.—Hydrogen system.

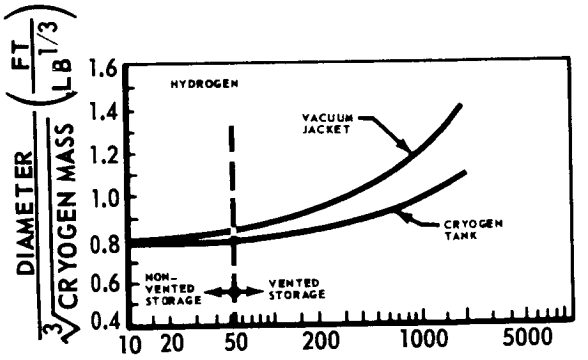

FIGURE 11.—Tank sizes of optimum LH_2 storage systems (ref. 3).

Tank sizes of optimum LH_2 storage systems are given in figure 11, and both tank and jacket sizes are based on the computer program results (ref. 3).

Figure 4—the storage vessel filling schematic diagram—is based on the conservation of cryogens. If sufficient quantities of cryogens are available, the reliquefication phase can be eliminated. Only vacuum and a supply of cryogens are needed.

Preliminary design calculations for actual systems are shown in the Appendix.

CONCLUSIONS

Small quantities of hydrogen (50 to 200 lb) and oxygen (200 to 1000 lb) can be stored for 6 to 12 months on the lunar surface if the proper materials are selected and the designs are properly made. Insulation degradation can be held at 2 for design purposes. Storage system weights increase almost linearly with the lunar mission duration. Freezing of the fluids increases the length of lunar storability by a factor of 1.5 for oxygen and a factor of 1.38 for hydrogen.

APPENDIX

Preliminary Oxygen System Design

A sphere containing 200 lb of lox with 10-percent ullage:

lox = 71.17 lb/ft^3, 200/71.17 = 2.78 cu ft + 10 percent = 3.058 cu ft

3.058 × 1728 = 5270 cu in. ($V = 4/3\ \pi r_i^3$)

$r_i = \sqrt[3]{5270/4.188} = 10.8$ in. $r_i + 3 + .25 + .125 = 3.375$

$r_o = 14.175$ in. Do − 28.35 in.

$Am = \sqrt{A_i \times A_o}$ $A = \frac{4\pi r^2}{144}$

$Am = \sqrt{10.16 \times 17.5} = 13.33$ sq ft

Use 3 inches of superinsulation.

$Q = 13.33 \times 2.5 \times 4 \times 10^{-5} \times 4400 = 5.87$ Btu/° F

with outside painted white and using figure 3 for outside temperature.

LMTD = 353° R

4400 × 353 = 1,550,000° R hr

Supercritical to solid O_2 (see figure 5 LMTD). Temperature 221 ° R.

4400 × 221 = 972,000 ° R hr

$\frac{1550{,}000 - 972{,}000\ ^\circ\text{R hr}}{4400} = 131\ ^\circ\text{R}\ \Delta t.$

5.87 × 131 = 771 Btu through the insulation in 6 months.

Connection heat leak.

2 1/2-in. aluminum tubing fill and vent 3 in. long.

2 No. 24 sensor wires copper

2 No. 24 heater wires copper

assume each 3 ft lead for copper

K = 223.5 for copper

K = 66.5 for aluminum

$$\text{Heat flow} = KA\frac{\Delta T}{L}$$

No. 24 wire

$$Q = \frac{223.5 \times .02^{-2} \times .785 \times 131 \times 4}{144 \times 3}$$

$$= 0.0852 \text{ Btu/hr}$$

1/2-in. aluminum tube Q − 66.5

$$\frac{(.5^{-2} - .37^{-2}).785 \times 131}{144 \times 3} \times 2 = 4.75 \text{ Btu/hr}$$

Total 4.8352 Btu/hr

Connection losses: $4.8352 \times 4400 = 21{,}200$ Btu in 6 months

Insulation losses: = 771 Btu in 6 months

Total 21,971 Btu in 6 months

Allowable heat leak 22,000 Btu in 6 months

From these preliminary design calculations, it appears that this system will contain 200 pounds of oxygen for 6 months with no loss due to venting.

Preliminary Hydrogen System Design

If hydrogen is to be stored on the Moon for 6 months to a year, an even better system must be designed. Storage of hydrogen for 6 months without loss is the objective of this study. A quick set of preliminary calculations will show that it is physically impractical to store hydrogen for 6 months without loss on the Moon with the oxygen type system. To store 70 pounds of hydrogen for 6 months on the Moon, the frozen hydrogen would have an enthalpy of 20 Btu/lb, while 300 psi supercritical hydrogen would have 210 Btu/lb or a net increase of 190 Btu/lb:

$70 \times 190 = 13{,}300$ Btu in 6 months storage.

One sphere containing 70 lb of hydrogen with 10-percent ullage with wall thickness to hold critical pressure.

Hydrogen − 4.43 lb/ft^3 $70/4.43 = 15.8 + 10$ percent = 17.38 cu ft

$17.38 \times 1728 = 30{,}200$ cu in. ($V = 4/3\pi r^3$)

$r_i = \sqrt[3]{30{,}000/4.188} = \sqrt[3]{7180} = 19.2$ in. r_i

Use 6-inch insulation

$+6 + .25 + .125 = 6.375$ in.

$r_o = 25.575$ in. Do = 51.15 in.

$$Am = \sqrt{Ai \times Ao} \qquad A = \frac{4\pi r^2}{144}$$

$Am = \sqrt{32.3 \times 56.9} = 42.1$ sq ft

$Q - 42.1 \times 2.5 \times 2 \times 10^{-5} \times 4400 = 9.26$ Btu/° F

with outside painted white (see figure 2).

For outside temperature LMTD = 50° R

$4400 \times 50 = 220{,}000$° R hr

$$\frac{1550{,}000 - 220{,}000}{4400} = 303\text{° R } \Delta t$$

$9.26 \times 303 = 2800$ Btu through insulation in 6 months.

Connection heat leak

2-1/2 in. Teflon tubes. Fill and vent capable of critical pressure.

2 No. 24 sensor wires

2 No. 24 heater wires

assume each lead 3 feet long

K = 223.5 for copper

K = .41 for Kel F

$$\text{Heat flow} = KA\frac{\Delta T}{L}$$

No. 24 wire

$$Q = \frac{223.5 \times .020^2 \times .785 \times 303 \times 4}{144 \times 4}$$

$$= .143 \text{ Btu/hr}$$

1/2 in. Kel F tube Q

$$= \frac{.41 \times (.5 - .37^2).785 \times 303 \times 2}{144 \times 4} = .505 \text{ in.}$$

Total 0.648 Btu/hr

Connection losses $.648 \times 4400 = 2850$ Btu in. 6 months

Insulation loss = 2800 Btu in. 6 months

Total 5650 Btu in. 6 months

Allowable leak 13,300 Btu in. 6 months

From the above preliminary calculations, it would appear that 70 pounds of frozen hydrogen can be stored on the moon for 6 months without loss if special 6-inch insulation and Teflon tubing is used for the system.

REFERENCES

1. WEINSTEIN, A. I.; FRIEDMAN, A. S.; AND GROSS, U. E.: Cooling to Cryogenic Temperatures by Sublimation. Advances in Cryogenic Engineering, Vol. IX. 1963.
2. MAKAY, J. B.: Space Power Plants. Prentice Hall Space Technology Series, 1963.
3. WILKES, S. G.; SNYDER, E. F.; AND BOBO, W. S.: Lunar Storage of Cryogenic Reactants. Proceedings of the Conference on Long-Term Cryo-propellant Storage in Space, NASA–George C. Marshall Space Flight Center, pp. 31–53, Oct. 1966.
4. STEWART, R. B.; AND JOHNSON, V. J.: A Compendium of the Properties of Materials at Low Temperatures. Phase II, National Bureau of Standards, 1961. Published as WADD TR 60–56, Part 4 A D 272769.
5. OLIVER, J. R.; AND MCCOMBS, W. M.: Lunar Storage of Small Quantities of Cryogenic Fluids. NASA–TR–4–4–42–2–D, Kennedy Space Flight Center, Jan. 1964.

GERD A. KLEINEBERG, Ph.D. and ANTHONY A. THOMAS, M.D.
Aerospace Medical Research Laboratory
Wright-Patterson Air Force Base, Ohio

Toxicological Screening of Space Cabin Materials

The advent of manned space flight initiated the demand for information concerning the effects of long-term continuous exposure to low concentrations of environmental contaminants. To control toxic contaminants in space cabins and to identify individual gas-off products, stringent material selection and analytical gas-off studies are performed. Since 1965, 278 materials have been analyzed prior to toxicological evaluation. Criteria for the screening process (TGA) and methods for detailed gas-off studies are described. The effects of reduced atmospheric pressure and oxygen-rich atmospheres on the characteristics of truly uninterrupted long-term exposure to toxic trace contaminants are also studied. A brief description of the altitude inhalation exposure facility (Thomas Domes) is given. Toxicological screening is performed by continuously exposing rats and mice to the gas-off products of candidate materials within a closed-loop life-support system which in turn is located inside a Thomas Dome. Two hundred and ninety materials have been screened for 7-day acute toxicity, and 102 materials have been studied for a 60-day duration. Results of the toxicological evaluations are discussed.

INTRODUCTION

In the beginning of manned space flight there were no experimental data available on which to base prediction of man's tolerance to trace contaminants that could be expected in a space cabin atmosphere. This was indeed the case even though the idea of sustaining men in a closed system was not particularly new or unique. The results of about 40 years of research effort by the United States Navy on the environmental control of habitable submarine atmospheres were available. These compiled data, however, were of limited value in the case of spacecraft because it was realized immediately, although the problems in the two systems are essentially alike, that environmental control problems in spacecraft will be greatly influenced by both the external and internal environments of the vehicle. All experimental data on continuous exposures that were available at that time were at ambient pressure and air environments. The spacecraft, on the other hand, had an atmosphere of 100 percent oxygen at the reduced pressure of 5 psia. These conditions presented the possibility of an undesirable pulmonary reaction and the relative certainty that such an undesirable reaction would greatly reduce man's tolerance to certain contaminants that are generated by a number of sources in a space cabin. There was also another set of data available for a variety of toxic chemicals, i.e., the industrial threshold limit values (TLV's). TLV's are concentrations that are considered to be harmless for daily 8-hour exposures, 5 days a week, for at least 30 years' duration. These values were of no help to the toxicologist in predicting the effects of continuous, truly uninterrupted exposure of men for extended periods of time to these compounds. One should then think that a "corrected" TLV (i.e., a value for a three-fold increased dose—the factor of 3 would take into account a continuous exposure as compared to 8-hour interrupted periods) would be a valuable guideline for the toxicological evaluation of contaminant levels for a space cabin atmosphere. This assumption, however, cannot be made without great restraints; and unfortunately, to further complicate the situation, the astronaut will certainly be exposed to a complex mixture of contaminants. Such a situation always carries the threat of potentiation of

toxic effects by individual constituents within the mixture. Realizing these circumstances, the toxicologist remained very skeptical about the usefulness of these numbers. This skepticism was confirmed by later experiments when animals were continuously exposed to the concentrations of the appropriate industrial TLV of a variety of chemicals. It was found that this concentration was detrimental to the health of animals in many instances,* notably hydrazine, decaborane (candidate rocket propellants) and the mixture of indole, skatole, and methyl mercaptan (end products of metabolic processes) (ref. 1). Going back to the situation as it existed in the early days of manned space flight, it was evident that there was no toxicological information available and no hardware on hand with which to gather data concerning a long-term space mission with all its implications, i.e., zero gravity, reduced pressure, 100 percent oxygen atmosphere, continuous exposure to trace contaminants, and an unfavorable volume/man ratio.

SCREENING OF SPACE CABIN MATERIALS

Consequently scientists of the Toxic Hazards Division, Aerospace Medical Research Laboratory, started work in the field of trace contaminant toxicology. For this purpose a unique inhalation exposure facility has been built with the capability to study inhalation toxicology under continuous conditions. Thus the study of the influence of low atmospheric pressure and oxygen-rich atmospheres on the characteristics of truly uninterrupted long-term exposure to toxic gases and vapors that are encountered in a space cabin became possible for the first time (fig. 1).

The facility became operational in September 1964 and consisted of four dome-shaped altitude chambers. The Thomas Domes were conceptually designed by Dr. A. A. Thomas, Director of the Toxic Hazards Division, and were engineered and installed by the Aerojet-General Corporation. Four additional domes have been added since, and the facility is currently operated by the SysteMed Corporation jointly with Air Force personnel.

Among the other sources of trace contaminants (i.e., the life-support system and man himself), the construction materials of the space cabin, especially the nonmetallic materials, are the main target for detailed investigations in an effort to control the space cabin atmosphere. Before any toxicological investigations on the candidate materials are performed, a selection based on thermogravimetric analysis (TGA) data as well as detailed gas-off studies is made to identify those candidates that can be considered seriously as constructual components for the manned portion of the spacecraft. This screening is very helpful to avoid an undue workload and to cut back on expenditures for costly toxicological evaluations.

For the initial screening, approximately 10g of a material is placed into a thermogravimetric screening apparatus (fig. 2). The weight loss of the material is continuously recorded while the temperature is programmed from ambient to 68° C over a 30-minute period. The temperature is then maintained at 68 ± 0.5° C for a maximum of 20 hours or until the weight remains constant for at least 2 hours. Over the same time period, a hygrometer probe determines the amount of water vapor given off by the material and these measurements are also continuously recorded. All TGA procedures are performed in prepurified nitrogen at 5 psia under dynamic conditions. All materials that lose more than 1.0 percent of their weight, exclusive of water, under the experimental conditions are recommended for disqualification based on engineering criteria. Materials that yield volatiles in the range from 0.001 to 1.0 percent of their weight, exclusive of water, under the described conditions are selected for further detailed gas-off studies. Figure 3 shows a typical TGA pattern of such a material. Finally materials losing less than 0.001 percent of their weight (exclusive of water) are recommended for conditional acceptance because the evolved amount of volatiles is considered of no toxicological significance. As the technology of compounding nonmetallic space cabin materials progresses, an increasing number of candidate materials that fall into this category is received

*The concentration caused nearly 100-percent mortality in some cases.

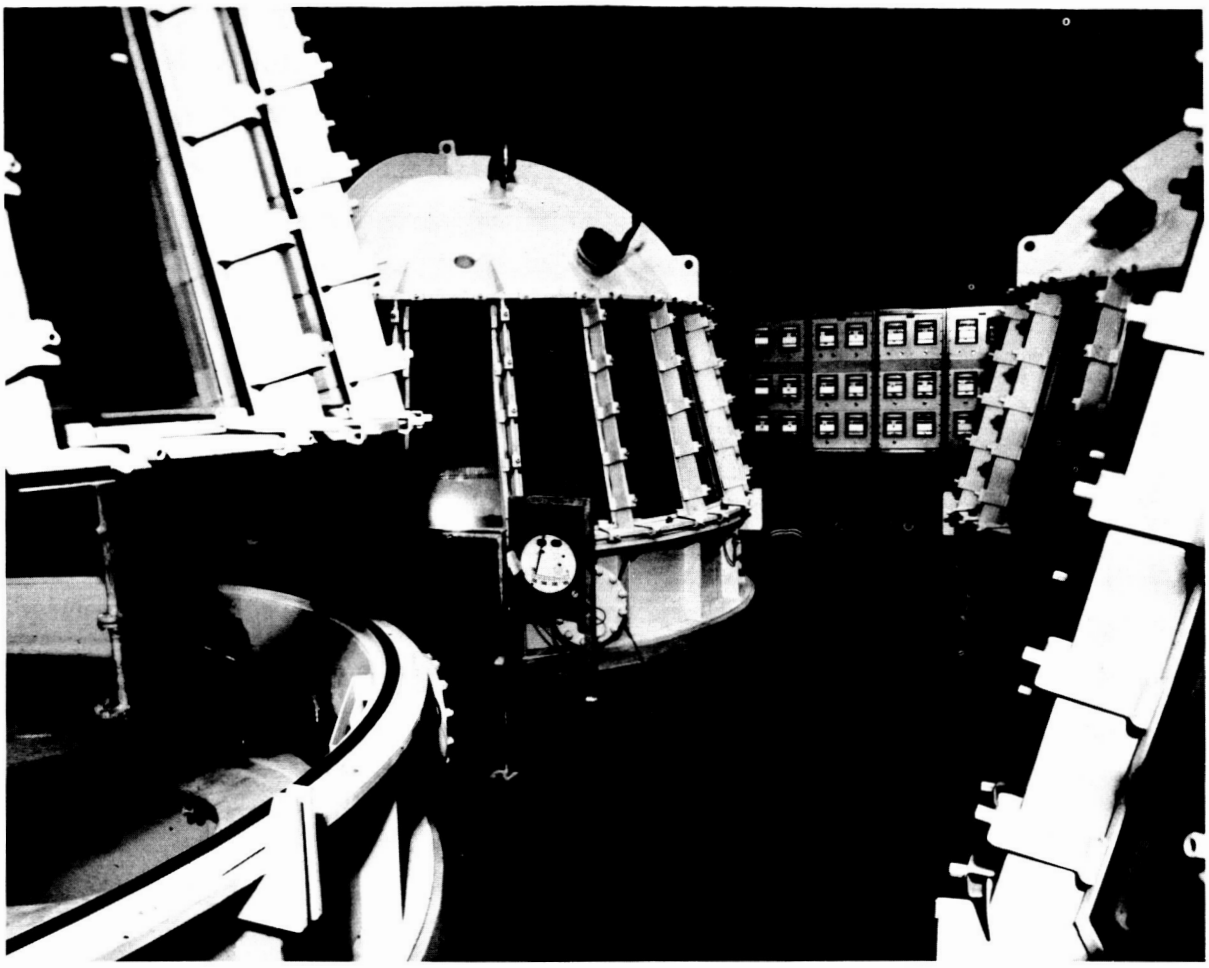

FIGURE 1.—Altitude exposure facility.

in our laboratory. At this point it should be emphasized that the lower limit of 0.001-percent weight loss may become subject to further critical review when the duration of manned space missions is extended beyond the presently encountered periods of about 2 weeks. For future prolonged space missions, the spacecraft design will have to be improved with respect to leak rates. Such improvement in the area of decreased leak rates, however, will further aggravate the problem of contaminant build-up in the space cabin.

The next step in the screening of a candidate space cabin material involves detailed gas-off analyses. The selected materials are stored in 9-liter boro-silicate glass chambers at 68 ± 2° C for 72 hours and at 25 ± 2° C for a period of 30 days. The atmosphere in the chambers is 100-percent oxygen at a pressure of 5 psia. The gaseous contaminants evolved from the test materials are identified by combinations of gas chromatography, mass spectrometry and IR-spectroscopy as needed. The sample preparation and the analytical procedures are far more complex than is evident in this brief summary. In table I the results of gas-off analyses are summarized for the same material for which the TGA curve was given in figure 3.

The composition of head-gas of this material is quite typical. The presence of all types of solvents in various amounts as they are used in the manufacturing process of the nonmetallic space

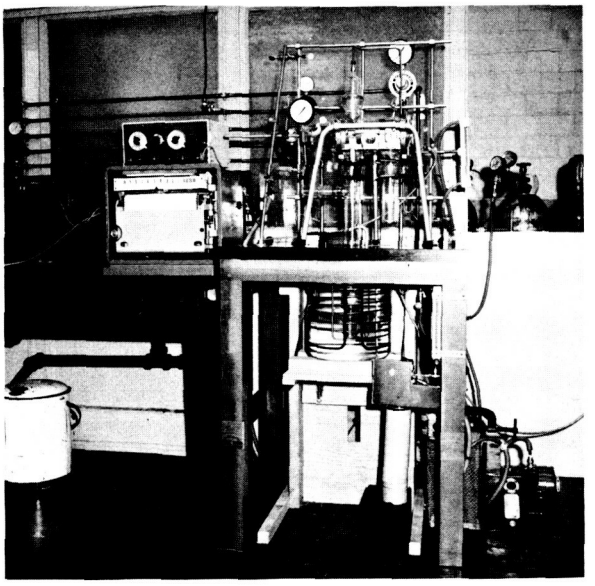

FIGURE 2.—Thermogravimetric analysis system.

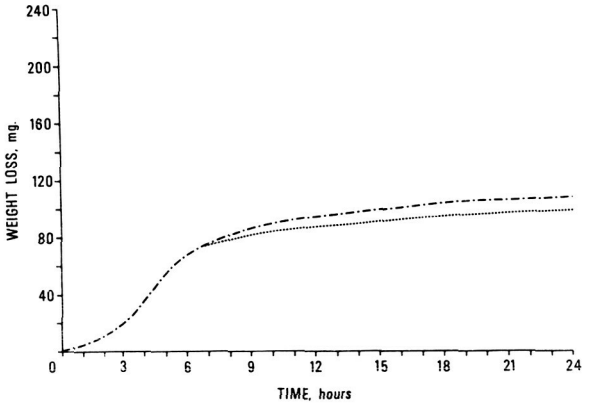

FIGURE 3.—Typical TGA pattern.

cabin material is observed frequently. The presence of the respective monomers in the case of polymeric materials is also very common. Methane and carbon monoxide contaminants have been observed in almost every material tested so far. To the latter trace contaminant we devote a great deal of attention because of its pronounced toxicological characteristics.

About 300 materials have been completely analyzed since 1965. Almost 200 different volatile contaminants have been identified during these studies, which were conducted until May 1969 by the Monsanto Research Corporation, Dayton Laboratory, under contract for the Air Force (refs. 2 through 5). The same effort is now being carried on in the laboratories of the Chemical Hazards Branch, the Toxic Hazards Division of the Aerospace Medical Research Laboratory. Assuming that the testing up to this point did not reveal any evidence of a possible toxicological hazard, either by the nature of one specific contaminant or by the amount of evolved volatiles, the candidate material still has to pass one further test. Since the biological responses to combinations of potential toxicants cannot be predicted from toxicological evaluation of the individual compounds of that mixture, due to additive, synergistic, and potentiating effects, actual toxicological testing of the entire mixture must be performed. To this end, test animals are exposed to the complex mixtures of gas-off products of candidate space cabin materials in the Thomas Domes.

TABLE I.—*Gas-off Products from Corfil 615 Adhesive*

Component	Weight of component (mg/10 gms candidate material)		
	72 hours (68° C)	30 days (25° C)	60 days (25° C)
Methanol	0.041	(*)	(*)
Acetone	0.045	0.037	0.052
Ethanol	0.27	0.17	0.20
Benzene	0.035	(*)	(*)
Toluene	1.3	1.1	1.2
Xylenes	0.050	0.025	0.030
C_3 alkylbenzene	0.015	(*)	(*)
Carbon monoxide	1.0	0.10	0.22
Methane	0.01	0.001	0.002

*Not detected.

This series of animal experiments was begun in 1965 on NASA's behalf for the toxicological evaluation of nonmetallic materials used in the construction of Apollo space cabins. The program has been expanded and now includes the testing of materials utilized throughout the entire manned space program. A schematic diagram depicting a closed-loop life-support system that is used in these studies is shown in figure 4. This equipment has been incorporated within a Thomas Dome that is used as an environmental envelope. The systems are operated at 5-psia pressure

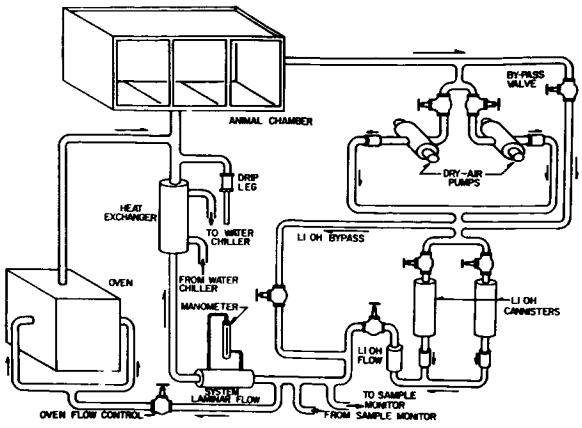

FIGURE 4.—Cabin material screening system.

either with a 100-percent oxygen-gas supply or with a mixed gas atmosphere of 68 percent O_2 and 32 percent N_2 utilizing a life-support loop comprised of a water vapor and carbon dioxide removal system. Carbon dioxide is usually controlled at 0.5 percent, but a bypass loop around a lithium hydroxide canister permits operation at CO_2 concentrations comparable to any actual space flight conditions.

The animal exposures are conducted in two distinct series of tests. Continuous 7-day exposures of rats and mice are performed for initial toxicological screening employing smaller groups of candidate materials (~ 25) followed by a 60-day exposure of the combined 7-day tested materials in an amount of up to 100 materials for a single test. A prepared group of materials is placed in a vacuum oven which is part of the closed-loop life support system. The oven is heated to 155° F (at 5 psia) and then the breathing atmosphere is passed through the oven and introduced into the animal exposure portion of the closed-loop with the added gas-off products. To control the temperature in the animal exposure portion, the recirculated gas-flow is split into an appropriate ratio of one part going back through the oven and the other part by-passed through a heat exchanger. Since oxygen is consumed for animal metabolism, it is replaced through a two-way pressure relief valve from the dome outer envelope operating with a 100 percent O_2 atmosphere. Inert gas losses in mixed gas atmosphere tests are made up manually from cylinder gas storage. The conditions are the same for both the short- and long-term exposures, except for the amount of cabin material utilized. This is 100g each for the 7-day experiment and 10g each for the 60-day studies. The 7-day exposures are designed for initial screening. This time period is sufficient to indicate the presence of a "bad actor" by comparison of control and test animals with respect to clinical symptomology, mortality, total body weight gain, organ weights, organ-to-body weight ratios, and gross pathology examinations at necropsy. These are the critical criteria utilized in these experiments for the assessment of toxicological effects. The necropsies are performed on both control and test animals in two groups at 2 and 4 weeks after exposure. If a toxic effect is observed, the relatively small group of candidate cabin materials can readily be sub-divided for repeat exposures until the material that releases the toxic agent is identified.

After about 100 materials have been screened in the described manner, these materials are then introduced into the continuous, long-term 60-day exposure of rats and mice to the gas-off products of these candidates. For these final studies, added criteria for the assessment of animal responses to toxic effects are histopathological examinations and, if warranted, electron microscopic investigations. During a particular 60-day exposure to gas-off products from 100 Apollo space cabin materials, groups of 20 rats (110–135g) and 25 mice (15–30g) all male, representing a typical animal population for these studies, were used as test animals. The recorded body weight data of the rats from this experiment were randomly selected as an example for the demonstration of the results. The data are illustrated in figure 5. It can be seen that the mean weight gains closely parallel each other for the 2 weeks' pre-exposure. For the post-exposure period, one might suspect some differences. However, statistical comparison of the mean body weight gains indicated no significance at the 95-percent level of confidence; the large standard deviations tended to negate any seemingly real difference (ref. 6). Based on all criteria used for assessment of effects, no measurable response was observed in rodents exposed continuously for 60 days to the gas-off products

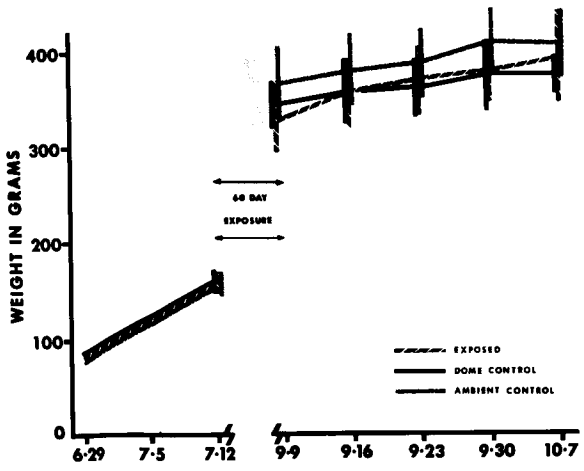

FIGURE 5.—Mean total bodyweight gain data (rats).

of 100 Apollo space cabin materials in a 100-percent oxygen, 5-psia environment.

The outcome of this study can be looked at from two different viewpoints. One approach would give unequivocal satisfaction over the result that no evidence of any measurable toxicological effect could be detected in the test animals. This is assuming, of course, that the data can be extrapolated to man. The alternate way of judging the negative result of the experiment could be to question the necessity for these involved and costly investigations, since as many as 100 materials showed no evidence of an adverse effect, even under the exotic test conditions. Both approaches, however, have their weak points. The shortcoming in the first one is the somewhat tenuous extrapolation of animal data to man; therefore, more toxicological data are required. The drawback to the second approach is much more serious because it may result in a possible oversight of just one dangerous material. Only one toxic compound is needed to set the stage for a catastrophe (ref. 7).

The experience with carboxynitroso rubber (CNR) very explicitly illustrates the necessity for a constant lookout for the one bad material. Carboxynitroso rubber is a synthetic polymer with rubber-like properties and has the added advantage of being noncombustible. Due to its nonflammability, CNR was selected as a candidate material for use in the Apollo spacecraft as a replacement for combustible materials with similar properties. Under normal conditions carboxynitroso rubber is a harmless material. However, its properties under emergency situations, for instance a localized overheating in the circuitry where CNR is utilized as insulating material, were not known. CNR was submitted to our laboratories for determination of flammability in 100-percent oxygen and for chemical analysis of pyrolysis products formed. It was found that complete decomposition occurred at about 300° C, as illustrated in figure 6. The pyrolyzate had very pronounced irritative properties to the nasal passages and bronchial tubes as experienced by one experimenter. Consequently animal experimentation was conducted to define the acute toxicity of the pyrolyzate. Based on information that approximately 65g of CNR would be used in a space cabin having a free volume of about 8 m^3, an inhalation exposure concentration of 7.65 mg/l was selected for testing. A group of five rats was placed in a 30-liter chamber filled with 100 percent O^2. The sample of CNR was heated in a nichrome wire basket until spontaneous decomposition of the rubber occurred. Dense, white fumes filled the chamber in which the rats were caged. Four of the five rats died during the 30-minute exposure period, and the remaining animal expired immediately upon removal to ambient air.

The composition of the volatile decomposition products of a sample from the same batch of carboxynitroso rubber was analyzed at different

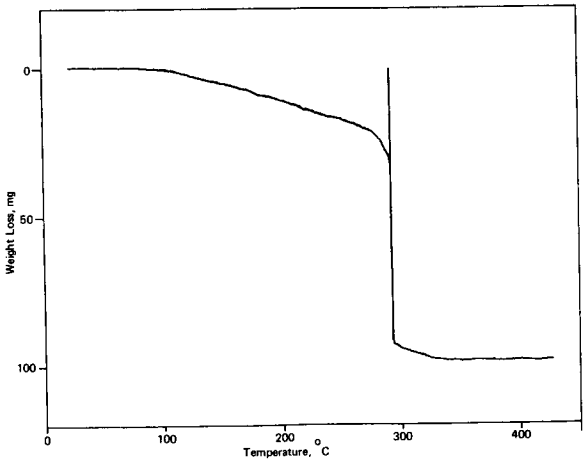

FIGURE 6.—TGA pattern of CNR sample.

TABLE II.—*Volatile decomposition products of CNR MSC 1549*

Components		Mole ratios of components relative to carbon dioxide			
		tested for 1 hour at			
		125° C	250° C	350° C	350° C*
Carbon dioxide	CO_2	1.0	1.0	1.0	1.0
Carbon monoxide	CO	0.01	0.4	0.5	0.6
Nitrogen dioxide	NO_2	ND	trace	0.1	0.1
Nitric oxide	NO	ND	trace	0.02	0.01
Silicone tetrafluoride	SiF_4	ND	0.2	0.3	0.1
Carbonyl fluoride	COF_2	0.06	0.2	0.02	0.02
Trifluoromethyl isocyanate	$CF_3N{=}C{=}O$	0.009	0.04	0.04	0.02
Perfluoro-methyl methylenimine	$CF_2{=}N{-}CF_3$	0.08	0.3	0.05	0.04
Uncharacterized	Silicon component	ND	ND	0.006	trace
	Perfluorocarbons	0.06	0.005	0.03	0.006
Hexafluorodimethylamine	$(CF_3)_2NH$	ND	trace	ND	0.02
TGA results		< 1% wt loss	~ 10% wt loss	> 95% wt loss	

*Performed in stainless-steel bomb.

temperatures. The results of these analyses are tabulated in table II. The observed toxic response to CNR pyrolyzate cannot be readily explained with respect to a specific causative agent. With the exception of perfluoro-methyl-methyleneimine, none of the compounds identified in the CNR pyrolyzate have been reported to be as highly toxic as was observed. This could very well mean that the imine is the causative agent. In this case a concentration of about 300 ppm breathed for a 2-minute period is lethal, and a concentration of about 65 ppm inhaled for a 30-minute period would prove fatal. The possibility exists that synergistic or potentiating effects were involved.

CONCLUSIONS

The toxicological evaluation of materials associated with manned space flights is performed to establish tolerance limits for contaminants that will inevitably be present in cabin atmospheres. This is an enormous task that requires the concerted efforts of a diversified team, recruited from a wide spectrum of scientific disciplines. Scientists involved in these investigations include physicians, toxicologists, pathologists, clinical and analytical chemists, and electron microscopists as well as facility engineers. With the prospect of future 1000-day space missions, it will take an all-out effort from the above mentioned scientific talent to establish man's tolerance to trace contaminants for this time period so that the information will be available when it is needed in the next few decades.

ACKNOWLEDGMENT

The research reported in this paper was conducted by personnel of the Aerospace Medical Research Laboratory, Aerospace Medical Division, Air Force Systems Command, Wright-Patterson Air Force Base, Ohio. This paper has been identified by Aerospace Medical Research Laboratory as AMRL–TR–69–53. Further reproduction is authorized to satisfy needs of the U.S. Government.

The experiments reported herein were conducted according to the "Guide for Laboratory Animal Facilities and Care," 1965 prepared by the Committee on the Guide for Laboratory Animal Resources, National Academy of Sciences-National Research Council; the regulations and standards prepared by the Department of Agriculture; and Public Law 89–544, "Laboratory Animal Welfare Act," August 24, 1967.

REFERENCES

1. THOMAS, A. A.: Man's Tolerance to Trace Contaminants. AMRL-TR-67-146.
2. PUSTINGER, J. V., JR.; HODGSON, F. N.; AND ROSS, W. D.: Identification of Volatile Contaminants of Space Cabin Materials. AMRL-TR-66-53.
3. PUSTINGER, J. V., JR.; AND HODGSON, F. N.: Identification of Volatile Contaminants of Space Cabin Materials. AMRL-TR-67-58.
4. PUSTINGER, J. V., JR.; AND HODGSON, F. N.: Identification of Volatile Contaminants of Space Cabin Materials. AMRL-TR-68-27.
5. PUSTINGER, J. V., JR.; HODGSON, F. N.; AND STROBEL, J. E.: Identification of Volatile Space Cabin Materials. AMRL-TR-69-18.
6. HAUN, C. C.: Toxicological Screening of 100 Space Cabin Materials. AMRL-TR-67-200. Proceedings of the 3rd Annual Conference on Atmospheric Contamination in Confined Spaces.
7. SAUNDERS, R. A.: A Dangerous Closed Atmosphere Toxicant, Its Source and Identity. AMRL-TR-66-120. Proceedings of the 2nd Annual Conference on Atmosphere Contamination in Confined Spaces.

H. A. HOLLENDER and MARY V. KLICKA
US Army Natick Laboratories
Natick, Massachusetts

Feeding Man in Space*

In 1961 President John F. Kennedy established a goal that resulted in the initiation of manned space flights that have offered unique challenges to many scientific personnel. The food technologists have also been challenged by the many constraints placed on the design and fabrication of foods suitable for consumption in space. For example, the following list gives various space food criteria:

(1) Acceptability
- Liked by astronauts
- Familiar flavor and texture
- Assure sustained consumption for flight duration

(2) Physiologic
- Nutritious
- High caloric density
- Digestible
- Low residue
- Non-gas producing
- Wholesome
- Cause no gastric disturbance

(3) Stability
- Biologically, chemically, and physically stable without refrigeration
- Withstand flexible packaging under 25-torr pressure (i.e., 29 in. vacuum)
- Withstand storage for:
  - (a) GEMINI
    - 136° F for 3 hours
    - 100° F for 2 weeks
  - (b) APOLLO
    - 0 to 130° F for 100 hours
    - 75° F for 400 hours
  - (c) MOL
    - 0 to 100° F for 30 days

(4) Utility
- Crumb free at time of consumption
- Reconstitute in 80° F water (GEMINI)
- Reconstitute in 45° F and/or 155° F water (APOLLO and MOL)
- Meet quality assurance provisions
- Small volume
- Lightweight

The problem of designing space food was not only one of maintaining high nutritional and acceptability levels; consideration had to be given to weight and size, the non-availability of refrigeration, the temperature of the water available for rehydration, and the fact that the food was to be consumed in a weightless environment. All this pointed to the need for highly stable "convenience type" food. Toward this end, five basic approaches were taken in the development of food suitable for use on Projects Mercury, Gemini, Apollo, and ultimately the Manned Orbiting Laboratory (MOL) program of the Air Force. The five categories of foods used are sterile semi-solid foods, bite-size dehydrated foods to be eaten dry, precooked dehydrated foods (rehydratables) to be reconstituted with water by the astronaut before consumption, thermally stabilized flexibly packaged wet foods, and intermediate moisture foods. All five categories were included in the Apollo 10 and 11 menus.

Prior to the first flight of Project Mercury, limited experimentation by the Air Force demonstrated that it was possible to eat and drink while in a weightless condition. As the period of weightlessness experienced was of less than 1 minute's duration, extreme caution was exer-

* This paper reports work undertaken in cooperation with NASA (Project No. NASA T-20541-G) and the Air Force (AF MIPR AM6-40061) in developing food for space feeding use.

cised in the selection of the food for the first Project Mercury flights. Thus the first feeding system used in Project Mercury was drawn with little or no modification from that used by the Air Force for feeding pilots operating under conditions requiring pressurized head gear. Semi-solid, sterile meat combinations and fruits developed for Air Force high-altitude flight use were adapted to Project Mercury use. These products were of the consistency of junior baby foods and were packaged in collapsible aluminum tubes (approximately 5-oz capacity) having a non-toxic, food-grade organic inside coating. A polystyrene extension tube, called a "pontube," screwed onto the aluminum tube and permitted ready passage of the comminuted food into the astronaut's mouth. Astronauts Glenn, Carpenter, and Schirra were supplied these semi-solid foods.

Project Mercury also utilized bite-size pieces of dehydrated food and low moisture confection items. For example, John Glenn's semi-solid applesauce was supplemented by compressed chocolate malted-milk tablets. Several of these bite-size foods were adapted from operational rations previously developed for the armed forces. These items, while acceptable, presented several technical problems, most immediate of which was a reliable method for preventing the formation and release of crumbs in the cabin during orbital flight. Crumbs could have been aspirated by the astronaut, obscured his vision, and even caused equipment malfunction.

Experience from the first Mercury flights supported the position that semi-solid, sterile foods, although convenient to eat, were not suitable for extensive space flight use. The pureed foods were not well accepted as a steady diet. In addition, since these products contained about 80-percent water, they provided relatively few calories for their weight and cube. Moreover, the availability of water as a by-product of the spacecraft fuel cell operation and the knowledge that it could be made potable dictated the use of dehydrated foods as the most economical method of food supply. Since most of the weight of food is water, use of dehydrated foods permits a major weight savings.

Two approaches on the use of dehydrated foods were pursued: bite-size foods and rehydratables. The availability of acceptable prototypes of bite-size and rehydratable foods resulted in the elimination of the semi-solid foods from the final Mercury flight menu. This menu included four products to be rehydrated in and consumed from special 0g sealed packages. In addition, a variety of bite-size pieces to be consumed by placing directly in the mouth were available as shown in figure 1 (ref. 1).

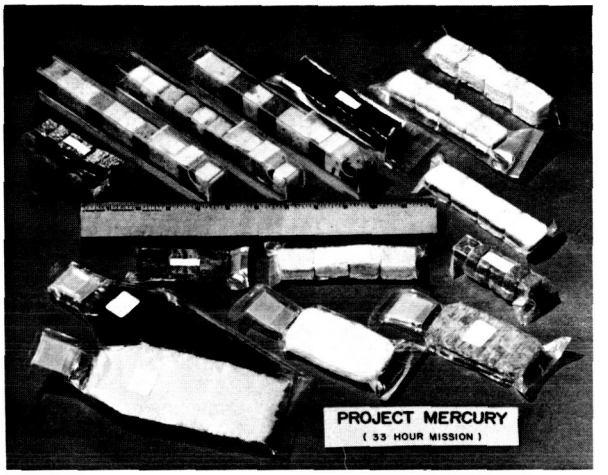

FIGURE 1.—Food samples from Project Mercury.

Semi-solid foods were not used on any of the 10 manned Gemini flights or on the first three Apollo flights. The two semi-solid items, ham salad and chicken salad, provided for both the Apollo 10 and 11 menus at NASA's request, are quite different from their early Mercury predecessors. These products were specially formulated to approximately 60-percent moisture content and were processed in a hyperbaric chamber to minimize texture and flavor changes normally occurring in heat-processed foods. These salads are to be used as sandwich fillings.

BITE-SIZE FOODS

The simplest, most convenient approach to space feeding is the use of bite-size units since these require no preparation by the astronaut (fig. 2). In the form of cubes or rectangles, they pack efficiently with a favorable ratio between food and packaging material. Special formulation and dehydration in conjunction with compression permit high nutrient content per unit of weight and

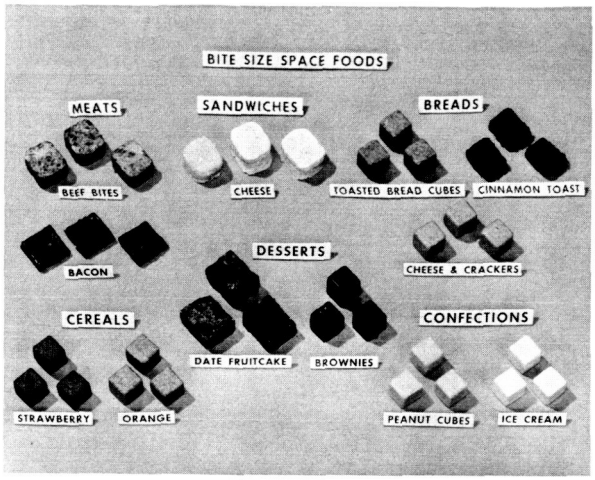

FIGURE 2.—Bite size space foods.

cube and improve stability after packaging. Freeze drying is generally the preferred method for dehydrating meats, fruits, sandwiches, and desserts, since few deleterious changes occur during drying, and the resulting products are capable of rapid rehydration in the mouth. Technological problems arose in the design and fabrication of bite-size foods to make them withstand the mechanical stresses associated with space flight. The problem of eliminating crumbs at time of consumption was especially troublesome.

Prevention of crumbling is in itself a unique problem. Control has been accomplished in several ways, primarily through careful product formulation. Binders in compressed food, gelatin in molded freeze-dried products, and careful control of fat content have aided in the control of crumbling. A variety of processing techniques have also contributed. A practical expedient has been the application of edible protective coatings. These are applied to all bite-size foods except bacon. The compressed bacon squares have been packaged under vacuum in a flexible package, resulting in a crumb-free, smooth, hardened surface. An investigation is still underway looking toward the development of a reliable coating which can be applied by an automated procedure to all bite-size foods.

Most bite-sized foods are now coated with one of three basic coatings. Compressed cereal and bread cubes and fruitcake pieces are compatible with a simple gelatin solution. For the high fat confection products, a zein-in-alcohol solution proves most satisfactory. Other products are coated with an emulsion comprised of sodium caseinate, oil, glycerine, gelatin and water. All coatings are applied as liquids, and the excess moisture or solvent is removed by drying, usually freeze drying. After drying, the coating becomes firm and protects the food from damage in subsequent handling. Table I exemplifies the research and development expended on coating problems with bite-size foods. Experimental coatings tried, but found unsuitable prior to space flight, have been omitted from this summary.

The coating problem was intensified by the requirement that all space food be packaged in non-rigid containers evacuated to approximately 29 in. of mercury at the time of sealing and withstand storage at 100° F under atmospheric pressure. The pressure differential between the atmosphere and the internal pressure in the flexible package subjects the contents to a con-

TABLE I.—*Evolution of Coatings for Sandwiches* and Meat Bites*

Where used	Coatings used	Reason discontinued
Mercury 9	Acetylated monoglycerides (mp 109° F)	Flight cabin temperature exceeded 109° F; coating melted.
Gemini 3	Hydrogenated palm kernel oil (mp 136° F plus a high amylose starch film overcoat).	Coatings were incompatible; starch film flaked badly and turned bitter on storage.
Gemini 4 through 8	Hydrogenated palm kernel oil (mp 136° F), 2 coats	Unacceptable to astronauts (inhibited hydration in mouth and covered roof of mouth); poor digestibility, steatorrhea.
Gemini 9 through 12	Sodium caseinate, fat, sugar emulsion	Sweetness not liked on non-sweet products.
Apollo	Sodium caseinate, fat emulsion (standard coating)	(Still in use).

*All sandwiches are coated with gelatin during manufacture.

stant force which in some foods has produced undesirable changes (refs. 2 and 3). For example, compressed baked gingerbread, brownies, and fruitcake pieces exuded oily fluids when so packaged. To correct the problem, it was necessary to change the ingredients and the coatings and to lower the moisture level in the products. Freeze drying the fruitcake pieces corrected the exudation problem and also eliminated the need for the starch wafers which had been applied to absorb the free moisture (fig. 3).

Application of the standard coating requires considerable technological skill and has been the cause of many problems. Poor adhesion, cracking, brittleness and toughness in the coating, sloughing of product during coating and partial coverage (i.e., bare spots) are some of the difficulties experienced. These are partially due to shrinkage during drying and are influenced by the thickness of the coating and the amount that soaks into the product. The mineral content of the water used as a plasticizer in the coating affects its viscosity and subsequent performance. Therefore, it has been necessary to specify the use of distilled water.

Uncompressed baked items such as pound cake bites and fresh bread collapse when packaged in a flexible pouch under low pressure. Since their resultant textures are gummy and unappetizing, the only naturally baked product used in current menus is fruitcake. All bread items now used are either compressed (i.e., toasted bread cube) or freeze dried (i.e., sandwiches, cinnamon toast). Production costs of freeze-dried sandwiches are exceedingly high due to the amount of labor required. Splitting of the product during drying causes poor yields, a high rejection rate, and other quality control problems. The sandwiches are still a potential crumb hazard; therefore, appropriate replacements are urgently desired.*

Although the Space Food Prototype Production Guides furnished brand names of ingredients used in developmental work, their use was not mandatory. As a consequence, occasional problems arose when other components were substituted. A typical problem was one that occurred with cinnamon toast pieces when, in order to better satisfy quality assurance requirements, a continuous mix bread was substituted for the firmer non-uniformly textured specialty bread used in the development work. This was done to meet an initial requirement (which subsequently has been changed) for products having no holes

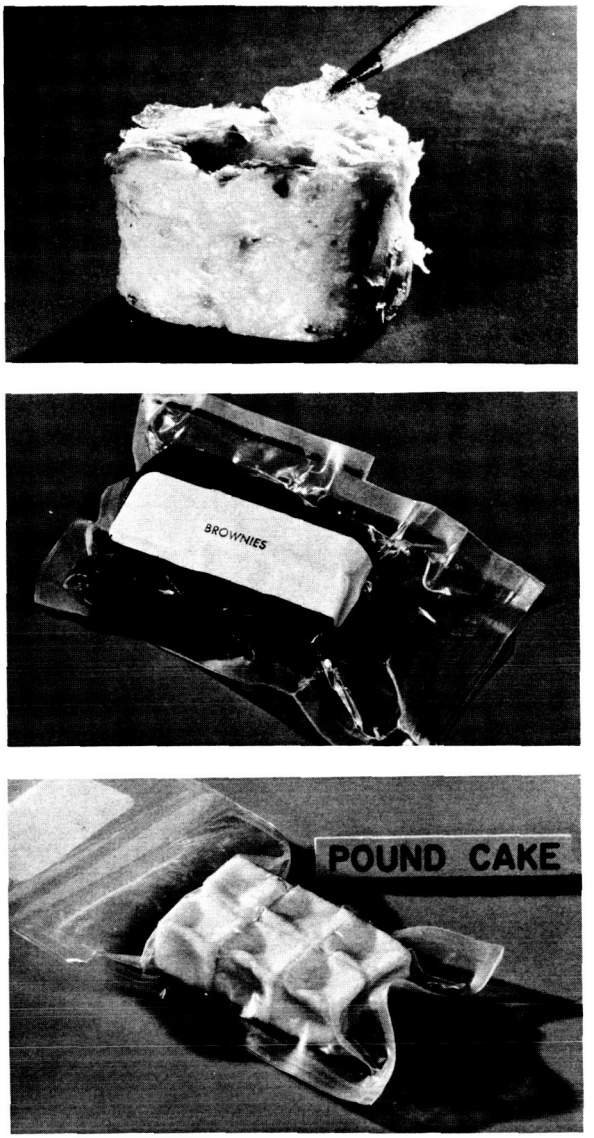

FIGURE 3.—Problems encountered in development of bite-size foods: poor adhesion of coating to bite, exudation of fluid from baked products, and collapse of uncompressed baked products with vacuum packaging.

*Subsequently NASA added fresh bread (white, rye, and cheese) packaged under a slight positive nitrogen pressure to the Apollo 11 flight menu.

or voids exceeding 1/8 in. in any dimension. However, the finer textured continuous mix bread crushed under the stress of 29 in. vacuum and resulted in a completely unusable product. Use of the specified bread results in an acceptable cinnamon toast.

Common problems which have been met in bite-size compressed foods are fragility, splitting, lack of cohesion, relaxation after compression, variable density, nonuniformity in size and shape, loss of palatability and extreme variability in texture between lots. Experience has shown that adjustments either in formulation or procedures are almost always necessary to adapt to different types of pressures. Physical and chemical changes occur on prolonged storage, and with exposure to high temperatures (i.e., the required 136° F for 3 hours) some bites harden, others soften. These changes are difficult to predict and control. On the other hand, compressed bite-size foods provide needed variety and have proved generally acceptable. They require neither preparation for consumption, nor special equipment, only a simple transfer to the mouth. They pack with maximum efficiency and have a high caloric density on both a weight and volume basis. One factor that remains critical to their continued or even frequent use is their extreme dryness, particularly when consumed without benefit of a swallow of water.

REHYDRATABLE FOODS

For a decade prior to NASA's requirement for special foods, scientists at Natick Laboratories were active in the production of freeze-dried foods and in their application to military operational rations. Particular attention had been directed toward the development of a feeding system in which the major components required only the addition of water and a brief holding period prior to consumption. A number of such products were rapidly adapted to the more exacting requirements of NASA and in many cases have been improved through further effort. A major problem was the attainment of acceptable meats, stews, and vegetables when only 80° F water was available for their reconstitution. The use of pregelatinized starches solved the problem for most of these products. In addition, new families of freeze-dried products, such as meat salads, have been developed and proved suitable for space feeding. In fact, these space flight salads have also been adopted by industry and are being marketed commercially to restaurants and institutional feeding companies. Figure 4 shows a variety of rehydratable foods.

The Army too has benefited from its space food development program since "spin off" permitted improvement and redesign of the precooked dehydrated entree items of the Food Packet, Long Range Patrol (fig. 5) within a record 3 months' period. The redesigned packet is extremely popular in Vietnam. The long range patrol formulas have greater caloric densities per unit of weight and larger component piece sizes than do the space food counterparts from which they were derived. For these reasons beginning with Apollo 10, five long range patrol formulas—chicken and rice, spaghetti and meat sauce, beef stew, chicken stew and pork with escalloped potatoes were adopted for space flight use. NASA is having these products packaged in a newly designed "spoon and bowl" type rectangular zero gravity feeder (figs. 6 and 7).* The feeder will have a valve to facilitiate rehydration of the food with the standard hot water probe provided on the Apollo capsule. Consumption of the foods after reconstitution will be with a spoon. Therefore, the mouth port (polyethylene tube) provided on the standard 0g feeder will be replaced by two parallel reclosable zippers. The lower zipper, in the open mode, serves as a scraper to prevent contamination of the top zipper which serves as a closure system. After food contents have been removed and the antimicrobial waste stabilization agent has been added the zippers are closed and the package stored in the waste storage area.

Credit for the introduction of spoon eating in space goes to the Air Force. Through a series of experiments in the F–100 and C–135 aircraft, they proved that food can be consumed with a spoon in zero gravity. Completely liquid foods are the exception. In zero gravity food mixtures exhibit considerable surface tension and adhere

*NASA Contract NAS–9–9032, Whirlpool Corporation, St. Joseph, Michigan.

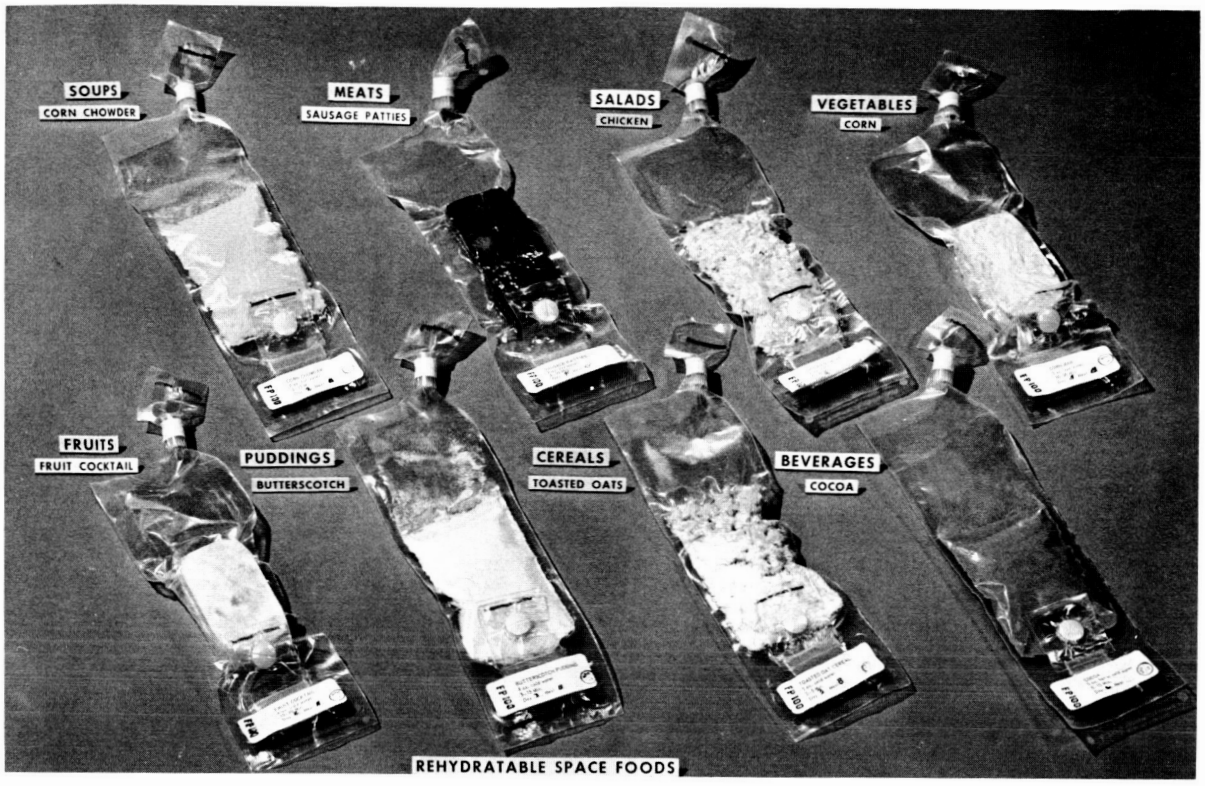

FIGURE 4.—Some rehydratable space foods.

FIGURE 5.—Samples of the Army Long Range Patrol Food Packet.

to both the bottom and top of the spoon with equal ease. Therefore, special feeders provided with a means for scraping excess food from the bottom of the spoon are required.

High caloric soups were formulated by using a non-dairy coffee whitener as a creaming agent. The use of calcium cyclamate permitted a reduction in the sucrose content of sweetened fruits and resulted in better control of bulk density (fig. 8). Experience has shown that high sugar levels potentiate the problem of foaming and thawing during freeze drying. Rehydratable fruits and natural fruit juices packaged in flexible pouches under high vacuum caked and fused when held at 100° F for 2 weeks. For applesauce the solution of this problem was attained only by starting with freshly peeled, cored, and cooked apples; removing and discarding 50 to 60 percent of their juices; freeze drying the pressed apple pulp; comminuting it; and adding sufficient sucrose and malic acid to replace the fruit sugars and flavor lost in the juice extraction step. No solution has been found to prevent natural fruit juices from hardening under these conditions. As an expedient, the astronauts are drinking formulated fruit flavored drinks as a substitute for natural citrus and other juices.

FIGURE 6.—Spoon and bowl type feeder.

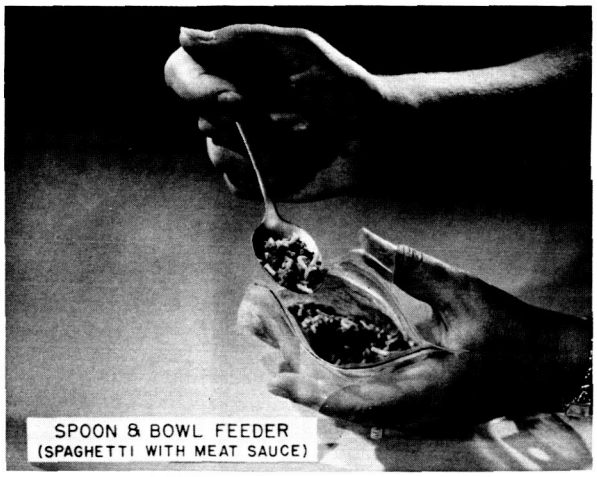

FIGURE 7.—Newly designed rectangular zero gravity feeder.

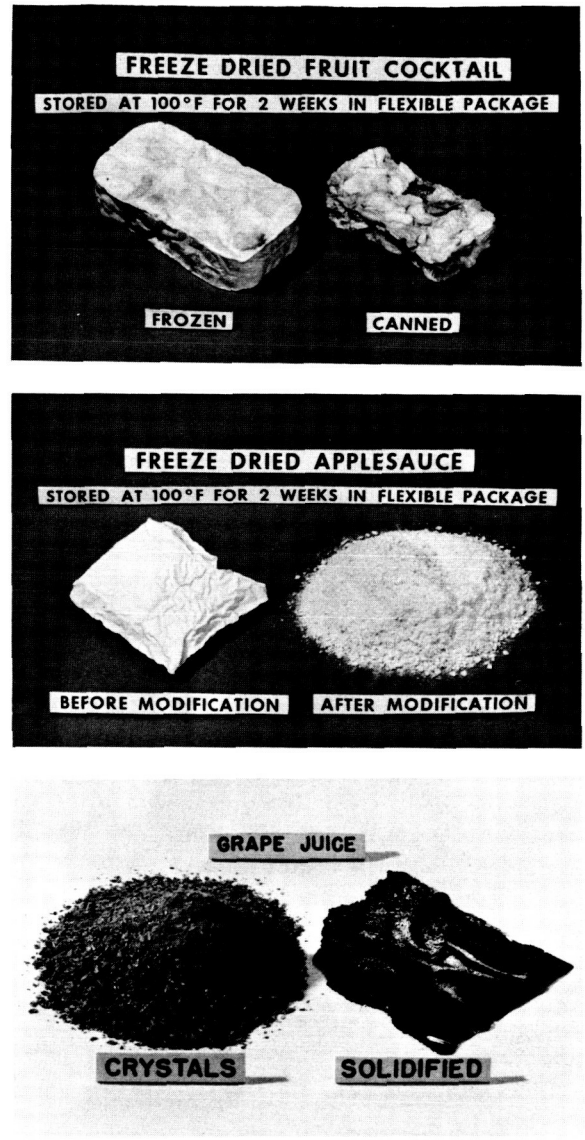

FIGURE 8.—Problems encountered in development of rehydratable fruits and juices due to requirement for vacuum packaging.

THERMOSTABILIZED WET PRODUCTS

With the Apollo 8 flight, NASA introduced a fourth class of food into the inventory of space flight foods. Each astronaut was provided with a single serving of heat sterilized turkey and gravy processed in a flexible pouch. This product carried a normal moisture content. It was extremely well accepted by the astronauts and was the first eat-with-a-spoon food provided U.S. astronauts. The turkey was cut into pieces, 3/4 by 3/4 by 5/8 inch, and the gravy thickened with starch so that once the top of the foil laminate pouch was cut open the contents would not readily disperse into the cabin atmosphere. The product adhered to the spoon and was consumed without problem. The food item was highly acceptable primarily because it was familiar in appearance, flavor, and texture. Three thermostabilized wet meats were included on the Apollo 10 menu, i.e., ham and potatoes, beef and potatoes, and turkey and gravy (fig. 9).

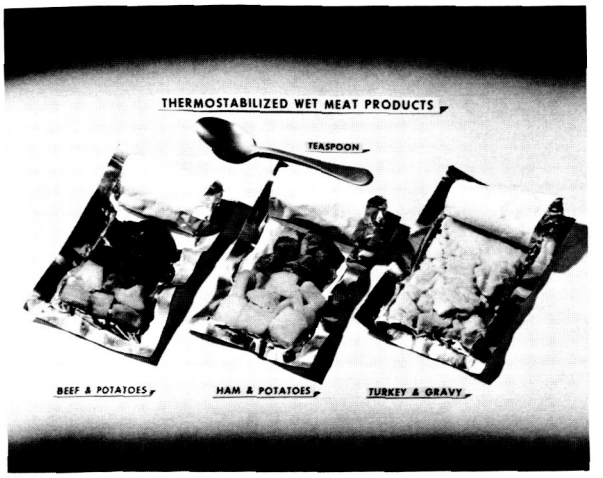

FIGURE 9. — Three meals included on the Apollo 10 menu.

These same products will be used on Apollo 11 plus frankfurters and a cheese spread.

Most of the technological problems associated with processing wet products in flexible containers had been worked out in earlier research and development for the U.S. armed forces. The foil-laminated material used for the package was a thoroughly tested material with a known history of performance. The integrity of the container seals when subjected to pressures of 1×10^{-6} torr, however, was not known and had to be determined. This test was a criterion established for the packaging of foods that might be exposed to the vacuum of space during extravehicular activity.

INTERMEDIATE MOISTURE FOODS

Commercially produced dried apricots, peaches, and pears (approximately 27 percent by weight moisture), were vacuum packaged and included on the Apollo 10 menu and are planned for continued use on subsequent flights. Foods such as these fruits fall into the intermediate moisture food category. They owe their microbiological stability to a reduced water activity but contain too much water to be classified as dry.

Intermediate moisture foods are potentially advantageous for special military and space feeding situations. Being low in moisture content they provide a concentrated source of calories. Being plastic they can be molded to any desired form. Being moist they are suitable for direct consumption without giving rise to the sensation of harsh dryness usually concomitant with the direct consumption of freeze-dried foods. Furthermore, the texture of intermediate moisture foods is much closer to normal food than the crisp or rigid structure of freeze dried and other fully dehydrated foods.

Current research towards the attainment of a wide variety of intermediate moisture foods of high acceptability has been reported by Brockmann (ref. 4). The desirability of such foods for space flight use has been reported by Smith (ref. 5).

PACKAGING

A clear, four-ply flexible laminate comprised of an inner and outer layer of polyethylene with fluorohalocarbon and polyester layers between is used for packaging of all dehydrated foods and intermediate moisture foods. A heat processable, laminated packaging material (modified polyolefin-aluminum foil-polyester) is used for all wet foods. A flame-proof fluorohalocarbon film is employed as a meal overwrap material (fig. 10).

At the maximum pressure that could be developed from exposure to the vacuum of space, 1.003 kg/cm^2 (14/7 psi), no difficulty should have been anticipated from the laminar plastics used for packaging. A problem that has been encountered with the present material has been

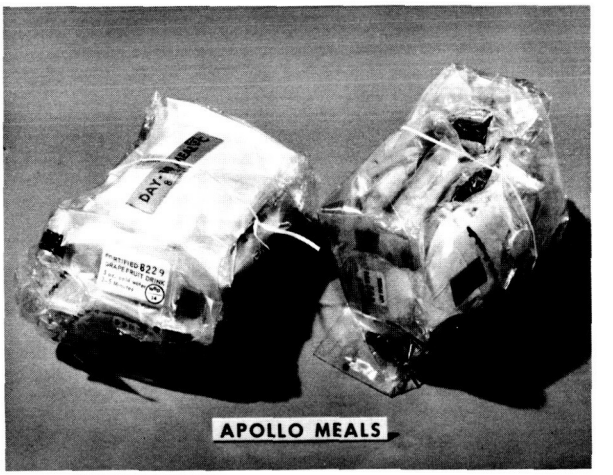

FIGURE 10. — Flame-proof overwrap material used on Apollo flights.

delamination. When delamination occurs, the basic strength component of the structure (polyester) is unable to contribute to the overall strength of the package, and failure results at the points of highest stress, i.e., the seal area. The solution rests with the development of improved techniques for laminating to the fluorohalocarbon or finding a substitute material that will satisfy the requirements (barrier properties) necessary to protect freeze dehydrated foods from damage as a result of permeation of water vapor and/or oxygen through the package. The present material is a compromise with strength being sacrificed for environmental protective qualities provided by the fluorohalocarbon.

MENUS

Menus are planned for each flight. Initial plans for Gemini feeding called for four meals a day. This schedule was adhered to for the 4-day Gemini 4 flight but abandoned for the 8-day Gemini 5 flight when it was learned that the volume allocated for food was the same for both flights. For Gemini 5, the same nutrition was consolidated into three meals. The three-meal schedule has been adhered to ever since because it is more acceptable to the astronauts. A 4-day menu cycle is used with repetition as dictated by the flight schedule.

HUMAN FACTORS

The daily food requirements for astronauts are broadly controlled by nutritionists and medical advisors. Such controls, however, relate to requirements for protein, calories, specific minerals and vitamins, limitations on food residues and fat, and a prohibition of several groups of foods, such as those known to produce intestinal gas. The menu planner is given no guidance as to specific foods, and menu planning is performed without insight into the time or division of attention that can be invested in the preparation and consumption of a meal. Yet, each item of every menu should be of unequivocal acceptability for its intended customer.

NASA interviews each astronaut regarding his food likes and dislikes. These have proved to be of value. To a considerable degree present food choices are based on experience and reliance on items of general acceptability. While astronauts are familiarized with their food supply prior to flight, no attempt is made to condition them to specific foods or to change existing food attitudes.

CONTROLS ON FOOD PRODUCTION AND DEVELOPMENT

Wholesomeness of all dehydrated foods (rehydratable and bite size) is monitored through prescribed microbiologic standards that must be met by all food produced for flight use:

Total aerobic plate count	Not greater than	10,000/g
Total coliform count	Not greater than	10/g
Fecal coliform count	Negative in	1g
Fecal streptococci count	Not greater than	20/g
Coagulase positive staphylococci	Negative in	5g
Salmonellae	Negative in	5g

Wholesomeness for the packaged wet foods is assured by incubating randomly selected production samples, half at 32° C and half at 55° C, for 20 days and then applying a special sterility test. This latter test is applied to half of each lot of incubated samples and involves further incubation in Tryptic Soy broth for 5 to 7 days at 32° C and 55° C.

PRESENT SPACE FEEDING PROBLEMS

All Apollo flights have used fuel cell water for drinking and for reconstitution of rehydratable foods in the command module. Sufficient water is carried aboard initially to last approximately 12 hours. To assure potability at the point of consumption, the water is chlorinated by the astronauts. Difficulties encountered in getting the chlorine dispersed in the water supply have not been resolved. As a result, water with varying levels of chlorine content is dispensed.

The Lunar Module (LM) water is stored aboard prior to launch. NASA is using iodine as the water purification agent. In-house studies conducted prior to making this decision indicated that water treated with metallic iodine did not significantly alter the taste of space foods at levels of up to 30 parts per million. At this level an iodine flavor was detectable in water. Feedback data from Apollo 9 indicates that the LM water seemed to be preferred over that used in the Command Module.

Another problem that has caused difficulties

has been the fact that the command fuel cell water contains considerable free hydrogen. The hydrogen is difficult to dispel from the food package. This also makes food reconstitution more of a problem since gas must be expelled from the package to add enough water for adequate rehydration. Reports from the astronauts indicate that the currently available fuel cell water is not acceptable. The variability in chlorine content is a contributing factor. However other objectionable and unidentified flavors have been reported. Analysis of samples of fuel cell water from the Apollo 10 flight should help define this problem so that it can be solved.

MANNED ORBITING LABORATORY*

The Air Force MOL program will involve two men who will orbit in a modified Gemini spacecraft that will be attached to an orbiting laboratory. They will live in this laboratory for 30 days. The space allocated for food is 195 cubic inches per man per day or 1.7 lbs of packaged food per man per day. A feeding system comprised solely of dehydrated food is now being evaluated by the Air Force in order to obtain an optimum feeding system for the MOL flights. Both bite-size and rehydratable foods are included. These are similar to those currently being used on Project Apollo. Many changes are expected to be made in both the food and package concepts prior to the adoption of a final flight qualified system. As for Project Apollo, hot water and cold water will be available for reconstitution of the foods.

APOLLO APPLICATIONS PROGRAM

NASA's Apollo Applications Program (AAP) will follow on the heels of the Apollo program. The AAP will involve making a S4B spent fuel cell habitable. The S4B is the second stage of the Saturn 1B rocket. Once the fuel has been used and staging has been accomplished, the crew in the Apollo capsule will dock with it and the men will vent any residual fuel into space and convert its approximately 11 000 cubic feet into a habitable environment. Three AAP missions are now scheduled to be flown—one 28-day mission and two 56-day missions. The first two flights, the 28-day and one of the 56-day missions, will be primarily medical flights and will determine man's ability to adapt to living in space. It will include a habitability study and a nutrition and musculoskeletal function study. The third flight will be primarily to obtain astronomical data.

Appropriate feeding systems for the AAP will be required. The feeding system aboard the AAP will be as good as the conventional feeding systems currently in use and must be compatible with the medical experiments to be conducted aboard. Weight requirements have been somewhat relaxed for these experiments. Two to three pounds of packaged food will be allowed per man per day. An oven and refrigeration will be available for food preparation. Storage facilities will be better than those currently available for nominal Apollo flights (ref. 6).

Beyond AAP the United States can look forward to long-term space missions. Projected programs can be grouped into three basic areas:

(1) Earth orbital program
(2) Lunar program
(3) Planetary program

During the next decade we can look forward to Earth orbital space missions carrying crews of from 8 to 12 members and lasting approximately 180 days. (This is 13 times as long as previous flights.) Space stations will probably be assembled in space; they will have a hangar and docking area, and resupply of expendables will be by shuttle. For the lunar program we will probably have a lunar base with resupply of crew and expendables.

For planetary spacecraft launch, we can look forward to a Mars or Venus flyby during the next decade with a Mars landing predictable by 1984. For planetary missions, food will be critical and at some point we must consider closing the life-support system. Recycle of water and oxygen will probably occur for flights in excess of 100 man-days. At the present time, it is anticipated that food regeneration will be necessary somewhere between 1000 and 10 000 man-days of flights. However, it is not expected that any system will be completely closed but that some type of a composite system comprised of stored and regenerated foods will be used.

*The Air Force has subsequently cancelled this program.

REFERENCES

1. KLICKA, MARY V.: Development of Space Foods. J. Am. Dietetic Association, vol. 44, no. 5, May 1964, pp. 358–361.
2. HOLLENDER, H. A.; KLICKA, MARY V.; AND LACHANCE, P. A.: Space Feeding: Meeting the Challenge. Cereal Science Today, vol. 13, no. 2, 1968, pp. 44–48.
3. KLICKA, MARY V.; HOLLENDER, H. A.; AND LACHANCE, P. A.: Foods for Astronauts. J. Am. Dietetic Association, vol. 51, no. 3, Sept. 1967, pp. 238–245.
4. BROCKMANN, M. C.: Development of Intermediate Moisture Foods for Military Use. 29th National Meeting Institute of Food Technologists (Chicago, Ill.), May 13, 1969.
5. SMITH, MALCOLM C., JR.; AND ASHBY, WILLIAM T.: Intermediate Moisture Foods for Manned Space Flights. 29th National Meeting Institute of Food Technologists (Chicago, Ill.), May 13, 1969.
6. RAMBAUT, PAUL C.: Apollo Application Program Requirements. Presented at Aerospace Food Technology Conference, University of South Florida (Tampa, Fla.), April 15–17, 1969.

THOMAS R. McGETCHIN
Institute of Technology
Wright-Patterson Air Force Base, Ohio

Titanoclinohumite and Other Hydrous Minerals in the Earth's Interior and the Problem of Lunar Water

Titanium-rich clinohumite and layered structure minerals are observed in kimberlite and as inclusions in pyropic garnets from the Moses Rock dike, a kimberlite-bearing breccia dike in San Juan County, Utah. Associated clinopyroxenes observed as inclusions within similar pyropes and also in kimberlite are estimated to have equilibrated at depths ranging from about 50 to 150 kilometers at modest temperatures generally less than 1000° C. The presence of titanoclinohumite, a high density, hydrous phase is of considerable interest as a possible site for volatiles in the Earth's upper mantle. The dehydration of hydrous phases such as titanoclinohumite within the upper mantle may provide water as a free phase. Other minerals that may play a similar role in the Earth's mantle include mica (especially biotite and phlogopite), serpentine, amphibole, and possibly hydrous pyroxenes.

The localization of water within the Earth's mantle may play a key role in determining the character of the large scale tectonics of the Earth because, (1) it has been demonstrated at high pressure and temperature that the presence of small amounts of H_2O drastically reduces the strength of quartz (SiO_2), and possibly other silicate minerals as well; (2) water lowers the melting point of silicate systems by 200 to 300° C at upper mantle depths where pressures are of the order of 10 kilobars or more; (3) hydration reactions commonly involve a volume change (approximately equal to the specific volume of the water). Such effects undoubtedly are important in (1) the production and localization of magmas in the Earth's upper mantle and resulting volcanism; (2) convection of the mantle itself and hence drift of continents and observed motion of sea floor; (3) the presence of the seismic low velocity zone in the Earth's mantle; (4) regional vertical motions of the Earth's crust, such as the tertiary epeirogenic uplift of the Colorado Plateau province. Probably, it is safe to assert that if the Earth's mantle were anhydrous, the geology of the Earth's surface would be quite different.

Geologists and geophysicists are beginning to piece together a coherent picture of the physical and chemical state of the Earth's upper mantle by combining laboratory observations of rocks apparently derived from the mantle, with progressively more highly resolved geophysical models for the upper mantle. Among the best sources of such rocks are certain kinds of volcanoes; kimberlite pipes, alkali-basalt diatremes and maars, and basaltic volcanoes. High resolution photography of the lunar surface (Ranger, Orbiter) has revealed many structures similar in morphologic detail to these volcanoes. Among the best examples are the dark halo craters in Alphonsus. Hence, there is reason to believe that scientific exploration of such lunar features may provide us with deep seated rock fragments. From such rocks we can expect to extract useful information regarding the Moon's interior, its composition, physical state and history, and also the presence of water and its role in geologic processes in the Moon's interior. Such knowledge, of course, would provide valuable clues about where the search for near-surface water should be directed.

ISIDORE ADLER
Goddard Space Flight Center, NASA

Methods of Water Determination (Surface and Orbital)

INTRODUCTION

The subject of water on the Moon is an important one for several reasons. Water constitutes an essential resource in continuing space exploration, both as a life support requirement and a possible source of engine fuel. It can also serve as a highly significant indicator of various geochemical processes. A number of investigators have examined the questions of possible lunar water sources, conditions for recovery, and potential yields (refs. 1 and 2). Arguments have been presented for sources consisting of basaltic and granitic rocks that may be widely distributed in large quantities; serpentine and other hydrated minerals that may be localized in fumarolic vents; and finally water in the form of ice trapped in permanently shaded cold spots in the polar regions. Gold (ref. 3) has considered the likelihood of a permafrost layer at modest depths, and Urey (ref. 4) has proposed that the sinuous rilles are in fact dry river beds.

A summary of possible water sources on the Moon has been given by Lopik and Westhusing (ref. 5) and is shown in table I.

TABLE I.—*Possible Water Sources on the Moon*

Free water	Bound water
Solid condensates	Crystalline volcanic
Liquid interstitial	Hydrates meteoritic
Gas adsorbed	Ultra basic

These authors go on to state that the presence of water in one form or another may be reflected in differences in physical properties between "deposits and country rock." They propose that if suitable instruments can be developed for detecting these differences, they can then be exploited in the search for water. Some of the potentially useful physical phenomena suggested are as follows:

(1) Density measurements
(2) Thermal properties
(3) Acoustic or seismic velocities
(4) Electromagnetic emission or absorption
(5) Radioactivity
(6) Structure
(7) Albedo

Many of these phenomena can, however, only yield inferential information, and there is a continued searching for more specific methods or procedures. Three such methods will be discussed in this presentation. Two are under consideration for surface missions and one for orbital missions. In the interest of realism it must be stated that these methods are in early stages of development and are still to be tried in the actual framework of an actual lunar mission. They are presented here as techniques having some promise.

ALUMINUM OXIDE HYGROMETER

The first method to be discussed is based on the aluminum oxide hygrometer developed by the Panametrics Corporation. It is a sensor that has been successfully flown on rockets for determining the water vapor distribution at high altitudes.

The water sensor consists essentially of an anodized aluminum substrate into which a thin layer of gold is evaporated. The aluminum substrate and gold film act as the detector cell electrodes. Figure 1 is a diagram of the cell construction. In a general way changes in ambient water

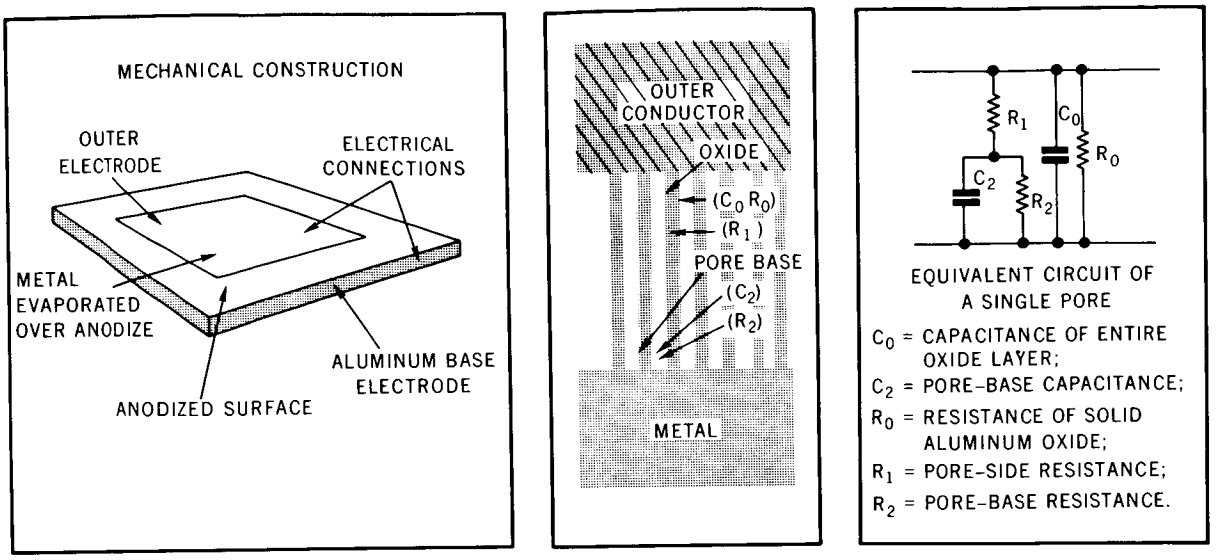

FIGURE 1.—Principle of aluminum oxide water sensor.

vapor concentration effect changes in the amount of water absorbed by the oxide structure which in turn produces corresponding changes in cell impedance (resistive and capacitive). The variations in impedance are related to moisture by a type of calibration curve shown in figure 2. These sensors have been studied in great detail by Del Pico (ref. 6) and Chlech and Brousaides (ref. 7). Del Pico was able to demonstrate that the film structure of the anodized aluminum consists of roughly hexagonal crystals with a diameter of about 50 000 A° and that the crystals contain pores of approximately 150 A° diameter. It is in these pores that the water is adsorbed affecting in turn the impedance of the sensor.

As a result of their investigations, Chleck and Brousaides of Panametrics have drawn the following conclusions:

(1) The sensor response is related to the absolute water vapor concentration and is independent of the total pressure. The dynamic range is large covering the range from ground conditions to moistures corresponding to dew points as low as −90° C.

(2) Response is rapid—of the order of 2.5 seconds for 63 percent change.

(3) The temperature coefficient is small.

(4) The sensor element is very small in size.

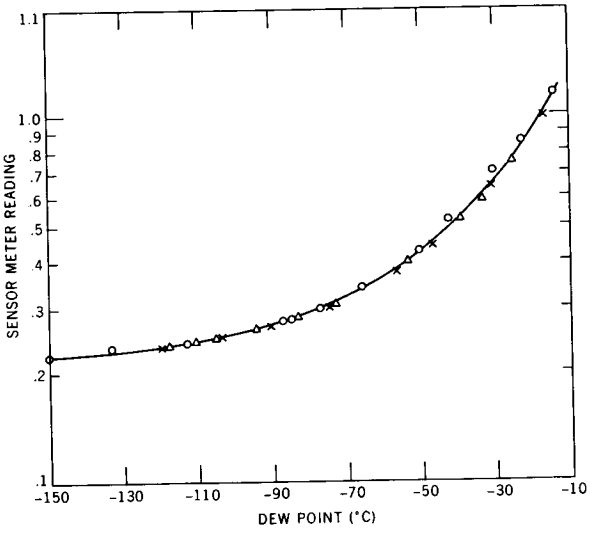

FIGURE 2.—Typical calibration curve of water vapor sensor.

(5) The sensor is not affected by common air pollutants or high humidities.

Our own determination of sensitivity has given values of about 10^{-9} to 10^{-10} g/cm^3 at pressures of 10^{-1} torr or less.

With the above sensor in mind, the following proposals have been advanced for surface exploration of the Moon: A surface device utilizing solar heating to look for bound water in the lunar

surface materials and a sub-surface probe to attempt moisture profiles.

Figure 3 is a conceptual sketch of a possible surface probe. One can conceive of a hand-held probe to be driven partially into the lunar surface. Heating would depend on solar radiation, and hopefully the lunar material would provide a barrier permitting the evolved moisture to rise to a value within range of the detector sensitivity. An assumption of 0.01-percent moisture in the surface material can yield enough water to be detected by several orders of magnitude.

A second concept is shown in figure 4, which shows a subsurface probe for determining moisture profiles. This probe would consist of a series of discrete moisture cells having a number of independent water and temperature sensors. The probe would be driven into the surface to a depth of about 1 foot. Each cell would be made of sintered metal permitting the free passage of water vapor from the adjacent soil. This type of device would be expected to give some notion of water gradients and "currents." While it is difficult to predict how successfully this type of probe can be operated in inactive regions of the Moon, one would certainly expect exciting results in the vicinity of fissures and regions of volcanic activity if in fact such regions occur.

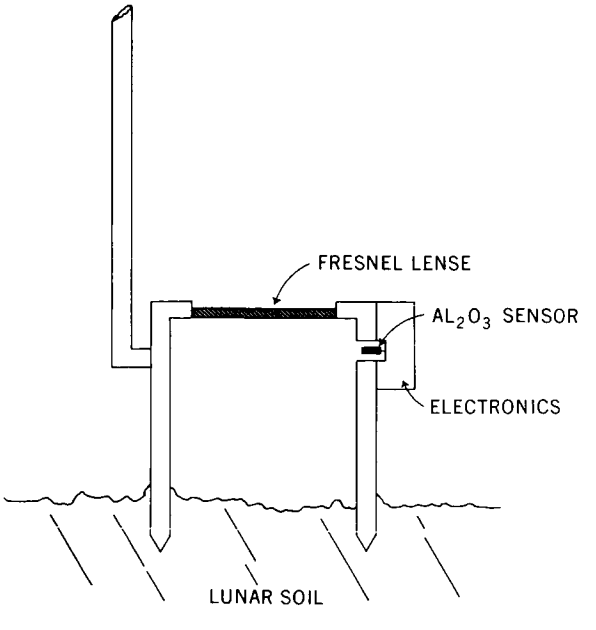

FIGURE 3.—Schematic of a possible lunar surface water probe.

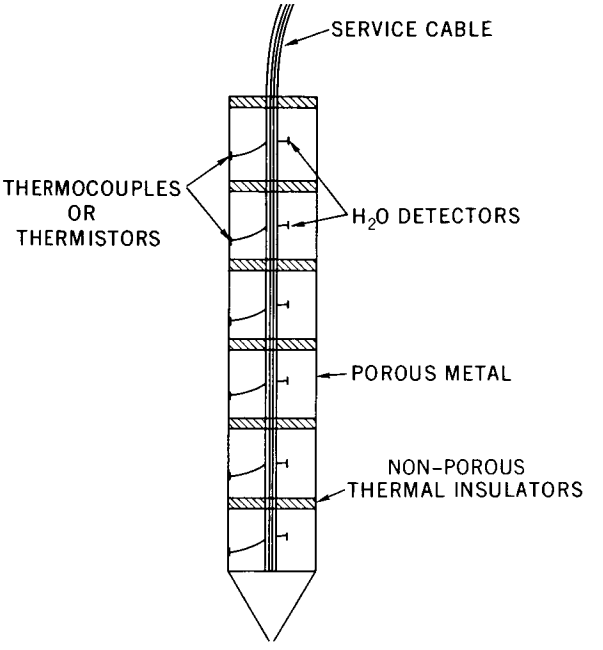

FIGURE 4.—Schematic of a possible sub-surface water probe.

NEUTRON-GAMMA EXPERIMENT

A second possible technique for mapping the Moon for water on the lunar surface is the method of neutron die away. This is one aspect of a neutron-gamma experiment which is under study as a technique for compositional mapping of the lunar surface either in a manned or unmanned mode. A thorough description of this technique has been given by Caldwell et al. (ref. 8) and Mills and Givens (ref. 9), and it will be reviewed briefly here.

The Neutron-analysis method depends on either the spectral or temporal characteristics or both of the gamma rays produced by the interaction of the neutrons with matter. Four types of phenomena have been proposed for determining elemental composition: (1) prompt, (2) capture and (3) activation gamma production, and (4) neutron die away. Prompt gamma rays arise from the inelastic scattering of fast neutrons. The emitted gamma rays are discrete and characteristic of the scattering nucleii. Capture gamma

rays are due to the decay of excited nucleii after neutron capture. In this instance the radiation is characteristic of the compound nucleus. Activation gamma rays arise from either fast neutron reactions, for example (n, p); (n, α) or $(n, 2n)$, or due to the capture of thermal neutrons. The unstable nucleii decay by emitting alpha particles and gamma rays. The temporal character of this emission is shown in figure 5 for a pulsed neutron source. The prompt gammas appear immediately with the neutron irradiation. The capture gamma rays build up rapidly and then decay off. The activation gamma rays continue to build with continued pulsing.

The fourth parameter that can be analyzed in order to determine composition is the rate at which thermal neutrons die away after a burst of fast neutrons. The neutron die away can be conveniently measured by a time analysis of the decay of the capture gamma rays. This last process, if one determines the die away of epithermal neutrons, can be used to obtain an estimate of the hydrogen in the near surface which can in turn be used to estimate the amount of water present.

Figure 6 shows the geometrical arrangement of the neutron probe with relation to the lunar surface. The source, attenuator, and detector are arranged in a straight line. In practice a miniature, pulsed accelerator neutron source is used. This uses a deuterium-tritium reaction to generate 14-meV neutrons. While high fluxes are required for the activation mode, substantially lower fluxes can be used for the prompt, capture,

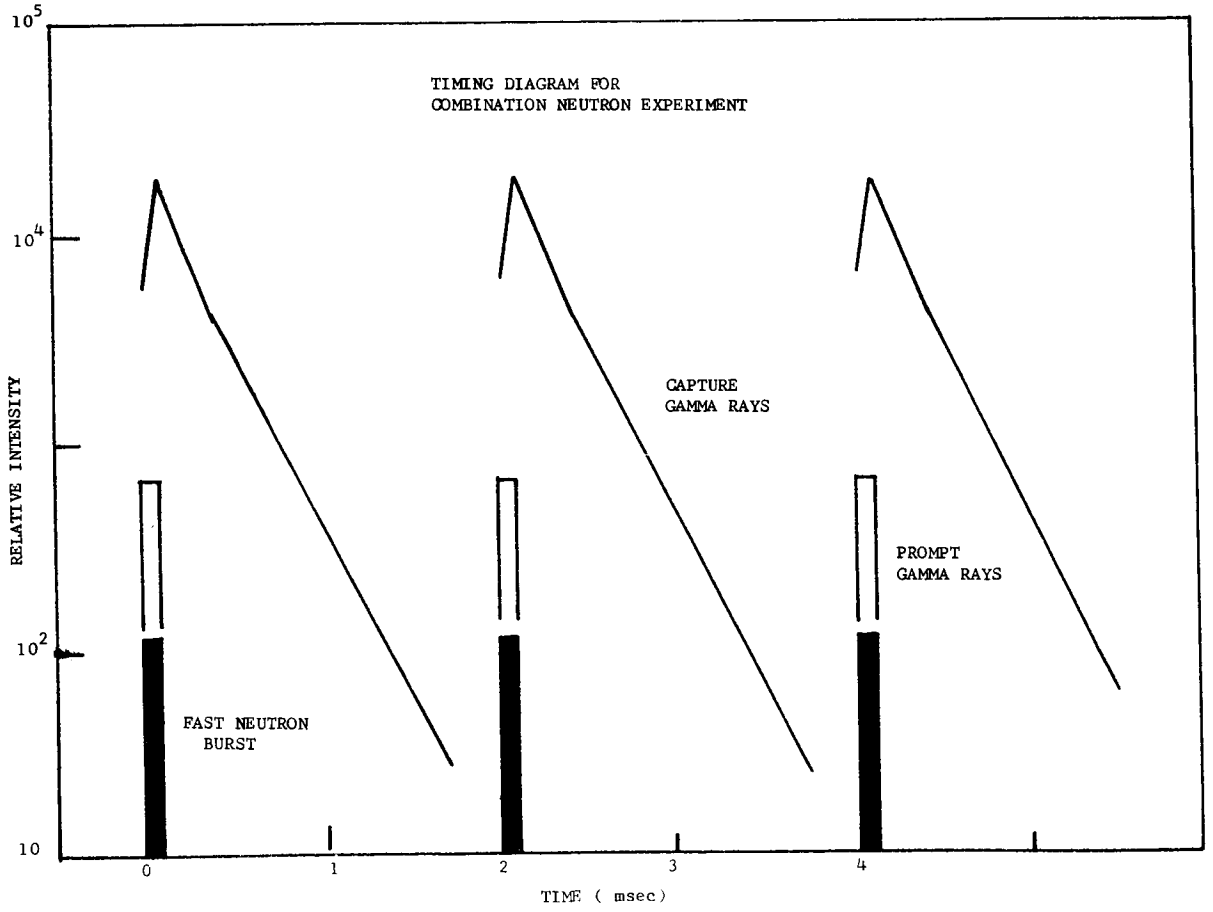

FIGURE 5.—Timing diagram for combination neutron experiment.

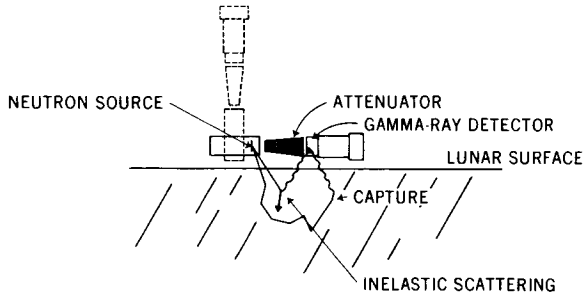

FIGURE 6.—Schematic of combined neutron experiment.

and die away experiment (about 5000 neutrons per pulse at approximately 200 to 1000 pulses/second). The die away of the epithermal neutrons can be discussed in terms of an epithermal removal cross section which includes the removal of neutrons from the epithermal group by absorption and by the slowing down to thermal energies. Since the cross sections for absorption vary as v^{-1}, the absorption process in the epithermal range would tend to remove fewer neutrons than would the moderating or slowing down process. This is especially true if hydrogen is present. Because hydrogen would dominate the slowing down process, the removal cross section should be very sensitive to the presence of even small quantities of water. Thus the die away of epithermal neutrons would provide a very sensitive method for the determination of water in a rock matrix.

In a recent report Mills and Givens have studied the epithermal die away process on three different materials: crushed basalt, crushed granite, and solid granite. Their report indicates that while a measurement of gamma ray intensity die away is convenient, it does not yield the same meaningful information as a direct determination of the removal of the epithermal neutrons. They have made the direct neutron measurements with a Cd-cladHe^3 detector, which in effect fails to detect thermal neutrons. (The thermal neutrons are absorbed in the cadmium.) From these measurements the conclusion is that there is in fact a very sensitive response to the water content. Die away constants have been obtained which semi-quantitatively reflect the amount of water in the rocks.

NEUTRON ALBEDO MEASUREMENTS

The final technique, lunar neutron albedo measurements, involves water determinations to be performed from orbit. In principle we know that cosmic rays interacting with the surface nucleii of the Moon produce neutrons some of which leak out through the surface. The energy spectrum of this emergent albedo will depend strongly on the composition of the surface, especially on the hydrogen content. Thus a measurement of the ratio of slow-to-fast neutrons should serve as an index of the hydrogen content in the lunar surface.

Ligenfelter, Canfield, and Hess (ref. 10) have published detailed calculations on the cosmic-ray-induced leakage spectrum for several model compositions. The results show a variation with mineral type and a strong sensitivity to hydrogen content. Figure 7, taken from the paper of Ligenfelter et al., shows the expected leakage for several compositions including (for chondritic material) two different values of H/Si atomic ratios.

The accuracy of the H/Si absolute measurement is limited by two factors:

(1) The statistical precision with which the ratio of slow-to-fast neutrons can be determined.

(2) The accuracy with which the thermal neutron macroscopic absorption cross section

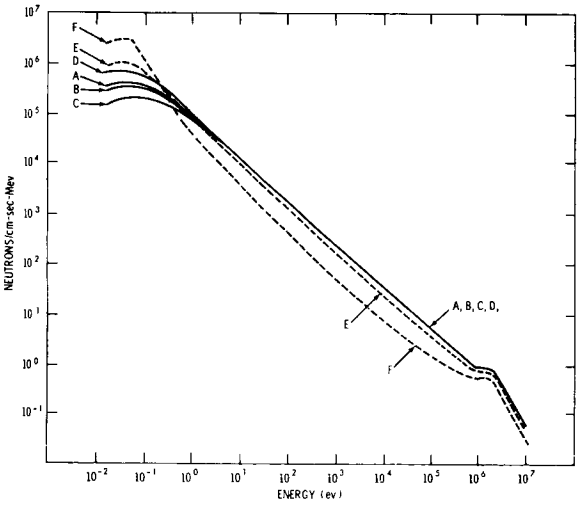

FIGURE 7.—Expected neutron leakage for several soil compositions.

is known. This second factor depends on a knowledge of the lunar surface composition, particularly the concentration of such elements as iron because of the very strong absorption. This information should be supplied by the gamma and X-ray measurements.

Ligenfelter et al. have calculated that hydrogen may be detected by a neutron albedo measurement if the H/Si ratio is 0.05 or greater. The atomic ratio in chondrites where water is approximately 0.3 percent by weight is approximately 0.05. In granite, one finds H/Si ratios of approximately 0.1—twice the minimum detectable ratio.

From present estimates, statistical limitations do not seriously affect the accuracy of the H/Si determination. The relatively high neutron fluxes expected should allow the measurement of slow/fast neutron ratios to approximately ± 10 percent in 30 seconds of sampling time. For H/Si ratios of approximately 0.1, this would only contribute an approximate 10-percent uncertainty to the ratio.

The problem of thermal neutron absorption cross section of the surface material is more serious. For example, if a ±20-percent uncertainty in cross section exists, then the H/Si ratio of 0.1 can only be known to approximately ±30 percent.

In order to perform the previously described measurement, one requires detectors for slow and fast neutrons. Two unmoderated proportional counters filled with BF_3 are proposed for detecting the slow neutrons. These two counters are identical except for ratios of B^{10} to B^{11}. One tube

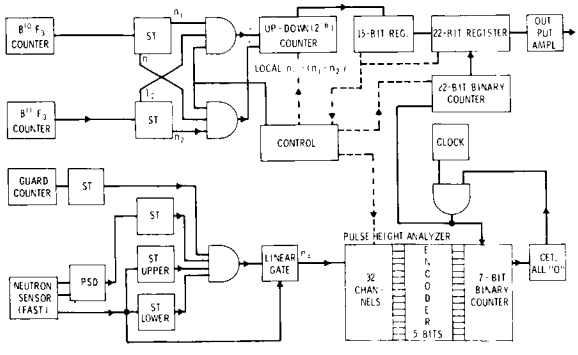

FIGURE 8.—Block diagram of neutron albedo measurement system.

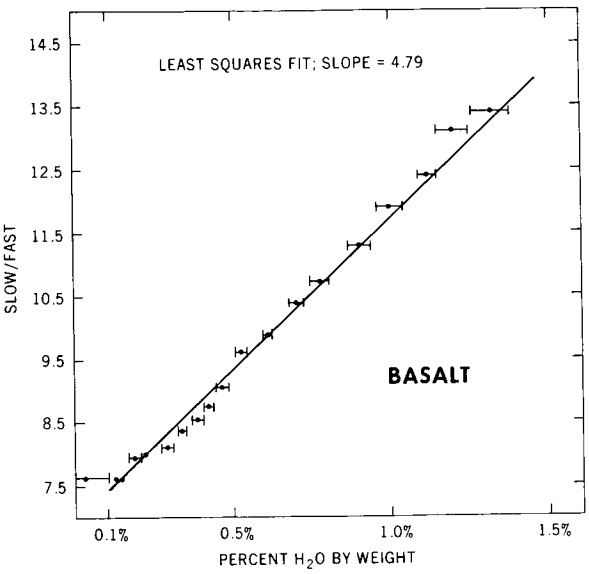

FIGURE 9.—Fast/slow neutron ratio for varying compositions of water in a basalt.

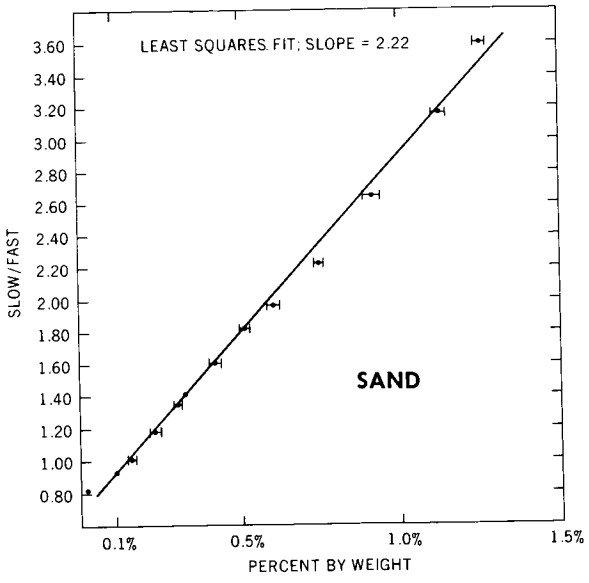

FIGURE 10.—Fast/slow neutron ratio for varying compositions of water in a sand.

contains 96-percent B^{10}, and the second tube uses 10-percent B^{10} and 90-percent B^{11}. The B^{11} isotope does not react appreciably with neutrons; the B^{10} undergoes a (n, α) reaction, forming Li. The reaction has a $1/v$ dependence, where v is the neutron velocity, hence the high sensitivity

to slow neutrons. The method consists of comparing the difference in counting rates between the two detectors and solving the simple simultaneous equations

$$A = 0.96n + b$$

$$B = 0.10n + b$$

where A and B are the respective count rates, b the backgrounds, and n is related to the density of the slow neutrons.

The fast neutrons are detected through the (n, p) elastic scattering process. A special, organic scintillator sensitive to neutrons, is coupled to a photomultiplier. The readout system may consist of a simple multi-channel analyzer, although in this instance one would use the analyzer described earlier. In order to eliminate charged particles such as cosmic rays and gamma rays, an inorganic scintillator is used in the anti-coincidence mode. A block diagram is shown in figure 8.

Finally in figures 9 and 10 from a report by Haymes (ref. 11), we see an example of laboratory measurements made on a basalt and a sand. There is a distinct sensitivity to water concentration which seems, therefore, to warrant further development.

REFERENCES

1. GREEN, J.: Lunar Exploration and Survival. Douglas Paper 4038, June 1966.
2. WEBER, J.; BRINDLEY, G. W.; ROY, R.; AND SHARP, J. H.: Materials Research Laboratory Report, Oct. 1965.
3. GOLD, T.: On the Detection of Water on the Moon. Planetary and Space Science, vol. 15, April 1967.
4. UREY, H. C.: Water on the Moon. Nature, vol. 216, 1967.
5. VAN LOPIK, J. R.; AND WESTHUSING, K.: Exploration for Lunar Water. Proceedings of Lunar and Planetary Exploration Colloquium, vol. 111, Nov. 1963.
6. DEL PICO, J.: Performance of Thin Film Humidity Sensors. Scientific Report No. 1, AFCRL-67-0543.
7. CHLECK, D.; AND BROUSAIDES, F. J.: A Partial Evaluation of the Performance of an Aluminum Oxide Humidity Element, Humidity and Moisture. Vol. I. Reinhold Publishing Corp.
8. CALDWELL, R. L.; MILLS, W. R.; ALLEN, L. S.; BELL, P. R.; AND HEATH, R. L.: Combination Neutron Experiment for Remote Analysis. Science, vol. 152, 1966.
9. MILLS, W. R., JR.; AND GIVENS, W. W.: Neutron Die-away Experiment for Lunar and Planetary Surface Analysis. Final Report to NASA, April 1967.
10. LINGENFELTER, R. E.; CANFIELD, E. H.; AND HESS, W. N.: Lunar Neutron Flux. J. Geophys. Res., vol. 66, 1961.
11. HAYMES, R. C.: Feasibility Study of Lunar Neutron Albedo Experiment. Final Report, NASA Grant NGR-44-006-044, 1969.

S. H. WARD and G. R. JIRACEK
Department of Materials Science and Engineering
University of California
Berkeley, California

W. I. LINLOR
Ames Research Center, NASA

R. J. PHILLIPS
Jet Propulsion Laboratory
Pasadena, California

Electromagnetic Detection of Lunar Subsurface Water

Detection of lunar subsurface water appears possible from a satellite in orbit around the Moon, by use of electromagnetic techniques. Plane-layered models of the Moon have been analyzed in the frequency range of 10^4 to 10^8 Hz, yielding values of reflection coefficient, surface impedance, apparent dielectric constant, and apparent conductivity, for normally incident plane waves. The variation of these quantities with frequency is dependent on the presence or absence of subsurface water (in either liquid or "permafrost" form); that is, a fraction of 1 percent of water, for a wide range of materials that might exist on the Moon, yields characteristic signals. Measurements of other geophysical quantities are described. A typical system for the measurements is described based on the ISIS-A satellite. An orbit around the Moon at an altitude of about 100 kilometers is suitable.

INTRODUCTION

Useful information has been obtained by radar observations of the Moon from earth-based stations. From the echo intensity one may infer the reflectivity of the surface. If the reflectivity were found to be near unity, one would suspect a surface containing considerable water, or perhaps an ionosphere. Because the measured power reflection coefficient is about 6 percent, it may be attributed entirely to an average dielectric constant, found to be 2.8 ± 0.7 for a homogeneous surface layer at least tens of meters in thickness. Measurements have been made of the difference between backscattering coefficients of waves polarized in, and perpendicular to, the local plane of incidence. Such results are in agreement with a lunar model consisting of a tenuous top layer having dielectric constant of 1.8 and thickness of the order of meters, underlaid by a denser layer having dielectric constant of about 5. For such measurements the conductivity of the lunar surface is negligible.

The Earth-based radar wavelengths ranged from 22 meters to 8 mm with a frequency range of approximately 10^7 to 10^{11} Hz. The Earth's ionosphere reflects waves below about 10^7 Hz. The proposed electromagnetic (EM) exploration of the Moon involves measurements having a frequency range from 10^4 to 10^8 Hz, corresponding to wavelengths of 30 kilometers to 3 meters, respectively.

In the proposed system, electromagnetic waves from a spacecraft in lunar orbit are transmitted to the Moon, reflected, and the signals returned to the orbiter are measured with regard to amplitude, phase, and possibly polarization. From these measurements are obtained the electrical conductivity σ and dielectric permittivity K_e of the lunar subsurface to yield four-dimensional mapping over the lunar globe, that is, (1) Variation with frequency, as one

coordinate (2) Variation with depth and area location, as three coordinates

OBJECTIVES

Lunar Interior

The four-dimensional mapping over the lunar globe of the electrical conductivity and the dielectric constant can be expected to provide information on the mineralogical and chemical composition, interstitial water distribution, and density distribution within the lunar interior. Thus any known, inferred, or postulated layering within the Moon (such as the debris layer, permafrost layer, and differentiated layers, as well as gross lateral changes associated with known, inferred, or postulated volcanism, igneous intrustion, mare-highlands contacts, meteorite impacts, mascons, "permafrost" accumulations, etc.), may be evident from the data obtained with the experiment. The fundamental objectives are therefore consistent with the general goals of lunar exploration which are to understand the major geological processes responsible for the character of the lunar surface, and to understand the processes of internal evolution and their surface manifestations.

Lunar Environment

Detection and characterization of a postulated lunar ionosphere is another objective of the proposed experiment. This is fundamental to an understanding of the interaction between the Moon and the solar wind and radiation incident upon it. Measurement of the sheath of charge on the sunlight side of the Moon is also an objective.

Lunar Subsurface Electrical Parameters

The electromagnetic measurements will yield values of the dielectric constant and the conductivity of the lunar subsurface. Such information would give a physical description of the lunar materials and in this sense provide a three-dimensional extrapolation of surface geologic mapping.

The depth of measurement is expected to be as great as 10 kilometers at the lowest frequency, and as great as 1 kilometer at the highest. The width of the sampled region is about equal to the orbital height. The circumference is the projection of the orbit on the lunar surface.

Frequency Dependence of Reflection Coefficient

Variation of the power reflection coefficient as a function of frequency has not been observed to date in Earth based measurements. Dependence of reflection coefficient on frequency in the range of 10^4 to 10^8 Hz would present new information, regardless of subsequent interpretation.

Detection of Layering

Discrete layers, if they exist beneath the lunar surface, will be measured. The details of layering will be evident from the data, as is the case for Earth measurements employing EM techniques.

Major layering within the Moon, such as the known debris layer, postulated ice layer, or differentiated layers, may be identified from the EM profiling. The depth and area of exploration is approximately that described above.

Detection of Gross Inhomogeneities

Gross lateral electrical property changes which arise in volcanism, igneous intrusions, meteorite impact, "permafrost" accumulations, etc. and which possibly will be associated with mascons, mare-highland contacts, and other major geologic contacts should be evident from the EM response. These changes may result from either endogenic or exogenic sources.

Detection of Conductive Materials

The presence of conductive iron, iron oxides, or other metallic minerals is expected to give characteristic EM response.

Detection of Mascons

The presence of shallow mascons in the vicinity of an EM sounder orbit may be evident in the sounder data. The composition of the mascons (i.e., whether they are dense, basaltic phases, or meteorites rich in iron or iron oxides) will determine the nature of the EM response, if such exists. Possibly the details of the response will indicate the size, location and/or the composition of the mascons.

Detection of Lunar Subsurface Water

The presence of subsurface water is evident in characteristic "signatures" obtained in theoretical studies of elementary models of the Moon. Absence of these characteristic signatures implies a dry lunar subsurface.

The depth of measurement is about 1 to 10 kilometers. Presence of water (in pore liquid or permafrost form) can be identified, for amounts greater than a fraction of 1 percent. The width of the sampled region is about equal to the orbital height. The circumference is the projection of the orbit in the lunar surface.

Detection of Lunar Ionosphere

The presence of a lunar ionosphere will be measured if the plasma density is 1 electron/cm^3 or greater, with a reflecting horizon greater than approximately 30 km away from the spacecraft. A density of 10^6 electrons/cm^3 represents the upper limit to the measurement (as in the case of the Earth's ionosphere), although so high a density is not expected.

Variation of the lunar ionosphere with position relative to the Sun may be measured.

Solar Wind EM Noise

Measurements during programmed transmitter-off intervals will yield values for EM noise caused by solar wind interacting with the Moon, as well as natural plasma oscillations within the solar wind. These measurements can be related to the spacecraft position relative to the Sun; when the spacecraft is shielded from the Sun by appreciable lunar mass, solar wind EM noise may be absent.

Cosmic Noise

A passive measurement during programmed transmitter-off intervals can yield values for EM noise of cosmic origin. These measurements can be related to the spacecraft position relative to the Sun and Earth.

Earth Transmissions

Measurements during programmed transmitter-off intervals will yield values for EM Earth transmissions in the frequency range above Earth ionosphere cutoff. Bistatic measurements of lunar subsurface electrical parameters then become possible.

Earth Receptions

At frequencies above the Earth ionosphere cutoff, reception of transmitted lunar EM sounder signals may be possible. If so, then bistatic measurement of lunar subsurface electrical parameters will be possible.

Development for Future Lunar and Planetary EM Experiments

Experience gained at an early date with a lunar EM sounder would be invaluable in designing EM systems for such important missions as the orbital detection of water on or below the Martian surface, orbital detection of the presence of an ionosphere, and the mapping of major geologic units on Venus.

SIGNIFICANCE

Electromagnetic exploration of the Moon is significant in the knowledge to be gained from the electromagnetic sounding of the distribution of rock types and water in the lunar crust. This information is extremely important in terms of the origin, evolution, and current state of the Moon. In particular, the four dimensional mapping of the dielectric constant and conductivity is expected to provide information regarding the lunar subsurface chemical composition, distribution of interstitial water, and possibly temperature distribution within the lunar interior (although temperature may not markedly affect the electrical parameters to depths of approximately 10 km beneath the lunar surface). Major layering within the Moon (such as the known debris layer, postulated permafrost layer, or differentiated layers, as well as gross lateral changes associated with volcanism, igneous intrusion, mare-highlands contacts, meteorites, mascons, and similar features) may be evident in the data from the EM sounding from lunar orbit.

Characterization of the geometry of subsurface physical changes associated with mascons will greatly enhance our understanding of these features. The association of subsurface water with the mascons and its distribution would

also be a line of evidence bearing on a volcanic or impact origin for the anomalies. Both of these lines of information on the mascon problem are amenable to study by EM sounding.

In addition, the identification of such potential natural resources as water, carbon, or metallic minerals in oxide or sulphide form may have important implications for life support on the lunar surface or as resources for other space missions. Detection and measurement of a lunar ionosphere would have important implications regarding the interaction between the Moon and the solar wind. A sheath layer at the Moon's surface, if detected, would have implications concerning interaction between solar radiations and the lunar surface.

The important recent results derived from deep EM experiments through ice and low loss rocks and soils on Earth, strongly suggest that electromagnetic sounding through anticipated low loss materials beneath the lunar surface will provide a three-dimensional picture of lunar geology and structure to depths as great as 10 km.

LUNAR WATER

Let us review published material regarding the possibility of occurrence of water or ice on the Moon. Basically our position is that we take no strong stand one way or the other, but we believe that EM measurements from lunar orbit can provide a meaningful answer. The possibility of the occurrence of water or ice on the Moon has been discussed by Kopal (refs. 1 to 3); Gold (refs. 4 to 6); Gilvarry (ref. 7); Hapke and Goldberg (ref. 8); Urey (refs. 9 to 11); Lingenfelter et al. (ref. 12); and others. Gold estimates the upper boundary of the permafrost to be about 30 meters below the surface, and the lower boundary to be between 1 and 10 km. Kopal suggests an upper boundary at about 50 kilometers. Research at Jet Propulsion Laboratory (Pasadena) indicates that permafrost may even be associated with lunar surface features.

MAJOR ASSUMPTIONS

Let us now define the major assumptions for this paper. The first is perpendicular incidence of plane waves. Although finite sources would be used in any experiment, this approximation is adequate for providing a first appraisal. The second assumption is that of plane-layered models; that is, we take a zero-curvature model of part of the lunar surface. Third, we assume that scattering from discrete objects, lateral inhomogeneities, and other anisotropic features may be ignored. This assumption is justified provided that the wavelengths used are long relative to the dimensions of the scatterer. It implies that the depth to an interface is large compared with the local topographic relief, and that the Moon is radially layered in the gross sense, in such a manner that the plane wave impedance decreases with depth. For a substantial fraction of the lunar surface it is probable that the above conditions will be met for frequencies less than 10^6 Hz. The fourth assumption is related to the one just discussed, namely that we have true specular reflection from the mean surface of a layer. Such an approach is taken routinely on Earth, with full realization of its limitations, to obtain depths to impedance discontinuities.

Although sharp radial boundaries are not nearly as likely as gradual transitions, it is convenient to represent a radial change by one or more step-function changes in the electrical parameters. Such an approximation can be refined by recalculations on a computer utilizing a large number of incremental changes to approximate any smooth change. At the present time, however, our estimate of the distribution of electrical parameters of the Moon has such great ranges of uncertainty that a lengthy calculation would have little merit. Major subdivisions of the lunar interior can be recognized as being the dry outer shell, a wet or somewhat conducting shell, and the hot interior. Later we shall specify the layer models more precisely.

The fifth assumption is that Moon materials in the wet or dry states will have electrical properties similar to Earth materials in the corresponding states. The validity of this basic input information is unknown at present. The sixth, and last of our major assumptions, is that the measurement of the EM reflections will have an accuracy of at least $\pm$ 1 db, or $\pm$ 10 percent in amplitude. Absolute accuracy to this precision is not re-

quired, but rather relative measurements to compare selected regions with each other. It should be noted that all six assumptions are being verified by further theoretical work and will be checked by experiment with suitable scaled models.

THEORETICAL BASIS FOR CALCULATIONS

The complex plane wave impedance Z, for an $e^{i\omega t}$ time dependence, of a homogeneous, non-magnetic half space is

$$Z = Ze^{i\phi} = \frac{i\mu_0\omega}{\gamma} = \pm\frac{E_j}{H_k}; \qquad j \neq k \tag{1}$$

where ϕ is the phase and $|Z|$ the modulus of Z, ω is the angular frequency, μ_0 is the magnetic permeability of free space, γ is the wave number of the half space, and E_j and H_k are orthogonal electric and magnetic intensity pairs. The wave number is

$$\gamma = [i\mu_0\omega(\sigma' + i\epsilon'\omega)]^{1/2} \tag{2}$$

in which the dielectric permittivity ϵ', and the conductivity σ' are real functions of frequency. The loss tangent is defined by

$$\tan\delta = \frac{\sigma'}{\omega\epsilon'} \tag{3}$$

The amplitude reflection coefficient for normal incidence is

$$r = \frac{Z - Z_0}{Z + Z_0} \tag{4}$$

where Z_0 is the plane wave impedance of free space. At high frequencies such that $\frac{\sigma'}{\omega\epsilon'} \ll 1$, γ is imaginary so that Z and hence r are real. We could replace (2) by

$$\gamma^2 = i\mu_0\omega\sigma \tag{5}$$

where

$$\sigma = \sigma' + i\epsilon'\omega \tag{6}$$

is a complex conductivity which can account for both real conductivity and dielectric constant. This complex conductivity is then related to the impedance as follows:

$$\sigma = \frac{i\mu_0\omega}{(Z)^2} = \frac{i\mu_0\omega}{|Z|^2 e^{i2\phi}} \tag{7}$$

$$\sigma' = \frac{\mu_0\omega}{|Z|^2}\sin 2\phi \tag{8}$$

$$\epsilon' = \frac{\mu_0}{|Z|^2}\cos 2\phi \tag{9}$$

For an n-layered structure, we may use the formulation

$$Z_a = Z_1\frac{\hat{Z}_2 + Z_1\tanh\gamma_1 h_1}{Z_1 + \hat{Z}_2\tanh\gamma_1 h_1} \tag{10}$$

$$\hat{Z}_2 = Z_2\frac{\hat{Z}_3 + Z_2\tanh\gamma_2 h_2}{Z_2 + \hat{Z}_3\tanh\gamma_2 h_2} \tag{11}$$

$$\hat{Z}_{n-1} = Z_{n-1}\frac{\hat{Z}_n + Z_{n-1}\tanh\gamma_{n-1}h_{n-1}}{Z_{n-1} + \hat{Z}_n\tanh\gamma_{n-1}h_{n-1}} \tag{12}$$

where $Z_j = \frac{i\mu_0\omega}{\gamma_j}$ is the characteristic impedance of the jth layer. $\hat{Z}_j$ is the impedance at the top of the jth layer, and Z_a is the *surface impedance* of the structure, equal, at any given frequency, to the impedance of an equivalent homogeneous half space. The h_j are the thicknesses of the layers in the structure. The nth layer is semi-infinite, therefore, $\hat{Z}_n = Z_n$.

Thus the amplitude reflection coefficient for an n-layered structure is

$$r = \frac{Z_a - Z_0}{Z_a + Z_0} \tag{13}$$

and the complex apparent conductivity, the real apparent conductivity, and the real dielectric permittivity are from equations (7), (8), and (9), respectively

$$\sigma_a = \frac{i\mu_0\omega}{|Z_a|^2 e^{i2\phi_a}} \tag{14}$$

$$\sigma_a' = \frac{\mu_0\omega}{|Z_a|^2}\sin 2\phi_a \tag{15}$$

$$\epsilon'_a = \frac{\mu_0}{|Z_a|^2} \cos 2\phi_a \qquad (16)$$

In terms of dielectric constant rather than permittivity,

$$K' = \frac{\mu_0}{\epsilon_0} \frac{1}{|Z|^2} \cos 2\phi \qquad (17)$$

and

$$K'_a = \frac{\mu_0}{\epsilon_0} \frac{1}{|Z_a|^2} \cos 2\phi_a \qquad (18)$$

where ϵ_0 is the dielectric permittivity of free space.

LUNAR PARAMETERS

For the region above the lunar surface we have assumed free space values for the electrical parameters. On the sun-lit side of the Moon, there may be a lunar ionosphere as well as a plasma sheath, whose electron plasma frequency may be as high as 10^5 Hz, and therefore would compromise measurements at this or lower frequencies. However, measurements can be made of the Moon on its dark side (and thus eventually for an appropriate orbit, all of the moon can be so measured), where the electron plasma frequency is expected to be lower than 10^4 Hz.

The magnetic permeability of the Moon is quite unknown, because we have no knowledge of the composition or magnetic history of any magnetic minerals that might be present in lunar rocks. Recent results from the Surveyor 5 show apparent agreement with the amount of magnetite expected in a basaltic rock. For this reason, and because the permeability of Earth rocks is confined to the relatively narrow range of 1.00 to 1.25, we shall assume for simplicity the free-space value of unity for the magnetic permeability in all our calculations.

We next consider the values of frequency-dependent parameters of hypothetical lunar materials. These are given in figures 1, 2, and 3, respectively for dielectric constant, conductivity, and loss tangent as functions of frequency. It is assumed that these curves may be representative of lunar materials in the wet or dry states; at least such frequency dependence of the parameters can be considered to be a first approximation to actual lunar materials. The

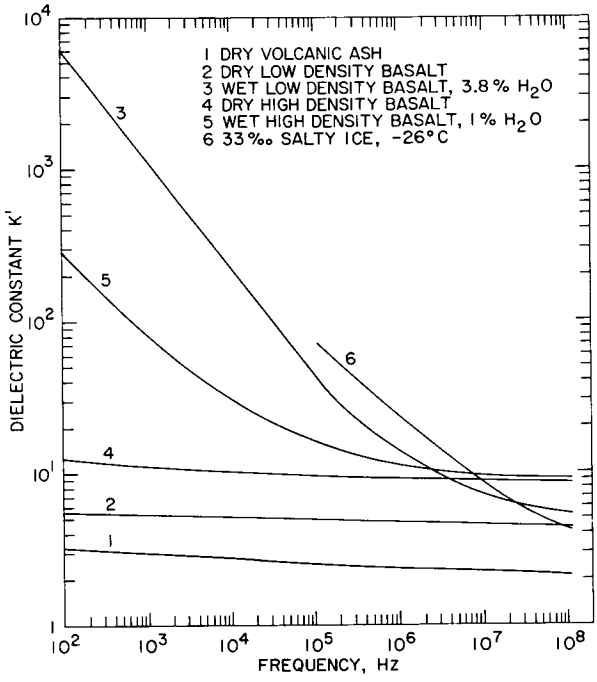

FIGURE 1.—Variation of dielectric constant with frequency.

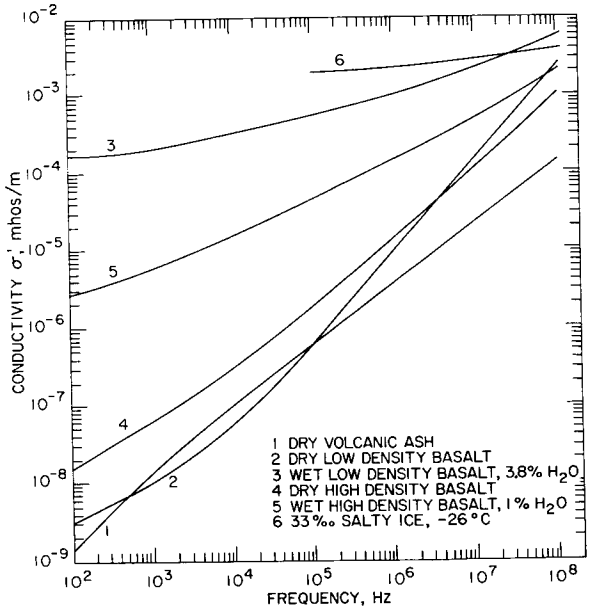

FIGURE 2.—Variation of conductivity with frequency.

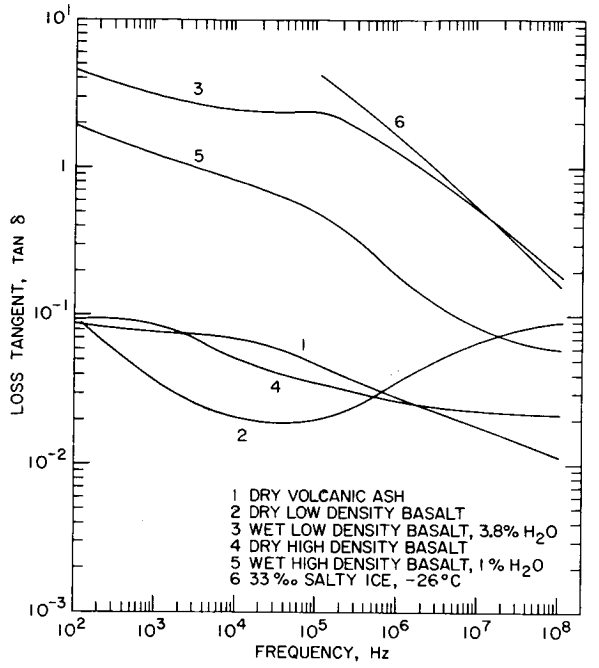

FIGURE 3.—Variation of loss tangent with frequency.

results are from measurements made at the Massachusetts Institute of Technology Laboratory for Insulation Research. The samples consisted of loose volcanic ash soil with dry density 0.76 g/cm³, low density basalt with dry density 1.4 g/cm³, and high density basalt with dry density 2.7 g/cm³. The conductivities and dielectric constants were measured at room temperature, following heat treatment at 105°C for 3 days. Percentage of water present is indicated on the curves, the water resistivity being 10-ohm meters.

LUNAR MODELS AND ASSOCIATED RESULTS

The effect of lunar subsurface water is shown by various models. It should be kept in mind that although a variety of models can be postulated which will give the same value of apparent impedance at a given frequency, the variation with frequency greatly reduces the ambiguity; furthermore, the variation appears to be uniquely correlated with the presence of water or permafrost. To demonstrate this, the amplitude of the reflection coefficient versus frequency is shown for representative models which are described below.

Figure 4 describes a dry model, 1a, and a wet model, 1b; the water content for the wet model is 3.8 percent. For these two models, figure 5 shows the amplitude of the reflection coefficient plotted versus frequency. The difference in the curves for models 1a and 1b is quite pronounced.

Figure 6 describes a model that is somewhat similar to the preceding one; the dry model, 2a, is compared to a wet model, 2b. The water content for model 2b is only 1 percent. Despite the low water content, the amplitude of the reflection coefficient plotted versus frequency in figure 7 shows a definite difference in the response between the wet and dry models.

The effect of a layer of permafrost is shown in the next case. Figure 8 gives the layer characteristics; as in the preceding two cases, a layer of dry volcanic ash 10 meters thick constitutes the top layer. The permafrost layer is taken to

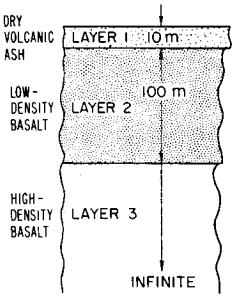

LAYER	k' (SEE FIG 1)	σ' (SEE FIG 2)	CONDITION	MODEL
1	CURVE 1	CURVE 1	DRY	1a
2	CURVE 2	CURVE 2	DRY	
3	CURVE 4	CURVE 4	DRY	
1	CURVE 1	CURVE 1	DRY	1b
2	CURVE 3	CURVE 3	"WET"	
3	CURVE 5	CURVE 5	"WET"	

FIGURE 4.—Illustrative model of lunar layers, models 1a and 1b.

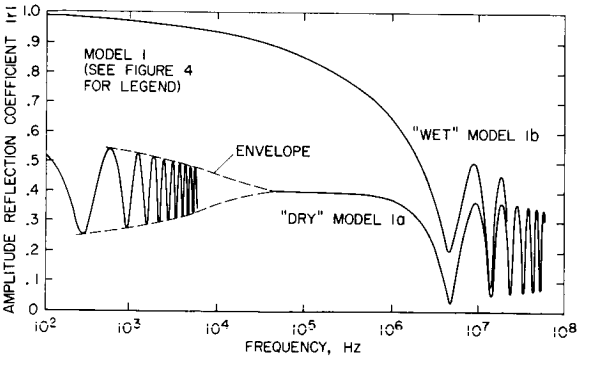

FIGURE 5.—Amplitude of reflection coefficient versus frequency, model 1.

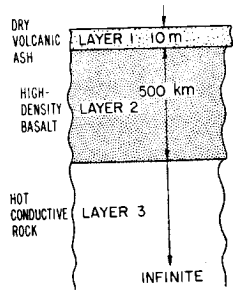

LAYER	k' (SEE FIG 1)	σ' (SEE FIG 2)	CONDITION	MODEL
1	CURVE 1	CURVE 1	DRY	2a
2	CURVE 4	CURVE 4	DRY	
3	100	10^{-2} mhos/m	–	
1	CURVE 1	CURVE 1	DRY	2b
2	CURVE 5	CURVE 5	"WET"	
3	100	10^{-2} mhos/m	–	

FIGURE 6.—Illustrative model of lunar layers, models 2a and 2b.

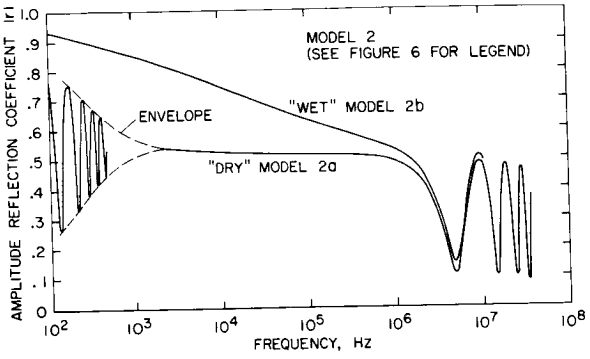

FIGURE 7.—Amplitude of reflection coefficient versus frequency, model 2.

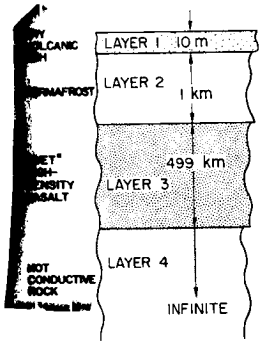

LAYER	k' (SEE FIG 1)	σ' (SEE FIG 2)	CONDITION	MODEL
1	CURVE 1	CURVE 1	DRY	3
2	CURVE 6	CURVE 6	"WET"	
3	CURVE 5	CURVE 5	"WET"	
4	100	10^{-2} mhos/m	–	

FIGURE 8.—Lunar model with permafrost.

be 1 kilometer thick. Because the characteristics of the permafrost are known only to 10^5 Hz, the amplitude of the reflection coefficient versus frequency is plotted in figure 9 only to 10^5 Hz. The shape of the curve demonstrates a pronounced "signature" that is characteristic of the presence of water.

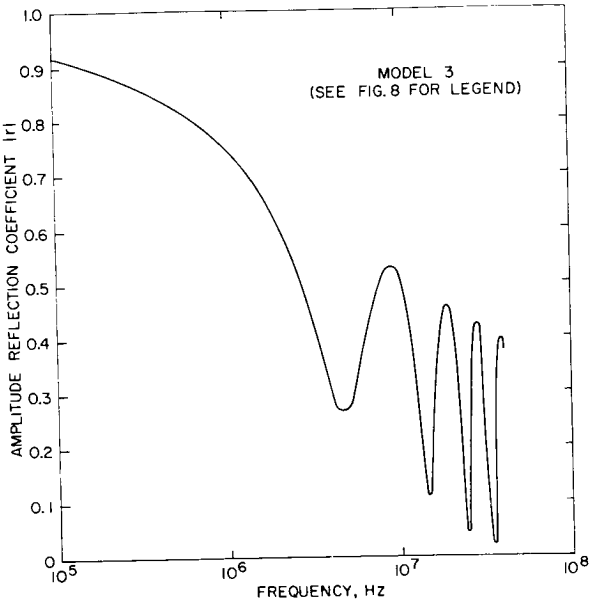

FIGURE 9.—Reflection coefficient versus frequency, permafrost model.

In all of the preceding cases, the models had dry volcanic ash 10 meters thick for the top layer. In order to see the effect of a varying thickness of dry volcanic ash, three thicknesses were analyzed, each on top of a second layer alternatively dry basalt, basalt with 1-percent water, and permafrost. The combinations are given in table I.

TABLE I.—*Effect of Dry Volcanic Ash*

Model	Layer 1 (meters)	Layer 2		
		k'	σ'	Condition
4a.....	1000	curve 4	curve 4	Dry
4b.....	1000	curve 5	curve 5	1-percent water
4c.....	1000	curve 6	curve 6	Permafrost
5a.....	100	curve 4	curve 4	Dry
5b.....	100	curve 5	curve 5	1-percent water
5c.....	100	curve 6	curve 6	Permafrost
6a.....	10	curve 4	curve 4	Dry
6b.....	10	curve 5	curve 5	1-percent water
6c.....	10	curve 6	curve 6	Permafrost

NOTE: Layer 1 consists of dry volcanic ash; see figure 1, curve 1 for k' and figure 2, curve 2 for σ'. Layer 2 has a thickness of 500 km in each case; see figure 1 for k' curves, and figure 2 for σ' curves.

The variation of the amplitude of the reflection coefficient versus frequency is given in figure 10. It will be noted that regardless of the thickness of the top layer (i.e., whether 10, 100, or 1000 meters), the asymptotic value of the reflection coefficient approaches a value of about 0.5, for a dry second layer. However, for wet basalt or permafrost as the second layer, the reflection coefficient exhibits a dependence on frequency that can be identified as a "water signature."

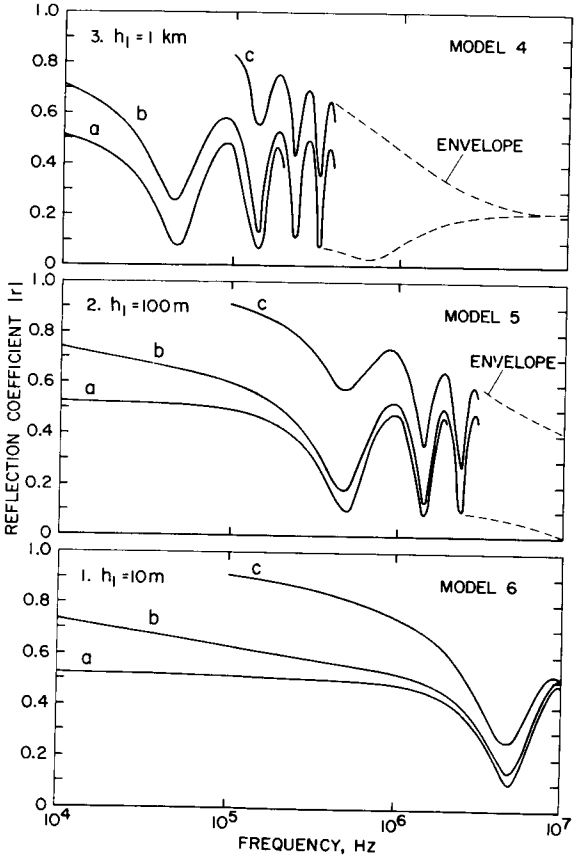

FIGURE 10.—Reflection coefficient versus frequency, models in table I.

BRIEF DESCRIPTION OF POSSIBLE ORBITAL SYSTEM

As an illustration of a flight-rated system that can be employed for EM exploration of the Moon, we consider an ISIS–A sounder aboard an Apollo Command and Service Module, as indicated in figures 11 and 12. The ISIS–A

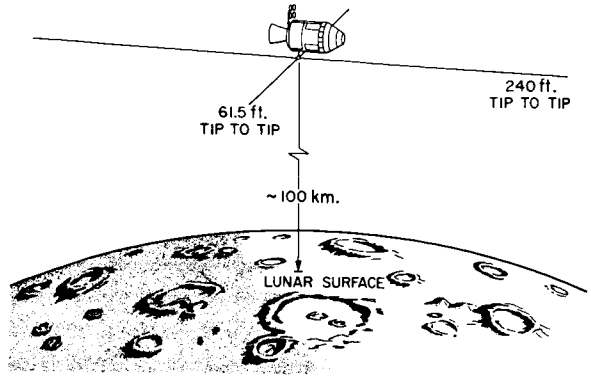

FIGURE 11.—Command and Service Module Sounder antennas.

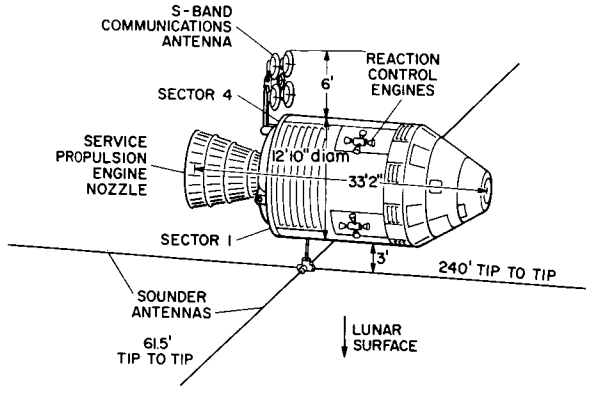

FIGURE 12.—Command and Service Module with antennas deployed.

sounder characteristics are described below (figs. 13 and 14):

(1) Antennas
  Two crossed dipoles, 61.5 ft and 240 ft tip to tip

(2) Power output
  - 400w at 30 pulses/sec (100 μsec pulse)
  - 100w at 30 or 60 pulses/sec

(3) Power input
  30w (average)

(4) Weight
  38 lb instruments
  32 lb antennas
  70 lb total

(5) Frequency
  - Swept: 0.1 to 20.0 MHz in 27 sec

- Fixed: 0.25, 0.48, 1.0, 1.95, 4.0 or 9.3 MHz

(6) Receiver

Switched input filters and low noise preamp single I.F. 24.0167 MHz, bandwidth 55 kHz linear-logarithmic AGC, 50 db dynamic range post-detection bandwidth: dc to 15 kHz

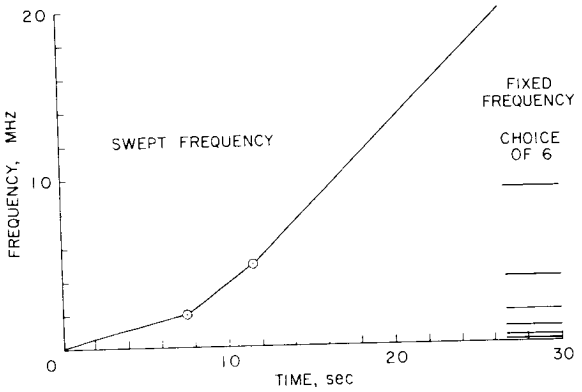

FIGURE 13.—ISIS-A Sounder frequencies in graph form.

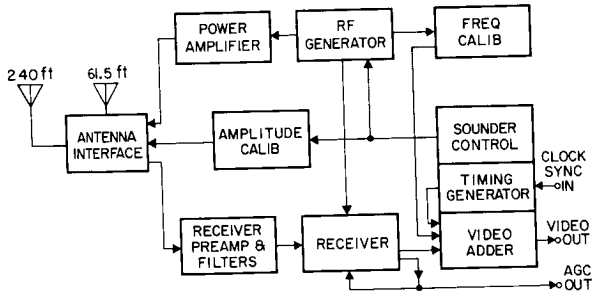

FIGURE 14.—ISIS-A Sounder block diagram.

Experimental Concept

A center-fed electric dipole antenna of an ISIS-A topside ionospheric sounder, mounted in sector 1 of the service module of the Apollo spacecraft, transmits sinusoidal electromagnetic waves in pulses at a repetition rate of 30 per second. Subsequent to each pulsed transmission, the antenna is used for reception. The outgoing electromagnetic wave is reflected from the lunar surface, and possibly from interfaces above or beneath the lunar surface; the reflected wave is monitored by the dipole antenna used in the receive mode. If the shape, amplitude, or time of the received pulse is known relative to the shape, amplitude, or time of the transmitted pulse, then information on the electrical parameters to depths as great as 10 km within the Moon can be obtained. Information on the character and particle content of any assumed lunar ionosphere might be obtained also. The carrier frequency is swept from 10^5 Hz to 2×10^7 Hz in 26 seconds via three linear segments of a frequency-time plot; this is the swept frequency mode. A 4-second flyback time permits the sweep system to recover from the sweep. During this time, the transmitter and receiver may be used in a fixed frequency mode wherein any single frequency may be used. A number of alternate modes of operation are available via a programmed sequencer.

Method and Procedures for Carrying Out the Experiment

The antennas are mounted on a boom in sector one of the Apollo Service Module. First the boom is deployed from sector one, then the antennas are deployed from the boom. The transmitter and receiver are turned on for a period of time ranging from one lunar orbit to 3 days. Measurements are made at the rate of 30 per second while the Command and Service Module (CSM) is in steady-state orbit. The measurements are transmitted to Earth via PCM and video channels. On the anti-Earth side of the Moon, data is stored on magnetic tape for replay. The video data reveal the amplitude, shape, and time of all received pulses at all frequencies while the PCM data reveals only the amplitude of the first reflected pulse. The data from PCM and video channels are stored on Earth based magnetic tape for subsequent processing and analysis.

When the experiment is completed, the system is turned off and the antennas and boom are retracted. Alternatively, the boom and/or antennas may be pyrotechnically jettisoned.

Choice of sequence of permissible modes of operation (swept frequency, fixed frequency, and combinations thereof) is selected by preprogramming.

Measurements To Be Made and Ranges of Numerical Values Expected

In the PCM channel, amplitudes of reflected pulses are obtained at the rate of 30 per second and are expected to range from 0.2 to 1.0 times the transmitted pulse amplitude, decreased by the path losses from antenna to lunar surface to antenna. In the video channel, the times, shapes, and amplitudes of the reflected pulses, as modified by the transfer function of the data link, are to be recorded at the rate of 30 per second.

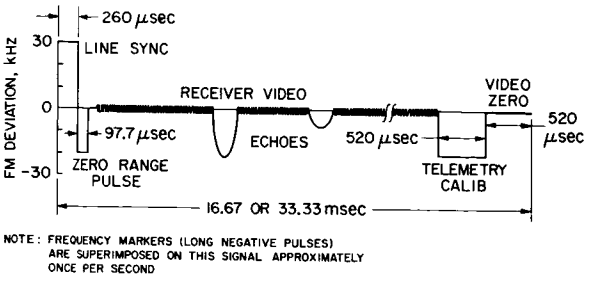

FIGURE 15.—ISIS-A Sounder line format.

Interpretation Procedures

Interpretation of the data will proceed as in the case of Earth based EM exploration in the broad sense. That is, alternative initial models will be evident from a preliminary scan of the data, then iterative procedures will narrow the selection of models. Further refinement may be obtained through additional information from companion experiments such as photography, radar measurements, etc. The form of the data is given in figure 15. The received echo pulse (or pulses) is transmitted to Earth via several modes of transmission which are discussed separately.

TV Video Link with 500 000-Hz Bandwidth

This mode of transmission permits accurate reproduction of the amplitude, shape, and time of arrival of the echo pulse. Correction for the receiver and data link transfer functions permits extraction of the complex reflection $r(f)$ coefficient for the frequency range employed in the sounding. Although one may interpret the complex $r(f)$ directly, physical understanding is aided by analysis employing the apparent conductivity, $\sigma_a(f)$, and the apparent dielectric constant, $\epsilon_a(f)$, given by

$$\sigma_a(f) = \frac{1}{z_0} \operatorname{Imag}\left(\frac{1-r(f)}{1+r(f)}\right)$$

$$\epsilon_a(f) = \frac{1}{2\pi f z_0} \operatorname{Real}\left(\frac{1-r(f)}{1+r(f)}\right)$$

where z_0 is the impedance of free space, 377 ohms. In the preceding relations it is assumed that the lunar material is magnetically non-permeable, and that the region above the lunar surface exhibits the electrical characteristics of free space. These assumptions are not necessary, but are convenient to illustrate interpretation procedure.

The plots of $\sigma_a(f)$ and $\epsilon_a(f)$ may be used directly to determine the distribution of electrical parameters with depth, on the reasonable assumption that the depth of sounding is inversely proportional to frequency.

The important point to be noted is that Fourier analysis (with the Fast Fourier Transform or FFT) yields the frequency spectrum of the returned pulses. Because considerable spectral overlap exists in the successive pulses, it is possible to cross-check various Fourier components of the signals, despite the fact that successive pulses differ slightly in transmitted frequency and are reflected from slightly different lunar locations. The preceding interpretation dealt with the frequency domain. We now consider the time domain.

The arrival times of distinct received pulses from various geologic horizons or strata involve the product of the path length and the dielectric constant. Interpretation is analogous to the seismic reflection method, which is well-established in terrestrial situations.

The shapes of the pulse envelopes and the amplitudes of the individual pulses each can be quite diagnostic of the nature and distribution of lunar rocks and soils. This is particularly true when rocks that are dry are compared with rocks having 1 percent or more of moisture (ref. 13). From the pulse shape Morrison et al. (ref. 14) have demonstrated a quantitative means of interpretation; they have also demonstrated the concept of

time dependency of apparent conductivity in time domain interpretation. In the latter case, the time axis is the depth sounding axis. This type of interpretation, while novel, is based on well-established and sound physical principles.

PCM Mode

In the PCM mode, which is available for most of the lunar circumference, only the amplitude of the received signal (i.e., the first echo) is measured. This can be plotted versus frequency in the manner shown in figure 5. The subsequent interpretation depends on the construction of a model of the lunar subsurface that matches the observed data. In figure 5, for example, the variation of the amplitude of the reflection coefficient versus frequency is markedly dependent on the presence of water.

Areal Extent of Return and Surface Roughness

For specular reflection, the Fresnel zones for a particular frequency dictate the areal extent of the return because of the essentially unconstrained antenna pattern and the fact that the return is in the vicinity of normal incidence. The effect of roughness is to produce signal returns from regions outside the major Fresnel zones. This has a dispersion effect in time, and possibly may cause interference with the dispersion produced by conductivity within the lunar subsurface. From a knowledge of the lunar surface statistics, the dispersion due to roughness scattering may be removed (deconvolved). Information on lunar surface roughness may be deduced from (1) Earth based radar information, (2) orbiter photography, (3) altitude radar and metric cameras aboard the CSM on which the proposed experiment is mounted, and (4) altitude radar and metric cameras aboard earlier or later Apollo missions. The influence of roughness may be studied by means of scaled models in which the photographed lunar surface roughness is reproduced, and possibly by calculation.

Effect of Solar Plasma on Lunar Interior Studies

For average solar wind conditions, the effect of the plasma should not complicate the interpretation (refs. 15 and 16). The presence of a lunar ionosphere greater than 100 electrons per cm^3 may possibly complicate the Moon echo interpretation at the low-frequency portion of the sweep. On the dark side of the Moon this problem is not expected.

Lunar Ionosphere

The form of the data is given in figure 15. The transmitted pulse consists of a sine wave of frequency f Hz, truncated by pulse boundaries having time extent τ_p. The value of τ_p for ISIS–A sounder is 97.7 μsec.

The condition for transmission of the sine-wave pulse is given by *approximately:*

$$f \geq 0.9 \times 10^3 \sqrt{N_e} = f_p \text{ Hz}$$

where N_e is the number of electrons per cm^3. When f is equal to f_p, the wave is reflected.

The distance h from the spacecraft at which the wave is reflected is given by *approximately:*

$$h = c\tau/2 \text{ km}$$

where c represents the speed of light in kilometers/second and τ is expressed in seconds. The time τ is the travel time of the pulse from the spacecraft to the reflecting region and back to the spacecraft. Thus the measurements of f and τ yield values for N_e and h, which represent the electron number density profile of the lunar ionosphere. The minimum value of τ for non-ambiguous interpretation is, of course, the value of τ_p (sounder pulse time). For $\tau_p = 97.7$ μsec., the minimum value of h is about 15 km.

It is clear from the transmission and reflection conditions discussed at the beginning of this section that the sounding can measure only an electron density that increases with distance from the spacecraft. The lowest frequency employed is 10^5 Hz; this corresponds to a density of about 100 electrons per cm^3.

At present, theories regarding the density profile of the lunar ionosphere are based on quite arbitrary assumptions. It is not at all certain whether a maximum in electron density will occur above or below the spacecraft nominal altitude of 100 km. However, whether such a maxi-

mum does indeed occur above or below the spacecraft, the electron density profile to such a maximum can be measured. If the maximum lies between the spacecraft and the lunar surface, this may be determined by effects on the pulses whose frequencies barely permit penetration through the plasma, are reflected by the lunar surface, and return through the plasma to the spacecraft.

CONCLUSIONS

We have employed elementary two-, three-, and four-layer planar models of the Moon to calculate the reflection coefficient, apparent dielectric constant, and apparent conductivity for normally incident plane waves in the frequency range of 10^4 to 10^8 Hz. Values can be obtained for the lunar subsurface electrical parameters, and thicknesses of some layers. Of particular interest is the possibility of determining the presence or absence of water (in pore liquid or permafrost form) if the measurements are sufficiently precise. The power return to an orbiting antenna, on the pessimistic side, may only differ by 2 to 3 db (or even less) between a dry and a wet Moon, and this may be just within the limits of current technology. On the other hand, the power return between a dry model and either a wet model or a permafrost model may differ by 5 or 6 db or more.

The lower the frequency, the greater the difference between reflection coefficients for dry and wet (or permafrost) models. The low-frequency end may be set by technological considerations rather than plasma problems, for measurements taken in the plasma void on the dark side of the Moon.

An upper frequency limit of about 10^8 Hz will assure that discrete scattering from objects smaller than about 10 meters in mean dimension will be negligible. Scatterers larger than this should represent geologically significant items. Electromagnetic returns from them will contribute information useful for three dimensional geological mapping.

The sparsity of reliable spectra of conductivity and dielectric constant under variation of rock type and composition, percent saturation, pore water salinity, temperature, and pressure represent the greatest single uncertainty in the theoretical analysis of lunar electromagnetic experiments. Much of this uncertainty can be removed by laboratory tests with suitable simulated lunar material.

REFERENCES

1. KOPAL, Z.: The Internal Constitution of the Moon. Planetary and Space Sci., vol. 9, 1962, pp. 625–638.
2. KOPAL, Z.: Stress History of the Moon and of Terrestrial Planets. Icarus, vol. 2, 1963, pp. 376–395.
3. KOPAL, Z.: An Introduction to the Study of the Moon. Gordon and Breach, 1966.
4. GOLD, T.: Processes on the Lunar Surface. In: *The Moon*, Symposium No. 14, International Astronomical Union, edited by Z. Kopal and Z. K. Mikhailov, Academic Press, New York, 1962.
5. GOLD, T.: The Presence of Ice Under the Moon's Surface. Trans. AGU, vol. 46, No. 1, 1965, p. 139.
6. GOLD, T.: The Moon's Surface. In: *The Nature of the Lunar Surface*, Proceedings of the 1965 IAU–NASA Symposium, Baltimore, The Johns Hopkins Press, 1966.
7. GILVARRY, J. J.: Evidence for the Pristine Presence of a Lunar Hydrosphere. Publ. Astron. Soc. Pacific, vol. 76, No. 451, pp. 245–253.
8. HAPKE, B. W.; AND GOLDBERG, L. S.: Molecular Flow Through Soils and the Possibility of Lunar Permafrost Layers. Trans. AGU, vol. 46, No. 1, 1965, p. 139.
9. UREY, H. C.: A Review of Atomic Abundances in Chondrites and the Origin of Meteorites. Rev. Geophysics, vol. 2, 1964, p. 1.
10. UREY, H. C.: Meteorites and the Moon. Science, vol. 147, 1965, pp. 1262–1265.
11. UREY, H. C.: Water on the Moon. Nature, vol. 216, No. 5120, 1967, pp. 1094–1095.
12. LINGENFELTER, R. E.; PEALE, S. J.; AND SCHUBERT, G.: Lunar Rivers. Unpublished manuscript, University of California, Los Angeles, 1968.
13. PHILLIPS, R. J.; AND MORRISON, H. F.: Lunar Sounding With Transient Electromagnetic Fields. Trans. AGU, vol. 49, 1968, p. 745.
14. MORRISON, H. F.; PHILLIPS, R. J.; AND O'BRIEN, D. P.: Quantitative Interpretation of Transient Electromagnetic Fields Over a Layered Half-space. Geophys. Prosp., vol. 27, 1969, p. 1.
15. PHILLIPS, R. J.: Dipole Radiation in the Lunar Environment. Trans. AGU, vol. 49, 1968, p. 744.
16. PHILLIPS, R. J.: Dipole Radiation in the Lunar Environment. NAS 489580, Thesis, U. C. Berkeley, Space Sciences Laboratory, 1969.

J. S. CHOATE, C. D. MOSBRUGER, V. M. KEMP, S. W. JOHNSON, and T. R. McGETCHIN
Air Force Institute of Technology
Wright-Patterson Air Force Base, Ohio

A Manned Lunar Mission for Water Exploration in the Marius Hills

Students in their final quarter of study for the M.S. degree in Astronautics/Space Facilities at the Air Force Institute of Technology are required to complete a design study on a subject chosen by the faculty. The results of this group effort carried out by the class which graduated in June 1968 were contained in a report entitled *A Manned Lunar Mission for Water Exploration in the Marius Hills.* This chapter is a condensation of that study. Many specific details of the planned 1978 time period mission have been deleted in favor of a shorter, more general look at both the problem and the solution.

Before such a mission as this is undertaken, it is obvious that maximum use should be made of water-detecting sensors flown on manned and unmanned orbiting spacecraft. Several techniques have been suggested for use from orbital altitudes, but the planning of a mission utilizing them was considered to be outside the scope of this study.

Several technical problems may reduce the efficiency of men and equipment on the lunar surface. Operation during the lunar night may be difficult, and some doubt yet exists as to the ease of trafficability and navigation across the lunar surface. Other problems may arise in the long-term operation of vehicles on the surface where lunar soil particles may adhere to vehicle surfaces and reduce visibility and increase problems with lubrication and airlock seals. For the purposes of this study, it was assumed that such problems will be solved.

INTRODUCTION

The establishment of a Moon base may be a first step in man's reach into space as well as a necessary station for lunar-based science, principally geology and astronomy. Lunar water resources will be useful, if not necessary, for both types of programs (ref. 1). Water will be required for life support at any station established for lunar based astronomy, the exploration of the Moon, or as a point of departure for interplanetary spacecraft. Furthermore, water could be used in this latter type of mission in the production of chemical rocket fuel or as a reaction mass for nuclear powered rockets. From this point of view, lunar bases could be used as refueling stations if useful quantities of water can be extracted from the near-surface (ref. 2). The purpose of this chapter is to outline a plan for a mission to explore for water in the Marius Hills region of the Moon. In the development of this mission plan, attention was given initially to the probable nature of lunar water sources, how they might be detected, and the most promising locations for a water exploration mission.

SOURCES AND METHODS OF DETECTION

As no lunar equivalent to the Earth's hydrologic cycle exists, recoverable water on the Moon, if not primordial water, must be juvenile water resulting from processes of magmatic differentiation and defluidization. This juvenile water could occur in traps of various types. On Earth, water is contained in most igneous rocks; on the Moon, water could possibly occur as a free phase or chemically or physically bound in rocks or minerals. For example, it could occur in the intergranular interstices of rock or trapped in small cavities of crystals of minerals such as quartz or as chemically bound constituents of hydrous minerals such as mica, hornblende, or

382-451 OL-70-6

serpentine. Another potential source of lunar water would be a free phase occurrence in a permafrost layer (ref. 3), which could exist a few meters below the surface (ref. 4), or as ice found in permanently shaded regions, which may act as cold traps (Watson, et al., ref. 5). Watson and his coworkers suggest that an accumulation of water-ice could exist for long geologic time in these cold traps. Other possible sources of free water (ref. 6) are postulated ice deposits below chain craters and rilles (figs. 1 and 2).

Chemically bound water, in the form of the hydroxyl ion, is probably the most likely useful source of lunar water. Clays produced from hydrothermally altered feldspar, such as those found around terrestrial fumarolic vents (fig. 3), contain 3 to 8 percent water (ref. 8) and are possible lunar water sources. Green has further indicated that a gallon of water could be extracted from such a rock containing 5 percent water by weight. Volcanic tuffs and serpentines would be other productive sources if they occur in the lunar environment.

Geophysical water exploration methods generally fall into two groups—one useful in locating possible water bearing structures, the second useful in detecting water itself. The first group includes seismic, magnetic, and gravity techniques. Direct detection of water is possible through the use of electrical, radiation, spectrographic, and photometric methods. The direct methods may be more appropriate for use in the type of mission under consideration because the indirect methods are time-consuming and often serve to locate potential water bearing structures rather than water itself. Techniques now in existence or anticipated for the 1978 time period will be considered for their potential usefulness in the determination of the presence of water through the measurement of a parameter or parameters having characteristic values for water in solid, liquid, gaseous, or hydroxyl form.

Detection of Free Water

Direct Sampling

Clearly, systematic sampling of surface and subsurface materials must accompany indirect techniques. Samples, some examined on the Moon and many sealed and transported to Earth, will yield valuable data in themselves as well as serving as calibration points for the indirect methods.

Electrical Resistivity

Electrical resistivity can be used to determine depth, thickness, and electrical conductivity of different subsurface layers in heterogeneous

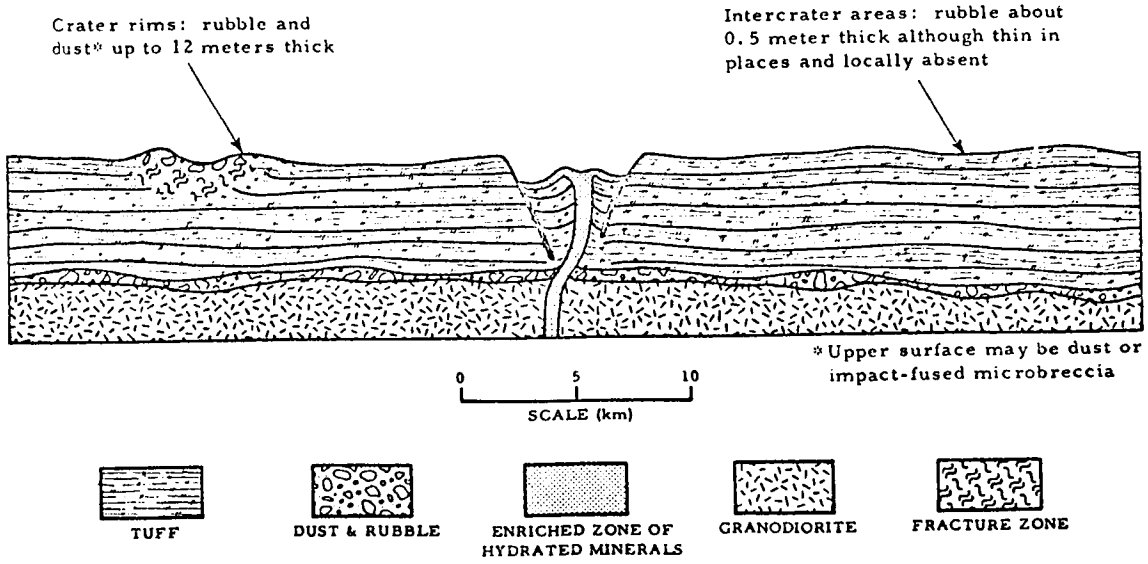

FIGURE 1.—Mare chain crater (ref. 7).

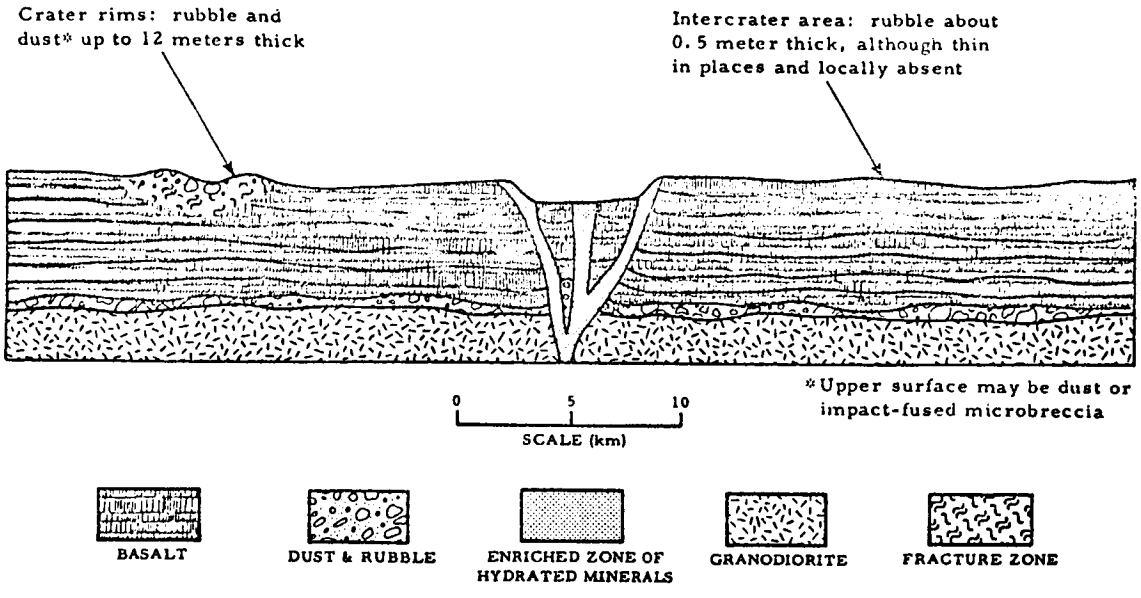

FIGURE 2. — Mare rille (ref. 7).

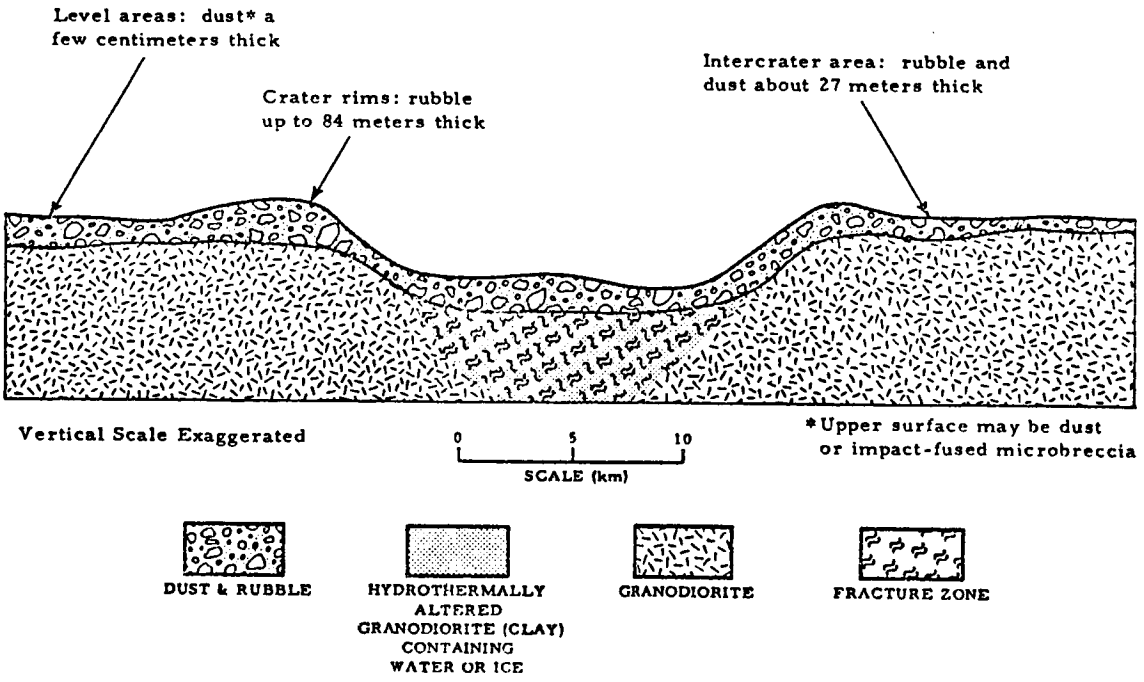

FIGURE 3. — Lunar crater with hydrothermally altered clays (ref. 7).

layered media (ref. 9). Electrodes are positioned on the surface and potentials are measured at various spacings between them. Since water has a large effect on the electrical conductivity of rocks and soils, resistivity is a potentially useful technique in detecting subsurface water. This technique is simple to use but is time consuming and requires a significant power source.

Neutron Logging

Radioactive or neutron logging techniques (e.g., ref. 10) involve the emplacement of a fast neutron source and return counter at the bottom of a borehole. This removes the device from any "outside" radiation effects. The medium around the hole is then bombarded with fast neutrons, and the gamma radiation or the slow neutron flux returning from the rock is measured. This method is simple to use and has the additional benefit of low power-size-weight ratios. It does, however, require a borehole. Furthermore, the interpretation of results may involve ambiguities requiring the sampling and analysis of possible water-bearing soil or rock.

Mass Spectrometry

A mass spectrometer could be miniaturized and made useful in the detection and measurement of volatiles escaping from the lunar surface (ref. 11). The probe of a mass spectrometer could be inserted into loose surface material. Heating or agitating the material would serve to increase chances of detecting and identifying the gases. Such a probe could be used in rilles or crater bottoms and at other locations where water sources are most likely to be located.

Alteration of Reflection Spectrum by Water

Ward et al. (refs. 12 and 13) show that the presence of even a fraction of a percent of free pore water will modify the reflection coefficient over a wide frequency range. In addition, the apparent conductivity and the apparent dielectric constant of natural materials will be changed, thereby permitting the detection of the presence of water in experimental samples by indirect means. This electromagnetic technique discussed by Ward is presently in the research and development stage, but it may be available for field use on the Moon by 1978.

Aluminum Oxide Hydrometer

Adler (ref. 14) suggests the use of the aluminum-oxide hydrometer in water exploration. As water is absorbed there are measurable impedance changes which can be related to amounts of subsurface and also bound water present.

Detection of Bound Water

Infrared spectrometry is one of the most promising techniques proposed for the detection of bound water. Certain emission and absorption bands are characteristic of minerals containing water in various bound forms. The infrared surveying equipment needed to accomplish the task envisioned for the proposed lunar mission has not yet been developed, but the principle has been successfully demonstrated (refs. 7, 15, and 16) and only requires field testing.

Summary of Detection Techniques

In addition to direct sampling, the following techniques may be developed for application to the problem of lunar water exploration by indirect means:

(1) For free water—electromagnetic reflection
(2) For bound water—infrared photometry
(3) For confirmation—neutron logging
(4) For mapping of subsurface layers—elect resistivity, etc.
(5) For analysis of volatiles—mass spectrometry

In addition, other techniques (ref. 14) such as the measurement of neutron albedo from lunar orbit and the use of the aluminum oxide hydrometer on the lunar surface may be developed for the detection of subsurface and bound water.

SITE SELECTION

Nine sites, all suggested in 1967 by the subcommittee of the NASA Group for Lunar Exploration Planning were considered in this study as potential sites for a water exploration mission. These sites included five craters (Censorinus, Littrow, Abulfeda, Copernicus, and Tycho), two rilles (Hadley and Hyginus), and two likely volcanic areas (Schroeter's Valley and the Marius Hills). Also considered were additional sites near the craters Aristarchus and Alphonsus. The Marius Hills region was selected as the general area for a lunar water exploration mission for the following reasons:

(1) The region consists of topographic domes inferred to be volcanic in origin (refs. 17 and 18), and water is typically associated with terrestrial volcanism.

(2) Geological and geophysical interest in the area indicates that a lunar base at the site may be desirable.

(3) Distance from the lunar equator was not large enough to cause any accessibility problems.

(4) Available photographic coverage (Orbiter V high resolution frames 211 to 217) indicated that the region was smooth enough for both landing and traversibility.

The specific landing site chosen, with approximate astronautical coordinates 14°40′ N. and 56°20′ W., was located in the center of an area between four domes in the northern section of Orbiter V medium resolution frame 213. This site can also be located on Lunar Chart LAC 56 prepared by the U.S. Air Force Aeronautical Chart and Information Center.

The mission plan was separated into two tasks to be performed in 90 days on the lunar surface. The first task was the thorough investigation of the main base area, the region surrounding the landing site with a radius of roughly 6 kilometers. The second task was to traverse a larger outlying area, investigating as many of the possible water bearing features as possible. A secondary task was the investigation of geologic features which occur along the traverse.

The most advantageous means of carrying out the mission in a 90-day stay time appears to be through the use of two three-man teams. Team A was assumed to consist of a pilot-astronaut, a geophysicist, and an engineer-mechanic. Team B will consist of a pilot-astronaut, a geophysicist, and a bioenvironmental engineer. All crew members will be cross-trained in aspects of medicine, equipment repair, and the piloting of the various transport vehicles.

MISSION PLAN

The payload and personnel will be soft-landed into the Marius Hills with two uprated 188 percent Saturn V rocket systems (ref. 19). The bulk payload consisting of the two living shelters (LSLM, MOBEX) for the astronauts will be transported to the Moon by a "cargo rocket," whereas the six crew members, other mobility aids, scientific equipment, and life-support expendables will be launched by a "passenger rocket." The cargo rocket can precede the passenger rocket by as long as 6 months provided that it can be confirmed by telemetry that the equipment landed by the cargo rocket is in a suitable location and in working condition.

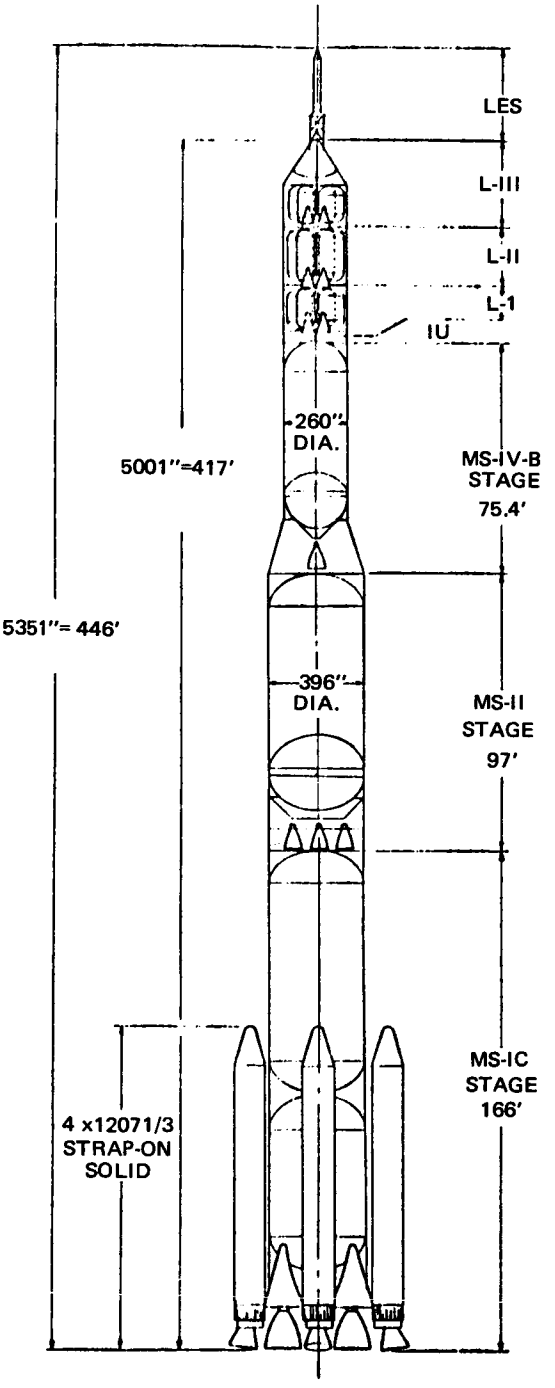

FIGURE 4.—Uprated Saturn V.

The proposed launch system is comprised of an uprated Saturn V rocket with four attached 120-inch, 7⅓ segmented solid propellent rocket motors (fig. 4). Approximately 450 000 kg will be put into a 100-n.m. circular Earth orbit. Only 86 260 kg will be injected into a translunar orbit, and after slowing down into a lunar orbit and finally landing on the Moon, approximately 30 000 kg will remain as payload. Tables I and II indicate the component masses injected into translunar orbit and the masses landed on the Moon, and table III presents the individual payload masses for both rockets. The passenger rocket will have Earth-return L–III stage) capability, but the cargo rocket will not require it. Both 188 percent Saturn V's have L–I and L–II stages; a lunar braking stage and a lunar descent and landing stage, respectively. A more detailed mass, volume, and power description of the scientific and life-support equipment is presented in table IV.

TABLE II.—*Mass Landed on Moon*

Item	Weight (kg)
Cargo rocket (at time = 0)	
Empty L–II stage	8356
Unmanned mode	530
Payload	29 739
Total mass	38 625
Passenger rocket (at time = 2 or 3 months)	
Empty L–II stage	8356
L–III stage	15 856
Adapter	400.4
Command module	7718
Payload	6294.6
Total mass	38 625
Total landed mass	77 250
Total landed payload (not including earth-return mass)	36 033.6

TABLE III.—*Payload Weights and Volumes*

Item	Weight (kg)	Volume (m^3)
Payload for cargo rocket	29 739	257
LSLM	20 095	82
MOBEX and trailer	9644	175
Payload for personnel rocket	6294.6	25.77
LSSM	500.0	11.00
LFV (2)	940.0	3.64
Scientific equipment	444.3	1.09
Expendables	4189.0	9.33
Communication and power sources	221.3	0.71

Team A

Team A will be assigned to the Lunar Shelter-Laboratory Module (LSLM), shown in figure 5, and located in the main base area. They will be equipped with mobility aids such as a Local Scientific Survey Module (LSSM) and possibly a Lunar Flying Vehicle (LFV) (figs. 6 and 7). The equipment necessary to conduct electromagnetic, infrared, neutron logging, and resistivity experiments; drill 30-meter holes; perform mass

TABLE I.—*Mass Ejected on Translunar Trajectory*

Equipment	Weight (kg)	Volume (m^3)	Performance
Passenger rocket			
L–I stage lunar orbit braking stage	24 209	187	1080 m/sec
L–II stage lunar descent and landing stage	31 782	224	2100 m/sec
L–III stage lunar takeoff and transearth injection stage (Earth return)	15 856	66	3125 m/sec
Adapter unit	400.4	25.77	.....
Command module	7718	25	.....
Payload for passenger rocket	6294.6	25.77	.....
Cargo rocket			
L–I stage	24 209	187	1080 m/sec
L–II stage	31 782	224	2100 m/sec
Unmanned mode (payload container)	530	257	.....
Payload for cargo rocket	29 739	257	.....

TABLE IV.—*Weight, Volume, and Power Requirements/Sources*

Equipment	Weight (kg)	Volume (m^3)	Power (watts)
Scientific equipment for MOBEX			
Mass spectrometer	12	.05	100 (plug in)
Electromagnetic device	18.6	.0115	250 (plug in)
n-γ device	50	.013	3.3 (plug in)
10m drill	13.6	.057	350 (solar cells and plug in)
Infrared device	45.4	.165	16 (plug in)
Microwave device (radar)	25	.1	
Scientific equipment for LSLM			
Mass spectrometer	12	.05	100 (plug in)
Resistivity device	9	.05	200 (plug in)
Electromagnetic device	18.6	.0115	250 (plug in)
n-γ	50	.013	3.3 (plug in)
Microscope	1	.014	1 (plug in)
Cutter-grinder	2	.028	5 (plug in)
30m drill	90.9	.34	3500 (solar cell and plug in)
Infrared device	45.4	.165	16 (plug in)
Baking oven	50	.013	100 (plug in)
Spring scales	1	.0084	
Communications			
For shelter (S-band)	[1] 45.5	.054	66.7 (plug in)
For MOBEX (S-band)	[2] 45.5	.054	66.7 (plug in)
6 belt packs (6-man)	[3] 10.92	.0054	9.6 (rechargeable battery)
Remote experiment (radio) over 100m away	17.3	.05	5.54 (battery)
Remote experiment (direct wire)	6.9	.0066	0.27 (plug in)
For LSSM	45.5	.054	66.7 (plug in)
For two LFV's	34.6	.1	11.08 (battery)
Miscellaneous			
2 preparation of food equipment	109.2	3.36	800 (plug in)
2 waste water treatment	77.2	.0326	362 (plug in)
2 atmosphere control (heating and cooling; one for MOBEX, one for LSLM)	500	1.02	5700 (plug in)
Extra power sources			
Roll-up solar cells (used for drills, supplementing the LSLM and MOBEX power units)	117	.5	Producing 3850

[1] Included in wt of shelter.
[2] Included in wt of MOBEX.
[3] Included in MOBEX and shelter.

spectroscopy; and laboratory equipment such as a polarizing microscope, a rock cutter-grinder, a scale, and an X-ray diffractometer will be available at the LSLM. During the first portion of the mission the LFV, which has a two-man capability, could be used to gather hand specimens from selected features around the main base area. One man will gather the specimens while the seond man will act as photographer and observer. The third man, during this period and throughout the mission, will remain at the LSLM and act as a communications monitor and cartographer.

The hand specimens will be labeled and returned to the LSLM. Upon completion of inspection and laboratory analysis of some of these specimens, any important findings will be transmitted to the second team for their information. The follow-on main base activities will include the drilling of eight 30-meter core holes and the horizontal and vertical mapping of a portion of the area with the resistivity equip-

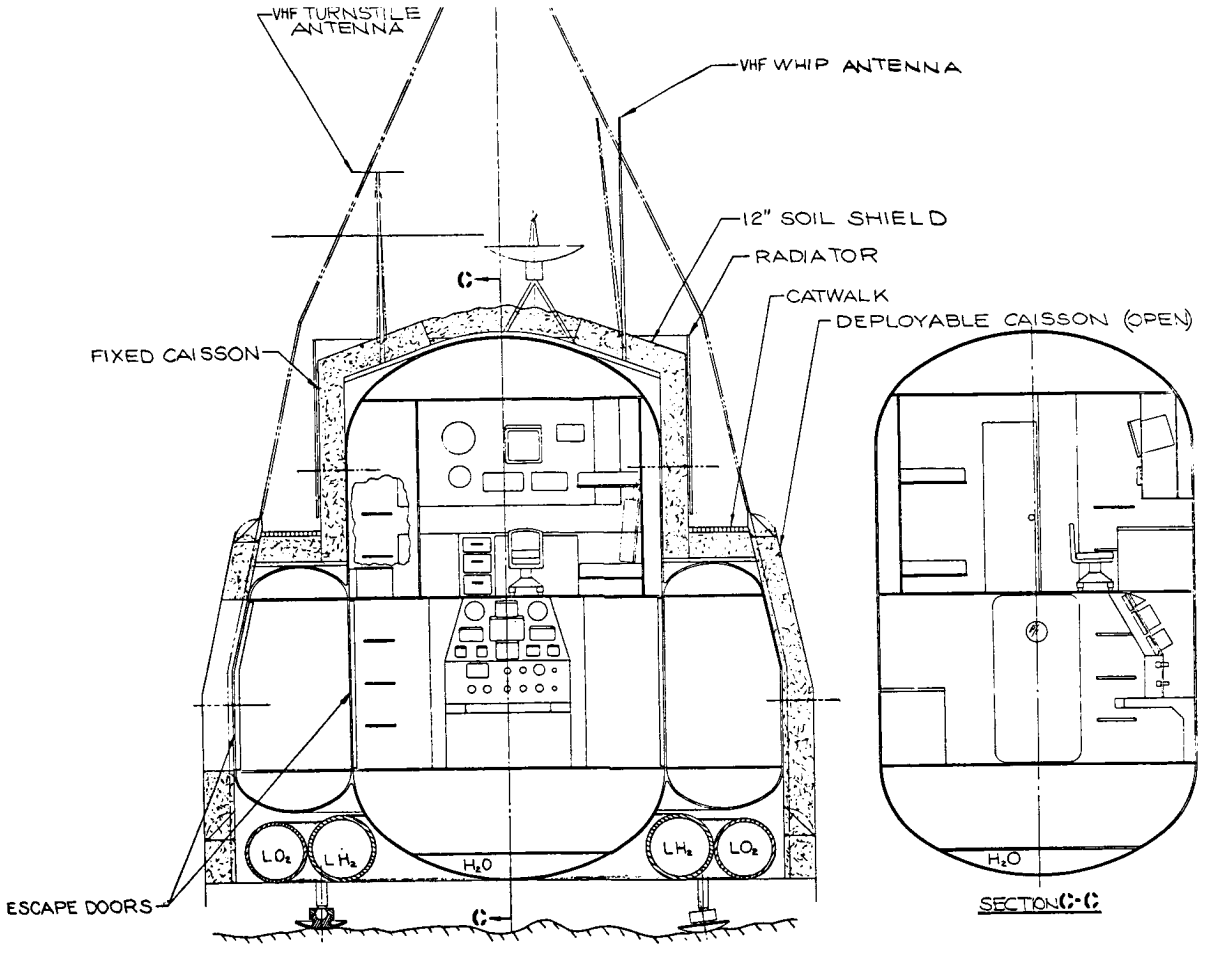

FIGURE 5.—Three-man shelter.

ment. The LSSM, which also has a two-man capacity, will be used for transportation as these tasks are performed.

Team B

The other three-man team will concurrently conduct the traverse of the surrounding region. This team will be equipped to conduct electromagnetic, infrared, neutron logging, and mass spectroscopy investigations. Their navigational or ranging radar system may be adapted to conduct a radar survey. A 10-meter drill is required. The surface vehicle used in this traverse is known as a MOBEX (fig. 8), for Mobile Excursion Vehicle (ref. 20), which can be used as a shelter and will support three men in a shirt-sleeve environment for the entire 90 days. The MOBEX will initially make a circular traverse of the main base at 5-km radius to check out its equipment and to conduct a reconnaissance survey of the area. It will then conduct the long traverse shown in figure 9.

The MOBEX has the capability also of carrying the second LFV supplied to the mission. This LFV will be used primarily for transportation to areas such as cratered dome fields which are inaccessible to the MOBEX. An important backup function of this LFV is that of an emergency rescue vehicle. The range of an LFV is 800 km, which is about 10 times as large as the maximum planned distance of the MOBEX from the LSLM.

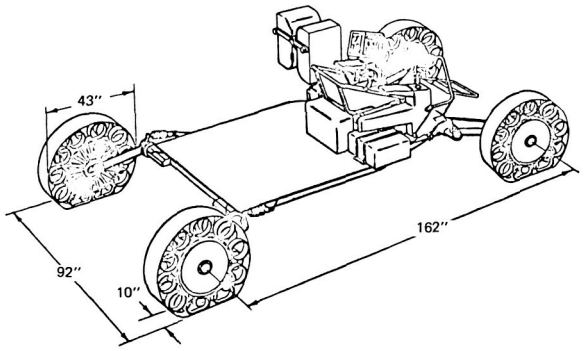

FIGURE 6.—LSSM configuration (ref. 21).

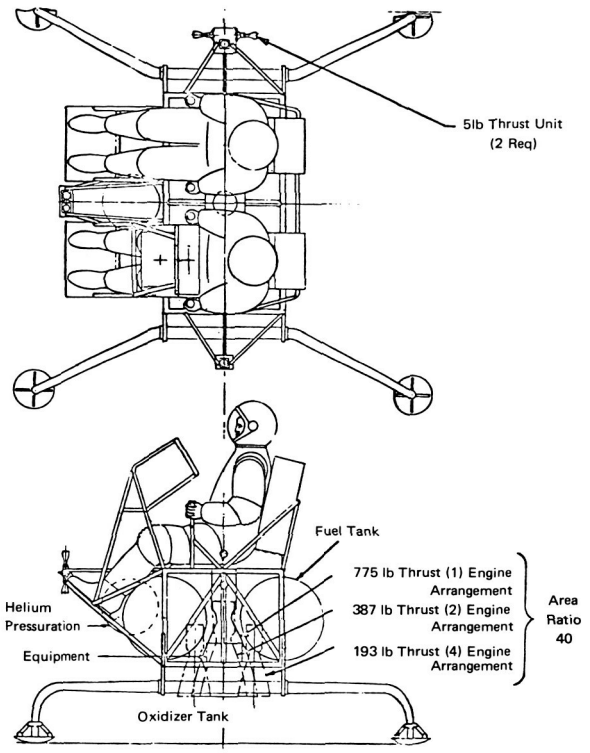

FIGURE 7.—Two-man lunar flying vehicle (ref. 22).

The mission plan calls for the MOBEX to follow a pre-planned path around the Marius Hills region along which specific tasks will be accomplished. Some flexibility will be permitted to allow for the unexpected.

At each of eight specified locations (fig. 10) the crew will spend from 2 to 8 days in a detailed exploration of the feature of interest. The duration of the stop will be a function of the amount of information being returned. The points of interest along the proposed traverse were selected from the high resolution Orbiter V photographs (table V). Upon completion of the 180-km traverse, the six astronauts will rendezvous at the LSLM, make final preparations, and return to the Earth.

Communication Links

A system of stations spaced around the Earth will provide continuous contact with the two living shelters (LSLM and MOBEX). This Apollo Ground Operation Support System from the early Apollo missions will accept the transmission of voice, digital data, and TV from the two lunar laboratories. The LSSM, LFV, and the astronauts will have communication systems provided for operational procedures on the lunar surface. Due to the curvature of the Moon, the line-of-sight transmission between the "belts packs" on the space suits is limited to 5.5 km. It will be necessary to employ Moon-Earth-Moon relay links for point-to-point communication on the lunar surface over long distances. Coaxial cables can provide data transmission from some experiments conducted

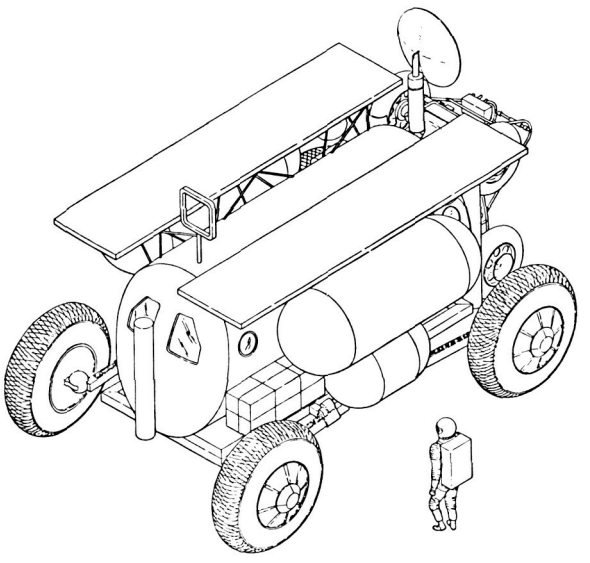

FIGURE 8.—MOBEX.

on the surface to the living shelters, thus allowing the astronauts the convenience of a shirt sleeved environment where they can monitor data collection. Communication links between the

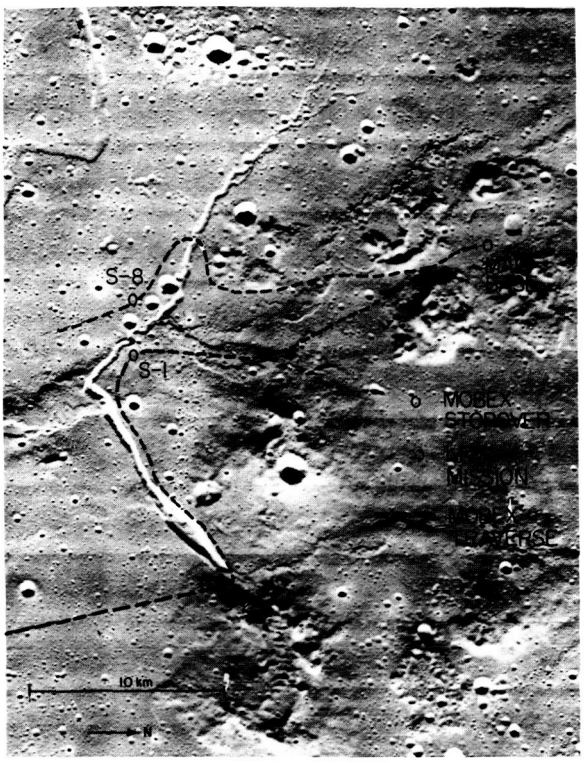

FIGURE 9.—MOBEX traverse through northern portion of Marius Hills region.

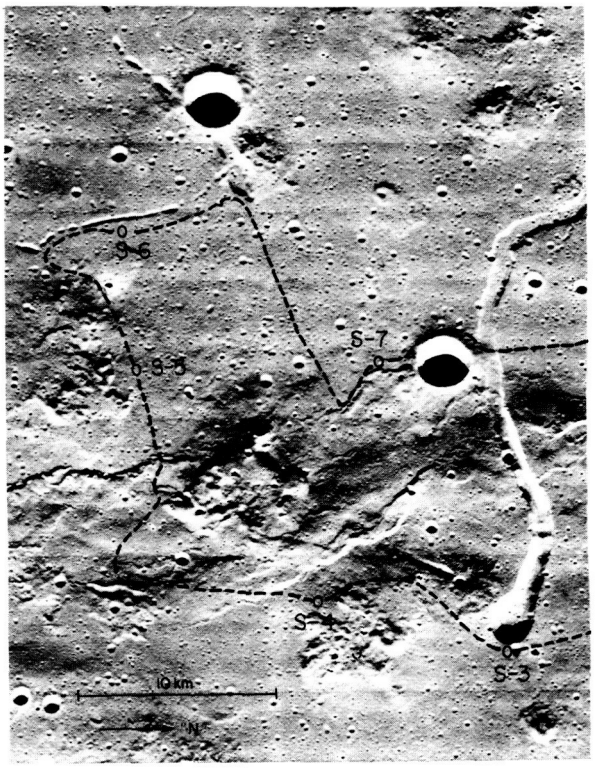

FIGURE 10.—Traverse through southern portion of Marius Hills region.

TABLE V.—*Marius Hills' Points of Interest*

Site	Description
S–1	The major point of interest is the intersection of a ridge and a rille. An attempt should be made to determine subsurface features and characteristics of the ridge and the rille.
S–2	An apparent transition from a sinuous rille to a tubular ridge suggests the possibility of a cave or permanently shaded area at this site. Such a site could retain ice near the surface. This location may also provide some information about the origin of lunar rilles.
S–3	The large crater at the head of the prominent north-south rille should be investigated for indications of the presence of water. Information concerning the origin of the rilles might also be available here.
S–4 and S–5	The two prominent clusters of possible volcanic domes should be investigated. The structures are typical of those postulated to be likely sources of lunar water. Samples will be collected.
S–6	The cratered trench adjacent to the indicated traverse should be examined for possible volcanic origins and for any evidence of water.
S–7	An effort should be made to expose the interior walls of this apparent impact crater. This should provide information about the stratigraphy underlying the region.
S–8	A north-south crater chain and rille system should be investigated to determine the character of these features.

Astrogeology 5, United States Geological Survey, Feb. 1968.

19. ANON.: Study of Mission Modes and System Analysis for Lunar Exploration (MIMOSA), 4 volumes. Lockheed Missile and Space Co., April 1967.
20. ANON.: Deployment Procedures—Lunar Exploration Systems for Apollo (LESA), volumes I, II, III. Lockheed Missile and Space Co., 1965.
21. ANON.: LSSM for Apollo Applications Program. Bendix Corporation, BSR-1495, 1967.
22. ECONOMOU, N.; AND SEALE, L. M.: A Study of Personnel Propulsion Devices for Use in the Vicinity of the Moon. Bell Aerosystems Company, Jan. 1966.
23. ANON.: Lunar Base Study: Communication and Control Subsystem. Final Report. Bendix Corporation, Oct. 1963.

JACK GREEN
Douglas Advanced Research Laboratories
McDonnell Douglas Corporation
Huntington Beach, Calif.

Hydrothermally Altered Rocks as a Lunar and Martian Water Source

Hydrothermally altered rocks are hydrous and may provide a source of water for the lunar and Martian base. Two major types of hydrothermal alteration thought to occur on the Moon and Mars are sulfur-acid and halogen-acid. Halogen-acid alteration may be confined to the termini or thickened zones of ash flow tuffs or to high temperature fumarolic centers at flow sources. In the latter case, the amount of hydrothermal alteration is relatively slight. Sulfur-acid alteration is more extensive. The hydrothermal envelopes surrounding volcanic vein-sulfur deposits can possibly provide over 150 liters of water per cubic meter of clay. Remote sensing techniques can be applied to detect sulfur compounds.

There are at least two possible candidates for a water source on planetary bodies that are volcanic, but lack near surface permafrost or ice. These two sources are hydrothermal clays and glassy zones in tuffs. The solar and nuclear power techniques for extracting water from Tumulo Creek tuff in Oregon have been discussed previously (ref. 1). This chapter will emphasize the nature and distribution of water in hydrothermal clays and will briefly discuss the localization of this resource on the Moon and Mars.

Two major types of hydrothermal alteration are sulfur-acid and halogen-acid. Of these, the sulfur-acid type is thought to be more important in evolving clays useful as a source of lunar and Martian water. Hydrothermal alteration characterized by the halogen-acids is, in general, of a higher temperature and often less hydrous than the sulphur-acid type. However, significant exceptions occur. For example, in the Valley of Ten Thousand Smokes in Alaska, Lovering (ref. 2) has shown that a considerable amount of water in the form of hydrothermally altered clays is present on the margins of halogen-acid fumaroles at the distal end of the 1912 ignimbrite flow (fig. 1). On the other hand, in the halogen-acid vents of the Guatamala volcanic highlands,

FIGURE 1.—Alteration haloes of clay around halogen acid fumarole, near terminus of ash flow of the Valley of Ten Thousand Smokes, Alaska.

most of the sublimates are anhydrous, and the aureole of water-bearing altered rocks is minimal (R. Stoiber, personal communication).

Therefore, sulfur-acid alteration, which is more abundant than halogen-acid alteration, and which

is almost always associated with hydrous rocks, has been studied from the standpoint of water potential on the Moon and Mars. The pertinent question arises, "How much of the Moon is volcanic and therefore associated with hydrothermal activity?" Probably over 95 percent of the major lunar surface features are volcanic (ref. 3); but of the volcanic area actually present on the Moon and Mars, only the vent areas will be hydrothermally altered. The area of a vent compared to the area of unaltered lava and ash flows is relatively very small. Volcanoes and, on a smaller scale, fumaroles are the most common vents in terrestrial volcanic provinces.

As figure 2 shows, the central mountains in Copernicus on the Moon resemble breached volcanoes on the Earth. The volcano on the lower left is that in the Fernandina caldera in the Galapagos Islands; on the right is the White Island volcano in New Zealand. Figure 3 shows an interior view of the andesitic volcano in New

FIGURE 3.—Interior of White Island volcano, view to north. Solfataras and hydrothermal clay in background.

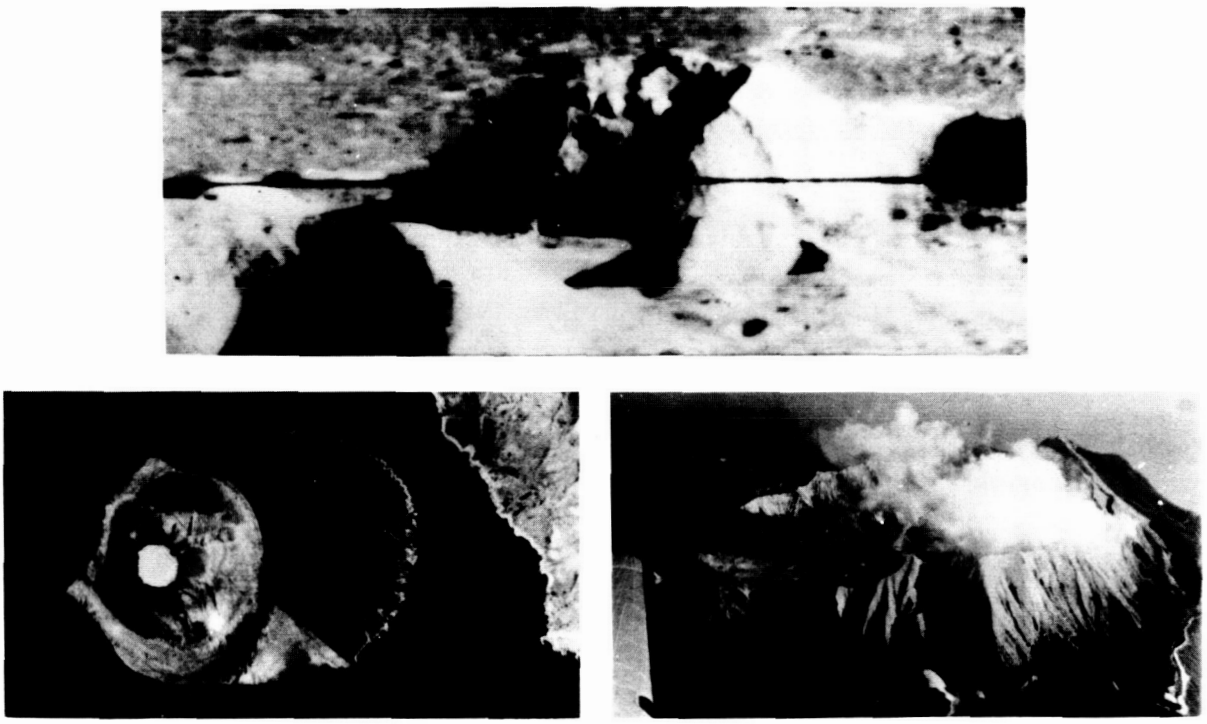

FIGURE 2.—*Comparison* of the central mountain in Copernicus (top) with Fernandina volcano in the Galapagos Islands (lower left) and White Island in New Zealand (lower right). The Copernicus mountain, about 300 meters high, appears to be breached by an explosion similar to the terrestrial volcanoes. The Fernandina volcano is 70 meters high and that of White Island about 500 meters high.

Zealand, which is characterized by abundant sulfur mineralization and hydrothermally altered clay. In addition to clay, siliceous opaline sinter occurs at the fumarole vents. Clear examples of the association of clay and opal—each having a water content that may exceed 135 liters of water per cubic meter of clay or opal (one gallon of water per cubic foot)—are found all over the world. Figure 4 shows opaline sinter associated with sulfur and clay on the eastern fault margin of the Kilauea caldera in Hawaii. The sinter contains 4 percent H_2O^+ (fig. 5), most of which is hydroxyl bonded at temperatures from 650 to 750° C. The same amount of water (H_2O^+) in the associated montmorillonite clay is contained within a more restricted and lower temperature interval maximized at 600° C.

In Japan, volcanic sulfur is invariably mantled with an envelope of hydrous rocks at depth. This relationship is clearly observed in vein-sulfur mine deposits in the Shojingawa, Ishizu, Iburi, Zao, Oshima, Shirane, Kuju, Azuma, Akan, and Nishiazuma mining districts. For the last named mining center, as Mukaiyama (ref. 4) has shown, the zoning from the fresh rock to vein sulfur is as follows: fresh rock, clay, alunite, opal, pyritized rock, sulfur (fig. 6). Surface expressions of sulfur deposits do not always indicate this clear cut zoning. In figure 7, for example, the alteration halo at the Atosanobori sulfur mine in Hokkaido shows mostly opaline sinter associated with gypsum and some pyrite produced by the ascending sulfur-bearing vapors.

Research by R. W. Wood (refs. 5 to 7) in the

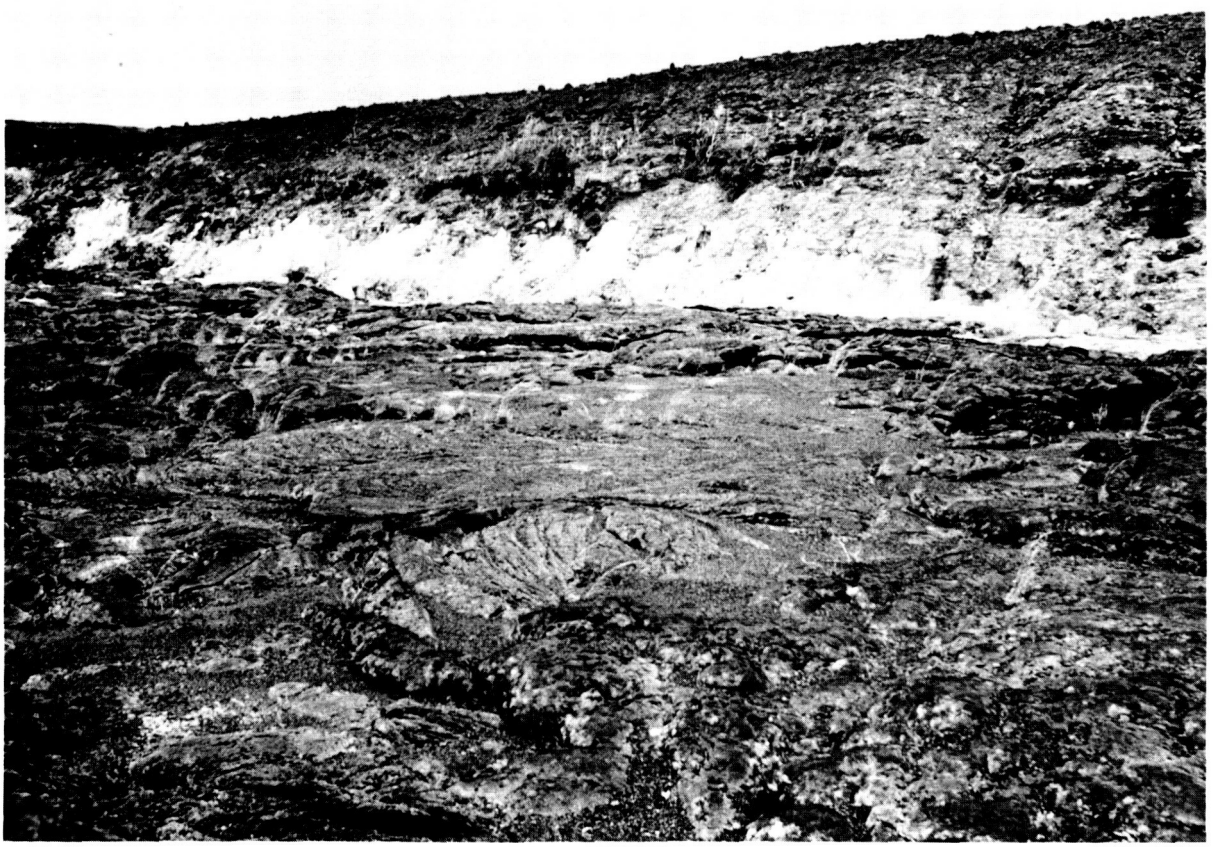

FIGURE 4.—Sulfur-rich fracture zone trending north-south on eastern margin of Kilauea caldera. The sulfur is associated with siliceous sinter and clay.

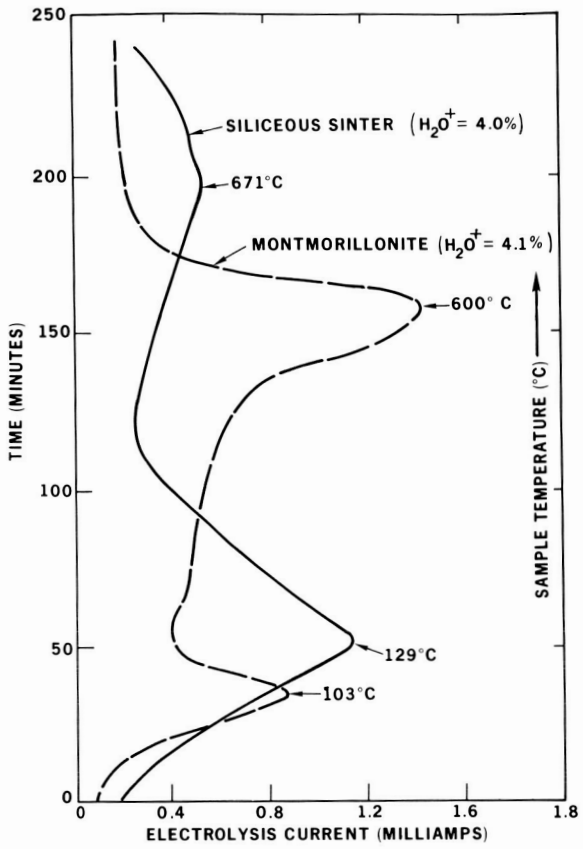

FIGURE 5.—Electrolytic hygrometry curve of siliceous sinter and clay collected in the alteration zone shown in figure 4.

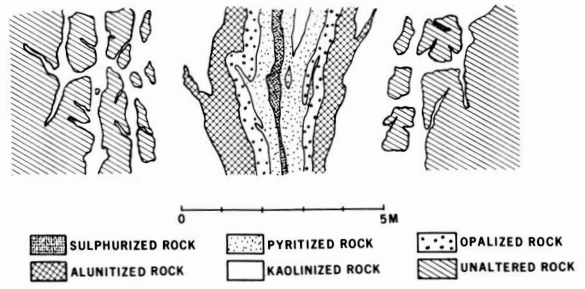

FIGURE 6.—Typical alteration sequence in the vein sulfur deposits of Hokkaido, Japan (after Mukaiyama, 1959).

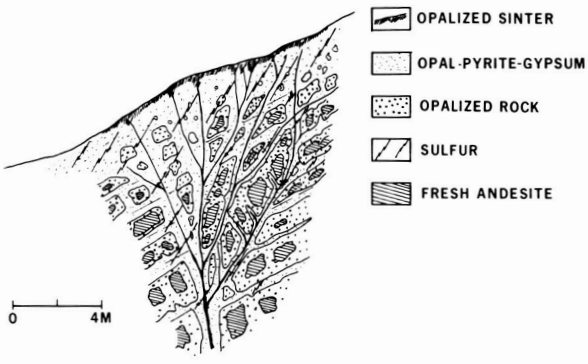

FIGURE 7.—Surface alteration halo at the Atosanobori mine, Hokkaido (after Mukaiyama, 1959).

early part of this century disclosed that certain parts of the Moon appeared dark when observed through a telescope with an ultraviolet filter. When a yellow filter was used, these spots virtually disappeared. Wood believed that a large area north of Aristarchus shown in figure 8 (the so-called Wood's Spot) was a sulfur deposit because of its unusual reflectance properties, namely high reflectance in the visible and high absorption in the ultraviolet. Zinc oxide also shows these characteristics. However, because sulfur is the most abundant volcanic mineral and because the Moon exhibits so many volcanic features, Wood thought that sulfur was the material producing the darkening effect in the ultraviolet.

However, native sulfur cannot be the material causing the Wood's Spot effect. As shown in table I, the sublimation rate of a centimeter

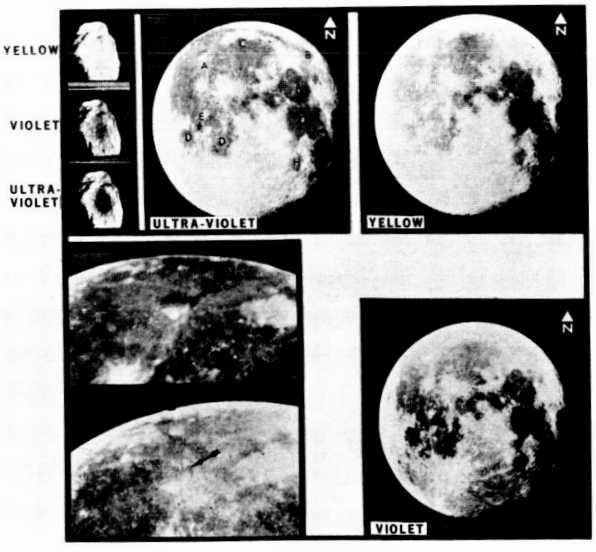

FIGURE 8.—Spectral data on dark spots of the Moon (modified after Wood, 1912).

TABLE I.—*Decomposition Rate of Sulphur**

Temperature	Number of years**
−150° C (lunar shadow)	10^{25}
0° C	10^{2}
+100° C (lunar subsolar)	10^{-3}

*Age of Earth-Moon crust is 4.5×10^9 years. B (rate of sublimation in cm/sec) $= 1.1 \times 10^{10} e^{-23,890/RT}$.

**Years required to vaporize a layer 1 centimeter thick in vacuum.

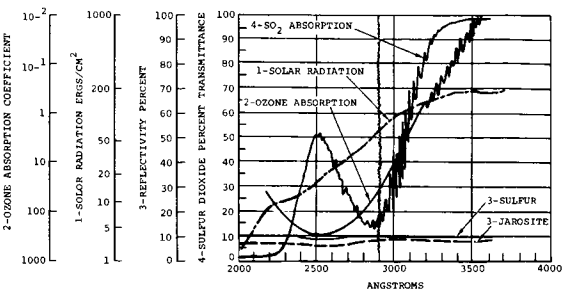

FIGURE 9.—Reflectance and absorption data on materials possibly causing the Wood's Spot anomaly.

thick layer of sulfur in vacuum under sub-solar conditions would evaporate this layer in 9 hours. Therefore, sulfur could not remain on the lunar surface very long under sunlit conditions unless the deposit were very thick or being regenerated. The mineral jarosite or some other yellow stable sulfur compound is a more reasonable cause for the darkening effect in the uv. Sulfur-bearing gases such as sulfur dioxide are also possible. The most likely explanation, however, is the simplest—quenching of luminescence in the Wood's Spot area by fresh iron-rich volcanics.

Figure 9 shows the flat reflectance response of sulfur and jarosite in the uv. We already have discounted sulfur. If Wood's observation is correct, that the darkening effect is maximized at 3100 and not at higher wavelengths (realizing that earthbound uv spectroscopy cannot go much below 3100), then sulfates such as jarosite may not be the answer either. This leaves the broad absorption band of SO_2 maximized at ~2900Å as an explanation for the spectral anomaly. However, uv photography of the fumarolically active Halemaumau crater in April 1969, showed no measurable darkening effects, presumably because of the low concentrations of SO_2 (~100 ppm) present. Unless the Moon is continuously emitting much higher concentrations of SO_2 that do not fluctuate during a lunation, sulfur dioxide appears only remotely possible.

Study of Orbiter photography of Wood's Spot shows what may be interpreted as fresh volcanics. Flow structures, sinuous lava (?) flow channels, and associate transients all in a region clearly outlined as a recent horst, point to very recent volcanism. Usually on Earth, the blacker the lava flow the more recent it is. The blackness may simply be a relative luminescence phenomenon with the quenching effect of the luminescence in iron-rich volcanics optimized at wavelength regions of high spectral activity. Significantly the wavelength region around 3100Å is spectrally active (refs. 8 and 9). Even if Wood's Spot is not directly caused by sulfur-bearing compounds, the recognition of recent volcanic centers by other effects is just as important in detecting hydrothermal alteration centers on the Moon and Mars. Recent volcanic areas would contain many recent hydrothermal alteration centers, especially at the source craters of sinuous rilles and intersection of grid fractures.

Because the alteration halo around sulfur-producing volcanic centers (solfataras) is composed of hydrous materials on the Earth, the possibility for this relationship also should exist on the Moon and Mars. The volume of these hydrous minerals (clay, opal, sulfates) is large compared to that of the sulfur. We might then regard sulfur or its compounds as indicators for water on the Moon and Mars. Because sulfur and many of its compounds have diagnostic absorption characteristics in the ultraviolet, visible, and infrared, they are capable of being detected by remote sensors. Thus, finding sulfur and its compounds on the Moon and Mars may be critical in locating the lunar or Martian base if we assume that sulfur equals water.

The volume of water in the alteration zones around an idealized vein-sulfur deposit is shown

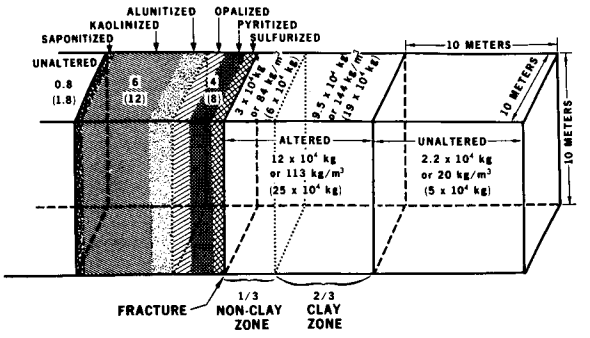

FIGURE 10.—Typical hydrothermal zoning and water yield in sulfur acid alteration sequence.

in figure 10. A cube 10 meters on a side of the hydrothermal clay could provide over 10^4 kg of water. Altered material is easier to process for water than fresh rock because it is much softer. Also, in prospecting for and locating such a deposit, not only the workability of the ore must be considered but also its extent. Ideally the pattern of a hydrothermal clay prospect on the Moon or Mars would consist of two parallel bands up to tens of meters wide on each side of a sulfur-bearing fracture. The sulfur itself, if abundant at depth, would also have application in lunar or Martian base technology.

REFERENCES

1. GREEN, J.: A Study of the Feasibility of Using Nuclear Versus Solar Power in the Water Extraction from Rocks. AFCRL 64–733 and AFCRL Final Report, July 5, 1963 to Sept. 30, 1965.
2. LOVERING, T. S.: Halogen Acid Alteration of Ash at Fumarole No. 1, Valley of Ten Thousand Smokes. Bull. Geol. Soc. Amer., vol. 68, 1957, pp. 1585–1604.
3. GREEN, J.: Volcanological Factors in the Selection of the Lunar Base. XXIII International Geological Congress, vol. 13, 1968, pp. 53–74.
4. MUKAIYAMA, N.: Genesis of Sulfur Deposits in Japan. Jour. Faculty Science, U. of Tokyo, Section II, Supplement to vol. XI.
5. WOOD, R.: The Moon in Ultraviolet Light. Monthly Notices, Royal Astronomical Society, vol. 70, 1910, p. 226.
6. WOOD, R. W.: The Moon in Ultraviolet Light and Spectroselenography. Pop. Astron., vol. 18, 1910, pp. 67–72.
7. WOOD, R. W.: Selective Absorption of Light on the Moon's Surface and Lunar Petrography. Astrophys. J., vol. 36, 1912, pp. 75–84.
8. HILL, R. A.: Trans. Faraday Soc., vol. 20, 1924, p. 107.
9. KORNFELD, G.; AND WEEGMANN, E.: Zeit. Electrochem., vol. 36, 1930, p. 789.

P. BLUM and M. J. HORDON
Norton Research Corporation
Cambridge, Massachusetts

Vacuum Adhesion and its Lunar Mining Implications

Selected equipment, procedures, and results from three experimental studies of vacuum adhesion are discussed: (1) self abrasion of basalt at 4×10^{-9} Torr to simulate lunar soil, (2) diamond wheel grinding of basalt at 0.1 and 4 Torr to simulate extraterrestrial geological sampling, and (3) friction and adhesion of selected metals at 5×10^{-13} Torr. Some of the implications are that a lunar vacuum may alter the size distribution of fractured rock, required increased energy and time to fragment it, and reduce the speed at which grinding, certain kinds of drilling, and other abrasion work can proceed. Remedies such as low pressure protective atmospheres and bearing surface lubricants are discussed, as well as their possible limitations.

INTRODUCTION

Three experimental programs concerned with vacuum adhesion, whose results have relevance to lunar mining and associated activities, are highlighted here and denoted by subsequent section headings. Discussions of the importance of vacuum comminution and descriptions of equipment and experiments are included in the lunar soil simulation section to elucidate relevant problems and insights pertinent to adhesion. The section on geological sampling studies extends to higher pressures the findings of the simulation work; the associated vacuum grinding equipment discussed here may be of interest as a versatile testing device for assessing the vacuum adhesional problems of machine tools and other comminution techniques. The third section discusses selected results of the adhesion and friction of metals in vacuum; only a small amount of the many studies of these phenomena are pertinent to the subject of this chapter. The description of associated equipment, due to its complexity, is omitted. The last section discusses potential lunar mining problems and associated implications derived from the combined results of all three studies.

LUNAR SOIL SIMULATION STUDIES

Numerous experimenters have studied the properties of silicate powders in a vacuum environment to learn about the properties of lunar soil (refs. 1 through 7). Associated work exists on the adhesion of crystals in vacuum, including those which are vacuum cleaved (ref. 8). It appears, however, that the study from which results here described are derived (refs. 9 and 10) constitutes the only one on vacuum comminuted powder, with the exception of parallel work on vacuum crushed olivine by Bell (ref. 11). Vacuum comminution is important because powder produced in air, or even in an inert gas, immediately adsorbs contaminating gases, and the last monolayers remain even when exposed to a vacuum environment. The inert gas is ineffective at contaminant protection because of preferential adsorption of impurity gases and of gases emitted from the rock itself. Once the contaminant gases are adsorbed, the vacuum environment is ineffective for desorption unless temperatures are used that are much higher than those common to vacuum chamber bake-out, so as to dissociate the resultant metallic oxides. Therefore, unless powder is vacuum comminuted

and other pertinent lunar conditions appropriately simulated, adhesive properties could differ appreciably from those of powder produced on the lunar surface, where an estimated 10^{-10} Torr vacuum exists.

Figure 1 shows major apparatus components of this study: a grinding motor supported on a vacuum chamber, in turn supported on an ion pump, and a magnetron gauge to measure pressure. Ion pumping eliminated the danger in diffusion pumping of oil contamination from pump oil back-streaming. A simplified internal view of the chamber is shown in figure 2. A cylindrical inner rock was revolved abrasively along the inside surface of a torroidal shaped outer rock by means of a shaft pivoting on a ball joint. A bellows welded to the shaft served as a vacuum seal for the grinding motion and also prevented the shaft from rotating on its own axis. The motion was such that a spot on the inner rock always faced in the same direction as the rock moved. As a result, freshly abraded rock surfaces are exposed over the circumference of each component for every revolution of the inner component.

One purpose of the design was to limit powder contact, prior to its collection in the pan below, to the freshly abraded surfaces, thus preserving powder cleanliness. A second purpose was to keep grinding surfaces exposed, to facilitate pumping the gases released during grinding, and thus to further minimize contamination and, of course, to simulate lunar conditions. Ultrahigh vacuum pumping was assisted with a liquid nitrogen cold wall surrounding the components.

Grinding initially caused a pressure burst to 2.6×10^{-8} Torr. This was followed by a rapid drop in pressure and then a slow leveling off. The mean pressure during grinding was 4×10^{-9} Torr. The pressure drop coincided with a gradual accumulation of powder on the grinding surfaces.

Figure 3 shows rock components after 17 hours of vacuum grinding. Adherent powder covers the entire grinding surfaces, which are the areas of intimate contact extending from the bottom to 75 percent of the height of the rocks. Some powder was pushed above the grinding surfaces. An unsymmetrical, but even, boundary separating abraded and unabraded areas is evident. (The uncovered area is a rock crevice.) The sticking of powder to these regions was one of the most significant results of vacuum grinding. Grinding in air produced only a thin dusting of powder on the grinding surfaces and none above them. The lower picture shows that flakes of powder removed from the upper area after release of the chamber to atmosphere were

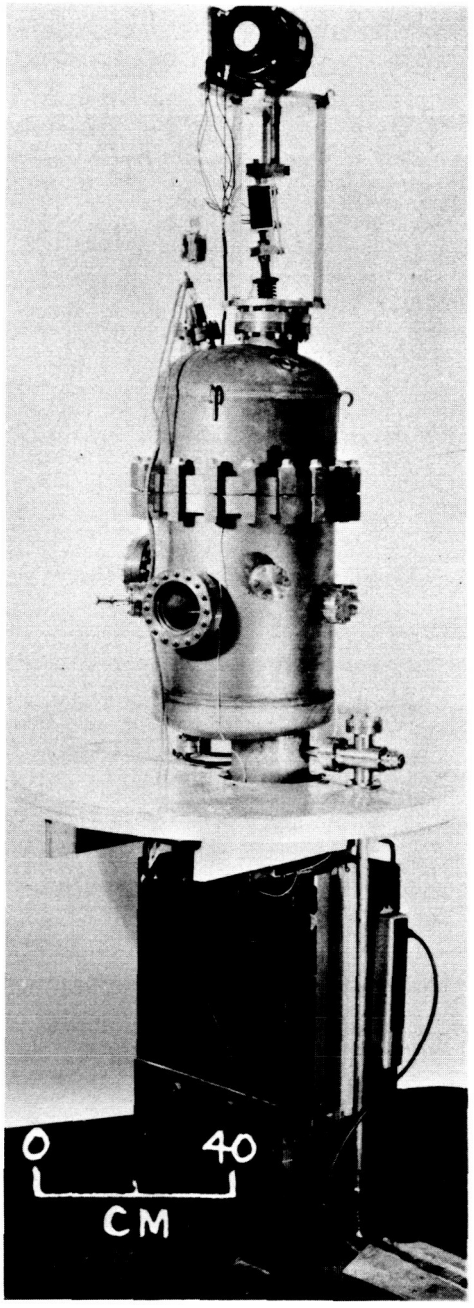

FIGURE 1.—Vacuum grinding system less electronic controls and rough-pump components.

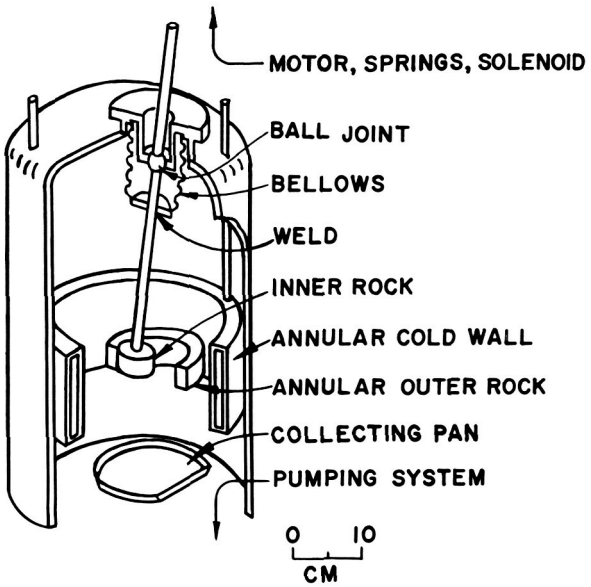

FIGURE 2.—Simplified sketch of vacuum chamber of internal components.

sufficiently self-adherent to support themselves on wire loops.

In the collection pan, the initially produced powder formed small spherical aggregates that jumped about due to vibrations. Subsequent powder became adherent, however, and angular aggregates were ultimately produced, as shown in figure 4, which gave the powder a gravel-like appearance. Air-ground powder also produced aggregates, but they were almost uniformly spherical, as shown in the bottom picture. A few exceptions are apparently small flakes from the grinding surfaces. Spherical aggregates also were noted in a funnel-shaped cup

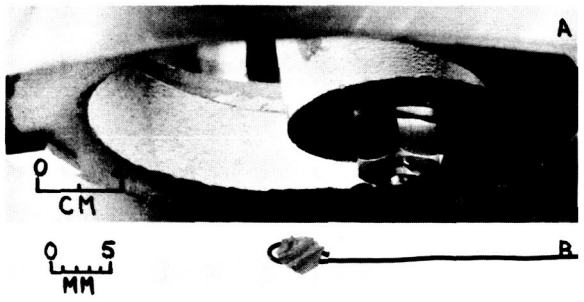

FIGURE 3.—(a) Vacuum-ground power adhering on and above rock grinding surfaces and (b) self-supporting flake of adherent powder from the upper area.

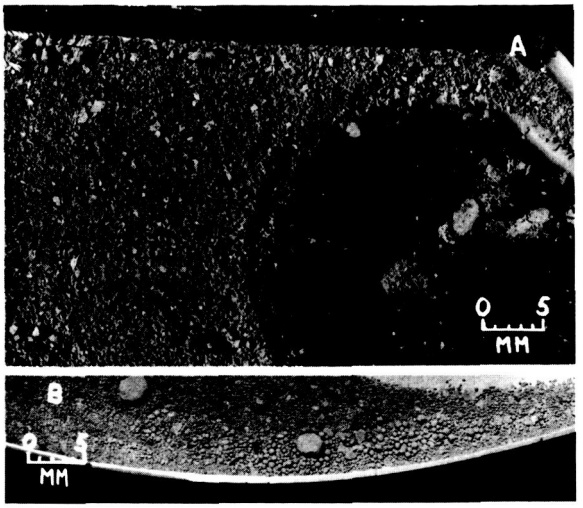

FIGURE 4.—(a) Aggregates produced on the collecting pan by vacuum-ground power and (b) aggregates produced on the collecting pan by air-ground powder.

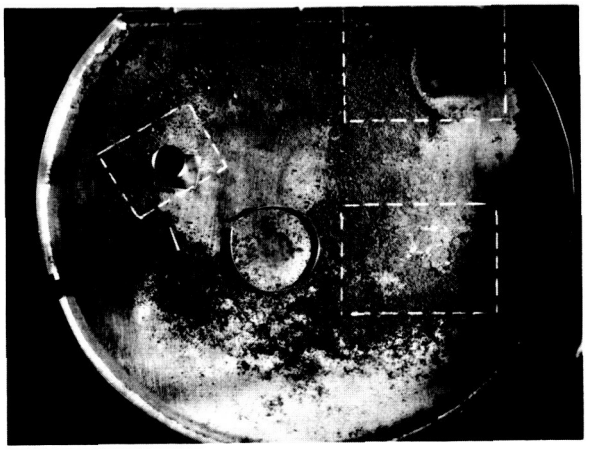

FIGURE 5.—Powder on the entire collecting pan after vacuum grinding. The circular, sparsely coated area near the center outlines the grinding perimeter; dashes outline other areas of interest.

in vacuum. It appeared that wherever contamination was greatest—in air, in the initially produced vacuum ground powder, and in a funnel where powder had to roll down an atomically unclean metal wall—that aggregates tended to be spherical. Where contamination was smallest, aggregates tended to be angular. This angularity appeared to be another indication of greater adhesiveness.

Figure 5 shows that vacuum-ground powder

was distributed over the collecting pan in a circular manner, roughly duplicating the shape of the annular rock above it. This distribution did not exist with the air ground powder, shown in figure 6, which indicated less adherence to the pan and more responsiveness to pan vibrations. In fact, the vibrations set up wavy patterns that were nonexistent in the vacuum-ground powder.

About 1 gram of powder was produced in vacuum compared with 4 grams in air in the same 17-hour period. The median vacuum-ground particle size was larger than the air-ground size, 1.25 microns vs 0.9 micron. An increase in vacuum comminuted particle size was also observed by Bell (ref. 11).

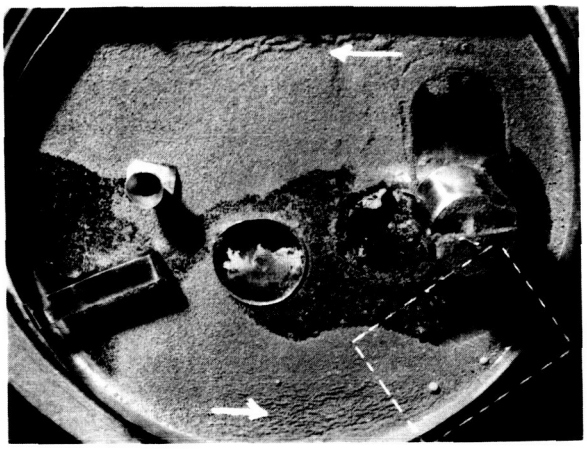

FIGURE 6.—Powder on the entire collecting pan after air-grinding. Arrows refer to wavy patterns. Dashed outline includes area previously shown enlarged.

It is seen that while observations of vacuum-ground powder are primarily qualitative, adhesion is demonstrably greater than for air-ground powder. While the strength is not extraordinarily high, it is sufficient to produce deceptive configurations, such as angular aggregates, which appear to account for some of the blocks seen in Surveyor photographs.

Correlations between Surveyor findings (ref. 12) and this work are noteworthy. Basalt, used in this simulation study, was concluded to be the makeup of lunar soil. The aggregates observed and the qualitative adhesiveness of simulated powders appear to approximate lunar soil observations. The median simulated powder particle sizes, at about one-seventh that estimated for lunar soil, is a fair approximation, although likely to produce somewhat greater adhesion.

GEOLOGICAL SAMPLING STUDIES

Rock comminution methods have been under development for acquiring powder specimens that are compatible with requirements for automated extraterrestrial geological analysis (refs. 13 and 14). A prime requirement was a method for producing a controlled rock particle size distribution. Reliance on sorting methods is thus avoided and thus possible mineralogical misrepresentation, since comminuted size ordinarily depends on mineralogy.

The optimal method developed entails first grinding a group of thin parallel ridges on the rock surface using dry ganged diamond wheels and subsequently removing these ridges by planing. The operations are illustrated in figure 7. The result is that powder size distributions are obtained, thus far on basalt and obsidian, that approach those desired for petrographic micros-

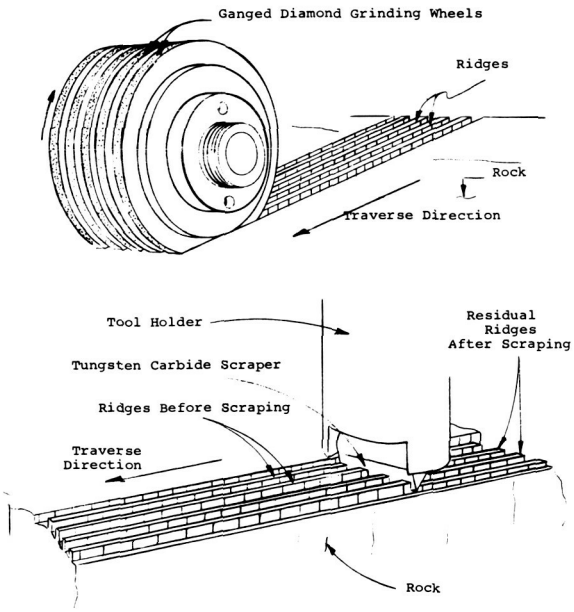

FIGURE 7.—Comminution method used for controlling particle size. Upper sketch shows ridge preparation; lower shows subsequent planning.

copy. Size distribution tests have been completed only at atmospheric pressure and are therefore discussed elsewhere (ref. 14). However, preliminary grinding tests of ridge formation have been performed in vacuum to observe potential grinding problems and particle trajectories relevant to powder collection.

Figures 8 and 9 show front and side views of the vacuum grinding system, which incorporates a commercial surface grinder, retaining its directional versatility, stability, and precision; movements are effected using the grinding machine's original controls. A large bell jar over the front of the chamber permits a full view and, by opening it, chamber accessibility.

Preliminary grinding tests were performed at 0.1 Torr to eliminate aerodynamic effects and at 4 Torr to simulate Martian pressures. Obvious powder swirling was observed at 4 Torr caused by grinding wheel generated air currents even at this low pressure, but only ballistic patterns were observed at 0.1 Torr. It was also observed that ridge formation was decidedly poorer at both vacuum levels. About 70 percent of the ridges were broken in vacuum compared with a negligible amount at atmospheric pressure. More powder clung to, or between, the grinding wheels in vacuum than at atmospheric pressure. This was concluded by running the wheels at high speeds after grinding and observing that considerably greater amounts of powder were thus flung out after vacuum grinding. These effects were most pronounced after brushing the grinding surfaces. Powder therefore appeared to be caked between the wheels and released after removing the outer "crust." The increased powder clinging to the wheels could help account for the poorer ridge forming capabilities in vacuum.

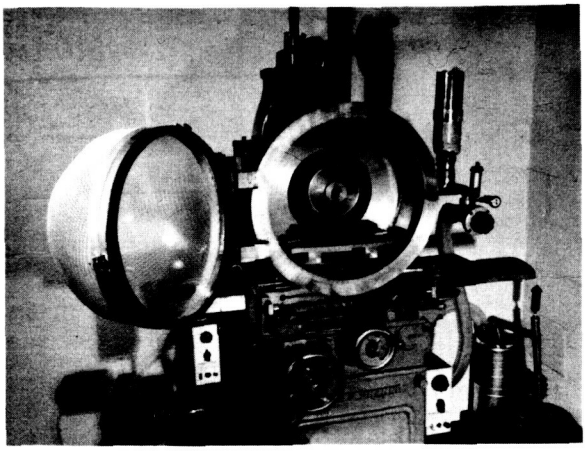

FIGURE 8.—Front view of vacuum grinding system.

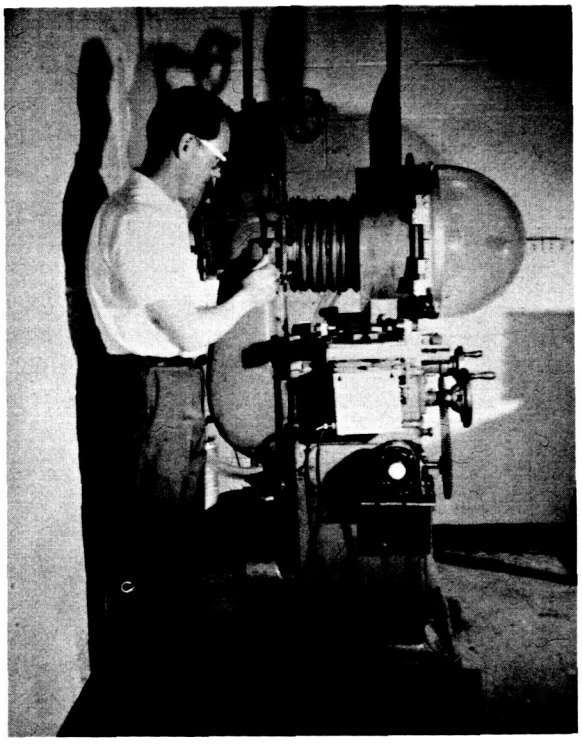

FIGURE 9.—Side view of vacuum grinding system.

METAL ADHESION STUDIES

Diverse studies of metal adhesion in vacuum exist, e.g., refs. 15 through 17. A review of theoretical and experimental work on this phenomena is presented in a report (ref. 18) from which results here described are derived. A distinguishing feature of this study is the extremely low pressure, 5×10^{-13} Torr, in which adhesion tests were administered. Other studies are believed limited to pressures higher than 1×10^{-9} Torr.

Materials were tested in an "extreme high vacuum" test facility described in ref. 18. The test procedure consisted in pressing together disk-shaped specimens in the 200° to 500° F temperature range and measuring the torque required to counterrotate specimens, both

while under load and after release of load. The shear stress was then calculated from the applied torque thus giving the corresponding frictional force and adhesional force, respectively. Adhesional forces were also measured following rotational loading. Representative data, including that for coated surfaces, obtained at 300° F, at 5×10^{-13} Torr, and for 100 psi loads are shown in table I. Comparative data at 760 Torr are included where available.

It is evident that substantial adhesional and frictional forces were generated even with hard materials. The vacuum environment increased adhesional forces having prior static loading by factors of 1.1 to 2.4, depending on material, as indicated. Vacuum adhesion under the same loading was also measured at 500° F. Forces, not shown in the table, were above 400 psi for softer materials such as copper and aluminum, reflecting large scale welding.

The table shows adhesional forces to be considerably greater for specimens with prior rotational loading than those with prior static loading, as might be expected. No comparative data exist at atmospheric pressure. Frictional forces are seen to increase by a factor of about 1.5 in vacuum for the three materials compared. The lowest frictional and adhesional forces are seen produced with molybdenum disulfide coated surfaces. This is in accordance with other studies of solid lubricants for vacuum bearing applications.

CONCLUSIONS PERTINENT TO LUNAR MINING

Some of the problems suggested by the three programs discussed include the following:

(1) More energy may be required in fragmenting solid rock into desired sizes. This is suggested by the larger mean particle sizes produced at 4×10^{-9} Torr than at 760 Torr under otherwise equivalent conditions.

(2) More time may be required in producing a given mean rock fragment size, for the same reasons as above.

(3) Both more time and more energy may be required in producing fragmented rock below some particular size, e.g., if powders are needed, regardless of specific size desired below that value. This is indicated by the four-fold increase in powder produced at 760 Torr compared with that at 4×10^{-9} Torr, independent of particle size.

(4) The size distribution of fragmented rock may differ regardless of mean particle size.

(5) Abrading devices used without fluids are likely to become more easily clogged, requiring frequent cleaning, as indicated in the abrasion sampling studies.

TABLE I.—*Frictional and Adhesional Forces in psi at 5×10^{-13} Torr (V) and 760 Torr (A)*

Material	Adhesion stress after 100 psi static load		Adhesion stress after 100 psi rotational load		Friction stress under 100 psi load	
	V	A	V	A	V	A
Al	12	10	155	.....	> 400	.....
Cu	28	15	141	.....	> 400	.....
17–4PH stainless	31	19	46	.....	> 400	350
440–C stainless	16	12	172	.....	310	250
Tungsten carbide	42	19	16	.....	78	46
Al_2O_3	12	.....	32	.....	450	.....
Cr_2O_3	12	.....	12	.....	140	.....
MoS_2	3	.....	10	.....	35	.....

(6) All three studies indicate that several factors may combine to make metal adhesion to metal a serious problem in certain kinds of equipment: (a) the increased adhesion of materials observed in vacuum; (b) the increased heating in abrading, fast moving, or other friction generating equipment, which results from a lack of convective cooling in vacuum; and (c) increased heating resulting from the effective dulling of abrading tools by powder clinging to the cutting edges. Such equipment may have to be limited to intermittant use to permit cooling. This would increase the time needed to perform certain tasks.

It appears that some of the potential problems discussed might be overcome by the use of very low pressure atmospheres, e.g., some of the rock fragment sizing problems. Bernett (ref. 1) observed no increase in silicate adhesion at 10^{-6} Torr. This is a possible argument for mining underground where a light atmosphere could be more easily maintained. However, other adhesional problems may require much higher pressures, e.g., the clogging of grinding wheels which was observed even at 0.1 Torr. This adhesion appears to have been promoted by heating due to the lack of convective gas currents and is likely to be primarily limited to small, friction-generating tools, e.g., hand drills and saws, as well as grinding wheels. Pressures above about 4 Torr may be sufficient for a gas pressure solution to these problems; the swirling powders observed at this pressure attested to appreciable convective currents. Thus far the best solution to metal adhesion problems appears to be MoS_2 lubrication, the use of hard bearing surfaces where possible, and cooling methods. The desireability of simulation studies to assess directly the lunar mining and associated problems implied by the foregoing studies is indicated.

ACKNOWLEDGMENTS

Results reported in this paper were derived from studies supported under NASA Contracts NAS1–5347 Task 2, NAS7–100 Subcontract 951422, and NASw–1616 and Air Force Contract AF04(611)–9717.

REFERENCES

1. BERNETTE, E. C.; ET AL.: Bearing Capacity of Simulated Lunar Surfaces in Vacuum. Am. Inst. Aeron. Astronaut. J., vol. 2, no. 1, Jan. 1964, pp. 93–98.
2. BROMWELL, L. G.: The Friction of Quartz in High Vacuum. Research Report R66–18, Mass. Inst. Technology, 1966.
3. HALAJIAN, J. D.: Soil Behavior in a Low and Ultrahigh Vacuum. Paper 64–WA/AV–14, Am. Soc. Mech. Engrs., 1964.
4. SALISBURY, J. W.; ET AL.: Adhesive Behavior of Silicate Powders in Ultrahigh Vacuum. J. Geophys. Res., vol. 69, no. 2, Jan. 1964, pp. 235–242.
5. SJAASTAD, G. D.: An Experimental Study in Lunar Soil Mechanics. The Lunar Surface Layer, edited by J. W. Salisbury and P. E. Glaser, Academic Press, 1964, pp. 23–66.
6. VEY, E.; AND NELSON, J. D.: Engineering Properties of Simulated Soils. J. Soil Mech. Found. Div., Proc. Am. Soc. Civil Engrs., vol. 91, no. SM1, Proc. Paper 4199, Jan. 1965, pp. 25–52.
7. WONG, R. E.; AND KERN, C.: Test Program for Determination of Soil Constants in Vacuum. Paper 64–WA/AV–11, AM. Soc. Mech. Engrs., 1964.
8. RYAN, J. A.; ET AL.: Adhesion of Silicates Cleaved in Ultrahigh Vacuum. J. Geophys. Res., vol. 73, no. 18, Sept. 1968, pp. 6061–6070.
9. BLUM, P.; ET AL.: Adhesion of Lunar Soil Simulated by Rock Comminuted in Vacuum. ASTM/IES/AIAA Second Space Simulation Conference, Am. Soc. Testing Mats., 1967, pp. 63–68.
10. BLUM, P.; ET AL.: Properties of Powder Ground in Ultrahigh Vacuum. NASA CR–66276, 1967.
11. BELL, P. R.: Vacuum Welding of Olivine. Science, vol. 153, no. 3734, July 1966, pp. 410–411.
12. JAFFE, L. D.: The Surveyor Landings. Science, vol. 164, no. 3881, May 16, 1969, pp. 775–788.
13. BLUM, P.; AND HORDON, M. J.: Study of Abrasive Techniques for Lunar and Planetary Solid Rock Geological Sampling. NASA CR–90328, 1967.
14. BLUM, P.: Development of Abrasion Sampling Techniques for Extraterrestrial Geological Analysis. Norton Research Corporation, Cambridge, Massachusetts, Final Report for NASA Contract NASw–1616, 1968.
15. GILBREATH, W. P.; AND SUMSION, H. T.: Solid-Phase Welding of Metals under High Vacuum, J. Spacecraft and Rockets, vol. 3, 1966, pp. 674–679.
16. HAM, J. L.: Metallic Cohesion in High Vacuum. Am. Soc. Lubrication Engrs. Trans., vol. 6, 1963, pp. 20–28.
17. WINSLOW, P. M.; AND MCINTYRE, D. V.: Adhesion of Metals in the Space Environment, J. Vac. Sci. Technol., vol. 3, no. 2, 1966, pp. 54–67.
18. HORDON, M. J.; AND ROEHRIG, J. R.: Study of Vacuum Welding, Air Force Tech. Report AFRPL–TR–66–105, Norton Research Corporation, Cambridge, Massachusetts, Final Report for Air Force Rocket Propulsion Lab. Contract AF04(611)–9717, 1967.

STANLEY A. FIELDS
Space Sciences Laboratory
Marshall Space Flight Center, NASA
Huntsville, Alabama

A Study of Friction and Adhesion in a Simulated Lunar Vacuum

A series of experiments has been conducted to determine the problems of friction and adhesion in a simulated lunar environment. The tests were made in a vacuum of 10^{-10} and 10^{-11} Torr.

The friction tests were conducted to determine the coefficient of friction between granular simulated lunar soils and metal test flats. The test flats were made of Steel AISI 1020 and Aluminum 7075. The granular soils were basalt and quartz in the size ranges 250 to 500 and 38- to 62-micron-diameter particles. The coefficient of friction for all samples was higher in vacuum than in air.

Several types of granular simulated lunar soils in varying size ranges were used in the adhesion experiments. The test results indicate that some materials adhere readily while others do not, and that particle size and shape are influential in the adhesive strength of soils.

This chapter relates the results of an experimental program conducted to determine the problems of friction and adhesion in a vacuum environment.

The friction tests were designed to determine the coefficient of friction between granular simulated lunar soils and plates of engineering materials. The materials used were basalt, quartz, steel AISI 1020, and aluminum 7075.

The adhesion tests were conducted using basalt, pumice, and serpentine soils of varying sizes. The soils were placed inside a 304 stainless-steel container for exposure to vacuum. This container was designed to allow various engineering materials to be inserted to study the adhesion of the soils to these materials. The coefficient of friction investigations and analyses were conducted in part by the Grumman Aircraft Engineering Corporation under Contract NAS8–5415 with the George C. Marshall Space Flight Center.

COEFFICIENT OF FRICTION

Test Apparatus and Procedure

The friction tests were conducted in an ion-pumped-vacuum system which was bakeable to 250° C. A detailed description of the friction-measuring apparatus can be found in reference 1. The test fixture was designed so that the test surfaces could be separated during pump-down and bakeout to allow outgassing of both surfaces. The surfaces were moved together before the rotation began and a normal load applied and held constant during the rotation of the metal disk. Separate heating elements permitted outgassing of either the metal disk or the soil, or both specimens simultaneously.

Quartz crystals from Hot Springs, Arkansas, and basalt from Somerset County, New Jersey, were crushed and sifted to obtain coarse particles ranging in diameter from 250 to 500 microns and fine particles ranging in diameter from 38 to 62 microns. The test sample was placed in a container 6.0 cm in diameter and 1.9 cm deep with the upper edge bent outward to prevent friction between the outer rim of the disk and the powder. The weights of the granular specimens were 65.6g for the coarse and fine basalt and coarse quartz and 53.6g for the fine quartz.

The metal disks were machined from Aluminum 7075 and Steel AISI 1020. The finished disks were 3.8 cm in diameter, with a cross-

sectional thickness of 0.063 cm. The surface of each disk was polished to a finish of less than 6 μ-in. The disk was rotated through a positive drive rotary seal by a motor located outside the vacuum chamber.

A strain gauge balance was used to measure the axial and torsional forces. A diaphragm section above the center of the unit was instrumented to measure axial loads, and a thin-walled vertical cylindrical member instrumented to measure the torsional forces. Normal forces were measured by means of a two-active-arm bridge and torsional forces by means of a four-active-arm bridge.

The vacuum system used for the friction test was designed for operation in the 10^{-10} Torr range with the test fixture and sample inside the chamber. The chamber was rough-pumped with liquid-nitrogen-cooled sorption pumps and a Welch Turbo-Molecular pump. The fine pumping was accomplished by an ion pump and a titanium sublimation pump with a combined pumping speed of approximately 700 liters/sec. Finally, when the pressure approached the ultimate value, a helium cryopump was activated. The system, test fixture, and sample were baked during the pump-down cycle to outgas the various components.

A new metal disk and granular sample were used in each test. Earlier tests indicated that the coefficient of friction increased with increased use of the two samples. The granular sample was placed in the container and positioned on the test fixture. A metal disk was positioned on the test fixture above the granular sample. If the test was to be a vacuum test, the two samples remained separated and the pumpdown started. The samples and system were baked during the pumpdown and allowed to cool to ambient temperature before conducting the test. The disk was loaded with a 1.13 kg weight and rotated at 3 rpm during all tests. The two surfaces were brought together before the rotation of the metal disk started.

The output of the strain-gauge amplifier generally resulted in a high initial torque followed by a cyclic lower torque. The initial value was only slightly higher for the tests performed in air, and, in most instances, significantly higher for the tests performed in ultrahigh vacuum.

Test Results

Torque values representative of the initial condition and the continued rotation were read from the strip chart. The coefficient of friction was computed from these torque values by the formula:

$$\mu = \frac{3T}{2WR}$$

where

μ = coefficient of friction
T = torque in inch-ounces
W = load in ounces
R = radius of disk in inches

Two tests were performed for each combination of metals and minerals (table I). The coefficient of friction was higher (both for the initial value and the dynamic value) in vacuum than in air. However, the increase was not as large as might be expected in the 10^{-10} Torr environment.

ADHESION

A series of tests has been conducted to determine potential problems to be encountered in a lunar environment due to the adhesion of gran-

TABLE I.—*Average Coefficient of Friction Between Rotating Metal Disk and Mineral Powder*

Material	ATM		10^{-10} Torr	
	μ_i*	μ_c**	μ_i*	μ_c**
Aluminum 7075 on quartz				
Fine	.27	.26	.45	.31
Coarse	.29	.26	.61	.28
Basalt				
Fine	.26	.19	.44	.24
Coarse	.34	.24	.80	.24
Steel 1020 on quartz				
Fine	.20	.17	.33	.33
Coarse	.30	.22	.43	.27
Basalt				
Fine	.23	.18	.33	.27
Coarse	.27	.20	.49	.26

*μ_i = initial value of coefficient of friction.
**μ_c = dynamic value of coefficient of friction.

ular particles to the surface of engineering materials. Three simulated lunar soils were selected for use in the tests and several size ranges of the materials were used.

Test Apparatus and Procedure

The test apparatus consisted of a 304 stainless-steel drum, a variable speed motor, and a magnetic rotary seal. The drum was 25 cm long and 15 cm in diameter. The drum contained four slats 1.3 cm high, which extended the length of the drum. The slats were 90° apart and were removable to allow slats of various materials to be used. One end of the drum was closed by a plate containing fine mesh wire to allow gas to escape. The other end was closed by a glass window to allow viewing of the sample while the test was in progress. The drum was attached to a magnetic-coupled rotary seal mounted on a port of the vacuum chamber. The variable-speed motor was used to rotate the drum. The vacuum chamber was completely oil-free using sorption, ion, and titanium sublimation pumps in the standard way to obtain the ultimate vacuum of 10^{-12} Torr. The pump-down procedure included a bake-out of the chamber at 250° C.

The test procedure consisted of crushing and sieving the sample to be used. After the sample had been sieved a specified amount, usually 180g, it was weighed, placed in the drum, and baked at 250° C in an atmospheric oven for 4 hours. The drum was transferred from the oven to the vacuum chamber while it was hot and pumped down as soon as possible. When the desired vacuum was obtained, the drum was rotated at 1 rpm until 100-percent adhesion occurred, or until it became obvious that complete adhesion would not occur. When all the particles would not adhere at the rotation rate of 1 rpm, the rate was accelerated to increase the force on the wall of the drum. The force on the surface of the drum is dependent on the rotation rate of the drum and the amount of material in the drum.

Test Results

The results of 16 tests are listed in table II, which shows that fine basalt particles adhere very quickly at a vacuum above 10^{-9} Torr. It also indicates that as the amount of sample is increased, or as the size is increased above 62 microns, the ability of the soil to adhere decreases.

As the drum rotated, the slats lifted the granular soil toward the top of the drum and allowed it to fall and expose the individual grains to the vacuum. The soil usually began to adhere as the drum started to rotate and continued to build up first on the stainless steel and then to itself until all particles had adhered at which time the drum was stopped.

In tests 10 and 11 the slats which were stainless steel in prior tests were changed to aluminum, copper, and Teflon. The adhesion to these materials was about equal, however, with a slight increase around one of the aluminum slats.

The initial tests (13 and 14) on pumice showed very weak adhesion forces. Additional tests determined that the pumice samples were almost impossible to outgas. However, when held under vacuum for a sufficient time, the pumice adhered as quickly as the basalt.

A test was made on serpentine because of its high chemical water content. Despite its chemical composition, it behaved very similarly to the basalt.

The experimental apparatus did not allow quantitative analysis of the adhesive forces to be made. However, from the experimental results and observations, it is concluded that although the soils do adhere to themselves as well as to engineering materials, the adhesive strength is weak.

SUMMARY AND CONCLUSIONS

The Surveyor program has confirmed that a portion of the lunar surface consists of fine-grain granular soil with an adhesive strength between 10 and 100 dynes/cm^2 (ref. 2). Also, the experiments carried out in the laboratory and reported here indicate that the soils tested exhibit some adhesive strength in a vacuum environment.

The coefficient of friction between the metal disks and the powder soils for all samples tested was higher in vacuum than air. In all tests the initial coefficient of friction was higher than the dynamic coefficient of friction. These values are

TABLE II.—*Adhesion of Simulated Lunar Materials*

Test number	Sample	Diameter (μ)	Weight (g)	Pressure (Torr)	Time for 100% adhesion (min)	Remarks
1	Basalt	10 to 20	180	1.7×10^{-11}	15	Adhesion began immediately with rotation of drum at 1 rpm.
2	Basalt	20 to 37	180	2.2×10^{-12}	15	
3	Basalt	37 to 62	180	ATM	.....	No adhesion after 12-hr rotation; small amount of sticking.
				1×10^{-6}	.....	
4	Basalt	37 to 62	180	1×10^{-9}	30	
5	Basalt	37 to 62	360	3.5×10^{-11}	100	24-hr rotation at 1 rpm—20% adhered; 100-min rotation at 20 rpm—100% adhered.
6	Basalt	37 to 62	600	2.0×10^{-10}	.....	2-hr rotation at 6 rpm—25% adhered; 6.5-hr rotation at 20 rpm—40% adhered; 2-hr rotation at 56 rpm—30% adhered.
7	Basalt	67 to 125	180	8.4×10^{-10}	65	100% adhesion at 21 rpm.
8	Basalt	125 to 250	180	7.2×10^{-10}	.....	Drum rotated at various rates up to 95 rpm for 24 hrs. Adhesion did not exceed 10%.
9	Basalt	10 to 37	180	1.8×10^{-10}	2	7 rpm.
10	Basalt	10 to 37	180	2.4×10^{-10}	8	2 Al, 2 Cu slats; heavy concentration around one Al slat; equal amount for other 3.
11	Basalt	10 to 37	180	1.3×10^{-10}	3	2 SS, 2 Teflon slats; uniform adhesion.
12	Basalt and pumice mix	20 to 37	200 P 200 B	8.0×10^{-11}	15	
13	Pumice	20 to 62	180	2.5×10^{-10} 2.5×10^{-9}	.....	Sample outgassing limited; ~ 20% adhered.
14	Pumice	20 to 62	180	4.5×10^{-11} 2.4×10^{-9}	.....	Similar results as in #13.
15	Pumice	10 to 37	180	8.0×10^{-11}	1	Sample under vacuum for 40 days.
16	Serpentine	10 to 37	180	9.5×10^{-10}	3	

significantly different in vacuum. It is believed that the initial value of the coefficient of friction was high because of an adhesive bond between the metal disk and the granular sample. The coefficient of friction between aluminum 7075 and the granular samples was higher in atmosphere than between steel 1020 and the granular samples. The coefficient of friction was greater between steel 1020 and the granular samples in a vacuum of 10^{-10} Torr than it was between aluminum 7075 and the granular samples. The only exception was for one test on coarse quartz.

The fine particles of basalt and serpentine adhered at a vacuum greater than 10^{-9} Torr. Only after prolonged exposure to vacuum did the pumice particles adhere. When the soil particle size was increased over 62-μ diameter, the adhesion decreased. The adhesion was similar for basalt to stainless steel, aluminum, copper, and Teflon.

It is concluded from the test program that adhesion and friction problems do exist in a vacuum environment. However, the problems do not appear to be severe for the materials and vacuum used in the program.

REFERENCES

1. MOHR, G.; AND KARAFIATH, L. L.: Determination of the Coefficient of Friction Between Metals and Nonmetals in Ultrahigh Vacuum. Final Report on Contract NAS8–5415, Dec. 1967.
2. CHRISTENSEN, E. M.; ET AL.: Lunar Surface Mechanical Properties. Surveyor VI Mission Report, Part II: Scientific Results, Technical Report 32–1262, Jet Propulsion Laboratory, Jan. 10, 1968, pp. 47–108.

WALLACE. W. ROEPKE
Bureau of Mines
Twin Cities Mining Research Center
Minneapolis, Minn.

Friction Tests in Simulated Lunar Vacuum

This paper describes techniques being used by the U.S. Bureau of Mines at the Twin Cities Mining Research to perform friction testing of mineral materials in ultrahigh vacuum. Under the assumption that lunar surface materials may be completely degassed and atomically clean surface conditions may be encountered in breaking and handling these materials, an attempt is being made to provide information on frictional behavior of mineral surfaces under this "worst case" situation. Preliminary experiments show that ultrahigh vacuum environment produces substantial increases in the kinetic coefficients of friction for quartz surfaces.

INTRODUCTION

The U.S. Bureau of Mines is studying the problems of using lunar surface materials under a contract funded by NASA's Office of Advanced Research and Technology. The objective of the studies is to help provide basic scientific and engineering information about the use of extraterrestrial mineral resources to support future manned space missions. The studies are being carried on as a series of coordinated research tasks at several different Bureau research centers (ref. 1). One of the studies, which is being performed in the Surface Properties Laboratory at the Bureau's Twin Cities Mining Research Center, is concerned with the frictional behavior of rock surfaces in lunar vacuum environment.

Since the exact surface states of rock on the Moon are not known, basic information on frictional behavior important to drilling, breaking, and handling lunar materials is needed over the range of possible conditions. If we assume the worst case for frictional behavior in the lunar environment, we must be prepared for the possibility that hundreds of millions of years of exposure to the hard vacuum, radiation, and particle bombardment of space may have produced a lunar surface that is totally outgassed to a considerable depth and rock surfaces that approach an atomically clean condition. Thus friction tests to simulate possible lunar situations must include not only ultrahigh vacuum environment but also well degassed test materials and a suitable surface cleaning technique.

LABORATORY SETUP

Experimental equipment being used in the friction studies includes an ultrahigh vacuum (UHV) system capable of simulating the lunar vacuum, auxiliary measurement devices capable of accurately determining conditions in the system while experiments are underway, and an apparatus for use in the system to measure friction between mineral and mineral-metal combinations. Also available for cooperative use in the studies are a 100-watt CO_2 laser and a scanning electron microscope (SEM).

The UHV system is an ion-pumped system with sorption forepumps and a titanium sublimator. It has a volume of 254 liters and a pumping speed of 400 liters per second at standard temperature and pressure. The system can reach a pressure better than 5×10^{-12} Torr when baked, clean, and empty. Pressure gaging, in addition to the pump current, includes a Bayard-Alpert gage and a Kriesmann cold cathode gage. However, the most critical pressure instrumentation is a quadrupole mass spectrometer with a bakeable head, a sensitivity of 1×10^{-15} amp/Torr

382-451 OL-70-8

for nitrogen, and a mass range from 1 to 500 amu, providing a rapid quantitative method of determining conditions in the chamber.

Figure 1 shows the UHV system in the Surface Properties Laboratory. Working space in the chamber is approximately 24 inches in height by 18 inches in diameter. Twelve ports are located on the circumference of the pump well for instrumentation or motion feedthroughs, and three ports are located on the chamber wall for viewing windows. Special windows with small germanium inserts capable of passing infrared radiation have been designed and constructed to permit visual and photographic observation simultaneously with use of the CO_2 laser shown in the figure.

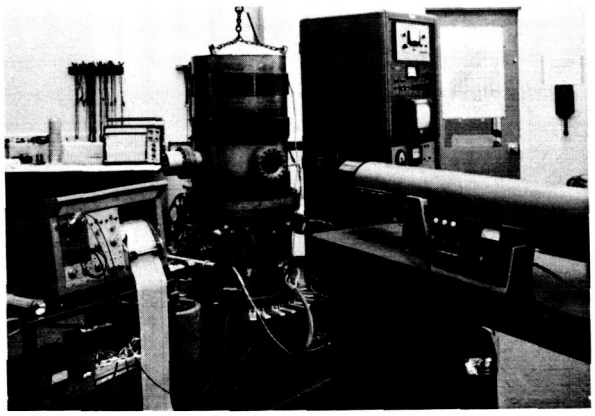

FIGURE 1.—Surface properties laboratory showing UHV system and CO_2 laser.

Accessory equipment includes an oil diffusion pumped, liquid nitrogen cold trapped high vacuum system, capable of a pressure of 5×10^{-8} Torr clean and empty, which is used for preliminary testing of techniques and devices designed for the UHV systems; a vacuum oven for specimen preconditioning; an ultrasonic vapor degreaser for cleaning components used in the vacuum systems; and a small bench-type spot welder for strain gage hookup.

The laboratory area is isolated as far as possible from extraneous contamination. A supplementary air conditioner and a continuously operating dehumidifier are used to help control the laboratory environment. The UHV system is not opened when the atmospheric water vapor content exceeds 6.8g per cubic meter. At 72° F this absolute water vapor content is approximately 35 percent relative humidity. Temperature can be controlled at $72° \pm 1.5°$ F.

A simple friction apparatus has been developed for use in the UHV chamber to measure kinetic friction coefficients at various loads between mineral samples and a metal or mineral probe. The apparatus is shown in figure 2 installed in the open chamber. It has only two major parts, the sample holder driven by a bellows-sealed wobble type rotary feedthrough, and the instrumented probe mounted on a ball screw driven by a second bellows-sealed rotary feedthrough. Normal load and rotational motion of the sample wheel are controlled independently from outside the chamber. Twelve samples 1.5 inches long, 0.5 inch wide, and $\frac{1}{8}$ inch thick can be mounted on the sample wheel. Thus a large number of

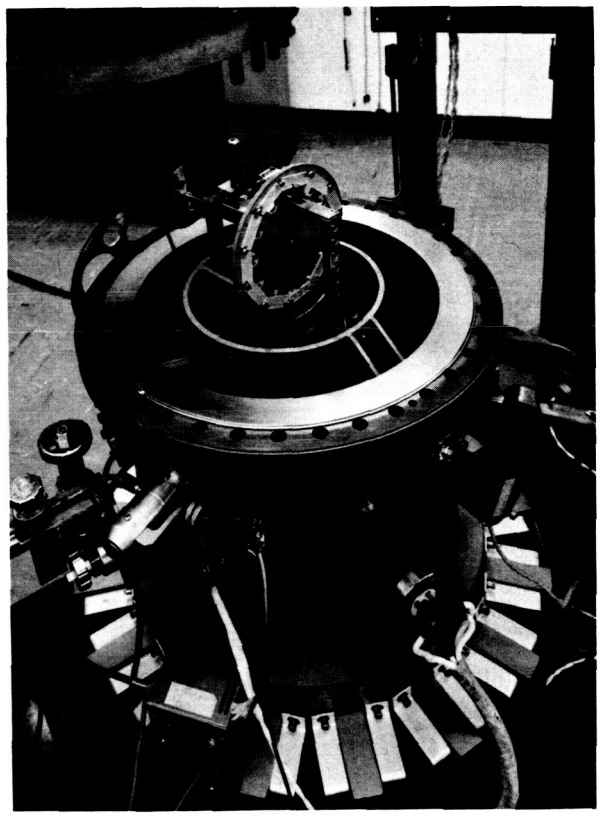

FIGURE 2.—UHV system in surface properties laboratory with friction apparatus installed.

test data can be obtained without opening the chamber.

Figure 3 shows a close view of the sample wheel and the probe assembly. The heart of the friction apparatus is the double bridge strain gage transducer shown in an enlarged view in figure 4. It is made up of two full bridges mounted on double beams at 90° angles. The bottom bridge gives a continuous measure of normal load applied during the test and the top bridge gives a continuous measure of the tangential force. Checkout with deadweight loads showed that interference due to twisting or other distortion between the two bridges was an insignificant 0.12 percent.

EXPERIMENTAL WORK

Preliminary work included obtaining valid baseline data for the empty UHV system, finding out whether rock samples could be handled by the system while still maintaining UHV, establishing sample preparation techniques compatible with system and test requirements, obtaining baseline data for various simulated lunar rocks, and acquiring outgassing data on these rocks. Careful sample preparation is crucial to any UHV tests. Samples are cut from the bulk and finished using only water as the cooling agent. When the samples are received in the laboratory they are placed in the vacuum oven at 130° C until the pressure falls to the ultimate of 5×10^{-3} Torr. Since water vapor is the main problem in any vacuum system, a major portion is excluded by filling the interstices of the samples with a dry gas. The samples are then transferred to a desiccator where they are stored until used.

Preliminary to friction measurements in vacuum, a considerable effort has been devoted to the measurement of the outgassing properties of several simulated lunar rocks. Outgassing, or the release of gases from a solid specimen into a vacuum chamber, can have a strong influence on

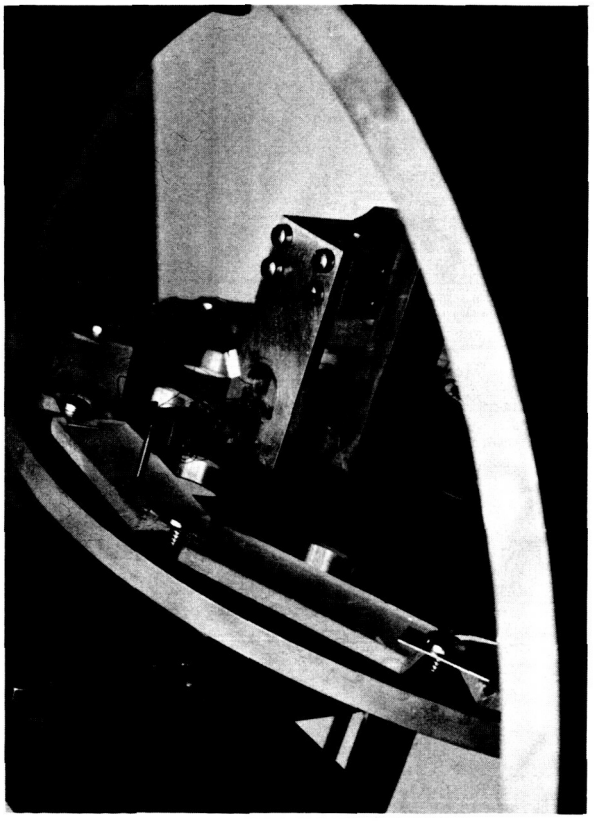

FIGURE 3.—Close view of sample wheel and force pickup probe on friction apparatus.

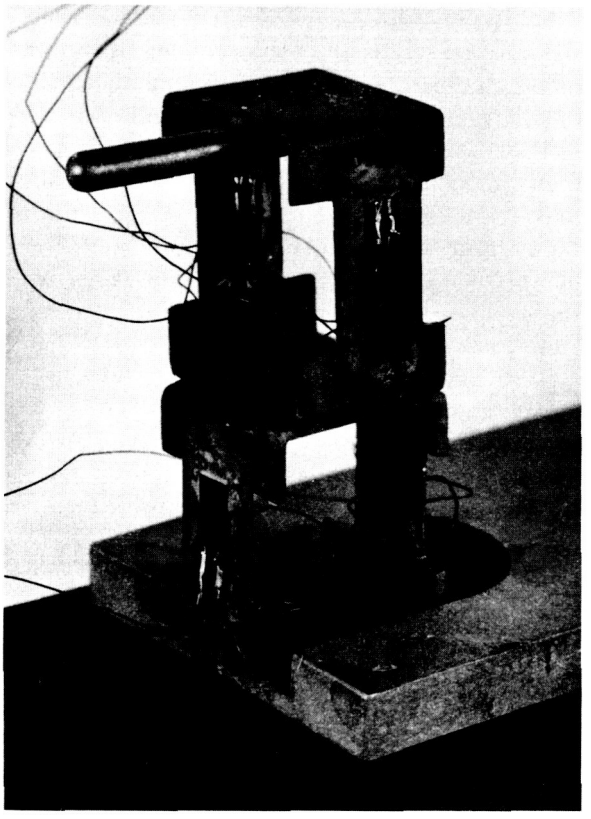

FIGURE 4.—Enlarged view of force pickup probe.

property measurements or behavioral studies. Also, outgassing of the test specimen imposes an additional load on the vacuum pump and lengthens the time required for the system to reach its ultimate pressure. In preparing to test rock specimens in vacuum, their outgassing characteristics need to be known so that it is possible to estimate the pressures that can be attained, the limitations on sample size, and the time required to pump the samples to an acceptable condition of steady-state pressure.

Results of the outgassing studies have been presented previously (ref. 2). They showed considerable difference in the behavior of the various rocks as demonstrated in table I, which represents data on 1-inch samples with bakeout temperatures no greater than 130° C. The pumice and tuff, having a high surface area and a porous texture, released a significant quantity of gas, but did so quite readily. In contrast the denser, more compact basalt released its adsorbed gases relatively slowly and reached steady-state pressure approximately one decade higher than the tuff. Dacite exhibited still another type of behavior. Virtually no additional pumping load was added to the chamber. The ultimate pressure was slightly lower than the tuff and almost equal to that of the empty chamber.

TABLE I.—*Outgassing of Simulated Lunar Rocks in Ultrahigh Vacuum*

Sample	Pressure at 14 hrs (10^{-10} Torr)	Net outgassing rate at 14 hrs (10^{-12} Torr liter/sec)
Empty chamber	1.5	.....
Dacite	2.0	nil
Pumice	2.5	2.0
Tuff	4.5	8.0
Serpentinite	7.0	8.0
Basalt	25	100
Granodiorite	30	250

Two additional long-term outgassing studies have been performed. The first of these studies was done to determine whether a 1-inch cube of basalt could be brought to equilibrium at a pressure below the 10^{-9} Torr range. Six weeks of baking and pumping on the 1-inch cube of basalt did bring it to equilibrium in the 10^{-12} Torr range. It therefore seems feasible to conduct experiments on larger basalt samples in a simulated lunar environment if sufficient pump-down time is available. The second long-term study was done on a 4-inch cube of dacite. The dacite outgassed readily as was expected, and in 1 week the chamber was in the mid-10^{-12} Torr range.

Several dozen friction tests of mineral-metal pairs have been conducted to establish operational characteristics of the friction apparatus and sensing equipment. The mineral used has been unoriented polycrystalline quartz while the friction probe has been 0.0635-inch (No. 52) carbide drill stock. The test surface of the quartz has been prepared with a 25-micrometer finishing material. The probes used have hemispherical tips with a radius one-half the diameter of the drill stock. The shape of the friction probe tip will allow an apparent area of real contact to be obtained by measuring the track widths with the SEM which, in turn, will allow a calculation of shear strength of the material at the sliding interface (refs. 3 to 5).

Tests have been conducted under four environmental conditions: ultrahigh vacuum cleaned, ultrahigh vacuum uncleaned, dry atmosphere, and normal (room) atmosphere. The results (see table II) show an increasing coefficient of friction as the environment changes from normal atmosphere through dry atmosphere to ultrahigh vacuum. Surface cleaning of the samples under light load (10g) resulted in a marked increase in friction coefficient.

TABLE II.—*Kinetic Coefficients of Friction Between Quartz and Tungsten Carbide*

Conditions	Normal load, g			
	10	50	100	150
Ultrahigh vacuum cleaned	0.50	(*)	0.42	(*)
Ultrahigh vacuum uncleaned	.33	0.34	.41	0.42
Dry atmosphere	.31	.25	.32	(*)
Normal atmosphere	.20	.23	.26	.27

*Data incomplete.

Work on preparing surfaces that approach atomically clean surface conditions is continuing. Several cleaning techniques were considered including high temperature baking, plasma or ion bombardment, sputtering, electron beam, cleavage, and wire brushing. None of these techniques provides a suitable surface for friction studies of the type planned. On the basis of literature study (refs. 6 to 9) the best choice for our study seemed to be a CO_2 laser emitting at 10.6 micrometers with a maximum 100-watt multimode CW output.

The laser energy must be presented to the sample surface in such a manner that it cleans without melting or damaging the surface. With a laser input to the surface of milliseconds duration and of sufficient intensity to raise the surface temperature hundreds of degrees Centigrade for this short duration, it appears to be possible to clean the surface without physical damage. Cleaning effectiveness is evaluated by monitoring the background species in the system with the quadrupole mass spectrometer and by examining the surface with the SEM after the sample is removed from the chamber. The area cleaned must be large enough to prevent surface migration from the uncleaned surface but not so large that the bulk of the material cannot act as a heat sink efficient enough to return the sample to the ambient temperature within milliseconds. Furthermore, the laser must be aligned on the sample in such a manner that for the given test velocity the sample is cleaned far enough from the probe to cool but not so far as to allow recontamination before the test. Precise alignment control and exact measurement of surface temperatures will require a high quality radiometer which is expected to be available in the near future.

The SEM will be used to evaluate surfaces of minerals before and after irradiation with the CO_2 laser and after the friction tests have been run. This work will provide data for correlations between beam energy, mass spectrometer data on degassing of the surface during irradiation, surface damage, if any, caused by the laser beam, and surface damage due to the friction probe. In addition to identifying the area of real contact and measuring the shear strength of the material, the SEM analysis will also provide information on cracking, surface fragmentation, plastic flow, and interfacial adhesion.

REFERENCES

1. ATCHISON, T. C.; AND SCHULTZ, C. W.: Bureau of Mines Research on Lunar Resource Utilization. Proc. of the Sixth Annual Meeting of the Working Group on Extraterrestrial Resources, NASA SP-177, 1968, pp. 65–74.
2. ROEPKE, W. W.; AND SCHULTZ, C. W.: Mass Spectrometer Studies of Outgassing from Simulated Lunar Materials in Ultrahigh Vacuum. Fourteenth National Symposium of the American Vacuum Society, Oct. 1967.
3. BRAITHWAITE, E. R.: Solid Lubricants and Surfaces. MacMillan Co., 1964, pp. 1–28.
4. BOWDEN, F. P.; AND TABOR, D.: Friction and Lubrication of Solids. Clarendon Press, pt. 1, 1958, pp. 1–24, 104–111; pt. 2, 1964, pp. 52–107, 159–212.
5. BOWDEN, F. P.; AND TABOR, D.: Friction and Lubrication. Methuen and Co., Ltd., 1967, pp. 1–82.
6. REDHEAD, P. A.; HOBSON, J. P.; AND KORNELSON, E. V.: The Physical Basis of Ultrahigh Vacuum. Chapman and Hall, 1968, pp. 37–87, 239–242.
7. FARKASS, I.: Problems of Producing a Clean Surface by Outgassing in Ultrahigh Vacuum–Fundamental Phenomena in the Material Sciences. Proc. of the Second Symposium on Fundamental Phenomena in the Material Sciences, vol. 2, 1966.
8. LEVINE, L. P.; READY, J. F.; AND BERNAL, E.: Laser Bombardment Effects on Vacuum Surfaces. Research and Development, Dec. 1965.
9. LEVINE, L. P.; READY, J. F.; AND BERNAL, E.: Gas Desorption Produced by a Giant Pulse Laser. J. Appl. Phys., vol. 38, No. 1, Jan. 1967, pp. 331–336.

J. A. RYAN and J. J. GROSSMAN
Space Sciences Department
McDonnell Douglas Astronautics Company
Santa Monica, Calif.

Comments on Lunar Surface Adhesion

Considerable interest in the ultrahigh vacuum adhesion of dielectrics has been generated in recent years because of the fear that adhesion of lunar materials may pose problems to lunar missions. This has resulted in various experimental studies which have shown that dielectrics, specifically silicates, do indeed adhere to each other, and to other materials, at equivalent lunar vacuum. Much of this work has been summarized by Ryan (ref. 1), Ryan et al. (ref. 2), and Grossman (ref. 3).

The Surveyor and Apollo lunar missions have verified that the lunar materials adhere. This adhesion has been likened in strength to that of damp sand (ref. 4). The success of Apollo 11 has demonstrated that this relatively weak adhesion does not pose serious problems to lunar missions, at least for those where the tasks performed are similar to those performed to date. The purpose of this chapter is to point out that under certain conditions adhesion could cause serious problems and, hence, that it is unwise to become complacent about the matter. Before discussing the conditions under which adhesion could be a problem, it is worth considering how the early laboratory findings compare with the Surveyor findings. This is important since it will indicate the degree to which terrestrially obtained data can actually predict lunar behavior, and we will be using recently obtained terrestrial data to predict potential lunar adhesional problems. In making this comparison, we take the rather parochial approach of using almost solely our own experimental data, with due apologies to other investigators.

A few years back we studied the adhesion, in ultrahigh vacuum, between silicate disks (apparent contact area of 0.3 cm) after touch contact, and after the application of a load force (ref. 1). The contact faces were fabricated in air and then chemically etched. The resultant surface roughness was between 3 to 6 microns peak-to-peak. Adhesion forces after touch contact were typically in the range of 1 dyne. (Actually the weight, ≈ 20 gm, of the upper sample and support was applied to the interface.) Surveyor found soil adhesion (cohesion) in the range of 7×10^2 to 1.2×10^4 dynes cm^{-2}. Our results cannot be precisely compared to the Surveyor results, but there are several ways in which we can obtain indications as to whether there are any obvious discrepancies between the two sets of data. The simplest way is to assume (rather naively) that our rough surfaces were equivalent to two layers of granular material in contact. With this assumption, we find that the touch contact lunar soil cohesion would be about 3 dynes cm^{-2}. This value is lower than the Surveyor values, but this is not unexpected since it is not necessary for more than three asperities to be in contact, for the disks. A more realistic assumption would be to assume that each grain of our hypothetical lunar soil touches an overlaying grain at a single point, structural stability coming from adjacent grains, and, hence, that the adhesion between each grain pair is about one-third that between the disks. Surveyor has indicated that the bulk of the lunar soil grains have diameters in the range 2 to 60 microns. If we assume that the basic soil matrix is supported primarily by the 60-micron grains, in a cubic packing, then the soil cohesion would be $\approx 3 \times 10^4$ dynes cm^{-2}. If the matrix is supported primarily by the 30-micron particles, the soil cohesion would be $\approx 10^5$ dynes cm^{-2}. These values are somewhat higher than the Surveyor

values but represent upper bounds in the sense that the lunar soil porosity appears to be higher than that of a cubic packing and a relatively wide range of grain sizes is present. Both factors would tend to cause significant decreases in the cohesion magnitude. We have tried several other ways of comparing the data, such as load force effects, and in all cases the results indicate compatibility. (The reader may find it interesting to try his own approaches.) In addition, Salisbury et al. (ref. 5) estimated adhesion forces between 5-micron particles as being $\approx 2\text{–}3 \times 10^{-4}$ dyne. In a cubic packing this would result in a soil cohesion of $0.8\text{–}1.2 \times 10^{3}$ dynes cm^{-2}. Also Stein and Johnson (ref. 6) estimated the adhesion between 140-micron particles as being 3×10^{-2} dynes, which for a cubic packing would give a soil adhesion of 1.5×10^{2} dynes cm^{-2}. It thus appears that the early terrestrial experiments are consistent with the findings of Surveyor. It should be noted that in all these early studies the contacting surfaces were contaminated by the presence of adsorbed gases. If we assume that the lunar and terrestrial data are indeed compatible, this would imply that the lunar surfaces are also contaminated to a degree, this contamination having been either present prior to the landings or produced by the landings. However, as will be seen below, it may be possible to have the same cohesion magnitude even if the surfaces are ultraclean.

Our recent work has consisted of cleaving and fracturing various silicates at ultrahigh vacuum (refs. 2 and 3), the purpose being to produce ultraclean surfaces. In doing this we found that the adhesion forces after touch contact were much larger (up to 2×10^{4} dynes); that considerable surface charging was produced (greater than 10 e.s.u. cm^{-2}); that the silicates would adhere strongly to any metal in the vicinity, generally without any indications of discharge; that the charge persisted for months; that it maintained itself up to system pressures of 10^{-2} Torr; and that, due to the long range nature of the forces, removing the silicate samples from the metal surface was much like trying to remove iron filings from a magnet. Let us consider what these findings indicate concerning potential adhesion problems.

First, the adhesion magnitude of the clean surfaces is relatively large—large enough to support the sample weight. The question arises as to how large a silicate block could be supported. We have found that the charge distribution consists of a mosaic of positive and negative charge patches over the crystal face and that the distribution of these is related to the dislocation densities and locations. One would expect the lunar material to have greater dislocation densities than the terrestrial material due to its exposure to a shock and radiation environment and, hence, exhibit larger adhesion than the terrestrial samples. But let us disregard this aspect.

Due to this mosaic distribution, it appears reasonable to assume that the adhesion force is proportional to the contact area. (Note that due to the long range nature of the forces, intimate contact is not required.) This adhesion will be most effective when the silicate is in contact with a conductive surface, since the electron mobility in the conductor will allow equal and opposite charge patches to be generated on the conductor surface. With the above assumptions, we can determine the largest silicate block that can remain attached to the underside of a large metal plate. The result, using the highest adhesion force we ever measured as a basis of calculation, is that a silicate block 7 meters thick could be so supported. Even if such a block were in the form of a cube, it would, under lunar gravity, weigh several tons. For typically observed adhesion forces (charge densities), a 2-meter thick block could be supported. Obviously one can argue that adherence of such large blocks is extremely unlikely because (1) the rougher the block surface the less the effective adhesion force, and (2) we have no experimental data to justify the assumption of proportionality between adhesion force (or electrical charge) and surface area (though on the face of it the assumption is not unreasonable). However, the main purpose of the calculation is to indicate that it is possible that massive adhesion could be produced if rocks and other debris are fractured or cleaved at the lunar surface.

Second, the charging produces a long-range attractive force. As a result, we have found it quite difficult to remove silicate fragments that have adhered to metal components. The chips can be pushed around and sometimes shaken loose, but they exhibit the frustrating behavior of

jumping back much like iron filings in the vicinity of a magnet (as noted earlier). It does not take much imagination to visualize the problems this behavior could cause.

Third, we noted that the charge persisted for several months. To this might be added the comment that at the end of this period the charge was still present, the runs being terminated simply because we became tired of waiting for something to happen, and in any case the system was needed for other related experiments. Although the charge did not disappear over this time period, it is reasonable to assume that it eventually would since silicates do have a finite, though small, electrical conductivity. One would also expect that on the Moon the charge would be neutralized more quickly, perhaps on the order of a few tens of hours during a lunar day, due to the action of the solar wind and solar ultraviolet. However, this possibly shortened lunar survival time is not sufficient to negate the potential problems, particularly if the surface to which the fragment is adhering provides shielding against the solar radiations.

Fourth, one might argue that the gaseous contamination from the landed vehicle and astronauts would quickly neutralize the charge. This would be true provided that the gas pressure in the vicinity of the fragment is at least $\approx 10^{-2}$ Torr, since we have found that the charge maintains itself over long periods of time at all pressures below this (10^{-2} Torr represents the minimum pressure in the experiments at which the critical Paschen voltage was reached, permitting plasma breakdown; adsorption of gases on the surface at lower pressures appeared to have relatively little effect on the charge magnitude.)

Finally it should be noted in passing that the large adhesion is produced primarily, if not entirely, by the electrical charging. It may be that when the charge is neutralized by electrical conduction, the resultant clean surface adhesion will be comparable to that found for contaminated surfaces. Hence the Surveyor and Apollo 11 findings do not prove conclusively that the lunar surface material is contaminated.

In summary, Surveyor and Apollo 11 have shown that, under the conditions of the missions, adhesion posed no problems. However, it is unwise to assume that this will be universally true, particularly if future missions involve fracture or cleavage of lunar material at the lunar surface.

As a final note, we are at present completing preparations for receipt of Apollo 11 lunar material. If a portion of this material is suitable, we plan to perform cleavage and/or fracture experiments upon it in ultrahigh vacuum. The results of these studies may confirm some of the predictions made in this chapter.

ACKNOWLEDGMENTS

This work has been supported by the National Aeronautics and Space Administration, Office of Advanced Research and Technology, under Contract NAS7-307.

REFERENCES

1. RYAN, J. A.: Adhesion of Silicates in Ultrahigh Vacuum. J. Geophys. Res., vol. 71, 1966, pp. 4413–4425.
2. RYAN, J. A.; GROSSMAN, J. J.; AND HANSEN, W. M.: Adhesion of Silicates Cleaved in Ultrahigh Vacuum. J. Geophys. Res., vol. 73, 1968, pp. 6061–6070.
3. GROSSMAN, J. J.: Electrostatic Charge Distribution on Ultrahigh Vacuum Cleaved Silicates. J. Vac. Sci. and Tech., vol. 6, 1969, pp. 233–236.
4. ANON.: Surveyor Project Final Report, Part II: Science Results. Tech. Report 32-1265, Jet Propulsion Laboratory.
5. SALISBURY, J. W.; GLASER, P. E.; STEIN, B. A.; AND VONNEGUT, B.: Adhesive Behavior of Silicate Powders in Ultrahigh Vacuum. J. Geophys. Res., vol. 69, 1964, pp. 235–242.
6. STEIN, B. A.; AND JOHNSON, P. C.: Investigation of Soil Adhesion Under High Vacuum. In: The Lunar Surface Layer, edited by J. W. Salisbury and P. E. Glaser, Academic Press, 1964, pp. 93–105.

ROBERT M. COX, JR.
University of Alabama

Explosives and the Lunar Environment

A number of potential uses for explosives exist in the post-Apollo exploration of the Moon. These include geological and geophysical exploration, construction of base camps and roads, and mining operations.

Both conventional high explosives and/or nuclear explosives may find applications. The possible uses and associated problems are presented in the following discussion.

HIGH EXPLOSIVES

The use of high explosives will be dependent to a large extent on two principal factors:

(1) Cost involved with the manufacturing, shipping, storage, and use

(2) Development of explosives that will be stable in the lunar environment

With regard to the hostile environment, the most suitable high explosive would be a blasting agent of rather high detonation velocity and high density. Such an explosive could be transported and stored as non-explosive components and then mixed just prior to use. This would allow for the greatest safety margin.

If a blasting agent cannot be developed for lunar use, other types of explosives will have to be packed in special containers that will protect them from the lunar environment, but not hinder their action during use.

The possible uses of high explosives include:

(1) Seismic exploration work
  (a) Geologic
  (b) Geophysical
(2) Lunar base construction
  (a) Rock excavation
  (b) Boulder fragmentation
(3) Lunar mining
  (a) Drilling
  (b) Tunneling
  (c) Open cuts

In general the applications would be similar to those in Earth-bound operations; however, due to the high cost of equipment and labor, relatively more explosives may be used. Two uses that may find lunar application to a greater extent than on Earth are explosive casting and shape charge drilling.

The throw-in blasting is directly proportional to the excess charge of the round (i.e., that portion of the charge in excess of that required to fragment; see fig. 1). Langefors and Kihlstrom (ref. 1) have presented data which show the relationship between throw and excess charge to be constant. If throw can be assumed to increase with a decrease in gravity, it is readily apparent that lunar material could be easily thrown with explosives for mining or construction purposes, thus reducing the need for some equipment and labor.

The principal disadvantage of using explosives for casting and other purposes may possibly be the ejection of small fragments into low lunar orbit, which creates an additional hazard to explorers and their equipment. In some cases,

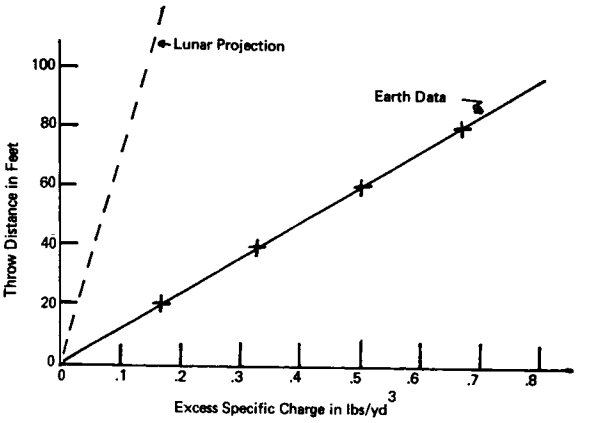

FIGURE 1.—Throw distance as a function of excess explosive charge.

this hazard may be overcome by using some type of blasting mat.

Lined-cavity shaped charges have a great potential use as a means of drilling shallow holes (15 to 25 in.) in lunar rock (ref. 2). Such holes could be used for the location of anchor pins for structures and equipment, as well as for the placement of explosives for mining or construction. Another potential use could be the fragmentation of surface boulders that might present an obstacle to base camp construction, or the movement of mobile exploration equipment. In the event the lunar surface is covered with a layer of dust or fine fragments, shaped charges could be used to clean the surface for building sites, geological exploration, or drilling.

The main advantage of using shaped charges are their compactness and simplicity of operation as compared to drilling machines considering the environment in which they will be used. The main disadvantage of shaped charges is that they can only be used once. The weight of a shaped charge necessary to drill a 2-ft hole is approximately 4 pounds.

NUCLEAR EXPLOSIVES

The possible application of nuclear explosives will probably be limited to: geophysical investigations, stripping overburden, and in situ fragmentation of rock and ore.

The use of nuclear explosives for generating seismic signals for study of the lunar interior is very promising for the geophysicist and most likely will be used in the future if nuclear explosives are not banned from the lunar surface by treaty.

The results of tests conducted in Operation Plowshare under the auspices of the AEC have proven the technical feasibility of excavation by cratering and in situ fragmentation utilizing nuclear explosives (ref. 3). The economics remain to be proved; however, for lunar operations, it may well be justified.

The use of nuclear explosives for surface excavation has two big disadvantages: (1) the possible radioactive contamination of the lunar environment and (2) the ejection of large volumes of material into lunar orbit. These factors may prevent this use.

The use of contained nuclear explosives to fragment large volumes of rock is very promising. In this case the radioactivity is contained in a small amount of rock and the environment is not contaminated. This method can be used either for fragmenting rock for surface mining or underground mining.

The main disadvantage for nuclear excavation is the large amount of material involved. Thus the use of these explosives may have to wait until the demands of a lunar base grow to justify large mining operations.

SUMMARY

It is hoped that this presentation will stimulate discussions on the uses of explosives in lunar exploration. The author holds the opinion that early explosive uses will be limited to small shaped charges as aids in limited excavation or construction projects. Also, small nuclear devices may be detonated for geophysical research.

REFERENCES

1. LANGEFORS, V.; AND KIHLSTROM, B.: Rock Blasting. John Wiley and Sons, Inc., 1963.
2. AUSTIN, C. F.: Lined-Cavity Shaped Charges and Their Use in Rock and Earth Materials. Bulletin 69, State Bureau of Mines and Mineral Resources, 1959.
3. BOARDMAN, C. R.; RABB, D. D.; AND MCARTHUR, R. D.: Contained Nuclear Detonations in Four Media—Geological Factors in Cavity and Chimney Formation. Third Plowshare Symposium, University of California, 1964.

REYNOLD Q. SHOTTS
University of Alabama

Early Water Mining on the Moon

INTRODUCTION

Apollo and the earlier post-Apollo landings will make use exclusively of water, fuel, and oxygen from the Earth. Even if easily accessible lunar free water (ice) is discovered very early, some auxiliary equipment must be landed and proved before its utilization is possible. If lunar water is found only in combined form, or in very small quantities (1 percent by weight, or less) as permafrost or fracture fillings, its utilization will be further delayed. Water regenerative systems probably will be in use in post-Apollo expeditions. These systems may also be capable of assimilating and processing any easily accessible free ice. Such ice probably could be gathered during the lunar night and delivered to the system under conditions permitting little evaporation. Chemically combined forms of water and low grade permafrost, however, will require specially designed water processing equipment. If water is found no closer to the lunar surface than 1 meter, no matter what its form, some type of "mining" will be required to produce the "ore." In the absence of water, oxygen must be extracted from the lunar rock by complex, high energy methods.

Paul (ref. 1) has estimated the water requirements for lunar expeditions from 1976 to 1985. He states that ". . . it is difficult to postulate large demands for liquid oxygen on the basis of life support or mobility system requirements; it is necessary, therefore, to conceive a crew transportation system which can utilize lunar produced propellants for the return trip to earth." Most of the oxygen demand shown in table I, from Paul, therefore, represents fuel for Earth return trips and not for life support.

A study of lunar surface mining has been made, based upon the rather large quantities of liquid oxygen needed in 1982 (refs. 2 to 7). A number of other studies (refs. 8 and 9) have presented elaborate, indirect, Frasch-type systems, also suitable for meeting high oxygen demands. It is proposed, in this study, to consider possible methods or systems that can be applied to earlier and smaller oxygen demands, to intermittent or part-time operation requiring primitive support facilities. Support facilities probably will be limited to small or intermittent power supply; limited, probably single-vehicle transportation; and primitive or non-existent maintenance shops. In addition, mining operations may be carried out by astronauts rather than by specially trained crews.

GENERAL AND ENVIRONMENTAL CONSIDERATIONS

It is proposed to assume the existence of a deposit or deposits of water, hydrous or oxygen-bearing mineral, reasonably close to suitable lunar landing sites and to consider only the problems of mining it. Because mining equipment and methods are largely determined by the nature of the mineral deposit, either (1) a single deposit or a group of deposits must be defined for application of mining equipment and methods or (2) a range of mining methods and equipment must be investigated, sufficiently broad for potential application to any and all conceivable lunar water deposits with limitations only as to depth or grade. This chapter contemplates the latter approach.

To study the problems that may be encountered in mining and in transportation connected therewith, not only must the nature and type of mineral deposit be investigated but every aspect of the environment should also be evaluated. Thus the nature of the terrain, of the surface materials, and of sub-surface materials including volatiles must be approximated as closely as

TABLE I.—*Postulated Lunar Operations Schedule*

	76	77	78	79	80	81	82	83	84	85
Scientific personnel (base size)	6	6	9	9	9	9	12	12	12	12
Plant operations crew	3	3	3	3	3	3	3	3	3	3
Total men on station	9	9	12	12	12	12	15	15	15	15
Number of three-man crew flights	6	6	8	8	8	8	10	10	10	10
Liquid oxygen requirements:	(thousands of pounds per month)									
Flight requirements	7.8	→	10.4	⟶			13	⟶		
Spillage allowance (15 percent)	1.2	→	1.6	⟶			2	⟶		
Misc. requirements	1	→	3	⟶			5	⟶		
Total lox demand	10	→	15	⟶			20	⟶		

possible. Conditions of temperature, pressure, lighting, high energy flux, particle flux, gravitational and magnetic field strengths and variations and other environmental factors should be considered. Problems of energy supply, lubrication, general maintenance and other engineering and logistics factors are also involved. Before mining methods can be selected and equipment designed, all these factors and perhaps others must be evaluated, specifically or within limits, and their relative influences on the mining operation itself must be estimated. Finally early mining must be done by nonspecialists who also attend to other tasks and methods cannot be too complex and controls should be highly automated.

Earlier studies of lunar mining and surface transportation had to be almost entirely speculative with regard to the composition, size consist, size distribution, structure, mechanical properties, and some other properties of the lunar surface and shallow subsurface. Almost everything that was known about the lunar surface was deduced from photometric studies. These were averages over relatively large areas and possibly represented only a millimeter or so of material, in depth.

Appendix A presents a summary of measurements or estimates of many lunar environmental factors. Some of these are pre-Surveyor values but have been generally confirmed. Others are estimates neither confirmed nor disproved by later information. A few are still highly problematical, and some were compiled 3 or 4 years ago (ref. 2) and may not represent the best present estimates.

Particularly scarce is "solid" information regarding the lunar subsurface below 10 meters. It apparently is firmer and coarser than the surface "regolith" (ref. 10), but may not be solid in the sense that solid rock is spoken of in Earth mining.

With customary reluctance to "stick my neck out," especially when a lunar landing is imminent, I will nevertheless suggest that it is doubtful "solid" rock will be encountered by any of the mining methods discussed here. From the fine-grained regolith encountered at all Surveyor sites, downward, the material probably consists of fine grains; fine grains mixed with fragments; blocky material further down and finally, highly fractured rock.

In the highlands, particularly, aeons of impacts have probably broken the "crust" badly, to hundreds of meters in depth. Indeed, most superficial "strata" are probably lenticular masses of fragments covered by still younger fragmental lenses. If shallow masses of lava, intruded or extruded, have been emplaced, these too have been broken in the same way, unless *very* recent in age. On the maria where impacts have apparently been less frequent, presumably because of

a younger age, the condition may be somewhat different. Lava beds or intrusions may be less severely broken up but if surface lavas are slightly distended and brittle or glass-like, after extrusion, they are likely to be badly fractured also, to considerable depth. Lava intrusions that cooled under the surface may come the nearest to representing true solid rock of any conceivable lithologic units. Certainly, if the maria are largely flows of fluidized fragments, as has been suggested (ref. 11), the material is, by definition, fragmental in nature. However, it is possible that fragmental material may be partly recemented at depth.

It has been suggested that the observed relative darkness of partly buried material (underside of fragments, for example), may be due to deposition of some strange "varnish," presumably from deeper under the surface (ref. 10). At moderate and great depths this same or other material may also produce a cementing effect, so that the nearest analogue to lunar solid rock, on earth, may be a conglomerate or cemented breccia. Cemented breccias and conglomerates may be, and probably have been, rebroken by subsequent high energy impacts, recemented, and again broken through several cycles.

All production of very fine particles in the lunar upper layers may not have resulted from direct crushing by micrometeorite impact. High energy shock waves, transmitted through fragmental material, should cause relative particle and block movement which, in turn, should produce some attrition breaking. The effect should be something like "autogenous" grinding of ores from slow tumbling. While high energy impact shock waves should be attenuated rapidly, especially horizontally, and each shock may produce only a small quantity of such attritus, many repetitions could produce considerable amounts of very fine-grained material. This material might even move downward due to "trickle stratification" (ref. 12).

In summary, shallow drilling and mining probably will encounter only fine to blocky material of quite small grain size. This condition may thwart our ambitions for obtaining pure, unmixed "moon rock" samples, particularly in the highlands, until deep into the post-Apollo era.

MINING BY DRILLING

Probably the first mining-type operation to be performed on the Moon will be drilling. As we have learned, design and testing of 10-foot and of 100-foot drills is well advanced.

On Earth, drilling is thought of as an exploratory and not a production operation, except when it is done for the emplacement of explosives. However, as drill holes penetrate ore and produce cores and/or cuttings, small quantities of ore can also be produced on proving water-bearing ores by drilling—and it is probable that water deposits will be proved, if not discovered, this way—drilling equipment will be available for production of some ore if this is deemed more desirable at the time than continuous drilling for discovery.

In addition to the ready availability of equipment, ore production by drilling has two advantages: (1) Some ore is produced from the very first hole reaching the orebody and from every hole penetrating it; (2) exploration and mining may be combined sequentially, using the same equipment. The most obvious disadvantage is that production will be very small and thus most inefficient by Earth standards. Actually overburden/ore ratios are the same as in strip mining. For example, removal of 1 foot of ore from a 31-foot hole gives a 30:1 volumetric overburden/ore ratio. Strip mining a 1-foot bed with 30 feet of overburden gives the same ratio.

Ore capacity per hole can be greatly increased by reaming or chambering the portion of the hole penetrating the ore zone. Replacement of the drilling bit by a reaming tool will require a design of the latter that enables cuttings removal to continue. If chambering of the hole with explosives is done, a fragment-removal tool of some sort must still be run into the hole as an additional operation.

The quantity of ore that can be recovered, per hole, from a 1-foot thick ore zone by a 3-inch hole is only $1/16$ that for the same hole reamed to 1-foot diameter. It is probable that hole enlargement beyond a few diameters may result in caving and resulting dilution of ore. To avoid hole collapse, surface spacing must exceed reaming diameter by a few inches.

On Earth, large diameter holes often are drilled,

not to produce ore, but to obtain large samples or to allow manned access for examination of the hole walls. In hard rocks, the method used to drill holes up to 6 feet in diameter is chilled shot or "calyx" drilling system (ref. 13).

In soft material, some type of auger or rotary bucket drill is used. Either system, on the Moon, would allow the extraction of much more material per hole but would, at the same time, necessitate the expenditure of more energy in removal and disposal of larger quantities of overburden.

The calyx drill can extract cores from "solid" rock but all auger products are soil-like or fragmental. The presence of boulders too large to pass through the auger flights will greatly inhibit or preclude the use of that method. Chilled shot drills probably will not work well in fragmental or brecciated material. Core removal will be difficult or impossible, and shot consumption through loss in cracks at the hole boundaries may be excessive.

Of the two systems, augering probably will prove superior, if usable. It is simpler mechanically and may be used for vertical, inclined, or horizontal holes. On Earth, calyx drill holes must be inclined at less than 35° from the vertical to prevent collection of the shot on one side of the hole; on the Moon, slightly greater inclination may be possible due to the lower gravity, but nothing like a low angle inclined or a horizontal hole will be possible.

Trenching tests by the SMSS attached to Surveyors III and VII indicate that holes in the regolith blanket should stand readily without caving. There is no reason to expect any less self-support from the lower, presumably more blocky, zones. Use of fluidless, mechanical chip removal systems are contemplated (ref. 14). A fluid cuttings removal system or the intersection of gaseous zones in the hole probably would result in caving and thus eventually require casing the hole. Any casing requirements will greatly increase the cost of drilling holes even if casing is recovered and reused. Prefabricated, light-weight plastic casing should be satisfactory in view of the probable low wall pressures to be expected in shallow lunar drilling.

INDIRECT MINING METHODS

If comparatively shallow deposits of free water (ice) are found to occur, it is possible to extract it by indirect methods similar to those used in the Frasch process for recovery of sulfur and in solution mining of salt beds. Soluble hydrous salts may be similarly mined but not as readily. Mining hydrous silicates by these methods will require more power than will be available in early mining.

Six indirect extraction methods have been suggested (refs. 8 and 9). They are

(1) Melting ice by circulating a non-freezing brine

(2) Melting or vaporizing ice by electrical resistance or atomic reactor heating

(3) Melting ice by circulating a heat transfer fluid through coils placed in holes

(4) Direct electrolysis of massive ice

(5) Vaporization of ice by laser beam or plasma torch

(6) Extraction of water via cultivated microorganisms

While all of these methods are technically feasible now—under suitable conditions—except the last one (and it may eventually prove feasible), all are too complex and require too idealized water occurrences to be used in early, primitive water mining. The non-thermal processes can be applied only to free water deposits. The thermal processes probably require more concentrated applications of energy than will be available in the early stages of mining.

CONVENTIONAL METHODS

What is left for consideration now are the conventional methods of mining employed on Earth. These may be divided into surface methods and underground methods. If the hydrous or oxygeniferous ores are near enough to the surface, surface methods are to be preferred.

The last statement is made despite the fact that, historically, underground mining methods have always displaced surface methods, where there was a choice, until comparatively recent times. This was due to the fact that historically not enough energy could be concentrated in mining operations to remove the much longer volumes of material that must be moved in surface methods. Early mining on the Moon could also be short on available energy but not to the

extent of having to depend altogether on human energy as did early terrestrial mining. If the analysis made above of the nature of the first 100 meters or so of the lunar crust is correct, the problem in underground mining will be roof support. Burrowing into the first few meters may be more like mining in alluvium or soft sediments on Earth, the most difficult of underground operations. Of course, if water deposits are so deep that surface methods are wholly impractical, underground mining can be done by carefully lining all shafts, slopes or drifts used in development and by extracting ore by caving methods. Caving methods require only partial or temporary support in working places.

Surface mining is essentially excavation. The range in size of equipment used for excavation is from hand shovels to large power shovels or draglines. The former is too small, and even small models of the latter have excess capacity. The problems of surface mining equipment with respect to type, mass, capacity, manpower needs, power requirements, constructional materials and some environmental factors have been studied in detail (refs. 3 to 7). Systems considered were tower scrapers, bulldozers, front-end loaders, scraper-loader ("carryalls"), power shovels and draglines. Within the constraints expected for early surface mining, the most suitable systems appear to be the front-end loader, scraper-loaders, and bulldozer, probably in that order.

Briefly the mode of operation of each type of machine is as follows:

(1) Front-end loader—Front-end loaders dig rather than scrape. They consist of a tractor and a bucket mounted on bars in front of the tractor (fig. 1b). The blade on the front of the bucket is thrust into the material until the bucket is partly or completely filled, lifted, trammed to the unloading point, and dumped at heights often greater than the tractor height. Some large models have buckets that are also articulated laterally. It is doubtful if the front-end loader can dig as hard, tough, or strongly cemented material as a bulldozer of equal power or capacity can scrape. Loading and transportation, however, are more satisfactory for the loader. Blocks of a diameter smaller than bucket width can also be handled by the front-end loader. No ramp or other aid is needed by the front-end loader for dumping its load. Front-end loaders, because of their versatility, are increasingly popular around coal mines for loading coal, cleaning the top of the coal bed, the removal of thin partings, and any other operations that formerly required great care or even hand work.

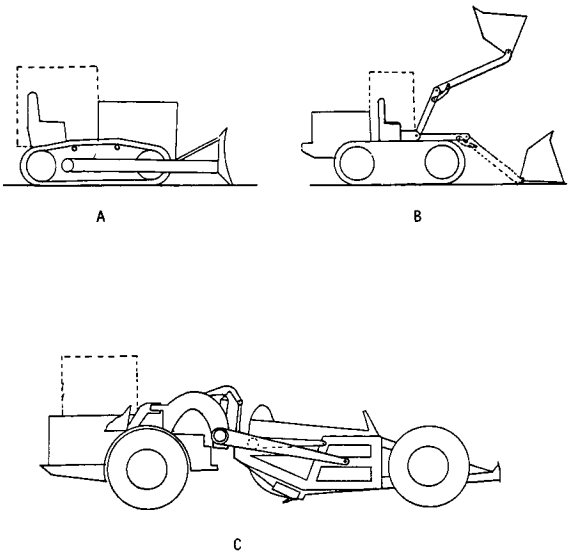

FIGURE 1.—Excavating machines: (a) bulldozer, (b) front end loader, and (c) scraper loader.

(2) Scraper-loader—The scraper-loader, or carryall, scrapes unconsolidated or small fragmental material, loading as it goes and then hauls the load to the dumping point (fig. 1c). Some large, heavy models have elevators for heaped loading. The small models are one-piece but, in some models, the machine is articulated to, and towed by, a tractor. These models are more complex, and heavy than early mining is likely to require.

(3) Bulldozer—Where only unconsolidated or deeply weathered overburden is present, some coal is uncovered, but not picked up and loaded, by the bulldozer at the present time. The bulldozer consists of a blade pushed by a tractor (fig. 1a). A layer of material is scraped off by the concave blade, piled against the blade and pushed ahead up a loading ramp and onto a truck, conveyor belt, or other transportation device. Better still, it is piled up and loaded by another piece of equipment. The bulldozer blade is much higher than the thickness of the layer

scraped so considerable material can be piled before the blade. The capacity of the bulldozer is based on its pushing ability. The figure used in table II, for bulldozer unit capacity, was calculated by assuming material piled at an angle of 45° against the entire blade area. Bulldozer mining is flexible and is adaptable to mining either large or small deposits. If lunar water mining proves to be a problem of exploiting many small deposits rather than a large one, bulldozers or front-end loaders should be particularly useful.

All three machines have the advantages of light weight and high mobility. All three can build their own roads and ramps with the bulldozer perhaps having the edge here. Unfortunately, however, the bulldozer cannot serve as both excavator and haulage vehicle. It can move ore and overburden by pushing, but the operation is slow; and when ore is pushed, it gets diluted and mixed with the material over which it is pushed, or part of it is lost. For handling overburden, the bulldozer is slow but efficient.

Both the front-end loader and the scraper-loader can excavate and transport. For a compact operation involving only short haulage distances, this is a great advantage. With longer haulage distances, a separate haulage unit or units may be desirable because the excavator is not excavating while it is hauling and vice versa. The front-end loader can dig in a fairly small, concentrated area, while the scraper-loader merely scrapes and must remove a greater quantity of material for a given depth of excavation.

If very large boulders are encountered, they can best be handled by the bulldozer. Exercising its great pushing ability, the bulldozer can "wrestle" large boulders aside that neither of the loaders can handle. In coarse, blocky material, the front-end loader may have difficulty digging and the scraper-loader probably cannot be used. In hard material, such as solid rock, conglomerate, or cemented breccia, breaking with explosives will probably be necessary before any of the three excavation methods can be used. Probably the bulldozer will require less complete breakage than will either of the loaders.

Table II, from previous work (ref. 6), shows unit capacities, masses and machine and manpower requirements for three bulldozers, three front-end loaders and two scraper-loader models. The 1982 water demand (ref. 1) on which these figures were based was far larger than contemplated for early mining. One machine of the smallest model should be sufficient for early operations. In the case of the scraper-loader, if it can be used, even the smaller model has large overcapacity.

RELATION OF MINING TO OTHER BASE ACTIVITIES

The problems of power, personnel and scheduling for surface mining have been studied briefly (refs. 3 to 7). Power, especially during the lunar night, may be a big problem. Manpower and scheduling probably are intimately connected with each other.

Before special mining crews are practical, mining must be done by personnel having many other duties about the lunar base. Mining, therefore, may be an intermittent activity. For a number of reasons, conducting surface mining activities only during the lunar night has been recommended (refs. 3 and 6). At night a uniform ambient environment may be maintained which is more difficult to achieve during the lunar day (ref. 6). Early mining equipment is likely to be small and powered by fuel cells. Ore transportation vehicles may be those used for other activities, such as exploration during the lunar day, and scheduling may not be as difficult as in the case of the equipment in demand concurrently. It has also been suggested that the night mining crew may operate the processing plant during the day (refs. 3 and 6). By processing only during the day, almost unlimited solar power may be available that is not available at night. For electrolytic processing, solar energy can provide much more electricity during the lunar day than can be stored in batteries during the night. The end products of processing water (hydrogen and oxygen), or oxygeniferous ores (oxygen), are conveniently stored and intermittent production will pose no problem.

Central power, whether it be from an atomic reactor, solar furnace or banks of fuel cells or batteries, may have to be carefully allocated to

TABLE II.—*Nominal Size, Rated Volumetric Capacity, Earth and Probable Lunar Design Mass, and Number of Machines and Personnel Required to Mine a Hypothetical Lunar Water Deposit* [a]

Machine number	Machine type and size	Unit capacity		Shift capacity		Unit design mass, lb.		System design mass, Moon		System requirements	
		m^3	yd^3	m^3	yd^3	Earth	Moon	kg	lb	Machines [b]	Men [c]
1	Bulldozer, 80″ × 24″ blade	0.38	0.49	101.5	132.8	8667	6070	11010	24280	4	5
2	Bulldozer, 110″ × 28″ blade	0.71	0.92	189.6	248.0	15275	10690	14550	32070	3	4
3	Bulldozer, 125″ × 34″ blade	1.18	1.55	315.0	412.0	21600	15120	13720	30240	2	3
4	Front-end loader	0.62	0.81	165.5	216.5	11010	7710	10490	23130	3	4
5	Front-end loader	1.00	1.31	267.0	349.2	17550	12290	16720	36870	3	4
6	Front-end loader	1.15	1.50	307.1	401.7	20080	14560	13210	29120	2	3

[a] 63.01 m^3 ore and 210.00 m^3 overburden must be mined, per shift, for total of 273 m^3

[b] Includes the one spare unit required in all systems considered here.

[c] One operator per *active* machine plus one maintenance man plus one extra man.

base activities in order to limit power demand, especially during the lunar night. Vehicles used for mine haulage, exploration and other surface activities can be designed with a common chassis and interchangeable bodies. Mine excavation machines can also be used for general excavation purposes when needed.

Thus, until diversification of lunar activities is so great that special mining and processing bases can be built, maximum flexibility can be ensured by tandem qperation of mining and processing plants and the close correlation of both with other base activities.

REFERENCES

1. PAUL, D.: Economic Analysis of Extraterrestrial Propellant Manufacture in Support of Lunar Exploration. Proceedings Fourth Annual Meeting Working Group on Extraterrestrial Resources, Air Force Academy, 1965, pp. 341–376.
2. SHOTTS, R. Q.; COX, R. M.; GRUBBS, D. M.; AND AHRENHOLZ, H. W.: A Study of Lunar Resources: A Preliminary Report on Surface and Some Other Mining Systems, Summary Report, NAS8–20134, Bureau of Engineering Research, University of Ala., NASA CR–77720, 1966.
3. SHOTTS, R. Q.; AND COX, R. M.: Lunar Resources: A Study of Surface Mining. Bureau of Engineering Research, University of Ala., Final Report, Contract NAS8–20134, 1967.
4. FIELDS, S. A.; WEATHERS, H. M.; COX, R. M.; AND SHOTTS, R. Q.: Problems and Techniques of Lunar Surface Mining. NASA TM X–5356, Marshall Space Flight Center, 1967.
5. COX, R. M.; SHOTTS, R. Q.; FIELDS, S. A.; AND WEATHERS, H. M.: Surface Mining on the Moon. Proceedings Fifth Annual Meeting of the Working Group on Extraterrestrial Resources, 1967, pp. 161–180.
6. SHOTTS, R. Q.: Systems for Lunar Surface Mining. In: Engineering Science in Space, Fifth Technical Meeting of the Society of Engineering Science, Inc. Reprinted as Alabama State Mine Experiment Station Technical Report No. 24, July 1968.
7. SHOTTS, R. Q.: Power for Lunar Surface Mining. Alabama State Mine Experiment Station Tech. Rep. 26, 1969.
8. SALISBURY, J. W.; GLASER, P. E.; WECHSLER, A. E.: The Implications of Water as a Lunar Resource. Lunar Planetary Colloquium, N. Amer. Aviation, Inc., vol. III, No. 3, 1963, pp. 39–53.
9. BENSKO, J.; AND SHOTTS, R. Q.: The Utilization of Lunar Resources. In: Advances in Space Science and Technology, Academic Press, 1965, pp. 147–214.
10. HIBBS, A. R.: Surveyor Results. Astron. and Aeron., vol. 7, 1969, pp. 50–63.
11. O'KEEFE, J. A.; AND CAMERON, W. S.: Evidence From the Moon's Surface Features for the Production of Lunar Granites. Icarus, vol. 1, 1963, pp. 271–285.
12. TAGGART, A. F.: Elements of Ore Dressing. John Wiley, 1951.
13. LEWIS, R. S.; AND CLARK, G. B.: Elements of Mining. 3rd. ed., John Wiley, 1964.
14. PAONE, J.; AND SCHMIDT, R. L.: Lunar Drilling. Proceedings of the Working Group on Extraterrestrial Resources, Brooks Air Force Base, NASA SP–177, 1968, pp. 107–117.

APPENDIX

Selected Value and Range for Certain Lunar Environmental Factors

Lunar environmental factor	Probable range	Selected factor		Reference
		MKS or Cgs	English	
1. Atmospheric composition	Ne^+, Kr^+, CO_2, H^+, H_2O	Kr^+, Xe^+	.....	6
2. Atmospheric pressure	1.03×10^{-8} to 10^{-6} N/m²	1.033×10^{-8} N/m²	1.5×10^{-12} psi	1
3. Temperature, surface, max., near 0° lat	390 to 410° K	407° K	273° F	7
4. Temperature, surface, min., near 0° lat	104 to 122° K	105° K	−270° F	6
5. Temperature, subsurface, depth > 1m	−270 to −220° K	233° K	−40° F	6
6. Gravitational acceleration		1.60 m/sec²	5.25 ft/sec²	6
7. Magnetic field max		3×10^{-4} gauss	.....	6
8. Surface electrical charge		+20 volts	.....	5
9. Dielectric constant, lunar surface grains	2.7 to 5.6	4.3	.....	4
10. Soil density near surface of maria	0.7 to 1.2 gm/cm³	[a] 1.0 gm/cm³	62.43 lb/ft³	2, 11
11. Soil density, a few cm below surface		1.6 gm/cm³	99.9 lb/ft³	11
12. Density rock fragment	2.4 to 3.1 gm/cm³	2.8 gm/cm³	175 lb/ft³	12
13. Soil porosity	0.8 to 0.5	0.7	.....	2, 11
14. Particle size	2 to 60 M (most particles)	[b] < 100 M	3.94×10^{3} in	11
15. Soil permeability	1×10^{-8} to 7×10^{-8} cm²	[c] 5×10^{-8} cm²	7.85×10^{-9} in	10
16. Angle, internal friction	35 to 40°	0.65 rad	37°	9, 10
17. Dynamic bearing strength, maria	2 to 7×10^{4} N/m²	2.4×10^{4} N/m²	3.5 lb/in²	2, 8–11
18. Static bearing strength, maria	$1\times10^{3}+05.5\times10^{4}$ N/m²	3.4×10^{4} N/m²	4.9 lb/in²	2, 9, 10
19. Static bearing strength, Tycho rim (2–5 cm)	2 to 3×10^{4} N/m²	2.5×10^{4} N/m²	3.6 lb/in²	12
20. Cohesion, maria	1.5×10^{3} to 7×10^{3} dynes/cm²	500 N/m²	0.07 psi	9
21. Cohesion, maria (vernier and attitude control jet firing)	0.007 + 00.17/N/cm²	1000 N/m²	0.15 lb/in²	2, 11
22. Adhesive strength, material impacting photometric target [d]	10 to 100 dynes/cm²	5 N/m²	7.3×10^{-4} lb/in²	11
23. Chemical composition, maria regolith	Granite-peridotite	Basalt or gabbro	Basalt or gabbro	10, 11
24. Chemical composition, highland regolith	Granite-peridotite	Basalt or gabbro	Basalt or gabbro	12
25. Chemical composition, maria rock	Granite-peridotite	Basalt or gabbro	Basalt or gabbro	Inferred
26. Chemical composition, highland rock	Granite-peridotite	Basalt or gabbro	Basalt or gabbro	Inferred
27. Bulk density, entire maria regolith		[e] 1.7 gm/cm³	106.1 lb/ft³	Estimated
28. Bulk density, solid maria rock	2.7 to 3.5 gm/cm³	[f] 3.00 gm/cm³	187.3 lb/ft³	Estimated
29. Thickness of regolith, Flamsteed crater	1 to 2 M	~ 1 M	3.28 ft	2, 8
30. Thickness of regolith, Mare Tranquillitatis		~ 5 M	16.4 ft	2, 9
31. Thickness of regolith, Sinus Medii	10 to 20 M	~ 15 M	49.2 ft	10
32. Thickness of regolith, Tycho ejecta blanket		~ 10 cm	0.33 ft	12
33. Meteoroid flux (particles larger than 1 gm)		8.8×10^{-14} part.	0.82×10^{-4} part.	Calculated from ref. 3

APPENDIX

Selected Value and Range for Certain Lunar Environmental Factors—Continued

Linar environmental factor	Probable range	Selected factor		Reference
		MKS or Cgs	English	
34. Micrometeoroid flux (particles > 10 μ radius)		/m²/8 hr $8.8 \times 10^{-1.7}$ part.	/ft²/8 hr $0.82 \times 10^{-1.7}$ part.	Calculated from ref. 3
35. Solar wind—average proton flux		/m²/8 hr 2×10^{10}/m²	/ft²/8 hr 1.86×10^{11}/ft²/	13
36. Solar wind—average α-particle flux		sec 0.3×10^{10}/m²	sec 2.79×10^{10}/ft²	13
37. Solar storm—average proton flux		sec 2×10^{11}/m²	sec 1.86×10^{12}/ft²	13
38. Solar storm—average α-particle flux		sec 3×10^{3}/m²	sec 2.79×10^{4}/ft²	13
39. Sputtering rate, max		sec [g] 0.34 Å yr	sec 1.39×10^{-9} in	13

[a] Average, first few centimeters
[b] Mean size
[c] Permeability of earth silts
[d] Lunar material *pressed against* spacecraft parts apparently did not adhere
[e] Before Surveyor VI—estimated as 1.9 gm/cm³ and used in some calculations
[f] Before Surveyor V—estimated as 3.25 gm/cm³ and used in some calculations
[g] Stony materials

REFERENCES

1. ELSMORE, B.: Radio Observations of the Lunar Atmosphere. Philosophical Magazine (London), vol. 2, 8th Series, No. 20, 1957, pp. 1040–1046.
2. HIBBS, A. R.: Surveyor Results. Astron. and Aeron., 1968, pp. 50–63.
3. MCCRACKEN, C. W.; AND DUBIN, M.: Dust Bombardment on the Lunar Surface. In: The Lunar Surface Layer, J. W. Salisbury and P. E. Glaser, eds., Academic Press, 1964, pp. 179–214.
4. O'KEEFE, J. A.; AND CAMERON, W. S.: Evidence From the Moon's Surface Features for the Production of Lunar Granites. Space Sciences, Goddard Space Flight Center, vol. 1, 1963, pp. 1284–1298.
5. OPIK, E. J.; AND SINGER, S. F.: Escape of Gases from the Moon. J. Geoph. Res., vol. 65, pp. 3065–3070.
6. SALISBURY, J. E.; ECKHARD, D. H.; AND HUNT, H. S.: The Lunar Environment. In: Handbook of Geophysics and Space Environments, S. L. Valley, Sc. Ed., U.S. Air Force, 1965.
7. SINTON, W. M.: Temperatures on the Lunar Surface. In: Physics and Astronomy of the Moon, Z. Kopal, Ed., Academic Press, 1962, pp. 407–428.
8. ANON.: Surveyor I Mission Report. Part II: Scientific Data and Results, Technical Report 32–1023, Jet Propulsion Laboratory, Sept. 10, 1966.
9. ANON.: Surveyor III Mission Report. Part II: Scientific Results, Technical Report 32–1177, Jet Propulsion Laboratory, June 1, 1967.
10. ANON.: Surveyor V Mission Report. Part II: Science Results, Technical Report 32–1246, Jet Propulsion Laboratory, Nov. 1, 1967.
11. ANON.: Surveyor VI Mission Report. Part II: Science Results, Technical Report 32–1262, Jet Propulsion Laboratory, Jan. 10, 1968.
12. ANON.: Surveyor VII Mission Report. Part II: Science Results, Technical Report 32–1264, Jet Propulsion Laboratory, March 15, 1968.
13. WEHNER, G. K.: Sputtering Effects on the Lunar Surface. In: The Lunar Surface, J. W. Salisbury and P. E. Glaser, Eds., Academic Press, 1964, pp. 313–322.

REYNOLD Q. SHOTTS
University of Alabama

Gas Wells on the Moon

Surveyor photographs have invariably shown the material lying just under the lunar surface to be darker, on exposure, than surface material (refs. 1 and 2). It is not known if this is due to a bleaching action on surface particles by the solar wind, or results from a coating of, or reaction with, some material from under the surface. If "sputtering" of surface material by the solar wind tends to free light-weight atoms and thus to concentrate heavier ones like iron and titanium (ref. 3), the surface should be darkened, not lightened. Observation that rock fragments, freshly turned over, are also dark on the underside, as well as the generally darker nature of below-surface material, led the Surveyor evaluation team to suggest the buried material is covered by some type of "varnish," similar to "desert varnish," which slowly disappears on surface exposure.

If this explanation is accepted, and it is an entirely reasonable one, it may constitute direct evidence that relatively volatile materials exist below the lunar surface. Curves given by Green (ref. 4) indicate that at the probable lunar subsurface temperature of about 230° K (−43° C) (ref. 5), ice has a vapor pressure of about 0.3×10^{-2} mm of mercury. The vapor pressure of mercury is 10^{-6} mm; HF, 50 mm and Cl_2, 700 mm. If volatiles are leaking from within the Moon, they could produce the change observed. Solids (like water) and liquids (like mercury), with appreciable vapor pressures at 230° F, will contribute. Other substances, not shown on Green's chart, may also be present.

If volatile substances exist under the lunar surface, some of them, including permanent gases, may be trapped in considerable quantities. The observations of Kozyrev confirmed the escape of some low pressure volatiles, possibly including acetylene (ref. 6).

It is known that the Earth's crust contains many reservoirs of gases entrapped in rocks. Entrapment occurs, although most rocks exhibit some degree of porosity and permeability, when completely free of liquids. However, in cases where permeability in an overlying layer has been eliminated by deposition of mineral matter or by the presence, in the pores, of a high surface tension liquid (water), traps are formed. Water is not displaceable from fine pores by hydrocarbon and other fluids not readily soluble in it. Frozen water may serve to close larger pores and cracks.

It appears likely that on the lunar highlands, the surface is badly fractured and brecciated to depths of hundreds of meters or even tens of kilometers. The layers nearer the surface may be largely lens of fragmented material ejected from older craters and covered by other lens of material ejected from younger ones. In the absence of liquids or condensed solids for pore and crack filling, such material could not form gas traps. Thus on the highlands the presence of entrapped gases and vapors may be dependent upon the presence of condensed volatiles below the surface.

On the maria, cratering is less extensive and the upper layers may not be fragmented quite as deeply as on the highlands. At hundreds of meters depth there may even be solid rock, in places. If there are layers of intruded lava, these may constitute solid rock. Surface lavas, however, should have been "frothy" and distended by escaping volatiles on extrusion into the lunar vacuum. If exposed long before being covered by later lavas or by collision crater debris, they probably have been pounded into fine, glassy fragments by micrometeorites.

Thus, unless the maria are also filled by fragmental material rather than lava, the chances for finding both volatiles and entrapped gases at depth appear to be better there than under the

highlands. Indeed, maria margins are considered likely places for finding entrapped volatiles (ref. 7). Other suggested places are at any contact between old highland surfaces and maria flood lavas or in breccia underneath major impact craters (ref. 8).

Except for possible fuel substances, gases and vapors have received little attention as potential lunar resources of value. Regardless of composition, however, they may have value as heat transfer media. This should be particularly true of those that change state within the lunar sunlight-shadow temperature range (120° to 410° K). Inert volatiles like N_2 or CO_2 also can be used in the atmosphere of shelters. If available, many other uses may be found for gases and vapors on the lunar surface.

On both the maria and the highlands it is likely that if entrapped volatiles are present at all, rather deep drilling will be required to produce them.

On Earth, drilling can be done against considerable fluid pressure. The gas retention function, in both rotary drilling and percussion or churn drilling on Earth, require the use of heavy drilling fluids that also serve for cuttings removal and bit cooling. On the lunar surface, these methods cannot be used in an open hole because water or other liquids would freeze or evaporate far too rapidly. Even if present in large quantities, their use will be limited. Probably gaseous fluids will be too scarce on the lunar surface for cuttings removal with consequent loss of fluid. A closed system of cuttings removal is possible, but the technical problems of maintaining such a system, even below depths at which lunar rocks become impermeable, may be great.

Figure 1 suggests a rotary drilling set-up. The upper part of the hole, penetrating permeable rubble, would be drilled by auger, percussion, or any suitable method with mechanical cuttings removal. The hole would be cased through the transition zone between rubble and rock. The division between the two may not be as sharp as indicated in figure 1. After the hole has penetrated a short distance into the impermeable rock zone, two seals would be installed. The drill pipe would operate through some type of packing glands. When it becomes necessary to remove the bit for replacement or for recovery

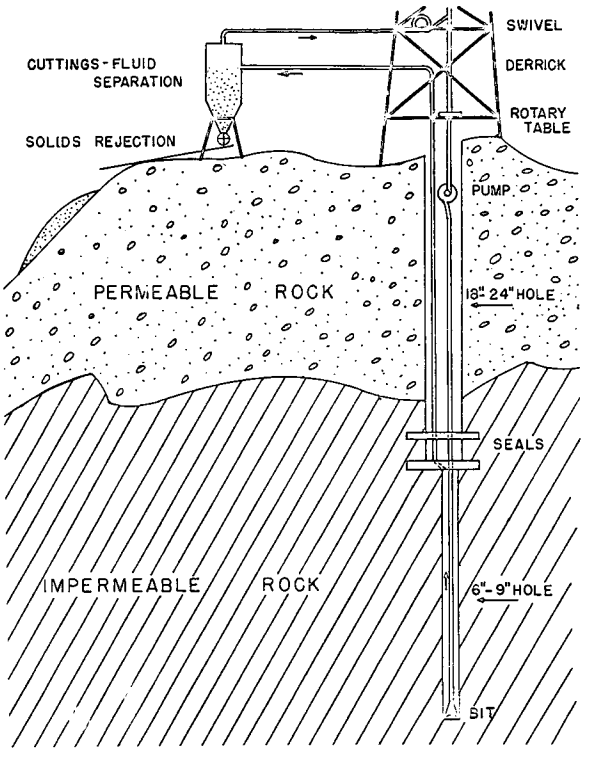

FIGURE 1.—Schematic arrangement for drilling and removing cuttings from a gas well penetrating into an impermeable zone and seeking gases under pressure.

of core, it can be removed through the double seals with escape only of the fluid between the seals. If a moving seal with flexible tubing to carry the fluid and cuttings to the surface could be designed and placed a short distance above the bit, it should provide a minimum volume of pressurized hole. A moving seal would be most difficult to maintain against pressure in a hole in anything but solid rock.

Figure 2 shows a similar scheme for extending the seal all the way to the surface. A drilling capsule is welded to the casing that was installed through the permeable material. The bottom of the casing is then sealed into the impermeable rock. The fluid and the cuttings would be picked up by the pump at the top of a hole being drilled and carried to the cuttings separation vessel. If a gaseous drilling fluid were used, a seal would still be needed to gather fluid and cuttings.

Even if deep subsurface lunar rock proves generally impermeable, deep crevices may be struck that will result in an instantaneous loss of all fluid to the surface. In this case, the hole

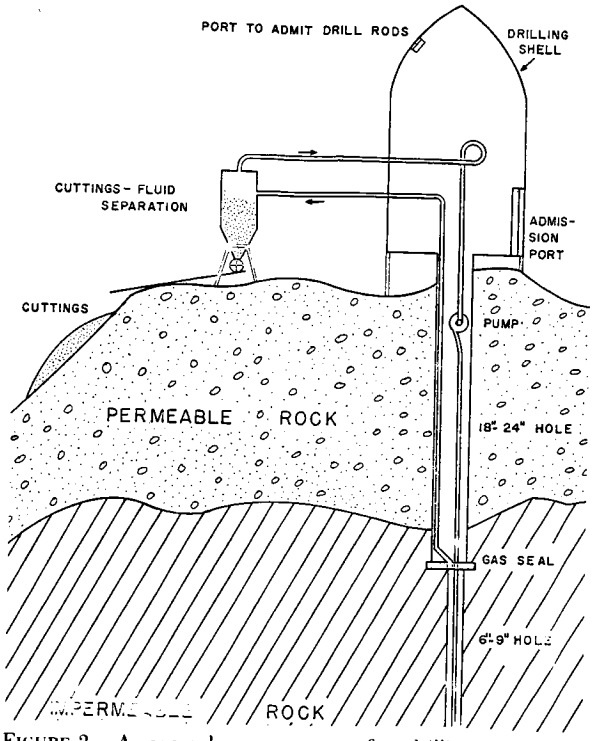

FIGURE 2.—A second arrangement for drilling and chip removal from a well seeking gases under pressure.

would have to be drilled across the crevice in some other fashion; the casing would have to be sealed in across the zone; and the fluid would have to be replaced for continued drilling.

Earth practice in the recovery of gases under pressure from wells passing through permeable or caving strata involves casing with steel pipe and cementing. Steel pipe will be too expensive and bulky to send to the Moon, although it will be easier to handle in the Moon's low gravity field than on Earth. Possible substitutes are plastic or light metal (aluminum). The initial cost of the latter is well beyond that of steel, but is small considering the cost of transportation to the moon is $5000.00 per pound (ref. 9).

Water-based cements cannot be used to cement casing in the lunar vacuum. Sulfur, if sufficiently plentiful, has been suggested as a cement (ref. 4). Perhaps some type of resin or cement that is not dependent upon evaporation of solvent for setting can be substituted. The choice appears to be between the use of expensive light metal or plastic casing and some new technology yet to be developed.

It can be concluded, therefore, that gas deposits of value may be encountered on the Moon, and the wells that produce them are not likely to be shallow. Conducting the gases to the surface may be difficult because of the fractured nature and permeability of the upper part of the lunar crust. To produce gases some sort of plastic or light metal casing may be required. The gases themselves should serve as the medium for conveying drill cuttings to the surface where they can be removed from the gas stream.

REFERENCES

1. ANON.: Surveyor III Mission Report. Part II Scientific Results, Technical Report 32-1177, Jet Propulsion Laboratory, June 1, 1967.
2. HIBBS, A. R.: Surveyor Results. Astron. and Aeron., vol. 7, 1969, pp. 50–63.
3. WEHNER, G. K.: Sputtering Effects on the Lunar Surface. In: The Lunar Surface, J. W. Salisbury and P. E. Glaser, eds., Academic Press, 1964, pp. 313–322.
4. GREEN, J.: Geophysics as Applied to Lunar Exploration (Final Report). AFCRC Document No. AFCRL-TR-60-409, Office of Tech. Serv., 1960.
5. SALISBURY, J. E.; ECKARD, D. H.; AND HUNT, H. S.: The Lunar Environment. In: Handbook of Geophysics and Space Environment, S. L. Valley, Sci. Ed., U.S. Air Force, 1965.
6. UREY, H. C.: On Possible Parent Substances for C_2 Molecules Observed in the Alphonsus Crater. Astrophy. J., vol. 134, 1961, pp. 268–269.
7. SALISBURY, J. W.: Natural Resources of the Moon. Nature, vol. 195, no. 4840, 1962, pp. 423–427.
8. SHOTTS, R. Q.: Pseudo-Volcanism and Lunar Impact Craters. Trans. Am. Geoph. Union, vol. 49, 1968, pp. 457–461.
9. PAUL, D., III: Economic Analysis of Extraterrestrial Propellant Manufacture in Support of Lunar Exploration. Proceedings 4th Annual Meeting Working Group on Extraterrestrial Resources, Air Force Academy, 1965, pp. 341–376.

R. L. SCHMIDT
Bureau of Mines
Twin Cities Mining Research Center
Minneapolis, Minn.

Developing a Lunar Drill: A 1969 Status Report

This discussion summarizes the mission of the lunar drill, reviews the problems associated with lunar drilling, and relates the status of the development program. A discussion of the work at the Bureau of Mines Twin Cities Mining Research Center in connection with the program is presented.

WHY A LUNAR DRILL?

Just as exploratory drilling usually precedes excavation on Earth, lunar drilling will be a prerequisite for lunar excavation. Exploratory drilling can provide solid core samples to determine subsurface geology and facilitate geophysical exploration. Instruments such as heat probes, radiation detectors, and seismic devices are often of necessity, or at least more effectively, placed at depth.

When full-scale lunar excavation becomes a reality, the technology acquired during the development of lunar exploratory drills may be the basis for production drills such as blasthole drills that will serve the same function on the Moon as they do on Earth.

PROBLEMS ASSOCIATED WITH LUNAR DRILLING

The difficult task of boring a hole in Earth rock is compounded by lunar logistics and the hostile lunar surface environment. Probably the least important of the environmental factors are the relatively high and low temperatures on the lunar surface. As no externally supplied flushing media will be used, the problem of operating a drill at lunar temperature will be no greater than that encountered when operating any other piece of equipment on the lunar surface.

The low lunar gravity, approximately one-sixth that of Earth, will present a problem to the early Apollo drill which will be hand-held and depend upon the weight of the astronaut for thrust and vertical stability. The larger moderate-depth lunar drill will be rigidly attached either to the spacecraft or to a lunar excursion vehicle. The weight of the vehicle will then supply the thrust and rigidity. As payload space and weight will be at a premium in any lunar excursion, all lunar rock drills must be constructed as light as possible; for this reason, extensive use will be made of aluminum and titanium alloys.

Perhaps the most severe environmental problem will be the hard vacuum plus the lack of available water that will preclude flushing the drill hole as is standard practice on Earth. In addition to cooling the drill bit, the flushing water, or air, removes rock cuttings from the hole bottom, and thus permits the bit to expend its energy on a clean rock surface. In lieu of flushing media, all lunar drill systems now under consideration have mechanical cuttings—removal systems which auger rock cuttings either to the surface or to a down-hole collection basket.

Another factor that must be considered in connection with the lunar vacuum is that of vacuum adhesion or vacuum welding. If this phenomenon acts to any appreciable degree on the rock cuttings generated by the drill, it can cause the particles to adhere to each other or to the drill rod. Agglomeration of cuttings could increase the torque load on the drill motor or might, in the extreme case, cause a drill stall. As will be explained later, laboratory experiments are under-

way at the Twin Cities Mining Research Center to determine if particle adhesion in vacuum will be severe enough to present significant problems in the design and operation of the lunar drill.

CURRENT LUNAR DRILL CONCEPTS

The first drill in space will be the Apollo Lunar Surface Drill (ALSD) which is scheduled for Apollo 13 in 1970. Designed and built by Martin-Marietta Corp. under contract to the Manned Spacecraft Center, Houston, Texas, this drill is a battery-operated, hand-held, rotary-percussive drill weighing less than 30 lb. Designed for operation by one astronaut, the mission of this drill is to bore two 1-in. holes to a depth of 3 meters in the lunar surface. Present plans are for the holes to be bored with solid, non-coring bits. Hollow, boron filament, Fiberglas drill rod will remain in the holes to serve the additional purpose of a hole-casing. These holes will be used for the placement of probes which are components of a heat-flow experiment. Time permitting, a third, shallower hole will be drilled with a core bit to obtain solid samples for return to Earth.

Design, engineering, and components testing are progressing on the moderate-depth lunar drill which will be the successor to the ALSD. Two companies, both under contract to the Marshall Space Flight Center, Huntsville, Alabama, are developing advanced systems with the capability of boring a 2-in. hole to a depth of 30 meters in the time frame of 1973 to 1975. The Westinghouse Defense and Space Center is offering a diamond rotary drill with a retrievable, wire-line innertube assembly patterned after the system in common use for Earth exploration.

The Northrop Space Laboratories has advanced a down-the-hole, gas-operated percussive drill. This concept is unique in that the drill rod will be flexible, being wound on and off a cylindrical drum as the drill is retracted or advanced. Both concepts are designed to recover a solid core sample.

U.S. BUREAU OF MINES PARTICIPATION

The U.S. Bureau of Mines, which has been conducting rock fragmentation research for over 3 decades, became involved in the lunar drill program in 1965. Bureau scientists first participated in a consulting capacity by assisting NASA in reviewing specifications and serving as an information center to companies developing lunar drill hardware. More recently the Bureau has undertaken laboratory investigations and hardware testing in support of the program.

Published results of diamond drilling research performed at the Twin Cities Mining Research Center during 1967 indicated that drilling with waterflush yielded a higher penetration rate then drilling with airflush or with no flushing media. This series of experiments also produced evidence that solid lubricants introduced to the bit-rock interface improved efficiency of a bench-mounted diamond rotary drill (ref. 1). Further experiments were performed in 1968 on a radial-arm drill (fig. 1) that was instrumented to record thrust, torque, and penetration rate while drilling with 1-in. diameter thinwall diamond bits. The penetration rates and the torque data were used to compute energy per unit volume, and a comparison of performance

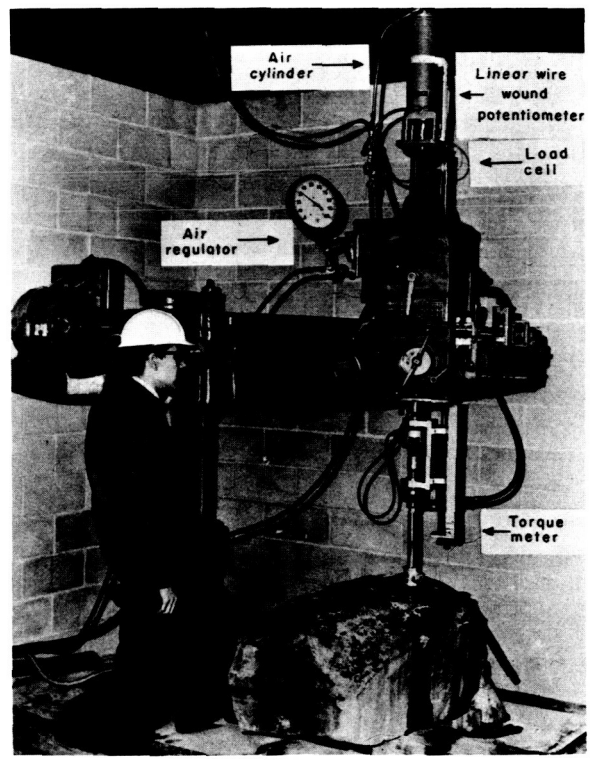

FIGURE 1.—Instrumented radial arm drill.

was made between drilling with waterflush, with airflush, with air plus powder graphite, and with air plus powdered molybdenum disulphide. The powdered lubricants were introduced into the airflush system by means of an aspirator in the air hose.

Figure 2 shows that airflush drilling with no lubricant consumes the highest energy per unit volume and is therefore least efficient from an energy standpoint. This is followed by air plus graphite, waterflush, and air plus molybdenum disulphide which is most efficient. A possible explanation of the poor relative performance of the graphite is that the graphite powder was relatively coarse-grained compared to the microfine molybdenum disulphide. A decision as to which dry lubricant yields better performance must await further experimentation with microfine graphite.

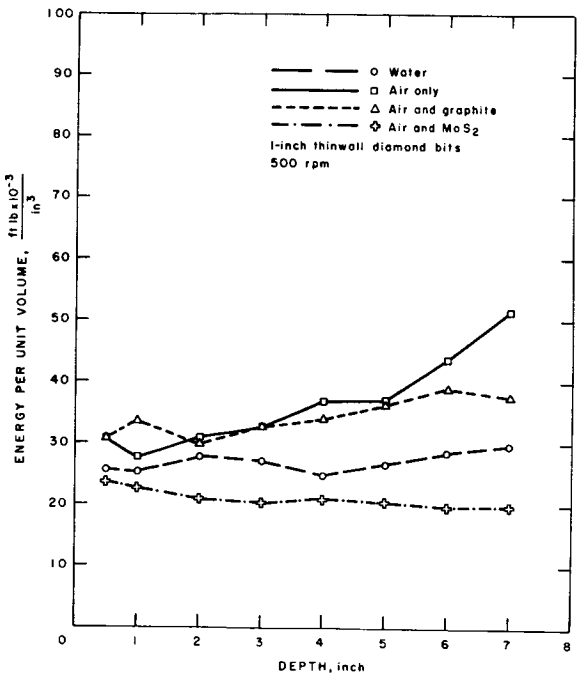

FIGURE 2.—Comparison of efficiency of flushing media in Dresser Basalt.

The exact function of the solid lubricant is not fully understood, but it appears to conserve torque by reducing friction between bit and hole wall. This is accomplished without significant decrease in penetration rate as evidenced by figure 3. This

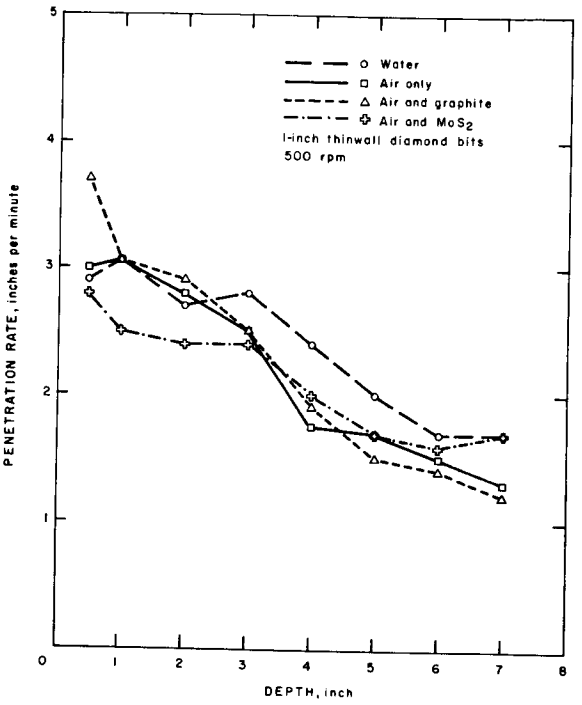

FIGURE 3.—Comparison of penetration rate of flushing media in Dresser Basalt.

decrease in friction may result in longer bit life, although this experiment was not extensive enough to draw any conclusions on this aspect. Previous experiments demonstrated that the addition of a lubricant to liquid flushing media resulted in longer bit life (ref. 2).

Another possible effect of a powdered solid lubricant is that it acts as a "glidant" (ref. 3) to improve the cuttings removal process. Further experimentation will be required to answer the academic questions surrounding the function of dry lubricants in drilling.

If it can be shown that dry lubricants have a positive effect on bit life, this, together with the demonstrated higher efficiency, would warrant their use in a rotary lunar drill. A method would have to be found to introduce the lubricant to the system by some means other than that used in the laboratory, as no flushing system is contemplated for the lunar drill. This might be accomplished with a cylindrical manifold inside the bit which would allow the lubricant to flow to the bitrock interface by centrifugal force.

At the Twin Cities Mining Research Center, a

program is underway to test bits for the moderate-depth lunar drills. A separate study is concerned with cuttings removal by mechanical means. In this study, laboratory tests are being conducted to optimize flute angle and rotational speed from a cuttings-removal standpoint.

As mentioned earlier, some observers are concerned that vacuum adhesion acting on drill cuttings will be a formidable problem for the lunar drill. Drilling experiments have already been conducted in vacuum chambers, both by NASA and by companies developing lunar drill hardware. These tests, however, were conducted in the vacuum range of 10^{-6} to 10^{-7} Torr, several magnitudes of pressure higher than the lunar environment. Since drill behavior in ultrahigh vacuum must be understood, the Twin Cities Mining Research Center has designed and built a vacuum drill apparatus. This apparatus, intended to be the first rock drill operated in ultrahigh vacuum, includes a means of measuring drill torque to compare energy per unit volume when drilling in vacuum and in atmosphere. High speed movies will provide additional comparative data on both vacuum and atmospheric drilling.

Aside from the ultimate objective of the lunar drill program, technology gained during this development program will be of immense value to design problems for Earth drills. Technological advances of the lunar drill development program have already been applied to the area of bit design. To cite a specific example, a drilling company which has developed bits for the diamond rotary lunar drill has significantly altered its procedure for manufacturing commercial diamond bits to take advantage of newly developed methods of diamond selection and orientation and bit crown configuration. This is another example of how the space program presents us with opportunities that would not have otherwise existed.

REFERENCES

1. PAONE, J.; AND SCHMIDT, R. L.: Lunar Drilling. Proc. of the Sixth Annual Meeting of the Working Group on Extraterrestrial Resources, NASA SP-177, Feb. 1968, pp. 107-117.
2. SELIM, A. ALY; SCHULTZ, C. W.; AND STREBIG, K. C.: The Effect of Additives on Impregnated Diamond Bit Performance. Proc. Fourth Conference on Drilling and Rock Mechanics, Preprint No. 2393, Jan. 14-15, 1969.
3. PIPEL, N.: The Cohesiveness of Powders. Endeavor, vol. 28, no. 104, May 1969, pp. 72-76.

D. G. KESTERKE
Reno Metallurgy Research Center
Bureau of Mines
Reno, Nevada

Electrowinning Oxygen from Silicate Rocks

One phase of NASA-sponsored research for the utilization of extraterrestrial resources is directed toward determining the feasibility of extracting oxygen by electrolysis of simulated lunar materials. The method is based on a modification of existing techniques for electrowinning metals from their oxides in fused-salt systems. Results of preliminary work leading to the electrowinning efforts are presented. The current status of the research effort is outlined, and operating conditions are described under which oxygen was successfully electrowon from fluoride-silicate mixtures.

INTRODUCTION

With the rapid advances being made in space technology, it is well within the imagination to envision large and complex lunar stations with personnel numbering in the hundreds. To support the inhabitants of such installations, it is obviously desirable to utilize extraterrestrial resources as much as possible. Of primary interest in developing a life-support system are potential sources of oxygen, one of which is the lunar surface material itself. This material is thought to be composed primarily of silicates, and the results obtained from the Surveyor program indicate that the composition of the lunar surface closely approximates that of some terrestrial basalts and that the constituent metals are present as oxides (ref. 1). Such silicate minerals contain about 50 weight-percent oxygen; however, many of the oxides are highly stable, and the extraction of free oxygen would require several processing steps, or a high-energy process such as can be provided by electrolysis.

Attractive possibilities exist for the electrowinning of free oxygen from silicate minerals through modification of the basic concepts and techniques developed for the preparation of various reactive metals by high-temperature electrolysis. The feasibility of metal production by electrolysis in fused-salt media has been widely demonstrated. Many of these procedures, such as the Hall process for aluminum, involve the dissolution and subsequent reduction of an oxide of the metal in question. The technique has also been demonstrated for preparing uranium and several of the rare-earth metals (refs. 2 to 5). In these methods, the anode reaction involves the discharge of oxygen ions at a carbon electrode and the resultant formation of carbon oxides, which consumes the electrode.

The objective of the present investigation conducted by the Bureau of Mines is to extend these methods to silicate-bearing mixtures. In this process, electrolytic energy would decompose the constituent metal oxides and yield oxygen ions that are discharged at a nonreactive anode, producing free oxygen which is evolved from the cell. In theory, electrolysis could also produce oxygen through the discharge of silicate anions as shown by the following reactions proposed by Bockris (ref. 6):

Silicate structure	*Reaction*
Orthosilicate	$SiO_4^{4-} \rightarrow SiO_2 + O_2 + 4e$
Pyrosilicate	$Si_2O_7^{6-} \rightarrow 2SiO_2 + \frac{3}{2}O_2 + 6e$
Rings and infinite chains	$(SiO_3)_n^{2n-} \rightarrow nSiO_2 + \frac{n}{2}O_2 + 2ne$
Chains	$(Si_4O_{11})_n^{6n-} \rightarrow 2nSiO_2 + \frac{n}{2}O_2 + 2ne$

The cathode reaction could entail the discharge of several different metal cations and the subse-

382-451 OL - 70 - 10

quent codeposition of these metals as dendrites or low-melting alloys.

Electrical conductivity and viscosity studies have been conducted at temperatures up to 1800° C by Bockris and associates on binary mixtures of SiO_2 and metal oxides of the alkali and alkaline-earth groups and others such as aluminum, iron, manganese, lead, and titanium (refs. 6 to 8). As the result of these investigations, it was determined that electrical conductance in these systems is primarily ionic. The conductance increases with the concentration of the metal oxide and is a function of the network-breaking effect of the metal oxide. Bockris also demonstrated that passage of direct current through the melt produces electrolysis and that, in many of the systems, Faraday's laws are obeyed within experimental error.

It is the purpose of this chapter to describe the progress made by the Bureau of Mines in studying the potentiality of oxygen preparation by electrolysis of silicate mixtures believed to be representative of the minerals found on the lunar surface. Silicate rocks selected for use in this study included several of the rock standards suggested by Green (ref. 9) as being representative of possible lunar surface materials. These included a basalt, an obsidian, a granodiorite, and a serpentine. Supplementary materials included a mixture of basalt plus sinter and a pumice.

EQUIPMENT

Cell and insulation components are enclosed in a 3-foot-diameter by 4-foot-long steel chamber. Essential features of the chamber are shown in figure 1. It is equipped with viewports, leadthroughs for bringing ac and dc power into the chamber, and has a full-diameter access door at one end. Manipulation of the electrode hoist mechanism is accomplished through gloveports and neoprene gloves. The chamber can be evacuated to a pressure of about 10^{-3} Torr by means of a mechanical pump. A refrigeration unit is available to cool the chamber atmosphere to permit the performance of necessary manual operations.

The initial phase of the investigation was directed toward a study of the relative physical characteristics of various silicate rocks and determining the effect of flux additions on these

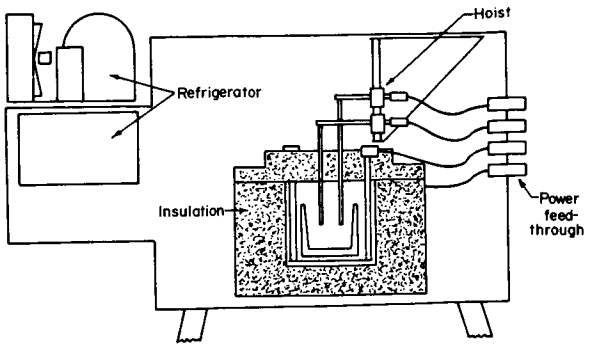

FIGURE 1.—Electrolytic cell in protective atmosphere chamber.

characteristics. For these experiments, a high-temperature cell and insulation system was used, as illustrated in figure 2. Graphite crucibles, 5 inches in inside diameter by 4 inches deep, were used for containing the silicate mixtures. Electrodes used in determining the relative electrical conductivity of the melts were 3/8-inch-diameter graphite rods, spaced approximately 2 inches apart. Surrounding the crucible were an enclosure and lid, also made of graphite. Thermal insulation was provided by boron nitride powder, alumina beads, and conventional firebrick. A specially designed graphite resistance heater-reflector combination located immediately below the crucible provided heat for melting the electrolyte

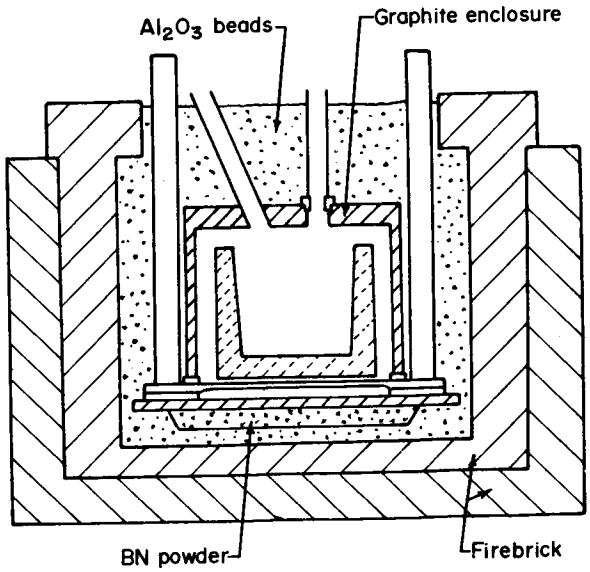

FIGURE 2.—High-temperature cell and insulation system.

and for maintaining the desired cell temperature during the experiment. An arc welder furnished alternating current applied to the resistor, and a silicon rectifier supplied the direct current.

Tungsten-rhenium or platinum-rhodium thermocouples immersed 1 inch into the melt were used to measure the temperature. Supplementary temperature measurements of the electrolyte surface were made with an optical pyrometer.

In recent experiments in which oxygen was prepared, major design changes were necessary to eliminate refractory materials that would react with free oxygen at elevated temperatures (fig. 3). A hot-pressed boron nitride crucible, 4 inches in inside diameter by 3½ inches deep, is used for containing the electrolyte. The selection of electrode materials for use with this cell was the subject of research which is described later. Thermal insulation is provided by castable alumina and firebrick. Six silicon carbide resistors heated by alternating current supply the requisite heat.

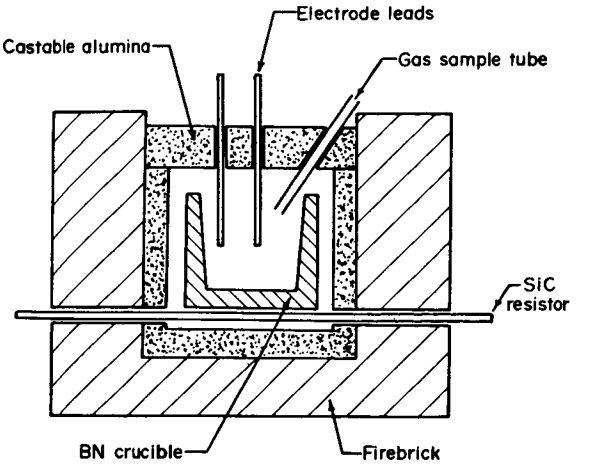

FIGURE 3.—Oxygen electrowinning cell.

PROCEDURE

Prior to assembling the cell components, the electrolyte constituents were dried to remove adsorbed moisture. After the cell components were assembled within the chamber, the cell was degassed by heating it to about 650° C under vacuum. The chamber was then backfilled with helium.

The electrolyte was melted by heat from the external resistor. About 15 kilowatt-hours was required to heat a 1000-gram charge of bath to 1100° C. After the desired bath temperature was attained, relative electrical conductivity determinations were made by applying a direct current to the electrodes.

In experiments to electrowin oxygen from the various silicate mixtures, direct current was applied to the electrodes and cell gases were sampled at a point near the anode and analyzed for oxygen by the Orsat method. Analysis for the presence of other gases was made by infrared spectrophotometry and by gas chromatography.

After each experiment the electrodes were withdrawn from the melt, and the cell was cooled to room temperature for disassembly and examination.

RESULTS AND DISCUSSION

Initial experimentation was directed toward determining whether electrolysis could be effectively performed in silicate mixtures without using fluxing materials to promote fluidity and electrical conductivity of the melt. Investigations were conducted at 1500° to 1775° C on a random mixture of various silicate rocks and on pumice, granodiorite, and basalt. In all experiments, the molten mixtures exhibited excessive fuming and remained quite viscous. Electrical conductivity determinations showed that the resistance of the melts was too high, even at temperatures greater than 1700° C, to permit effective electrolysis.

As an extension of this study, similar experiments were performed on selected synthesized minerals, including diopside, wollastonite, clinoenstatite, monticellite, and anorthite. Synthesis of these minerals was accomplished by fusion of the constituent oxides in the high-temperature cell and insulation system. Results of relative electrical conductivity determinations showed that none of the minerals was sufficiently conductive to be used as an electrolyte without the addition of a suitable fluxing agent.

In electrowinning operations conducted in fused-fluoride systems, the presence of lithium fluoride in the electrolyte serves to lower the melting point and promote the electrical conductivity of the melt. It was believed that LiF and

possibly other fluorides would have the same effect on silicate melts. In addition, oxide, borate, and phosphate additives are also used in various metallurgical processes to promote the fluidity of melts and slags.

A study was then conducted to determine the effect of various additives on the physical characteristics of silicate rocks. A basalt-plus-sinter mixture was chosen for use in determining the effect of selected fluxing agents on the relative electrical conductivity of the melt. Major constituents in this mixture in weight-percent are as follows: 46.5 oxygen, 25.8 silicon, 6.0 aluminum, 5.7 iron, 3.9 calcium, 3.2 sodium, and 1.5 magnesium. Conductivity determinations were made at temperatures of 1200° to 1300° C. The results are summarized in table I in which the conductivity is expressed as the amperage-to-voltage ratio. As indicated, the lithium fluoride-bearing melt was the most conductive.

TABLE I.—*Relative Electrical Conductivity of Basalt-Plus-Sinter Containing 10 Weight-Percent Additions of Various Fluxing Agents at 1300° C*

Flux	Amperage/voltage
LiF	0.66
CaF_2	.08
MgF_2	.0
Na_2O	.05
$NaBO_2$	.3
Na_3PO_4	.18
$Na_5P_3O_{10}$	.4

In table II, a comparison is made of the relative electrical conductivity of several rocks and minerals, each containing 10 weight-percent LiF.

Even with the considerable improvement in melt fluidity and conductivity that resulted from the addition of 10 weight-percent LiF, temperatures greater than 1400° C were required to obtain a more favorable current-to-voltage ratio. At lower temperatures, the relatively low-amperage, high-voltage conditions make the process less attractive from a power consumption standpoint.

Electrode-melt compatibility studies were made using various platinum-group metals to determine their corrosion resistance at the temperatures

TABLE II.—*Relative Electrical Conductivity of Silicates Containing 10 Weight-Percent LiF at 1400° C*

Rock or mineral	Amperage/voltage
Basalt plus sinter	1.8
Granodiorite	2.0
Pumice	1.3
Serpentinite	3.7
Diopside	2.5
Wollastonite	3.0

necessary for effective electrolysis. Iridium was evaluated by immersion in a mixture of diopside plus 10 weight-percent LiF heated to about 1500° C. Complete dissolution occurred in less than 30 minutes. The compatibility of iridium and platinum with a mixture of serpentinite plus 10 weight-percent LiF was similarly determined at temperatures up to 1450° C. Severe corrosion of the iridium and complete dissolution of the platinum resulted after only a few minutes of immersion.

The poor corrosion resistance of the materials thus tested necessitated a redirection of planning away from the initial concept of high-silicate, low-flux electrolytes. Subsequent experimentation was oriented toward a study of the characteristics of electrolyte systems in which silicates were the minor constituent. The primary objective was to develop melt systems that could be used at 1050° to 1150° C, thus increasing the possibility of finding suitable electrode materials.

Evaluation of the physical characteristics was made for melts containing 15, 25, and 35 weight-percent silicates, with the balance being BaF_2 and LiF in the mole ratio of 0.65 to 0.35. All three exhibited significantly improved electrical conductivity in that the current to voltage ratio was about 2.5 or 3.0 to 1 at 1100° C.

In further electrode-melt compatibility studies, iridium, platinum, and a platinum-13-percent rhodium alloy were tested at about 1250° C in a bath composed of 69.4 weight-percent BaF_2, 5.6 weight-percent LiF, and 25 weight-percent basalt plus sinter. Results showed that the platinum metal and alloy would dissolve in this mixture; however, the iridium did not corrode, and efforts were then directed toward determining the corro-

sion resistance of several refractory materials under the effect of an applied dc voltage. In addition to iridium, silicon carbide, and titanium and zirconium diborides were evaluated for use as anode and cathode materials in various fluoride-bearing silicate mixtures at temperatures up to 1250° C. Iridium exhibited the best stability of these materials when used as an anode, while silicon carbide was unattacked as a cathode material. Severe corrosion of both diborides occurred regardless of whether the polarity was anodic or cathodic.

Initial experiments to electrowin free oxygen used an electrolyte composed of 25.0 weight-percent basalt plus sinter, 69.4 weight-percent BaF_2, and 5.6 weight-percent LiF. Iridium sheet 0.02 inch thick, with a surface area of about 0.45 square inch on a side, was used as the anode material. The cathode was a ½-inch-diameter silicon carbide rod. Electrolysis was conducted at 1150° to 1250° C. In most experiments, at least 17 volts were required to decompose the oxides in the melt. The electrolysis current was temperature dependent and ranged from 25 amperes at lower temperatures to more than 60 amperes at temperatures near 1250° C. During these experiments, oxygen contents in the cell gases increased from zero percent at the start of electrolysis to 0.2 to 5.0 volume-percent after 30 to 40 minutes.

In a subsequent series of experiments, the silicate content of the melts was increased to 35.0 weight-percent. Barium fluoride and lithium fluoride contents were 60.0 and 5.0 weight-percent, respectively. Electrolysis temperature again ranged from 1150° to 1250° C, but the increase in oxygen yields was insignificant.

A considerable improvement in results was achieved by utilizing a bath composed, in weight-percent, of 35.0 basalt plus sinter, 48.5 BaF_2, and 16.5 LiF. The higher LiF content permitted electrolysis at 1050° to 1150° C, with no significant change in the voltage-amperage relationship. The maximum oxygen content of the gas over the cell during these experiments was almost 7 percent by volume. The remainder of the gas was primarily helium, with trace amounts of CO_2 and SiF_4. The carbon dioxide is a product of the reaction between free oxygen and the SiC cathode or heating elements, while the SiF_4 may result from a reaction between the SiC cathode and fluoride fluxing agents.

Increasing the anode surface area to about 0.85 square inch resulted in a further improvement in cell performance, and oxygen contents of over 12 volume-percent were achieved. Table III compares the conditions and results of typical experiments in which the anode area was 0.45 square inch, with those from experiments in which the area was 0.85 square inch.

In all experiments, a solid deposit of varying size accumulated on the cathode. This material consisted of metal dendrites and entrapped electrolyte, and most showed magnetic properties. Accurate analysis of the metal portion of the deposits was impractical because of the adhering bath; however, spectrographic analyses of selected dendrites that were relatively free of bath materials showed iron, aluminum, sodium,

TABLE III.—*Typical Operating Conditions and Results in the Electrowinning of Oxygen*

	Anode surface area			
	0.45 square inch		0.85 square inch	
Operating conditions:				
Melt temperature, °C	1050 to 1100	1050 to 1100	1070 to 1115	1060 to 1130
Average electrolysis current, amp	42	42	57	62
Cell voltage	17 to 19	17 to 18	18 to 19	18 to 19
Duration of electrolysis, min	40	42	42	40
Results:				
Maximum O_2 content over cell, vol pct	3.1	6.7	10.3	12.3
Anode loss rate, mg/amp hr	19.5	25.4	19.0	[1] 45.0

[1] High loss rate due to alloying with cathode deposit.

silicon, and barium as major constituents. Also present in significant quantities were manganese, titanium, calcium, molybdenum, and boron, while nickel, zirconium, copper, and chromium were present in lesser amounts. The boron, no doubt, originated from the BN crucible, while the molybdenum may have come from the tools or electrode connecting rods.

Another indication of the composition of the metallic portion of the cathode growth was obtained through analysis of the electrolyte before electrolysis and then again after 2½ hours of electrolysis. Metallic elements in the bath that showed a significant decrease could be assumed to have deposited on the cathode. The change in content of such metals is shown in table IV.

TABLE IV.—*Analysis of Metallic Elements in the Bath Which Decreased During Electrolysis*

Metal	Content in the bath	
	Before electrolysis	After electrolysis
Iron	2 percent	0.2 percent
Titanium	0.3 percent	0.1 percent
Vanadium	50 ppm	< 20 ppm
Cobalt	< 35 ppm	Not detected
Nickel	< 20 ppm	Not detected
Chromium	15 ppm	Not detected

The rate of loss of the iridium anodes ranged from 12.5 to about 60 mg per ampere hours. In some experiments, however, the loss was not due entirely to electrochemical processes or to oxidation, but was due partially to contact between the anode and the cathode growth. Alloying between the iridium and some of the metallic constituents of the cathode deposit caused severe embrittlement and promoted corrosion of the iridium. The average iridium loss rate for 20 experiments in which there was no contact between the anode and the cathode growth was about 25 mg per ampere hour. This showed that anodic dissolution of iridium under electrolysis conditions is negligible compared with loss rates that could occur based on electrochemical equivalents. The theoretical loss due to electrochemical dissolution is about 1800, 2400, or 7200 mg per ampere hour for a valence change of 4, 3, or 1, respectively.

SUMMARY

Bureau of Mines research has shown that oxygen can be electrowon from silicates dissolved in molten fluoride systems. The demonstrated ability to generate more than 12 percent by volume of oxygen in the cell gases is encouraging. However, no attempt has been made to collect and measure the total amount of oxygen evolved at the anode, and no estimate can be made of the faradic efficiency of the cell.

Before making the ultimate determination of whether the process is practical, uncertainties must be overcome. Of major importance is the problem of restricting the cathode deposit from the vicinity of the anode. The solution may be found through the use of compartmented cells.

Research using larger cells will also permit a more accurate determination of the effect of anode surface area and electrode geometry on cell performance. Further study of melt compositions will be conducted in efforts to find workable electrolytes that require lesser amounts of fluxing materials.

REFERENCES

1. TURKEVICH, A. L.; FRANZGROTE, E. J.; AND PATTERSON, J. H.: Chemical Analysis of the Moon at Surveyor VI Landing Site: Preliminary Results. NASA SP-166, March 1968, pp. 109–132.
2. KESTERKE, D. G.; FLECK, D. C.; AND HENRIE, T. A.: Direct Electrolysis of Uranium Dioxide to Uranium Metal in Fluoride Melts. Rept. of Inv. 6436, U.S. Bur. Mines, 1964.
3. STEVENSON, J. W.: Electrolytic Uranium Project Terminal Progress Report—Cell Operation. MCW-1514, Mallinckrodt Chem. Works (Weldon Spring, Mo.), Oct. 1966.
4. SHEDD, E. S.; MARCHANT, J. D.; AND HENRIE, T. A.: Continuous Electrowinning of Cerium Metal From Cerium Oxides. Rept.. of Inv. 6362, U.S. Bur. Mines, 1964.
5. MORRICE, E.; WYCHE, C.; AND HENRIE, T. A.: Electrowinning Molten Lanthanum From Lanthanum Oxide. Rept. of Inv. 6075, U.S. Bur. Mines, 1962.
6. BOCKRIS, J. O'M.; KITCHENER, J. A.; AND DAVIES, A. E.: Electric Transport in Liquid Silicates. Trans. Faraday Soc., vol. 48, 1952, pp. 536–548.
7. BOCKRIS, J. O'M.; KITCHENER, J. A.; IGNATOWICZ, S.; AND TOMLINSON, J. W.: Electric Conductance in Liquid Silicates. Trans. Faraday Soc., vol. 48, 1952, pp. 75–91.
8. BOCKRIS, J. O'M.; MACKENZIE, J. D.; AND KITCHENER, J. A.: Viscous Flow in Silica and Binary Liquid Silicates. Trans. Faraday Soc., vol. 51, 1955, pp. 1734–1748.
9. GREEN, J.: Selection of Rock Standards for Lunar Research. Ann. N.Y. Acad. Sci., vol. 123, art. 2, July 15, 1965, pp. 1123–1147.

U.S. GOVERNMENT PRINTING OFFICE : 1970 O - 382-451